Combination of Manumycin A and Mebendazole in Human Breast Cancer Cell Lines

A Dissertation Presented to the

Faculty of the Department of Pharmacological and Pharmaceutical Sciences

College of Pharmacy, University of Houston

In Partial Fulfillment of

The Requirements for the Degree of

Doctor of Philosophy

By

Rania Haddadin

November, 2010

AKNOWLEDGEMENT

Stars are always there in the sky but we can only see them in the dark. During the toughest times in our lives when we are surrounded by overwhelming darkness, shining stars send us beams of hope illuminating our path and breaking all the darkness. At times, my PhD pursuit was like the sky at night, dark but full of bright stars. To every one of them I dedicate this work with love. To my advisor Dr Diana Chow for all the support, advice, love and care she gave me. Thank you for sharing the Lord's love with me teaching me at all times that "His grace is sufficient". May the Lord bless you all the days of your life. To my committee members, Dr. Bippino Giovanella, Dr. Jim Yeung, Dr. Dong Liang and Dr. Richard Bond who gave me the time and guidance and helped get this work accomplished. To my best friend Dr. Hibah Awwad who was always there for me giving me a shoulder to cry on and a helping hand since the first day at UH. To Dr. Ozozuma Omoluabi who was a caring and faithful friend during the past year. To my colleagues at the lab as they all had an influence on my journey.

To my mom, my father-in-law, and my mother-in-law who lovingly dedicated their time to my daughters so that I can have this opportunity. To my dad who believed in me and supported me to fulfill my dream at all times. To my shining star, my beloved husband, Nader, who made this work possible by his surpassing love and continuous support. THANK YOU.

ABSTRACT

We evaluated the combination of MA and Mbz in wild-type and HER2 transfected MDA-MB-231 and MCF-7 human breast cancer cell-lines in vitro and in xenografted mouse model.

Methods: XTT colorimetric and SRB assays were used to determine cell viability in culture after single and combination treatment. Flow cytometry and western blotting were used to test the role of cell cycle arrest and apoptosis in cytotoxicity of single and combination treatment. We used PI for cell cycle and Annexin-V-FITC for apoptosis. We probed for Cyclins E and B and cleaved PARP. In vivo MDA-MB-231cell pair was used for dorsal subcutaneous xenogratfs in nu/nu Swiss mice. MA and Mbz were administered ip in single and combination treatments. The change in tumor volume was used to assess effectiveness.

Results: MA and Mbz were cytotoxic in all four cell-lines at micro-molar levels. Mbz is more effective in MDA-MB-231 cells. MA 1st and Mbz1st showed additional benefit in MDA-MB-231/ErbB2 and MCF-7/Her18 cells, respectively. MA arrested MCF-7cells at G1/S and MDA-MB-231 cells at G2/M phase. No cleaved PARP was detected at 89kDa in all four cell-lines. In vivo, concurrent treatment showed additional benefit in MDA-MB-23/ErbB2. Mbz1st treatment showed additional benefit in male but not female mice with MDA-MB-231 xenografts. Liver histopathology showed necrosic, apoptosic and microangiopathic changes with combination treatment.

Discussion: MA and Mbz were cytotoxic in all four cell-lines at micro-molar levels, with Mbz being more effective in MDA-MB-231 cells. Combination therapy showed additional benefit over single agent treatment in HER2 transfected but not wild-type cells. Apoptotic cell death did not play a major role in cytotoxicty. Sequence of drug administration, drug concentration, ratio of MA to Mbz, and targeted cells affect final outcome of combination treatment in vitro. Sequence of drug administration, type of cancer cells, and gender affect treatment outcome in vivo. Liver toxicity was observed with combination treatment.

Conclusion: We were able to identify factors affecting MA and Mbz combination outcome. This combination is antagonistic with some exceptions. We are the first to show anticancer activity of Mbz in breast cancer xenografts using a microemulsion formulation.

TABLE OF CONTENTS

LIST OF FIGURES

Dose Efficacy Studies:

LIST OF TABLES

LIST OF PICTURES

LIST OF ABBREVIATIONS

Cdk	Cycline Dependent Kinase
CI	Combination Index
ddH2O	De-ionized Distilled Water
DMSO	Dimethyl Sulfoxide
EGFR	Epidermal Growth Factor Receptor
EMT	Epidermal Mesenchymal Transition
ER	Estrogen Receptor
Erb B2	Human Epidermal Growth Factor-2 proto-Oncogene
FTIs	Farnesyl Transferase Inhibitors
GSH	Glutathion
HDAC6	Hydroxydeacetylase 6
HER-2	Human Epidermal Growth Factor-2 proto-Oncogene
IGF-1R	Insulin-like Growth Factor Receptor
i.p.	Intraperitoneally

kDa	Kilo Dalton
LMW-E	Low Molecular Weight Cyclin E
MA	Manumycin A
MAPK	Mitogen-Activated Protein Kinase
Mbz	Mebendazole
MEK	Mitogen Extracellular Kinase
MTOR	Mammalian Target of Rapamycin
NSCLC	Non-Small Cell Lung Cancer
OD	Optical Density
PARP	Poly (ADP-ribose) Polymerase
PBS	Phosphate Buffered Saline
PI	Propidium Iodide
PI3K	Phosphatidylinositol 3-Kinase
PR	Progesterone Receptor
PSN	Penicilline/ Stryptomycin/ Neomycin

rMETase	Recombinant Methioninase
ROS	Reactive Oxygen Species
SDS	Sodium Dodecyl Sulfate
SRB	Sulforhodamine Blue
STAT 3	Signal Transduced and Activator of Transcription 3
TBS-T	Tris Base saline- TWEEN 20
TCA	Trichloroacetic Acid
TC-complex	Tubulin-Colchicin complex
TGF-β	Transforming Growth Factor Beta

CHAPTER- 1- INTRODUCTION:

Our increased knowledge of cancer led to a dramatic increase in the number of anticancer drugs available for treatment. Yet, the improvement in survival rates and life expectancy among cancer patients was not proportionate. This reveals the need for preclinical studies to investigate new drug combinations and to optimize the regimens used to treat cancer in the clinical setting. Preclinical studies utilizing tumor cell cultures and cancer animal models help determine the optimal dose, dosing interval and sequence of drug administration in multidrug anti-cancer regimens used in human beings. These models improve our understanding of the mechanism behind drug cytotoxicity, and the drug-drug and drug-target interactions influencing it. A number of preclinical and clinical studies investigating the effect of anti-cancer drug combinations in different tumors revealed that the sequence of drug administration and the targeted tumor determine the cytotoxicity of combined anti-cancer drugs [Edelman et al 2001, Leo et al 2000, and Zoli et al 1999]. Recently, drug ratio dependent antagonism was identified as a new category of multidrug resistance in cancer treatment [Harasym et al 2009].

The odds of getting cancer in one's lifetime are 1 in 2 men and 1 in 3 women. Breast cancer is the second most common cancer among women accounting for 1 in 4 cancers diagnosed in women in the United States. In the year 2010, an estimated 207,000 new cases of breast cancer will be diagnosed [American Cancer Society, Inc. Breast Cancer Facts and Figures 2009-2010]. The impact this disease has on our society urges us to find

more effective drugs and drug combinations to cure patients and save lives. The heterogeneity of breast cancers contributes to the complexity of its management.

The combination of farnesyl transferase inhibitors (FTIs) and microtubule targeting drugs was synergistic when evaluated in a number of tumors including breast cancers [O'Regan and Khuri 2004, Nielson et al 2000]. FTIs were evaluated with taxanes that are microtubule stabilizing agents. It is believed that the synergism of this combination results from FTI stabilizing microtubule thus augmenting the effect of taxanes [Hussein and Taylor 2000, Sudakin and Yen 2007].

In our study we evaluated the combination of the FTI, Manumycin A (MA), and a microtubule destabilizing agent, Mebendazole (Mbz), in wild type MCF-7 and MDA-MB-231 breast cancer cell lines, which combined account for the characteristics of 70% of breast cancers [Charafe-Jauffret et al 2006]. Due to the aggressiveness of tumors expressing HER2 receptor, we also evaluated our combination treatment in the HER2 transfected cells MCF-7/Her18 and MDA-MB-231/ErbB2.

CHAPTER- 2 - LITERATURE REVIEW:

2-A-Breast cancer:

2-A-1-Breast cancer statistics:

According to the American Cancer Society, breast cancer is expected to account for 207,000 new cancer cases and more than 40,000 cancer deaths in the year 2010. It accounts for one in four cancer diagnosis in women in the United States and is the second largest cause of cancer deaths in women after lung cancer. Women diagnosed with this disease are mothers, sisters, daughters, teachers, colleagues and best friends. Their diagnosis and struggle leaves a scar not only on their bodies but also in the hearts of their beloved. Over the past decade, significant progress was made in understanding and managing breast cancer. Yet, despite increasing awareness and early detection of this disease death rates are still high, and many questions regarding the optimal treatment for this disease remain unanswered.

2-A-2-Breast cancer cell lines:

The term breast cancer defines a group of heterogeneous cancers that affect breast tissue. Based on microarray gene classification, breast cancers are divided into five subtypes; luminal A, luminal B, normal breast-like, human epidermal growth factor receptor 2, and basal like breast cancers [Hastak et al, 2010].

Molecular heterogeneity of breast cancer renders its treatment very complex. Treatment is effective only in 70% of cases. Based on the large scale gene and protein expression, breast cancer is classified into subtypes with different prognostic basis. Charafe_Jauffret et al profiled the genes of 31 breast cancer cell lines available for research. They divided breast cancer cells into two groups. Group I comprised of ductal carcinoma cell lines and are mainly ER-positive. Group II included mesenchymal like adenocarcinoma and ductal carcinoma breast cancer cells [Charafe_Jauffret et al, 2006].

Histopathology, estrogen and progesterone receptor status, and HER2 expression are some of the characteristics that help determine the choice of chemotherapy in breast cancer [Wiechec and Hansen, 2009]. Fifty to sixty percent of all breast tumors are estrogen receptor (ER) and progesterone receptor (PR) positive, while 15-25% of breast tumors are ER and PR negative [Lacroix and Leclercq, 2004]. Fifteen to thirty percent of breast carcinomas over-express human epidermal growth factor-2 proto-oncogene, also referred to as HER-2 or ErbB2. When translated, HER-2 gene gives the transmembrane tyrosine kinase receptor ($p185^{HER\text{-}2/neu}$). The $p185^{HER\text{-}2/neu}$ over-expression is associated with both poor prognosis and resistance to taxane derivatives [Hortobagy et al, 1996].

A large number of breast cancer cell lines are available for research. Most of the available cells were obtained from metastatic sites, mainly from plural effusion. Two thirds of all breast cancer research was done using three cell lines MCF-7, MDA-MB-231 and T-47D [Lacroix and Leclercq, 2004].

2-A-2a- MDA-MB-231 breast cancer cell line:

MDA-MB-231 cells are mesenchymal-like adenocarcinoma cells lacking ER, PR and HER-2 receptors. They are highly invasive in mouse models [Lacroix and Leclercq, 2004. Lostumbo et al, 2006] and over-express EGFR [Lostumbo et al, 2006]. Breast tumors that test negative for ER, PR and HER2 receptors are referred to as triple negative breast cancers. Triple-negative breast cancers lack therapeutic targets and are managed with conventional chemotherapy. Recently researchers are investigating the role of IGR-1R (insulin-like growth factor) in these tumors. They affect younger patients (<50 years), are more prevalent in African-American women, often present as invassive cancers, and are highly chemosensitive initially, but have a high tendency to reoccur, they are significantly more aggressive than tumors pertaining to other molecular subgroups [Bouchalova et al, 2009].

2-A-2b- MCF-7 breast cancer cell line:

MCF-7 cells were derived in 1973 and are by far the most commonly used breast cancer cells worldwide [Burdall et al, 2003]. They are luminal epithelial like cells that express ER and PR but lack HER-2 receptors. MCF-7 cells are weakly invasive in mouse

models [Lacroix and Leclercq, 2004. Lostumbo et al, 2006]. These cells do not show any EGFR over-expression [Lostumbo et al].

Despite identical morphological appearance of MCF-7 cells obtained from different laboratories, variation in cell growth rate,hormone receptor content and sensitivity to estrogen was detected [Burdall et al].

Numerous research was done on MCF-7 and MDA-MB-231cells only to show that they react differently to chemotherapy. Guisado et al studied the effect of resveratrol, a naturally occurring antifungal, on MDA-MB-231 and MCF-7 cells. MDA-MB- 231 died by non apoptotic process and MCF-7 underwent apoptosis, proving that target cell characteristics influence therapeutic outcome greatly [Guisado et al, 2002]. Wilson et al used MDA-MB-231 and MCF-7 breast cancer cells to study the effect of HER2 on TGF-β. HER-2 over-expression decreased TGF-β mediated gene response in MCF-7 cells, and promoted aggressive behavior in MDA-MB-231 cells by synergizing with TGF-β and increasing EMT. So in conclusion HER-2 abrogated the effect of TGF-β in MCF-7 but not in MDA-MB-231 due to the genetic differences between the two cell lines [Wilson et al].

EMT, epithelial to mesenchymal transition, is a fundamental process in the development and shaping of embryos. EMT is defined as a morphological conversion occurring at specific sites in embryonic epithelia to give rise to individual migratory cells that are needed for neural and cardiac development at the embryonic stage. EMT is also

important in the development of mammary glands. The role of EMT is to help tumor cells overcome the physical constraints of the primary tumor to detach and invade vasculature and surrounding tissue [Salomon and Thiery, 2003]. Epithelial cells have a rigid cytoskeletal network that restricts its motility. The transition to mesenchymal cells gives elongated cells with front-to-back polarized morphology that is less rigid and more suitable for cell migration. Microtentacles are microtubule based membrane protrusions that exhibit mesenchymal phenotypes and are linked to EMT. They were identified in breast cancer cells. Microtentacles are important for endothelial cell layers penetration and adhesion to vascular endothelium, a process prevented by microtubule destabilizing drugs [Whipple et al. 2010]. The claim that Mebendazole inhibits metastasis can be supported by their microtubule destabilizing activity that can influence the formation of microtentacles.

2-A-3- The epidermal growth factor receptor (HER-2 or erbB2):

The epidermal growth factor receptor, HER-2 or erbB2, is a member of the type I receptor tyrosine kinase family. HER-2 is over-expressed in different types of tumors especially breast and ovarian cancer. It is amplified in 15-30% of human breast cancers. Its amplification was linked to poor prognosis [Wilson et al]. The over-expression of HER-2 enhances cell mitogenesis and facilitates metastasis. It affects cell adhesion proteins such as catenins and E-cadherin [Martinez-Lacaci et al, 1999].

There are four closely related ErbB receptors (ErbB1/EGFR, ErbB2/Her-2/Neu, ErbB3 and ErbB4) that form hetero- or homodimers. ErbB receptor signaling can increase cell proliferation, decrease apoptosis and affect the survival and motility of primary and metastatic breast cancer cells. ErbB2 action also enhances signaling interactions with the cellular micro-environment and affects cell adhesion [Whyte et al, 2009].

Signaling through HER-2 receptor is mediated mainly through the ras/raf/MEK/ MAPK cascade. First HER-2 activates raf, a step that requires ras localization to the plasma membrane and raf kinase activation. Activated raf triggers the MAP cascade starting with the phosphorylation of MEK then MAPK. MAPK phosphorylates the nuclear transcription factor c-myc. This cascade is important for cell proliferation [Martinez-Lacaci et al, 1999]. Activation of ERK1/ 2 and PI3K-AKT signaling by ErbB receptors was also detected [Whyte et al, 2009].

Today HER-2 is a successful target for the monoclonal antibody trastuzumab (Herceptin) and the tyrosine kinase inhibitor lapatinib. Trastuzumab is used as a neoadjuvant treatment in patients with HER-2 positive breast tumors [Manabu et al, 2005]. The response rate to trastuzumab in matastatic HER-2 positive breast cancer is 17-35% [Freudenberg et al, 2009]. Trastuzumab cardiotoxicity makes it a choice only in patients whose clinical benefit out-weigh the risky side effects [Gruver etal, 2010]. Thus we aim at evaluating the combination of a farnesyl transferase inhibitor and an antimicrotubule agent in wild type and HER-2 transfected cells, as there is an increasing

demand for anticancer drugs that are effective in HER-2 positive tumors due to their aggressiveness.

2-B-1- Cell cycle and cell death mechanisms:

2-B-1a- Cell cycle:

The eukaryotic cell cycle is divided into four stages; G1, S, G2 and M phase. During G1 the cell integrates growth inhibitory and mitogenic signals and either proceeds towards S phase or exit the cell cycle. S phase stands for synthesis and is the stage during which DNA is synthesized. G2 is a gap that allows the cell to prepare for transition between S and M phases. The M phase is where mitosis happens, it starts with chromosome segregation into two nuclei and ends with the formation of two daughter cells [Johnson and Walker, 1999].

The cell cycle is regulated by a number of regulatory subunits called cyclins. At least 16 mammalian cyclins have been identified to date. Cyclin A functions in the S phase entry and transition, cyclins B1 and B2 are essential for G2 exit and mitosis. Cyclins C and D are important for transition from G0 (dormant cell) to S phase. Cyclin E controls the G1 to S phase transition. Cyclins execute their action after binding to cyclin-dependent kinases (cdk), binding induces a series of phosphorylations essential for cell division. Cyclin E is induced as the cell proceeds towards the S phase, it binds to cdk2 to facilitate the transition from G1 to S phase. Cyclins B1 and B2 and cdk1 are M phase

regulators. Cyclin B must be degraded for the cell to exit mitosis, thus accumulation of cyclin B delays the mitotic exit [Johnson and Walker, 1999].

Cell cycle checkpoints detect any defects during cell cycle progression. The gene p53 is an important checkpoint regulator that prevents the cell from progressing when DNA damage is detected. This gene is frequently mutated in human cancers. MDA-MB-231 breast cancer cells have a mutant p53 gene while MCF-7 cells do not [Johnson and Walker, 1999].

2-B-1b- Cell Death:

Cell death induced by anticancer treatment is classified into programmed and non programmed cell death. Programmed cell death is classified into type I (apoptosis) and type II (autophagy).Non-programmed cell death is also known as type III (necrosis) [Kim et al, 2006].

Apoptosis is a nontoxic model of cell death that is needed for development, homeostasis, aging, and as a defense mechanism [Hotchkiss et al, 2009]. It can affect single cells without producing inflammatory response in the surrounding tissue [Kim et al, 2006]. Apoptotic cell death is induced either via intrinsic (through the mitochondrial pathway) or extrinsic (through the death receptor) stimuli [Hotchkiss et al, 2009]. A number of enzymes called caspases control apoptotic death. Caspase 8 and caspase 9 regulate the extrinsic and intrinsic pathways, respectively. Upon their activation they

trigger caspases 3, 6 and 7 and induce their protease activity, this leads to cleavage of number of proteins including PARP and commits the cell to apoptotic death.

Autophagy is important for homeostasis. Today, the term autophagy is not used to describe cell death but to refer to a process that help the cell utilize its own resources when stimulated by nutrient starvation. Autophagy is continuously occurring at low levels and does not lead to cell death unless the nutritional starvation is prolonged this is refered to as autophagic cell death [Kim et al, 2006]. Bcl-2 proteins are essential in regulating the crosstalk between apoptosis and autophagy [Hotchkiss et al, 2009].

Necrosis is a non-programmed cell death triggered by acute hypoxia or ischemic injury. Reactive oxygen species, PARP and calcium ions all play a role in controlling necrosis. The main difference between necrosis and apoptosis is the role of the plasma membrane. In apoptosis the plasma membrane stays intact until later stages, whle it losses its integrity early in necrosis, allowing the influx of extacellular ions and fluids [Hotchkiss et al, 2009]. This criterion is utilized in apoptosis detection by flow cytometry, as cells are stained with annexin V that detects apoptosis and propedium iodide that detects late apoptosis and necrosis based on the integrity of the plasma cell membrane.

The cell cycle stage determines which cell death pathway will be activated [Hotchkiss et al, 2009].

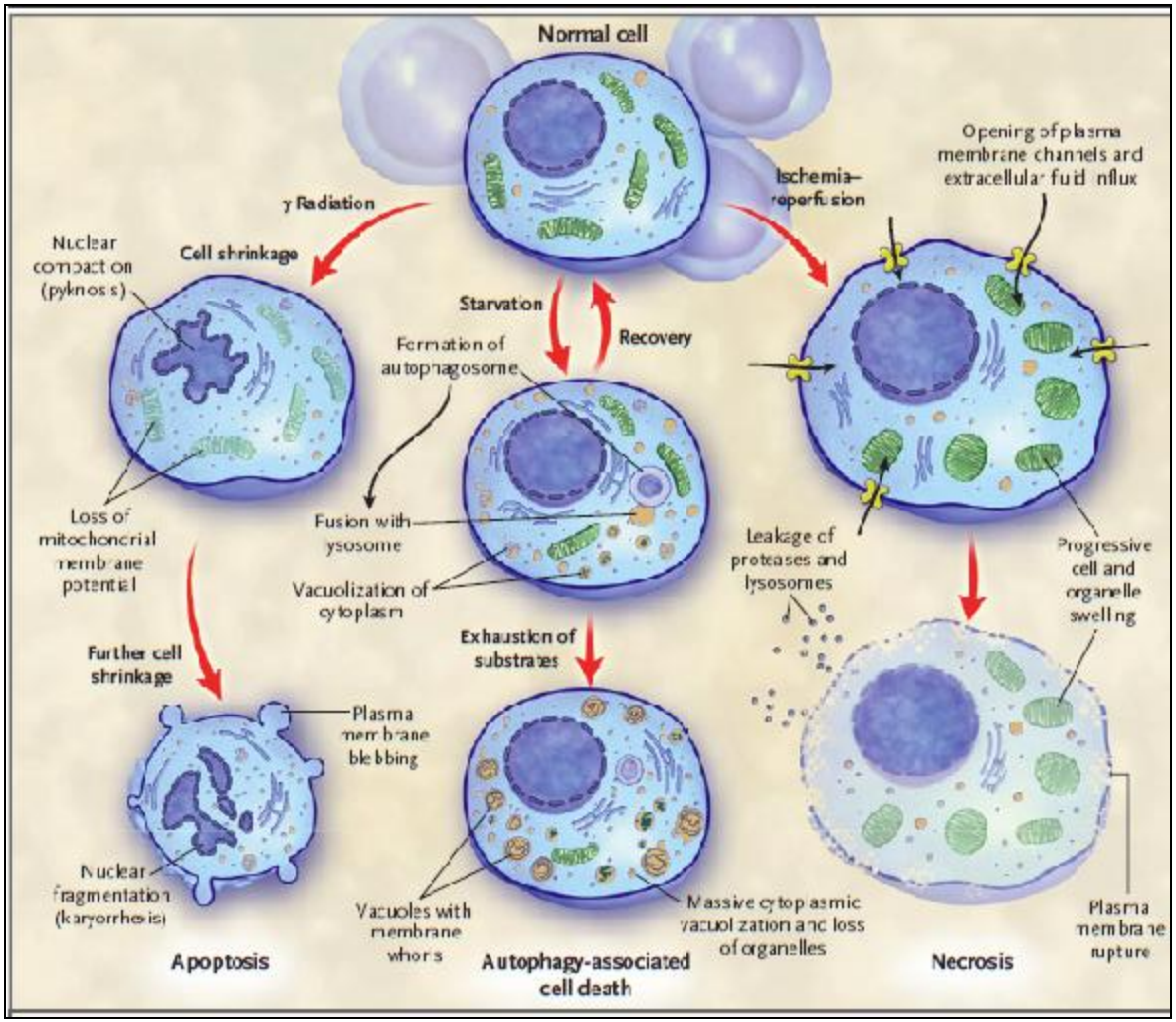

Figure 2-1- the three pathways of cell death- apoptosis, autophagy and necrosis. Figure obtained from Hotchkiss et al. Mechanisms of disease; cell death. The New England Journal of Medicine, 2009. Vol 361 page 1572.

Poly (ADP-ribose) polymerase (PARP) is an abundant nuclear protein that is activated when DNA is damaged. Chemotherapeutic agents cause single strand DNA damage and activate the PARP pathway [Annunziata and O'Shaughnessy, 2010].

Shah et al reported different patterns of PARP cleavage in HL-60 polymyelocytic leukemia cells. HL-60 cells were treated with etoposide or cytochalasin B to induce apoptosis or necrosis, respectively. Treatment with etoposide exhibited a stable band of PARP at 89kDa that underwent further cleaving to give a band at 47kDa after 24 hours of treatment indicating the occurrence of secondary necrosis. Cytochalasin B led to a cleavage pattern that is different from the apoptotic degradation. A major band was detected at 50kDa along with two minor fragments at 40 and 35 kDa [Shah et al; 1996]. These necrosis specific bands were detected at time points between 10 and 24 hours. Normal catabolic turnover of PARP gives minor bands at 32, 64 and 80 kDa [Shah et al; 1997]. A second pattern of PARP cleavage observed in apoptotic cells gives two bands, one at 64 kDa and one at 55 kDa. This PARP cleavage is mediated by granzyme B rather than Caspase-3,and occurs very early in apoptosis [Shah et al; 1997] PARP cleavage is a sensitive marker for cell death. Detection of PARP cleavage using western blotting is a very sensitive assay for apoptosis. It detects cell death very early and it can even detect apoptotic cell death occurring in a minor population of cells. When the 89kDa fragment

is detected, this is an indication of apoptotic cell death, and signifies the activation of caspase-3 [Shah et al; 1997].

2-C- Chemotherapeutic agents:

2-C-1a- Farnesyl Transferase Inhibitors:

Around 30% of all human cancers possess constitutively active ras onchogenes. Ras proteins are GTP-binding proteins that act as transducers of growth proliferative signals. Localization of ras to the inner surface of the cell membrane is essential for the function. A number of post translational modifications are required for this localization, starting with the addition of a farnesyl group to the cysteine in the CAAX moiety (where C refers to the cysteine) at the carboxy terminus of the protein via the enzyme farnesyl transferase (FT). The AAX part is then cleaved and the farnesylated cysteine is carboxymethylated and a palmitate residue is attached to facilitate ras attachment to the cell membrane [O'Regan and Khuri, 2004]. Farnesyl transferase inhibitors (FTIs) were developed to block FT and prevent the activation of ras [Barrington et al, 1998]. FTIs are divided into peptidomimetics that resemble the CAAX moiety, farnesyl phosphate (FPP) analogues and bi-substrate inhibitors that combine both properties [Servais et al, 1998, Mazierel et al, 2004].

Studies showed that FTIs are effective even in tumor cells lacking mutated ras. The fact that more than 20 mammalian proteins are farnesylated implies that the

mechanism of FTIs might be complex involving a number of target proteins. Among the proposed targets are RhoB, phosphatases PRl-1, 2 and 3, and the centromeric proteins CENP-E and CENP-F [Brunner et al, 2003]. So far, evidence of both cell cycle control and increased apoptosis was found with the use of FTIs. The mechanism of tumor regression depends on the genetic alterations present in the tumor [Suzuki et al, 1998]. Mazierel et al evaluated the FTI R115777 and reported that it produced an antiproliferative response in pancreatic cancer, an apoptotic response in melanoma, and an anti-angiogenic response in colon cancer [Mazierel et al, 2004]. FTIs modulate the cell cycle in human tumor cell lines leading to cell accumulation either in G0/G1 or G2/M phase. The G0/G1 blockade was correlated with p53 [Sebti S, 2003 and Mazierel et al, 2004]. FTase interacts with HDAC6 indirectly as they both bind to microtubules where the activity of FTase is required for HDAC6 activity. The use of FTIs increased tubulin acetylation and microtubule stability by interfering with tubulin deacetylase HDAC6 activity [Zhou et al, 2009]. This could be one way that FTIs interfere with cell cycle. Since breast cancer showed aberrant signaling through ras signal transduction pathways, ras became a new target in breast cancer treatment. The preclinical evaluation of FTIs in breast cancer models is promising [O'Regan et al, 2004]. Phase II studies favor the use of FTIs in glioma, leukemia and breast cancer [Mazierel et al, 2004].

Phase II studies revealed a lack of durable response with FTIs as single agents. Due to their distinct activity and mild cytotoxic effects, FTIs are very attractive adjuvant anticancer agents. FTIs were combined with a number of chemotherapeutic agents in

vitro and showed additive effects only. The only combination that showed synergism was that of FTIs combined with paclitaxel or epothilones [O'Regan and Khuri, 2004]. Moasser et al showed that a lower degree of synergism was observed in MCF-7 and MDA-MB-231 breast cancer cell lines with FTIs and taxanes.

Nielson et al. evaluated the combination of an orally available FTI, SCH66336, and taxanes; paclitaxel or docetaxel. The combination was synergistic in a number of lung, pancreatic, ovarian, and breast cancer cell lines in vitro. The two breast cancer cell lines; MDA-MB-231 and MDA-MB-468 were among the studied cell lines. When combined to paclitaxel, SCH66336 showed synergism with MDA-MB-468 and antagonism with MDA-MB-231, while the SCH 66336/ docetaxel combination showed synergism with MDA-MB-468 and an additive effect with MDA-MB-231 cells. In vivo single agent SCH66336 inhibited NCI-H460 xerografts growth by 52% and by 86% when combined to paclitaxel. [Nielsen et al, 2000].

2-C-1b-Manumycin A:

Manumycin A (MA), a naturally occurring product of the *Streptomyces parvulus* species, is a FTI active in both cell culture and nude mice xenographts. MA is a FPP analogue and competes for the enzyme FTase [Yeung et al, 2000].

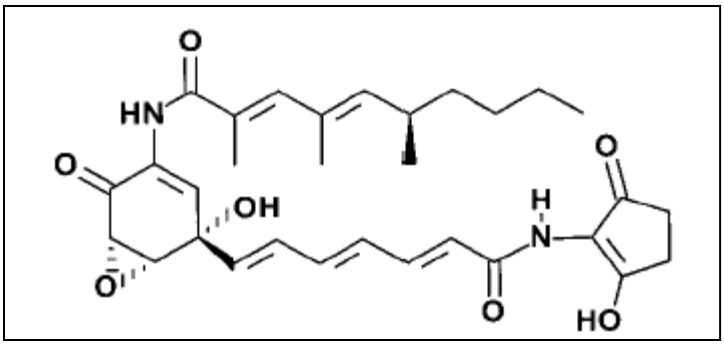

Figure 2-2: molecular structure of Manumycin A

Wang and Macaulay reported concentration dependent cell changes with MA treatment. At concentrations above 10 uM cells became rounded and detached from flask and an apoptotic peak was observed at about 12hr in all cell lines. They also reported that inhibition of ras farnesylation is maximum at 10 uM, and that apoptosis increases with increased concentration. No effect on cell cycle was observed in medulloblastoma with MA treatment [Wang and Macaulay, 1999].

Servais et al reported that in vitro experiments done on NIH3T3 cells showed that 10 ug/ml MA arrested cell growth. In vivo 6.3 mg/kg MA significantly inhibited tumor growth of fibrosarcoma (HT 1080) cells in animals. Growth inhibition induced by MA was rapidly reversed upon removal of the drug, indicating that its effect is mainly cytostatic. Another drawback was the decrease in host body weight at MA doses that induced tumor regression, this is an indication of toxicity [Servais et al, 1998]. Yeung et al compared sustained release MA to i.p. solution and showed improved antineoplastic effect with sustained release at lower cumulative doses [Xu et al, 2001].

The effect of MA on tumor cells is not restricted to FTase inhibition but is far more diverse. We will briefly review MA effects reported in literature. Yeung et al reported that MA induces the generation of reactive oxygen species (ROS), which mediate DNA damage leading to the formation of double stranded DNA breaks. DNA breaks stimulate apoptosis via a RhoB mediating pathway [Yeung et al, 2005]. She et al reported an increase in intracellular nitric oxide (NO) in KAT-4 cells treated with 54 uM MA that activated apoptosis via the intrinsic pathway. This increase was a result of GSH depletion [She et al, 2006]. Cancer cells can shift between autophagy and apoptosis once the cell is committed to die, recently reports showed that MA induced autophagy in human pancreatic cancer (Panc-1) and osteosarcoma (U2OS) cells. This effect was mediated through the PI3K/ Akt/ mammalian target of rapamycin (mTOR) pathway. mTOR negatively control autophagy. FTIs inhibit mTOR signaling, thus enhancing autophagy [Pan et al 2008]. Recently it was shown that manumycin induced ROS in glioma cells and led to apoptosis. The increase in ROS was accompanied with a decrease in signal transducer and activator of transcription 3 (STAT3) phosphorylation. STAT3 links extracellular signals to transcriptional control of proliferation and cell cycle progression. The decrease in its phosphorylation impairs its ability to promote cell survival [Dixit et al, 2009].

As with other FTIs, MA was evaluated in combination with other drugs. The combination with taxanes is by far the most commonly studied combination. Yeung et al used manumycin (54 uM) and paclitaxel (22 uM) either alone or in combination to treat

the anaplastic thyroid carcinoma ARO cells in vitro. This combination was compared to that of manumycin (54 um) and docetaxel (10 uM). Manumycin plus paclitaxel led to PARP cleavage into an 89kDa and 24kDa fragments that is characteristic of apoptosis. Manumycin alone or in combination with docetaxel showed a different pattern of PARP cleavage not characteristic of apoptosis. Both paclitaxel and docetaxel didn't have significant effect on PARP when used alone. In vivo, manumycin plus paclitaxel didn't show any additional benefit in ARO xerografts in nude mice but was superior to either agent alone in KAT-4 xerografts. Lack of synergism in vivo was attributed to ceiling effect [Yeung et al, 2000]. It is believed that the synergism of this combination elapses from an FTI induced microtubule stabilization, an effect that results from the influence of FTIs on the function of centromeric proteins. This effect is amplified in the presence of microtubule stabilizing drugs. Cenp-F is a cell-cycle regulated protein, its levels peak during G2/M phase and it is rapidly-degraded after mitosis. Cenp-F farnesylation is essential for its function and degradation. Manumycin A decreases Cenp-F farnesylation, decreasing its degradation leading to G2/M delay [Hussein and Taylor 2002, Sudakin and Yen 2007]. Our lab evaluated the combination of MA and the topoisomerase I inhibitor CZ48 in NSCLC cell lines in vivo. When using 5mg/kg MA in combination with 4mg/kg CZ48 tumor growth rates were statistically lower than control and survival was statistically higher in combination treatment compared to control [Pfuma, 2009].

We aim at evaluating the combination of MA and Mebendazole (Mbz), an anti-microtubule, in breast cancer cell lines.

2-C-2a- Anti-microtubules:

Microtubules are long cylindrical protein polymers composed of alpha and beta tubulin heterodimers. They are the major components of cell cytoskeleton and are involved in cell division, signaling, migration, transport and maintaining cell shape [Bhattacharya et al 2008, Zhou et al 2005 AND Jordan M A 2002]. Their role in cell survival made microtubules a very attractive target for anti-neoplastic agents.

Microtubule-targeted agents can be broadly divided into polymerization inhibitors (microtubule destabilizing agents) and polymerization promoters (microtubule stabilizing agents) [Bhattacharya et al, Zhou et al]. Taxanes are known to promote polymerization while colchicine and vinca alkaloids inhibit it. Different binding sites for taxanes, colchicine and vinca alkaloids had been characterized. Taxol and vinblastine bind to beta-tubulin and colchicine binds at the interphase of alpha and beta tubulin. Colchicine binds to microtubules leading to their dissociation to tubulin dimmers [Bhattacharya et al]. Aty high concentrations, colchicine depolymerizes microtubules, while at low concentrations it arrests their growth [Bhattacharya et al, Zhou et al].Cells in different stages of mitosis showed different sensitivity to colchicine. Cells in prophase are more sensitive to colchicine at low concentrations while cells at metaphase are only blocked when exposed to high concentrations of colchicine. A colchicine concentration of 50nM blocks all mitotic cells [Bhattacharya et al]. Mebendazole is a microtubule depolymerizing agent that is known to bind to the colchicine binding site and to destabilize microitubules.

Microtubule targeting agents have been used in the treatment of leukemia, lymphoma and solid tumors since the 1960s. Neurotoxicity is the main toxicity of microtubule targeting agents, an effect that is attributed in part to the inhibition of axonal transport by disrupting axonal microtubules [Huff et al].

Taxanes (paclitaxel and docetaxel) are widely used in breast cancer treatment. In HER-2 positive tumors, the addition of paclitaxel showed significant improvement in the five year survival regardless of the ER status. Paclitaxel is highly hydrophobic, it is administered in solution with alcohol and purified polyoxyethylated castor oil to aid in delivery. Hypersensitivity to polyoxyethylated castor oil may occur necessitating the premedication with dexamethasone. Resistance to taxanes triggered the search for other microtubule targeting agents for the treatment of cancer [Pusztai L 2007].

2-C-2b- Mebendazole:

Introduced by Brugmans and collaborates in 1971, Mebendazole (Mbz) (methyl 5-benzoyl-2-benzimidazole-carbamate) is a prototype benzimidazole carbamate that was initially used for the treatment of intestinal roundworms infections. Mbz exerts its anti-helmintic activity primarily by binding to β-tubulin, and inhibiting microtubule polymerization. Mbz binds to helmintic β-tubulin at a higher affinity than mammalian β-tubulin. Thus, it has a selective toxicity and exhibits low adverse effects in humans

[Goodman and Gilman]. Mbz is rapidly metabolized to less toxic metabolites by the liver; this could be another reason for its low toxicity. Yet, prolonged use of high doses led to liver failure, anemia, weight loss and deaths when Mbz was given orally to Wistar rats at a dose of 151.6mg/kg daily for 13 weeks [EMEA Mabendazole summary report 1999 and 2001, Dayan AD 2003]. Acute oral toxicity of Mbz was investigated in Wistar rats and rabbits. The oral LD50 is higher in male compared to female Wistar rats at 1434 mg/kg and 714mg/kg, respectively [EMEA Mabendazole summary report 1999 and 2001].

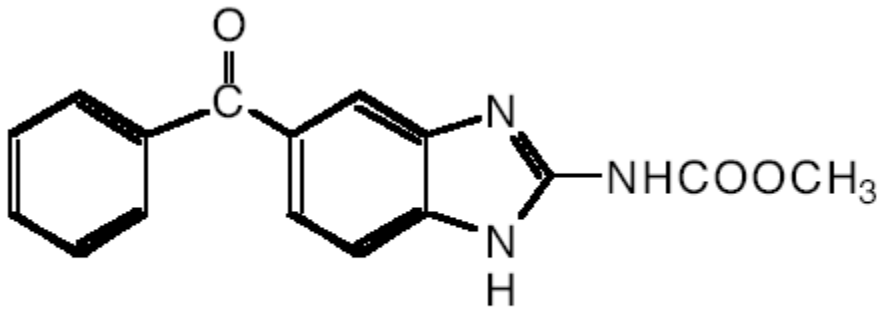

Figure 2-3: The molecular structure of Mebendazole.

It was not until the year 2002 that the anti-tumor activity of Mbz was unveiled. Mukhopadhyay et al. reported that Mbz induce a dose and time-dependent apoptosis in human lung cancer cell-lines. This effect is preceded by a G2/M phase arrest. An anti-angiogenetic effect was also detected both in vitro and in vivo. Mbz's growth inhibitory effect was also observed in breast, ovarian and colon cancers and osteosarcoma. Yet, no

cytotoxic effect was observed when Mbz was used with normal WI38 fibroblasts. Researchers speculated a defect in at least one mitotic checkpoint function in tumor cells leading to their higher sensitivity to mbz. In vivo, Mbz inhibited the growth of H460 NSCLC xenografts when administered orally at a dose of 1mg given once every other day for 4 weeks. No signs of toxicity were observed. Upon injecting human lung cancer cells A549 into the tail vein, Mbz treatment reduced the number of metastatic colonies in the lung by 80% compared to control. Histochemical staining revealed that colony size was also reduced following Mbz treatment [Mukhopadhyay et al, 2002].

Martarelli et al evaluated the effect of Mbz on human adrenocortical carcinoma cells (H295R) in vitro and in nude mice. Mbz inhibited the growth of cancer cells at concentrations of 1μM and higher, it did not have any effect on normal WI-38 fibroblasts even at high concentrations. Their final results indicate that Mbz induced apoptosis but did not affect angiogenesis. The authors suggest that Mbz is a microtubule inhibitor with pleiotropic effects. The in vitro dose response curve showed a decline in cell viability between 0.1 and 1 μM in H295R and SW-13 cells. Growth rate analysis of H295R xenographts in nude mice showed that Mbz was more effective during the initial phase of treatment, where tumor increment was minimal. In vitro studies using tumor spheroids are in agreement with this conclusion. Mbz affected the external layer of the tumor spheroids and took a couple of days to dissolve the entire tumor, while it rapidly killed the tumor cells in monolayer cell culture studies.[Martarelli et al, 2008].

In an effort to identify new anti-melanoma agents, Orlow et al screened 2000 small molecules including Mbz. Mbz inhibited cell growth and induced apoptosis in melanoma cells, but showed no effect on melanocytes. Mbz induced tubulin disruption mediating cellular response to Bcl-2 and apoptosis. Mbz altered tubulin structure both in melanocytes and melanoma cells, yet it only induced apoptosis in the malignant cells. Benzimidazole compounds are similar in structure to nucleotides, thus Mbz induced growth inhibition could be a result of its interaction with biomolecules in addition to microtubule disruption [Orlow et al, 2008].

Mbz was compared to paclitaxel in a metastatic model of A549 lung cancer cells. Mbz treatment significantly decreased the number of lung colonies compared to paclitaxel and showed lower toxicity [Sasaki et al, 2002]. It was noticed that Mbz's binding site is on the outside of the microtubule, which differ from that for paclitaxel and vinblastine, as they bind near the intradiamer interface, facing the lumen of the microtubule [Mukhopadhyay et al, 2002].

Cheung et al evaluated the combination of Mbz, Paclitaxel, docetaxel and iso-fludelone with recombinant methioninase (rMETase) in neuroblastoma cells in vitro. The combination of Mbz and rMETase was synergistic, with combination indices ranging from (0.37-0.6). Both microtubule stabilizing agents and depolymerizing agents were studied. In the 5NB cells tested, microtubule depolymerizing but not stabilizing agents were synergistic [Cheung et al, 2009].

2-D- Combination therapy in treating cancer:

2-D-1-Principals and rational behind combination therapy:

Current breast cancer treatment paradigms employ both classical and new chemotherapeutic agents. In vitro and in vivo studies are conducted to help evaluate the effects of the new agents and optimize the use of classical agents. Due to the increased resistance to single agent treatments evaluation of combination therapy is gaining more interest. Schedule-dependent synergism was observed with a number of combinations in clinical trials. Thus, both sequential and concurrent therapies should be evaluated with any new combination. Mathematical models for cancer treatment were suggested. Of the most interesting were Goldie, Coldman and colleagues, as well as Norton and colleagues. Goldie and Coldman et al. stated that "to avoid selection of doubly resistant mutants, multiple non-cross-resistant drugs should be used together rather than sequentially." On the other hand, Norton et al. recommended "individual drugs, not multiple drugs, should be given sequentially at their highest possible dose to treat cancers." Randomized trial on non-Hodgkin's and Hodgkin's lymphoma patients failed to prove Goldie and Coldman's model. Their model was overly simplified, not taking into consideration multidrug resistance [Norton et al, 1998]. Norton et al. conducted a clinical trial based on their model. Sequential cyclophosphamide, doxorubicin and paclitaxel were evaluated in women diagnosed with primary breast cancer with four or more positive lymph nodes.

Outstanding results were observed, with 80% 4-year disease free survival compared to 50% relapse rate at 4 years with the standard therapy of cyclophosphamide plus doxorubicin [Hudis et al, 1999]. The sequence of ecteinascidin 743 (ET-743) followed by doxorubicin is more effective than concomitant and the opposite sequence treatments in HT1080 and HT18 soft tissue sarcoma cells. When paclitaxel was administered before ET-743 the combination was synergistic, this effect disappeared upon concomitant and the reverse sequence administration [Takahashi et al, 2001].

The combination of gemcitabine and docetaxel was evaluated in vitro followed by clinical studies. In MCF-7 breast cancer and SAOS-2 osteosarcoma cells concomitant administration of the two drugs gave antagonistic effects in both cell lines, while sequential drug administration gave varying results depending on the cell line. Docetaxel first treatment was additive in MCF-7 cells and antagonistic in SAOS-2 cells, and the opposite sequence was synergistic in both cell lines, leaning more towards additivity in SAOS-2 cells. The combination was also evaluated in patients with bone and soft tissue sarcoma, but the authors did not come out with a conclusive observation and stated that more patients will be enrolled and evaluated [Leu et al, 2004]. Leu et al concluded from their studies and a review of other reports that the optimal sequence of drug administration is cell line specific and cannot be generalized for all tumors.

These results show that there is no one-size fits all approach in cancer treatment. Several elements should be taken into consideration including patient age, overall

performance, genetic disposition, comorbidity, tumor characteristics, and pharmacoeconomics [Chu E, 2008]. The effect of drug pharmacokinetics on the combination should also be considered. Drugs with very different half lives will have different interactions at different time points [Peters et al, 2000].

2-D-2- Ratiometric dosing and the synergy heat map:

2-D-2a- Ratiometric dosing:

Combinations of different drugs are usually used in treating cancer. Exposure of cancer cells to a combination of two anti-cancer drugs yields one of three outcomes; synergy, additivity, or antagonism. In the 1960s Frei and coworkers defined the bases for combination chemotherapy. Nowadays we do rely on Frei's fundamentals, yet our better understanding of cancer allows us to modify the different combinations optimizing their effect. There are three general principles in combination therapy; 1-combined drugs should have non overlapping toxicity and should be used at their maximal tolerated doses; 2- combined agents should have different mechanisms of action to prevent broad spectrum drug resistance; and 3- the full combination should be administered as early as possible in the disease.

The conventional wisdom that more is better is not always applicable in pharmacology. Increasing evidence reveals that certain ratios of two anticancer drugs can

be synergistic, while other ratios of the same drugs merely show additivity or can even be antagonistic. Taking this into consideration, some drug combinations utilizing the maximum tolerated dose of each drug might have failed, while it could have been very synergistic if the drugs were used at lower doses and different dose ratios [Mayer et al 2007]. This implies that after better understanding of ratio-dependant synergism one should revisit such combinations to determine the optimal ratio in vitro, and evaluate whether any synergism exists.

The phenomenon of drug ratio-dependent killing is based on the balance between pro-apoptotic and proliferating responses, which depends on the microenvironment and drug concentration; since many drugs have different pharmacological targets at different concentrations. Due to the dissimilarity of individual drug pharmacokinetics in vivo, achieving a constant drug1 to drug2 ratio is difficult unless the two drugs are pharmaceutically formulated to release the drugs at rates that maintain a constant drug-drug ratio at the tumor site.

Today drug ratio-dependent synergy is at its infancy and requires further in vivo investigation. Mayer et al found that a 5:1 molar ratio of cytarabin to daunorubicin is synergistic in vitro. They used leukemia bearing mice to test their drug ratio-dependent synergy theory, and were able to completely cure the mice using the 100 nm liposomes (CPX-351) to deliver these two drugs at this ratio and maintain the release for 24 hrs. CPX-351 was compared to an aqueous cocktail of the two drugs, which showed no long

term cure though higher doses were administered. A Phase I trial of 1:1 ratio irinotican to floxuridine showed significant anti tumor activity [Mayer et al, 2007].

Panllad et al treated glioma cells with concometant camptothecin and doxorubicin at molar ratio of 5:1 only to observe strong antagonism, when they used the drugs at a 1.5:1 ratio the combination was synergistic [Mayer et al, 2006].

Although drug-drug ratio antagonism is being recently perceived as a form of multidrug resistance [Harasym et al], little attention is paid to drug combinations yielding antagonistic effects. Drug combinations that showed synergy in vitro and antagonism in vivo should be revisited in term of ratiometric dosing taking into consideration drug pharmacokinetics.

2-D-2b- Synergy heat map:

Mayer et al studied the effect of ratiometric dosing of irinotecan and cisplatine on 20 tumor cell lines. The cells were treated with different molar drug ratios ranging from 1:64 to 64:1 irinotecan to cisplatine. Cell viability was evaluated, and the combination indices (CI) were calculated for each ratio at 80% cell killing (Fa=0.8). Data was presented in a heat map, see figure 1-4, where synergism was referred to by the color green, antagonism by red, and additivity by yellow. They referred to this presentation as the “Synergy heat map”. The irinotecan to cisplatine synergy heat map [Figure 2-4] showed two regions of synergy separated by a zone of antagonism between the ratios of

1:2 and 4:1 irinotecan to cisplatine. Information obtained from the synergy map was used to incorporate the two medications in liposomes that released them at a maintained ratio for 24hr, taking into consideration the different pharmacokinetic characters of the two drugs. The efficacy of the dual drug liposomes was evaluated in human xenografts tumor models against the free drug cocktail. The liposome formulation resulted in greater antitumor activity than the free drug cocktail. These results led to two ongoing clinical trials. The first uses floxuridine and irinotecan liposomes in colorectal patients, and the second uses cytarabine and daunorubicine liposomes in acute myeloid leukemia patients [Mayer et al, 2009].

We believe that the synergy heat map is a powerful tool that when combined with the pharmacokinetic and pharmacodynamic information will help determine in vivo dosing of drug combinations and will facilitate drug formulation into suitable dosage forms.

Cell lines screened	Tumor	CI at Fa = 0.8												
		1:64	1:32	1:16	1:8	1:4	1:2	1:1	2:1	4:1	8:1	16:1	32:1	64:1
LCC6	Breast	0.69	0.58	0.71	0.89	0.83	1.01	1.57	1.03	0.85	0.63	0.52	0.54	0.76
MCF-7	Breast	0.71	0.67	0.86	0.88	0.95	1.15	0.71	0.82	0.70	1.00	0.87	0.83	0.88
MB 231	Breast	1.02	1.01	0.90	0.90	0.70	0.87	1.54	1.34	0.90	1.10	0.76	1.40	0.61
HCT-116	Colon	0.38	0.36	0.37	0.33	0.62	0.84	1.50	1.73	9.40	0.71	0.76	0.82	1.06
Colon-26	Colon	1.22	1.67	1.40	1.16	1.00	1.21	1.04	1.38	1.10	1.03	1.31	1.25	0.82
HT-29	Colon	1.05	0.88	0.90	0.86	1.21	1.09	1.57	1.17	0.90	0.76	0.82	0.97	1.05
A549	Lung	0.67	0.61	0.67	0.56	0.44	0.39	0.44	1.65	1.31	0.49	0.37	0.41	0.49
H460	Lung	0.92	0.81	0.84	0.80	0.75	0.73	0.94	1.14	2.03	0.53	0.36	0.80	0.48
H322	Lung	0.47	0.52	0.68	0.96	0.57	1.28	1.24	0.95	0.73	0.54	0.44	0.52	0.54
H1299	Lung	1.07	1.08	1.12	1.09	0.76	0.98	3.01	2.57	1.83	0.65	0.64	1.49	0.82
H522	Lung	1.15	0.62	1.09	0.84	0.82	0.92	2.26	1.80	0.89	0.48	0.39	0.73	0.47
Ovcar-3	Ovarian	1.33	1.35	1.08	1.10	0.80	0.78	0.89	0.89	1.84	0.53	0.28	0.33	0.35
Ovcar-5	Ovarian	1.29	1.64	1.55	1.34	1.30	1.42	1.51	1.30	1.15	0.80	1.05	0.99	1.17
SK-OV-3	Ovarian	1.33	1.26	1.30	1.51	1.49	1.70	1.75	1.28	1.17	0.55	0.70	0.79	0.76
IGROV-1	Ovarian	1.16	1.16	1.16	1.00	0.95	0.95	1.23	1.20	1.16	0.77	0.78	0.71	0.75
A2780	Ovarian	0.93	0.94	0.81	0.75	0.80	0.81	0.87	0.70	0.81	0.81	1.20	1.03	1.25
Capan-1	Pancreatic	1.46	1.22	1.11	1.25	0.86	0.89	1.12	1.17	0.69	0.89	0.83	0.71	0.99
BXPC-3	Pancreatic	1.00	1.02	0.91	1.10	0.81	0.99	1.04	0.88	0.70	0.60	0.49	0.64	0.61
N87	Gastric	1.76	1.87	1.35	1.55	1.65	1.09	1.05	0.68	0.51	0.18	0.11	0.06	0.04
A253	H&N	0.85	0.84	0.81	0.92	0.76	0.63	0.79	0.78	0.86	0.83	0.90	0.82	0.84

NOTE: Irinotecan and cisplatin were simultaneously exposed to cells for 72 h at indicated molar ratios, and the dose-response curve for each cell line was determined by an MTT cytotoxicity assay. The dose-response curves were subsequently evaluated by the Chou and Talalay median-effect method to calculate the CI at ED_{80} (Fa = 0.8) and summarized in a heat map. Two areas of synergy are observed at <1:2 and >4:1 irinotecan/cisplatin ratios. Green indicates synergy (CI < 1); yellow indicates additivity (CI ~ 1); and red indicates antagonism (CI > 1). Results reflect compiled results from multiple experiments.

Figure 2-4 - Synergy heat map of irinotecan and cisplatine. Mayer et al. Moleculr Cancer Therapy 2009; 8 (8): 2268

CHAPTER- 3- OBJECTIVE AND SPECIFIC AIMS

3- A-Hypothesis:

We hypothesize that:

- A potential synergistic effect is obtained with the combination treatment of the farnesyl transferase inhibitor, MA, and the microtubule destabilizing agent, Mbz, compared to treatment with single agents MA or Mbz in wild type and HER2 transfected MDA-MB-231 and MCF-7 breast cancer cell-lines.
- The sequence of drug administration is a significant factor in combination therapy with MA and Mbz.
- The improvement in cytotoxicity with combination treatment is a result of both cell cycle arrest and apoptosis enhancement.
- The effect observed in cell culture will be correlated to that in tumor-xenograft nude mice.

3- B-Objectives:

The objectives of the project are:

To determine the single agent sensitivity for MA and Mbz in wild type and HER2 transfected breast cancer cell-lines: MDA-MB-231, MDA-MB-231/ErbB2, MCF-7 and MCF-7/Her18. The additive and/or synergistic nature of the combination treatment of

MA and Mbz will be characterized in the four breast cancer cell lines. We aim at determining whether the sequential administration of MA and Mbz will enhance the treatment responses compared to concurrent therapy. The role of cell cycle arrest and apoptosis in cell killing using the combination of MA and Mbz will be elucidated. We will also investigate whether the different cell-lines respond in the same way or differently to combination therapy. Finally, the in-vitro/ in-vivo correlation will be determined using tumor-xenografted nu/nu nude homozygous Swiss background mouse model.

3- C- Specific Aims:

The overall project includes the following studies, each presenting one of the specific aims:

3- C-1- To determine synergism/additivity of combined treatment in MDA-MB-231, MDA-MB-231/ErbB2, MCF-7 and MCF-7/Her18 breast cancer cell lines:

3- C-1a- Determine the dose-response curves for single agents MA and Mbz in each of the four cell-lines:

The sensitivity of each of the four breast cancer cell lines to individual agents, MA and Mbz, is to be established by constructing the dose-response curves. The IC_{25} and IC_{50} of

each agent in each cell-line will be derived from the dose-response curve. The percent viability will be determined using the XTT colorimetric assay.

3- C-1b- To evaluate the combination treatment with MA and Mbz in all four cell-lines:

MA and Mbz will be used concomitantly or in sequence (MA→Mbz, Mbz→ MA) in all four cell-lines. The percent viability will be determined in all cases to determine the additivity, synergism or antagonism of the combinations. The effect will be correlated with cell types and HER2 expression status. The effect of combination and sequential treatment will be evaluated using CalcuSyn® software. The combination index (CI) will be calculated based on the percent cell survival at varying doses of the treatment both alone and in combination. CI> 1 indicates antagonism, CI< 1 indicates synergism and a CI= 1 indicates additive effect.

3- C-2- To determine the role of cell cycle arrest and apoptosis in the cytotoxicity of combined MA and Mbz treatments in the four breast cancer cell lines:

The flow cytometry technique will be used to detect the extent to which cell cycle arrest and apoptosis occur in the previous treatment groups for all cell-lines. To better understand the effect of cell cycle arrest in cell killing, we will assay the change in the

levels of cyclin E and cyclin B using western blotting. To better understand the role of apoptosis we will detect the levels of cleaved PARP using western blotting.

3- C- 3-To determine the in vivo effect of MA and Mbz treatment using wild type and HER-2 transfected MDA-MB-231 breast cancer xenografts in nu/nu Swiss background nude mice:

The in vivo safety and combined anti-neoplastic effect with will be evaluated in nu/nu nude homozygous Swiss background mouse model.

3-C- 3a- Dose efficacy study of single agent treatment with MA and Mbz:

To determine the dose for dose efficacy study and evaluate single agent toxicity of MA and Mbz in nu/nu Swiss Background athymic mice.

3- C- 3b- Efficacy study of the combination treatment of MA and Mbz:

To determine if the combination of MA and Mbz is synergistic, additive or antagonistic in vivo taking into account the sequence of drug administration.

CHAPTER- 4- MATERIALS AND METHODS

4- A- Materials:

4- A- 1-Chemicals:

Acetic acid Glacial was purchased from EMD Chemicals (Cat # B10001-78) and used for SRB assay experiments.

Acetonitrile HPLC grade was purchased from EMD Chemicals. Cat # and was used in HPLC assay to determine Mb2 concentration in microemulsion.

Annexin V- FITC from human placenta (0.16 gr/ml) was purchased from Sigma (Cat # 9210-10UG) and was used to detect apoptotic cells using flow cytometry.

Bromophenol blue stimulate was purchased from Sigma (Cat # B5525) and used to visualize the running samples during electrophoresis.

Captex 200 (mixed diesters of caprylic/capric acids on prop. glycol) was purchased from Abitec corporations and was used to make Mbz microemulsion.

Dimethylsulphoxide was purchased from Sigma (Cat # D2438) and was used as a solvent in tisuue culture and animal treatment.

DL-Dithio-DL-threitol was purchased from Fluka Analytical (Cat # 43819-5G) and was used in loading buffer in western blots.

Ethyl alcohol 200 proof, absolute, anhydrous, ACS/USP grade was purchased from University of Houston Research stores (Cat # 111000200) and was used as antiseptic in cell culture room (70%).

Glycerol was purchased from Sigma-Aldrich (Cat # G 7893) and was used in loading buffer for western blots.

Glycin was purchased from Sigma (Cat # G8898) used in running &transfer buffers for western blots.

Hydrocortisone was purchased from Sigma-aldrich (Cat # H4001-1G) and used as an internal standard for Mb2 HPLC assay.

Manumycin A was purchased from Alexis Biochemicals through Axxora, LLC. (Cat # ALX350-241-M010) and used in in cell culture and animal treatment.

Mebandazole was purchased from Sigma (Cat # M-2523) and used in cell culture and animal treatment.

Methanol –HPLC grade was purchased from EMD chemicals (Cat # M X 0475-1) and used for transfer buffer in western blots.

Phosphate buffered saline (1X) pH 7.4, was purchased from Gibco. (Cat # 10010-031) and used for tissue culture and in treatment protocols.

Polysorbate 80NF (TWEEN 80) was purchased from PCCA. (Cat # 9005-65-6) and used in Mb2 microemulsion.

Propidium iodide solution (1mg/ml) in H2O was purchased from Sigma. (Cat # P4864-10ml) and used to determine cell cycle in flow cytometry ecperiments.

Ribonuclease A solution from bovine pancreas was purchased from Sigma. (Cat # R4642) used in flow cytometry assay protocol.

Sodium chloride was purchased from Sigma. (Cat # S-9888) and used in buffer preparation for western.

Sodium dodeayl sulfate was purchased from Sigma (Cat # L 3771) and used in buffer preparation for western.

Sulforhodamine blue sodium salt was purchased from Sigma. (Cat # S1402-5G) and used for cellviability assay.

Transcutol HP (diethylene glycol monoethyl ether) was purchased from Gattefosse SAS. (Cat # 111-90-0) and used for Mb2 microemulsion.

Trichloroacetic acid (TCA) 3% w/v was purchased from Sigma. (Cat # L 420090-01-900ML) and used in SRB assay.

Tris base was purchased from Promega. (Cat # H 5131) and used in buffer preparation for SRB assay and western blots.

Tris-HCl was purchased from J.T. Baker. (Cat #4103-02) and used in western blots.

TWEEN 20 was purchased from Sigma life Science (Cat # P 9416-100ML) and used in TBS-T preparation.

4-A-2- Supplies:

4-A-2a- Cell Culture:

Dulbecco's modified Eagle's Medium (DMEM/F12 (1:1) + L-glutamine, 15mM HEPES) was purchased from Gibco (Cat # 11330-057) and used for cell culture experiments to feed the cells.

Dulbecco's modified Eagle's Medium (DMEM) with the nutrient mixture F-12 Ham with L- glutamine and 15mM HEPES was purchased from Sigma (Cat # D8900-10X1L) and used for feeding the cells used to inoculate the mice**.**

(D) (+) Glucose solution (10%) was purchased from Sigma (Cat # G8644) to supplement tissue culture media.

Geneticin (50 mg/ml) was purchased from Gibco (Cat # 10131027) to supplement tissue culture media for HER2 transfected cells.

Fetal Bovine Serum was purchased from Invitrogen (Cat # 10082147) **For cell culture experiments** to supplement tissue culture media**.**

Fetal Bovine Serum was purchased from Phenix Research Products (Cat # FBS-500US-U) **For cells inoculated into mice** to supplement tissue culture media**.**

Trypsin 0.5% EDTA was purchased from Invitrogen (Cat # 25300062) and used to harvest the cells in cell culture experiments.

Penicillin-Streptomycin antibiotic was purchased from Gibco (Cat # 10378-016) **For cell culture experiments**, used to supplement tissue culture media**.**

Penicillin 5mg/ml, Streptomycin 5mg/ml, Neomtcin 10mg/ml antibiotic mixture 100X was purchased from Gibco (Cat # 15640-055100ML) **For cells inoculated into mice** and used to supplement tissue culture media**.**

Cell culture flasks:

BD falcon canted neck 75cm^2 Cat # 353135.

Centrifuge tubes:

50ml disposable graduated conical sterile from VWR Cat # 89039-656

15ml disposable graduated conical sterile from VWR Cat # 89039-664

Pasteur pipets 9” from VWR Cat # 14673-043.

Petri dish, sterile, slipable VWR Cat # 25384-302.

Pipette tips (1-10ul, 10-100ul, and 100-1000ul) from VWR were used for measurements.

Polystyrene round bottom tubes (5ml) from BD Falcon Cat # 352054

Serological pipets:

25ml VWR serological pipets Cat # 53283-710.

10ml VWR serological pipets Cat # 53283-708.

Tissue culture plates:

Costar 96-well cell culture flat bottom plates Cat # 3595.

Corning 6-well flat bottom tissue culture treated plates Cat # 25810.

4- A-2b- Western Blots:

Anti-CyclinE1 clone HE12 mouse monoclonal IgG antibody was purchased from Upstate Cellsignalling Solutions (Cat. #05-363) and was used to detect cyclin E in western blots

Anti-CyclinB1 mouse monoclonal IgG antibody was purchased from Chemicon International (Cat. # MA B 3684) and was used to detect cyclin B in western blots.

Anti-Cleaved PARP mouse monoclonal antibody was purchased from CellSignaling Technology (Cat # 95465) and was used to detect for PARP in western blots.

Anti-beta actin mouse monoclonal antibody was purchased from abcam (Cat # ab6276-100) and was used to detect for B-actin in western blots.

Sheep anti mouse IgG horseradish peroxidase conjugated antibody was purchased from Chemicon International (Cat # AP 300P) and was used as the secondary antibody in western blots.

Pierce ECL western blotting Substrate was purchased from Pierce (Cat# 32209) and used to visualize the bands in western blots.

ChemiLucent Plus Western Blot Enhancement kit was purchased from Millipore and consisted of antibody binding buffer (20X), chemilucent plus reagent, and chemilucent plus blocking reagent (Cat # 2650) and was used to enhance the signal in western blots.

See Blue Plus 2 pre stained standard was purchased from Invitrogen (Cat # LC5925) and used as a molecular weight marker for western blots.

Bio Rad 7.5% Tris-gylcine precast gels were purchased from Bio Rad Laboratories, INC.(Cat # 161-1102) and were used in sample electrophoresis to separate the proteins in western blots.

Supnitrocell, 0.2, 15 x15 cm nitrocellulose blotting membranes were purchased from Bio Rad Laboratories, INC.(Cat # 162-0147) and used in western blots.

Bio Rad protein assay kit was purchased from Bio Rad Laboratories, INC.(Cat #500-0006) and used to determine protein content of samples used for western blots.

Bio Rad protein assay standard II bovine serum albumin was purchased from Bio Rad Laboratories, INC. (Cat #500-0007) and used in protein assay to generate the standard curve.

Bio-Rad blot paper (8.6x13.5) cm was purchased from Bio Rad Laboratories, INC. (Cat # 1703967) and used in transferring the gel in western blots.

Cell lysis buffer (10X) was purchased from Cell Signaling Technology (Cat # 9803) and was used to lyse cells before running the western blots.

4-A- 2c- Animal Experiments:

Alcohol wipes from Webcol alcohol preps used in animal experiments.

Mouse decapicone disposable mouse restrainers from Braintree Scientific INC (cat # MDC-200).

Needles 27gauge ½ inch and 30 gauge 1/2 inch from BD Cat # 5109

Syringes 1ml from BD Cat # 309602.

4- A-3- Apparatus:

ABC electronic degetal caliper used to measure tumor volumes in nude mice xenografts.

Accuri C6 Flowcytometer (room 312) used to annexin V-FITC experiments.

Alpha Innotech FluorChem 8900 (room 514) used to visualize western blots protein bands

Aqua Solutions water purification Pure and Simple^{TM} (room 526) used to obtain dd H2O

Balance; Mettler AE100 (digital 0.0001 grams sensitivity) (room 508) used to weigh all the chemicals

Bewckman Coulter plate reader DTX 880 multimode detector (room 514) used to read 96 well plates for XTT,SRB and Bio-Rad protein assay

Bewckman Coulter microcentrifuge 16.

Carl Zeiss, INC microscope (room 422) used for cell culture.

Centrifuge 5810R Eppendorf 15amp version (room422) used to centrifuge the cells in flow cytometry and western blot sample preparation.

Corning hot plate and stirrer used to stir cell buffers and microemulsion.

Drummond pipet-aid used tomeasure volumes for cell culture experiments.

Mini Trans-Blot electrophoratic transfer cell from Bio Rad used to transfer Tris- glycine gels to nitrocellulose membrane in western blots

Mini PROTEAN 3 cell from Bio Rad used to run samples on gels for electrophoresis.

Nuaire NU-5510 DHD autoflow CO2 air-jacketed incubator (room 422) used to incubate cells at 37°C and 5% CO2

Nuaire biological safety cabinet class II type A2 (room 422) used to perform cell culture experiments under aseptic conditions.

Thermo Electron corporation ALC centrifuge PK 110 (room 422) used to centrifuge cells.

Vortex 2 genie from Scientific Industries used for mixing.

VWR Waterbath and sonicator model 150D used for cell culture and microemulsion preparation (sonicate Mb2- DMSO mixture)

4-A- 4-Software:

AlphaEase FC 8900 for windows used in the Alpha Innotech FluorChem 8900 western blot band detector.

CFlow Plus for the Accuri C6 flowcytometer.

Multimode detection software for Bewckman coulter plate reader.

CalcuSyn Biosoft software was used for CI calculations to determine synergism in cell culture.

Minitab student version 14 was used for statistical analysis.

GraphPad Prism 4 was used for statistical analysis and dose response curve plotting.

4-A- 5-Kits:

Cell proliferation kit II (XTT) was purchased from Roche Diagnostics (Cat # 1465015) and used to determine cell viability.

4-B- METHODS

4-B-1-To determine synergism/additivity of combined treatment in all four breast cancer cell lines:

4- B-1a- Cytotoxicity of the single agents, MA and Mbz, in wild type and HER2 transfected MDA-MB-231 and MCF-7 breast cancer cell lines:

We established the dose response curves for MA and Mbz in wild type and HER2 transfected MDA-MB-231 and MCF-7 breast cancer cell lines. We utilized the XTT colorimetric assay (Cell Proliferation Kit II from Roche) to determine the percentage of viable cells remaining after 48 hours of treatment at each concentration. XTT is converted to an orange colored formazan in the presence of metabolic activity. The intensity of color is relative to metabolic activity.

Five thousand cells in 100 µL culture medium were plated in each well of 96-well plates using DMEM/F-12 high glucose media supplemented with 10% fetal bovine serum (FBS) and 1% penicillin/ streptomycin antibiotic. Cells were incubated at 37°C and 5%

CO_2 for 18-24 hours. Plates were treated with either MA or Mbz at various concentrations of 0.25-500 µM and 1-100 µM, respectively. Plates were incubated at 37°C and 5% CO2 for 48 hours. Cell viability was determined according to the XTT colorimetric assay protocol by first removing 100 µl from each well using a multiple channel pipette. Fifty micro liters of XTT working solution, prepared by mixing 5ml of XTT labeling reagent with 100µl of the electron-coupling reagent, were added to each well. The plates were incubated for 4 hours at 37^oC. Optical densities (OD) were detected at 450 nm wave length using a Beckman Coulter DTX 880 multimode plate reader. The cell percent viability was calculated using the following equation:

$$\% \text{ Viability} = \frac{OD_{sample} - OD_{background}}{OD_{control} - OD_{background}} \times 100\%$$

Cells not receiving any treatment were used as control: control cells received 100 µl of 0.1% DMSO containing media and were incubated at 37^oC and 5% CO_2 for the same duration of 48hours. Background was determined by incubating 50 µl XTT solution with 100 µl blank media with no cells.

Drug stock solutions were prepared at 20 mM for MA and 10 mM for Mbz in sterile DMSO, and stored at 4°C. Dilutions were prepared using 0.1% DMSO media to enhance solubility.

Each experiment was performed in quadruplicates on at least two separate days

4-B-1b- Determining the synergistic/additive effect of combined MA and Mbz treatment in breast cancer cell lines:

Combination treatment of MA and Mbz was evaluated in wild type and HER2 transfected MDA-MB-231 and MCF-7 breast cancer cell lines, taking into consideration the sequence of drug administration. Percent of viable cells was evaluated using the sulforhodamine blue assay. Data was analyzed using the median-effect analysis method, where the extent of synergy or antagonism is defined by the combination index (CI) value calculated using CalcuSyn Biosoft software. A synergistic interaction is defined by a CI<1, an additive interaction is defined by a CI=1 and antagonism is defined by a CI>1.

Sulforhodamine blue assay:

Cell viability was determined using the sulforhodamine blue assay protocol described in Nature Protocols volume 1 number 3, 2006 [Vichai and Kirtikara]. A description of the protocol is stated here.

First the 96 well plates were prepared by adding 100 µl of 0.1% DMSO media containing double the desired concentration of the drug. Then 100 µl of cells containing media were added to each well at a density of 20 thousand cells /100 µl. For control, single agent and concurrent treatment groups the plates were incubated at 37 °C and 5% CO_2 for 48 hours. Sequential treatment groups were treated with the first agent for 24 hours, then washed with PBS and treated with the second agent after and incubated for another 24 hours.

After 48 hours 100 µl of cold 3% TCA was added to each well to fix the cells, the plates were incubated for one hour at 4 °C, then washed three times under running water and dried using paper towels. To each well 100 µl of 0.057% (w/v) SRB in 1% acetic acid solution was added, the plates were incubated at room temperature for 30 minutes. The dye was removed and plates rinsed three times with 1% acetic acid to remove unbound dye, then the plates were dried using a blow dryer. Two hundred microliters of 10mM Tris-base solution were added to each well and incubated for 30 minutes at room temperature.

Control plates from the day of the treatment were prepared by plating the cells in drug free media, incubating the cells for 3 hours at 37 °C and 5% CO_2, then running the assay as described for the treated cells with TCA, SRB and Tris base. The readings from these samples were averaged and the average was considered mean (OD_{day0}).

Finally the plates were read at 510nm using a plate reader. Cell viability was calculated as follows:

% cell viability =

(Mean OD $_{sample}$ - mean OD $_{day0}$) /(Mean OD $_{control}$ - mean OD $_{day0}$) x 100%

Fraction affected (Fa) was calculated as: (100 - %cell viability) /100

Fa was used to calculate CI using CalcuSyn Biosoft software.

4-B-1b-1- Combined treatment studies at a fixed (1:1) ratio of MA to Mbz in wild type and HER2 transfected MDA-MB-231 and MCF-7 breast cancer cell lines:

Using serial dilution, we treated all four breast cancer cell lines with MA and Mbz at a 1:1 dose ratio. The doses ranged from (0.061-500 µM). The two drugs were given concurrently or sequentially. With concurrent treatment the cells were treated with MA and Mbz for 48 hrs continuously. While with the sequential treatment, cells were treated with either MA or Mbz for 24 hrs, then washed twice with PBS and treated with the other agent for another 24 hrs. Cell viability was measured using the SRB assay described earlier. Each concentration was run in quadruplicates, and each experiment was repeated three times. CI values were calculated using CalcuSyn Biosoft software.

4-B-1b-2- Combined treatment studies at different ratios of MA to Mbz in wild type and HER2 transfected MDA-MB-231 and MCF-7 breast cancer cell lines:

4-B-1b-2a- Combined treatment studies at different ratios of MA to Mbz in MCF-7 and MCF-7/Her18 breast cancer cell lines:

We studied the sequential treatment with the combination of MA and Mbz in wild type and HER2 transfected MCF-7 breast cancer cell lines using different MA to Mbz ratios. MA was used at the concentrations (0.5, 2.5, 5, and 10 µM). Mbz concentrations were (0.5, 2.5, 5, 10, 25, and 50 µM). Cells were treated with MA or Mbz for 24 hrs then washed twice with PBS and treated with the other agent for another 24 hrs. Percent of viable cells was evaluated using the XTT cell proliferation assay described earlier (4-B-1a).

4-B-1b-2b- Comparing single agent to combination treatment with MA and Mbz in wild type and HER2 transfected MDA-MB-231 and MCF-7 breast cancer cell lines:

Combination treatment of MA and Mbz with different MA to Mbz ratios was evaluated in wild type and HER2 transfected MDA-MB-231 and MCF-7 breast cancer cell lines. The two drugs were given concurrently or sequentially. With concurrent treatment the cells were treated with MA and Mbz for 48 hrs continuously. While with the sequential treatment, cells were treated with either MA or Mbz for 24 hrs, then washed twice with PBS and treated with the other agent for another 24 hrs. Percent of viable cells was evaluated using the SRB assay described earlier. MA and Mbz were used at various concentrations in the four different cell lines. These concentrations are summarized below:

For MDA-MB-231 cells MA concentrations were 0, 0.5, 1.5, 2.25, and 4 µM, and Mbz concentrations were 0, 2.5, 5, 8.5, and 17.5 µM. For MDA-MB-231/ErbB2 cells MA concentrations were 0, 5, 15, 25.5, and 50 µM, and Mbz concentrations were 0, 2.5, 4.5, 8 and 22 µM. For MCF-7 cells MA concentrations were 0, 1, 4, 10, and 30 µM, and Mbz concentrations were 0, 1, 50, 55 and 60 µM. For MCF-7/ Her18 cells MA concentrations were 0, 15, 25, 30 and 60 µM, while Mbz concentrations were 0, 5, 10, 25 and 35 µM.

Data was analyzed using the median-effect analysis method, where the measure of synergy/antagonism is defined by the combination index (CI) value calculated using CalcuSyn Biosoft software. A synergistic interaction is defined by a CI<1, an additive interaction is defined by a CI=1 and antagonism is defined by a CI>1. Statistical significance of the difference between treatment groups was determined using one way ANOVA followed by Tuckey's test with $p<0.05$.

4-B-2- Determine the role of cell cycle arrest and apoptosis in the cytotoxicity of combined MA and Mbz treatments in the four breast cancer cell lines:

4-B-2a- Flow cytometry to detect both cell cycle and apoptosis:

Protocols for flow cytometry were obtained from to MD Anderson Cancer Center flow cytometry and imaging laboratory operating protocols.

Cells were seeded in 6-well plates at a density of 2 x 10^5 cells per well. Then they were treated with single agent MA at a concentration of 10 µM, single agent Mbz at a concentration of 5 µM, or one of the combination treatments in wild type MDA-MB-231 and MCF-7 cells and HER2 transfected MCF-7/Her18. Different MA and Mbz concentrations were used with MDA-MB-231/ErbB2, where MA was used at a concentration of 5µM and Mbz was used at a concentration of 1.25 µM. All drug solutions were prepared in 0.1% DMSO media, 3 ml of the drug solution at the desired concentration was added to each well. Drug free 0.1% DMSO media was added to control cells.

After 48 hours of treatment, cells were harvested and either fixed by ethanol based cell fixation for cell cycle analysis, or stained with AnnexinV-FITC without fixation to detect apoptosis. Staining was done as follows:

4-B-2a-1- Flow cytometry using propidium iodide staining:

At the end of the 48 hrs of treatment, cells were washed with PBS and harvested by incubating with 0.5 ml of trypsin for 2 minutes. Cells were centrifuged at 2400 rpm for 5 minutes, the supernatant was removed, and the pellet re-suspended in 300µl ice cold PBS in 5ml polyvinyl tubes. Then 700µl of cold 100% ethanol were added to the suspended cells and incubated at -20 ^{o}C for 30 minutes. Cells were centrifuged again and the pellet

re-suspended in 100µl cold PBS. An aliquot of 100µl of 1mg/ml ribonuclease A (Rnase, Sigma®) in PBS was added to each tube and incubated at 37°C for 30 minutes.Propedium iodide working solution was prepared by diluting the 1 mg/ml PI stock solution to 0.5 mg/ml using ddH2O, then diluting this solution (1:10) in Tris buffer. One milliliter of PI working solution was then added to each tube and the samples were incubated at room temperature for 30 minutes in the dark before flow cytometry analysis. Samples were read and analyzed using M D Anderson Cancer Center flow cytometry facility.

4-B-2a-2- Flow cytometry using Annexin V- FITC staining:

At the end of treatment cells were washed with PBS and harvested using trypsin as described above. Cells were centrifuged at 500g for 5 minutes, the supernatant removed and the pellet suspended in 200µl of Annexin-V binding buffer in 5 ml round bottom tubes. Two microliters of Annexin-V-FITC solution (from human placenta, Sigma®) were added to each tube, and incubated on ice for 10 minutes in the dark. The samples were read using the Accuri C6 flow cytometer, then 5 µl of propidium iodide was added to the samples and they were read again to help distinguish between necrotic and apoptotic cells. Controls were non stained non treated cells, propidium iodide stained non treated cells, Annexin V- FITC stained non treated cells, and non treated cells stained with both propidium iodide and Annexin V-FITC.

Annexin-V binding buffer is used to provide the calcium ions needed for Annexin-PS binding and was prepared as follows:

50mM HEPES/NaOH pH7.4, 750mM NaCl, 25mM KCl, 5mM $MgCl_2$, and 9mM $CaCl_2$.

4-B-2b- Western blotting for cleaved PARP, Cyclin E and Cyclin B to determine the role of apoptosis and cell cycle arrest in MA and Mbz cytotoxicity:

Wild type and HER2 transfected MDA-MB-231 and MCF-7 breast cancer cells were plated in 6 well plates at 0.5 million cells per well, and incubated at 37 °C and 5% CO_2 for 18-24 hours. Cells were treated with single agent MA, single agent Mbz, or one of the combination treatments. Drug free 0.1% DMSO cell culture media was added to control cells. After 48 hours of treatment cells were harvested and washed twice with cold PBS, then re-suspended with 300µl of 1X cell lysis buffer (Cell Signaling Technology) and incubated on ice for 30 minutes. Samples were centrifuged at 16000g for 20 minutes at 4 °C. Protein levels were assayed using Bio Rad protein assay kit (as described below) and samples were stored at -80 °C until the gels were run.

Samples were electrophoresed on precast 7.5% Tris-glycine gels in triplicates, and transferred to nitrocellulose membranes at 100V for 90 minutes at 4 °C. Membranes were blocked in 5% ChemiLucent Plus blocking reagent in TBS-T buffer (10mM Tris base, 150mM NaCl, 0.1% Tween20) for one hour. After three washes for 10 minutes each with

TBS-T buffer, the membranes were incubated with primary antibodies (dilutions used are described below) in 1X ChemiLucent Plus antibody binding buffer overnight at 4 °C. After washing with TBST buffer, membranes were incubated with horse-radish peroxidase conjugated sheep anti-mouse secondary antibody (at a dilution of 1:1500) in 1X ChemiLucent Plus antibody binding buffer for 90 minutes at room temperature. Bound antibodies were detected using Pierce ECL western blotting substrate, and the protein bands were visualized using the Alpha-Innotech Fluorchem 8900 CCD imaging exposure device. Densitometry was performed on the digital images using AlphaEase FC8900 software. The same membrane was then stripped by washing in distilled water for 5 minutes, followed by shaking in 0.6N NaOH for 5 minutes, and then washing again with distilled water for 5 minutes. The membrane was then blocked with 5% ChemiLucent Plus blocking reagent in TBS-T, and washed with TBST before re-probing it with another primary antibody with the above steps repeated. The dilutions for the primary antibodies used for immunoblotting were as follows:

Mouse monoclonal anti-Cyclin B1 antibody (1:1,000), mouse monoclonal anti-Cyclin E1 antibody (1:1,000), mouse monoclonal anti-Cleaved PARP antibody (1:1500), and mouse anti-β-actin antibody (1:1,000).

Protein concentrations were measured using Bio-Rad protein measurement protocol for 96 well plates. Three hundred microliters of 1X Bio Rad Protein Assay solution were added to each of the 96 wells, 5 μl of each standard concentration or of the treated cells sample were added to each 96 well. The plate was incubated for 5 minutes at room

temperature then mixed and read with the plate reader at 595 nm. Samples were run in triplicates.

Buffer preparation:

Buffers were prepared according to the protocol provided by Chemicon International.

Running buffer:

To prepare 1X stock solution 1.5 grams Tris Base, 7.2 grams Glycine and 0.5 grams SDS were dissolved in dd H2O to make 500 ml solution at a pH = 8.3.

Transfer buffer:

To prepare 20X stock solution 72.5 grams Tris Base, 36.25 grams Glycine, and 4.6 grams SDS were dissolved in dd H2O to make 500 ml solution at a pH = 8.3. This stock solution was then used to prepare 1X working transfer buffer by adding 40 ml of 20X stock solution and 200ml Methanol are added to 760ml dd H2O.

Washing buffer (TBS-T):

To prepare 20X stock solution 48.4 grams Tris Base and 160 grams NaCl were dissolved in 1 liter dd H2O and the pH was fixed to 7.4. The working solution was prepared by diluting 50 ml of the 20X stock solution with dd H2O to make 1 liter, then 1 ml TWEEN 20 was added.

Loading buffer: (2X SDS/DTT sample loading buffer)

Is prepared by dissolving 0.618 grams DTT and 0.4 grams SDS in 5 ml of 0.2M Tris buffer, then adding 0.2 ml of 1% Bromoplenol Blue (made by adding 0.01gr to 1ml H2O) and 2 ml glycerol.

4-B-3- To determine the in vivo effect of MA and Mbz treatment using wild type and HER-2 transfected MDA-MB-231 breast cancer xenografts in nu/nu Swiss background nude mice:

The effect of MA, Mbz and their combinations was tested in both wild type and HER2 transected MDA-MB -231 breast cancer cell lines in vivo. Adult male and female nu/nu Nude Homozygous-Swiss Background was used in our study. The cells were grown in cell culture, then harvested and inoculated subcutaneously in mid dorsal position. Each animal was inoculated with 20 million cells in 250 µl media.

4-B-3a- Cell culture and animal inoculation:

MDA-MB-231 and MDA-MB-231/ErbB2 breast cancer cell lines were grown at Stehlin Foundation facilities. High glucose dulbecco's modified eagle's medium (DMEM) with the nutrient mixture F-12 Ham, L- glutamine, 15mM HEPES and 15.6 g/L NaHCO3 and was supplemented with 10% fetal bovin serum, and 1% PSN antibiotic mixture.

The cells were cultured in 150 mm^3 tissue culture flasks and incubated at 37°C and 5% CO_2 until the day of inoculation. The cells were harvested and counted, then re-suspended at a cell density of 80 million cells per one milliliter media. Each animal was subcutaneously inoculated with 250 µl in the mid dorsal position using a 26 gauge needle. The tumors were monitored twice weekly until they reached a size of 250-400 mm^3. Using the Microsoft fox randomizer software, mice were randomized into different treatment groups of five based on their tumor size and body weight. Dose response and combination efficacy studies were conducted as follows:

4-B-3b- Determining the best dose of MA and Mbz for combination therapy in vivo (dose response study in nu/nu Nude Homozygous-Swiss Background mice):

For each breast cancer cell line five groups of MA and five groups of Mbz were studied, each group had five mice. Both MA and Mbz were administered intraperitoneally (i.p.). The MA groups were control, 1mg/kg, 2.5 mg/kg, 5 mg/kg, and 7.5 mg/kg for MDA-MB-231 and control 1 mg/kg, 1.5 mg/kg, 2.5 mg/kg and 5 mg/kg for MDA-MB 231/ErbB2. MA was prepared as stock solution of 10 mg MA in 1ml DMSO. Dilutions were prepared using 2.5% DMSO in DMEM/F12 tissue culture media. A final volume of 200µl was administered to each animal. Mbz groups were control, 0.5 mg/kg, 1 mg/kg, 2.5 mg/kg, 5 mg/kg, and 33 mg/kg for MDA-MB231, and 1 mg/kg, 2.5 mg/kg, 5 mg/kg

and 33 mg/kg for MDA-MB231/ErbB2. Mbz drug solutions were prepared either as a microemulsion formulation for MDA-MB231/ErbB2, or in 2.5% DMSO media for MDA-MB231 from 10 mg/ml DMSO stock solution. The microemulsion for ip administration was prepared according to [Gupta P, 2006] by mixing (5% w/w) DMSO, 1.9 mg/ml Mbz, Captex 200 (4.5% w/w), TWEEN 80 (20.25% w/w), transcutol (20.25% w/w) and 50% water. Mbz was dissolved in DMSO and sonicated for 30 minutes at 40 °C. Captex 200 was added to TWEEN 80 and transacutol, Mbz-DMSO mixture was then added to the oil mix. Water was then added drop-wise while stirring gently. Mbz final concentration was 1mg/ml, and was assessed using HPLC at the time of microemulsion preparation and once every week before the first dose. The 33 mg/kg group received 100 µl of 10mg/ml Mbz- DMSO stock solution. Control group for MA received 200 µl drug free 2.5% DMSO cell culture media, while control group for Mbz received 200 µl drug free microemulsion formulation in MDA-MB 231/ErbB2 cells.In MDA-MB231 there was only one control group that received 200µl of 2.5% DMSO media.

The drugs were administered ip twice weekly for a total of 8 doses. Animal body weight and tumor volume were measured on the first day of treatment (V_0) and twice weekly after that for 29 days. The volume recorded is calculated according to the following formula (V=L*W*H). Where L is the length or the larger dimension, W is the width or the smaller dimension, and H is the height or the thickness of the tumor. The efficacy is expressed as V/ V_0. Survival duration is defined as the period between the day of

sacrifice or death and the day the treatment started. Toxicity is expressed as body weight loss greater than 15%.

Mice were sacrificed if their tumor volume exceeded 10% of body weight or body weight loss was greater than 15%.

4-B-3c- Efficacy experiments in nu/nu Nude Homozygous-Swiss Background mice:

Seven treatment groups were used for each breast cancer cell line. The two control groups had five mice each while each treatment group had ten mice. The groups were control MA receiving 100 µl 2.5% DMSO media, control Mbz receiving drug free microemulsion, single agent MA, single agent Mbz, concurrent treatment with MA and Mbz, sequential treatment with MA given as the first agent, and sequential treatment with Mbz given as the first agent. Both MA and Mbz were administered intraperitoneally (i.p.), where MA was given at a dose of 2.5mg/kg to animals with both wild type and HER-2 transfected xenografts. Mbz was given at a dose of 1mg/ kg to animals with wild type xenografts and 5mg/kg to animals with HER-2 transfected xenografts. MA was prepared as 100µl of 2.5% DMSO in DMEM/F12 tissue culture media, while Mbz was prepared as the microemulsion formulation discribed in (4-B-3b).

The drugs were administered ip twice weekly for a total of 8 doses. Animal body weight and tumor volume were measured on the first day of treatment (V_0) and twice weekly

after that for the duration of treatment, then once weekly for 3 weeks following the last dose to detect any re-growth of the tumor. The tumor volume recorded was calculated according to the following formula (V=L*W*H) explained above (4-B-3b). The efficacy was expressed as V/ V_0. Survival duration was defined as the period between the day of sacrifice or death and the day the treatment started. Toxicity was expressed as body weight loss greater than 15%.

Mice were sacrificed if the tumor volume exceeds 10% of body weight or body weight loss was greater than 15%.

The readings from each group (10 animals) were averaged. The group average $\pm$ SD of (V/V0) was plotted against time from first dose (in days). The plot of survival was also compared. Differences among groups were tested using the software minitab 14 by repeated measures ANOVA followed by Tukey's post hoc test ($p<0.05$).

CHAPTER-5- RESULTS

5-A-To determine synergism/additivity of combined treatment in all four breast cancer cell lines:

5-A-1- Cytotoxicity of the single agents, MA and Mbz, in wild type and HER2 transfected MDA-MB-231 and MCF-7 breast cancer cell lines:

We tested the effect of MA on wild type and HER2 transfected MDA-MB-231 and MCF-7 breast cancer cell lines in vitro. MA inhibited cell growth in all four cell lines showing the same potency in wild type and HER2 transfected cells. There was no difference in sensitivity to MA between the two cell pairs (MDA-MB-231 and MCF-7) [Figure 5-1].

In wild type and HER2 transfected MDA-MB-231cells MA inhibited cancer cell growth at a dose as low as 0.25 µM with no additional effect observed at doses higher than 100 µM [Figure 5-2]. The Log EC_{50} values were (-3.195 $\pm$ 0.2755) M and (- 4.318 $\pm$ 0.01916) M for MDA-MB-231 and MDA-MB-231/ErbB2, respectively.

In wild type and HER2 transfected MCF-7cells MA inhibited cancer cell growth at a dose as low as 1 µM [Figure 5-3]. The Log EC_{50} values were (- 4.453 $\pm$ 0.0803) M and (- 4.498 $\pm$ 0.04539) M for MCF-7 and MCF-7/Her18, respectively.

The MCF-7/Her18 MA dose response curve shows percent cell viability higher than 100%, this warranted further investigations to determine whether such an increase in cell viability is a true reading or an artifact. Cell viabilities for dose response experiments

were obtained using the XTT (Formazan) assay. MA dose response curve for MCF-7/Her18 was generated using the sulforhodamine blue (SRB) assay (described in section 4-B-1b). Cell viabilities obtained using SRB did not exceed 100% [Figure 5-4]. The Log EC_{50} value for MA dose response obtained by SRB was (- 5.434 $\pm$ 0.04723) M.

The cytotoxicity of Mbz was tested on wild type and HER2 transfected MDA-MB-231 and MCF-7 breast cancer cell lines in vitro. Mbz inhibited the growth of all four cell lines with higher potency in the MDA-MB-231 cell pair [Figure 5-5]. Mbz had the same potency when comparing wild type to HER2 transfected cells for each cell line.

Mbz inhibited MDA-MB-231 and MDA-MB-231/ErbB2 cancer cells growth at a dose as low as 1.25µM [Figure 5-6]. It was effective in the range of (1.25-50) µM. The Log EC_{50} values were (-4.779 $\pm$ 0.141) µM and (-5.229 $\pm$ 0.1752) µM for the MDA-MB-231 and MDA-MB-231/ErbB2, respectively.

Cells growth was inhibited in both wild type and HER2 transfected MCF-7 cancer cells at a dose as low as 5µM [Figure 5-7]. The Log EC_{50} values were (- 1.282 $\pm$ 151) µM and (- 3.625 $\pm$ 3.215) µM for the MCF-7 and MCF-7/Her18, respectively.

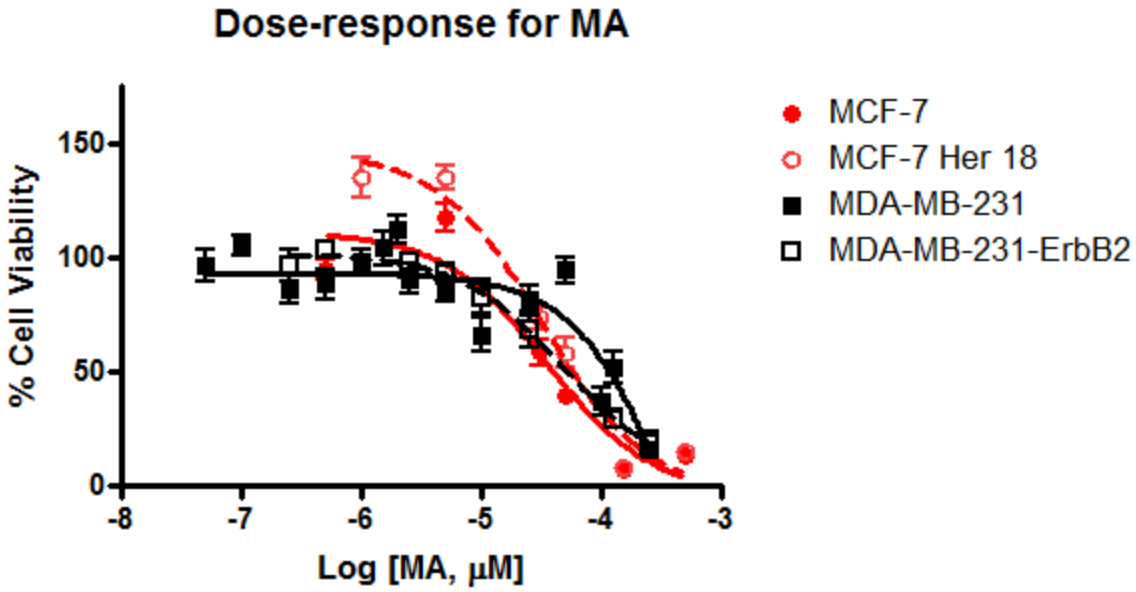

Figure 5-1: In vitro cytotoxicity of MA in wild type and HER2 transfected MDA-MB-231 and MCF-7 breast cancer cell lines. Values are presented as mean ± standard deviation (N=8 from two independent runs).

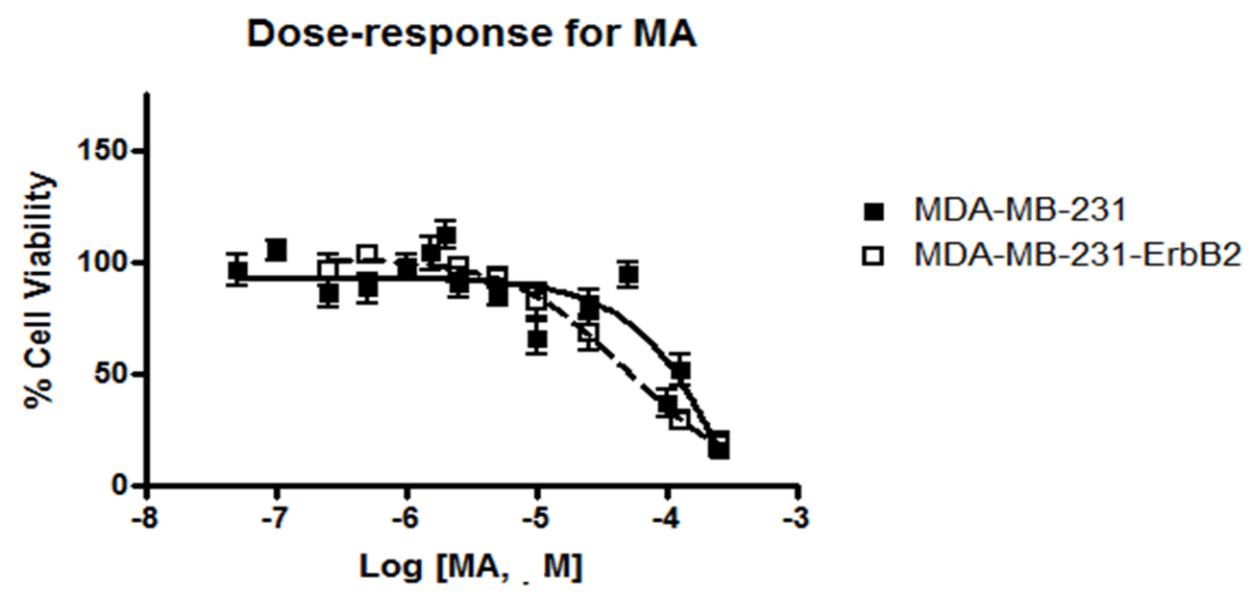

Figure 5-2: In vitro cytotoxicity of MA in wild type and HER2 transfected MDA-MB-231 breast cancer cell line. MA showed cytotoxicity at a range of (0.25-250) µM. Values are presented as mean ± standard deviation (N=8 from two independent runs).

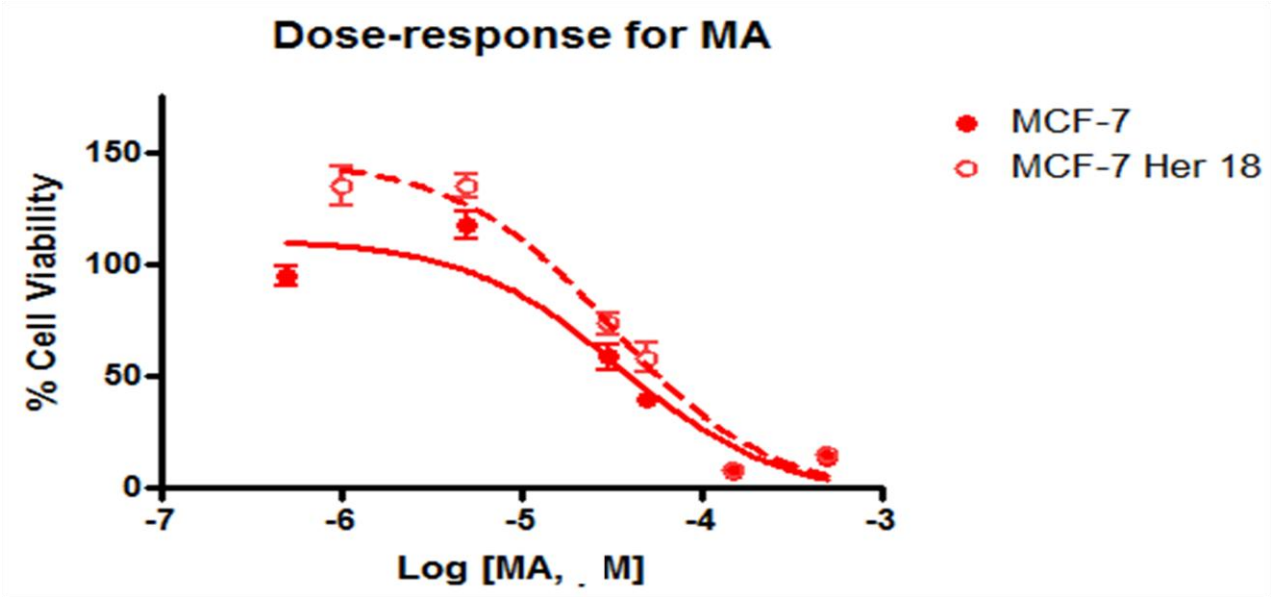

Figure 5-3: In vitro cytotoxicity of MA in wild type and HER2 transfected NCF-7 breast cancer cell line. MA showed cytotoxicity at a range of (1-500) µM. Values are presented as mean ± standard deviation (N=8 from two independent runs).

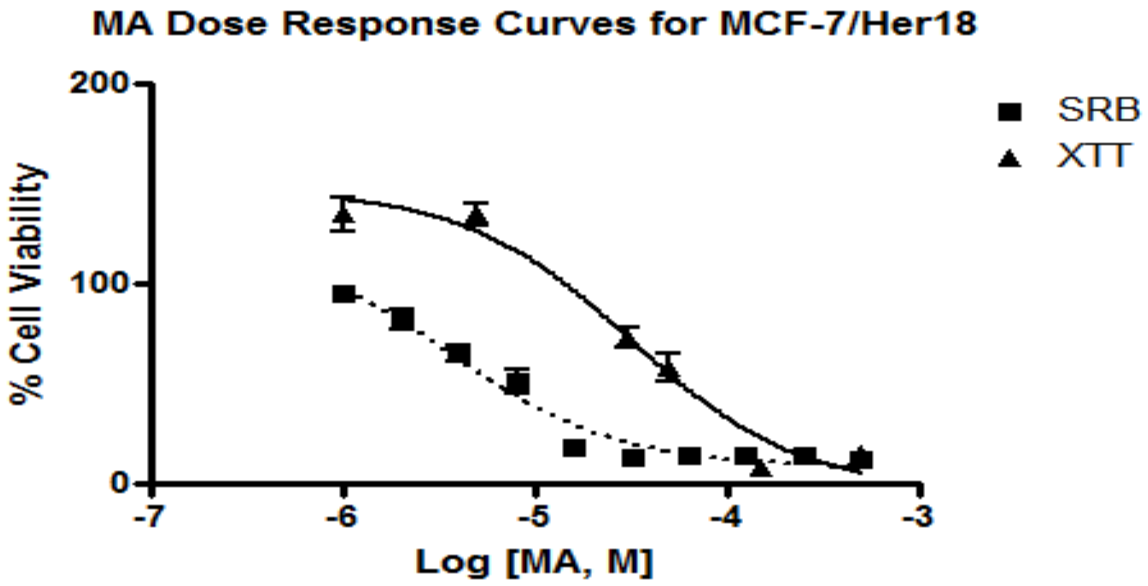

Figure 5-4: The MA dose response curve for MCF-7/Her18 was generated using XTT or sulforhodamine blue (SRB) assays. The Log EC_{50} values were (- 4.498 $\pm$ 0.04539) and (- 5.434 $\pm$ 0.04723) M for XTT and SRB, respectively. Cell viabilities exceeding 100% obtained using XTT assay are false readings due to experimental conditions. Values are presented as mean $\pm$ standard deviation (N=7-8 from two independent runs).

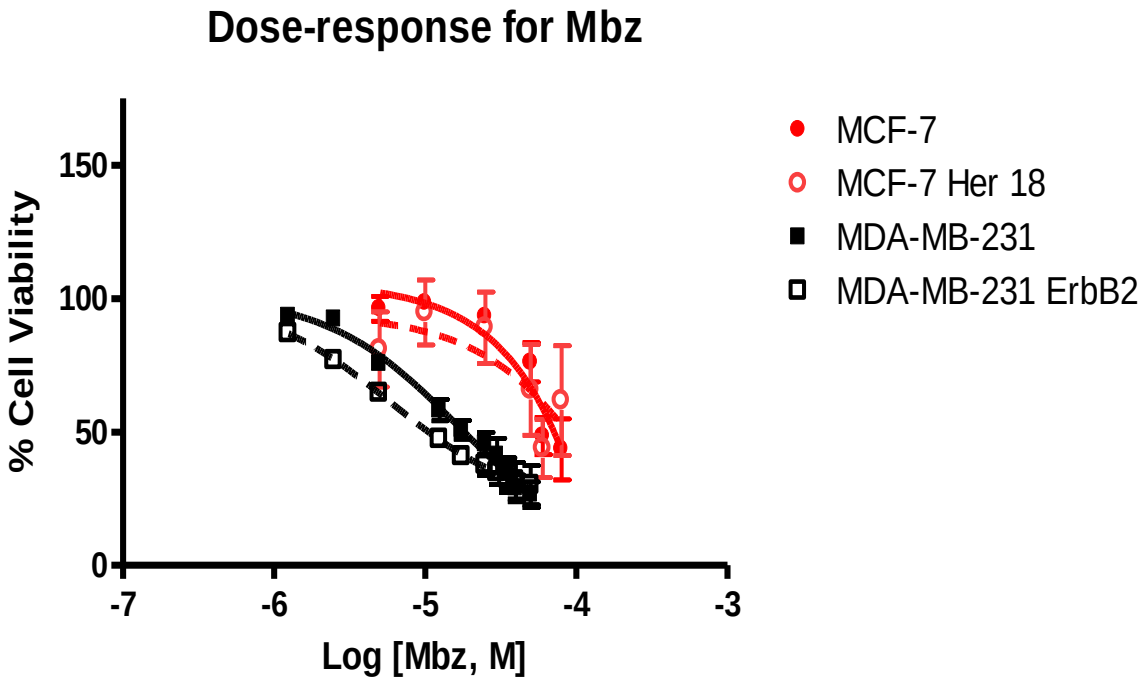

Figure 5-5: In vitro cytotoxicity of Mbz in wild type and HER2 transfected MDA-MB-231 and MCF-7 breast cancer cell lines. Mbz is more potent in MDA-MB-231 cells compared with MCF-7 cells. Cytotoxicity was not affected by HER2 expression. Values are presented as mean ± standard deviation (N=7-8 from two independent runs).

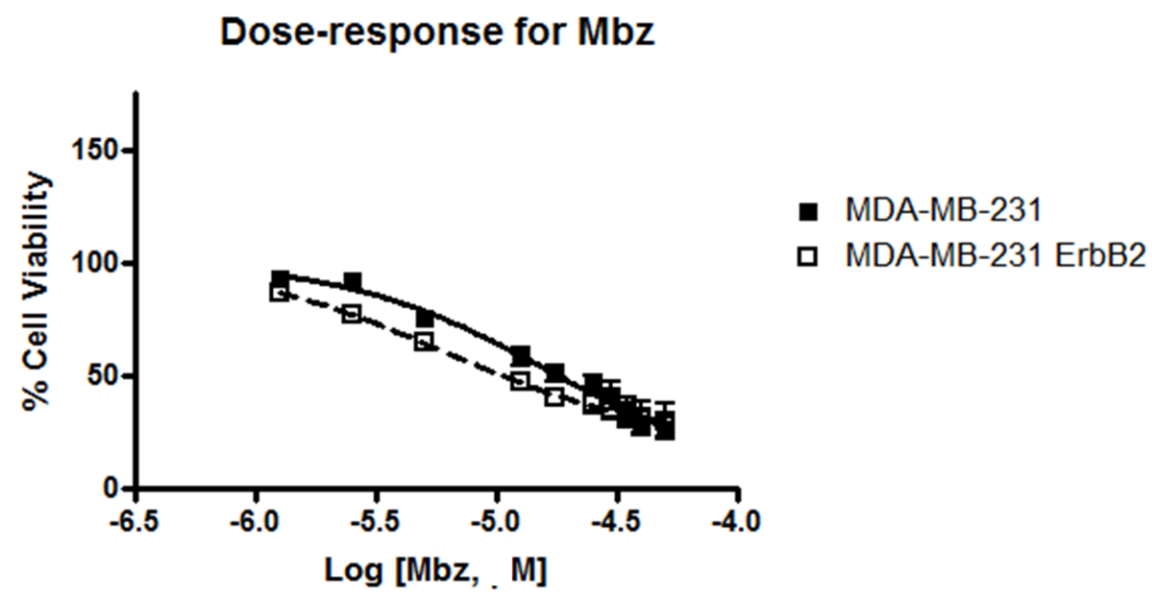

Figure 5-6: In vitro cytotoxicity of Mbz in wild type and HER2 transfected MDA-MB-231 breast cancer cell line. Mbz showed cytotoxicity at a range of (1.25-50) µM. Values are presented as mean ± standard deviation (N=7-8 from two independent runs).

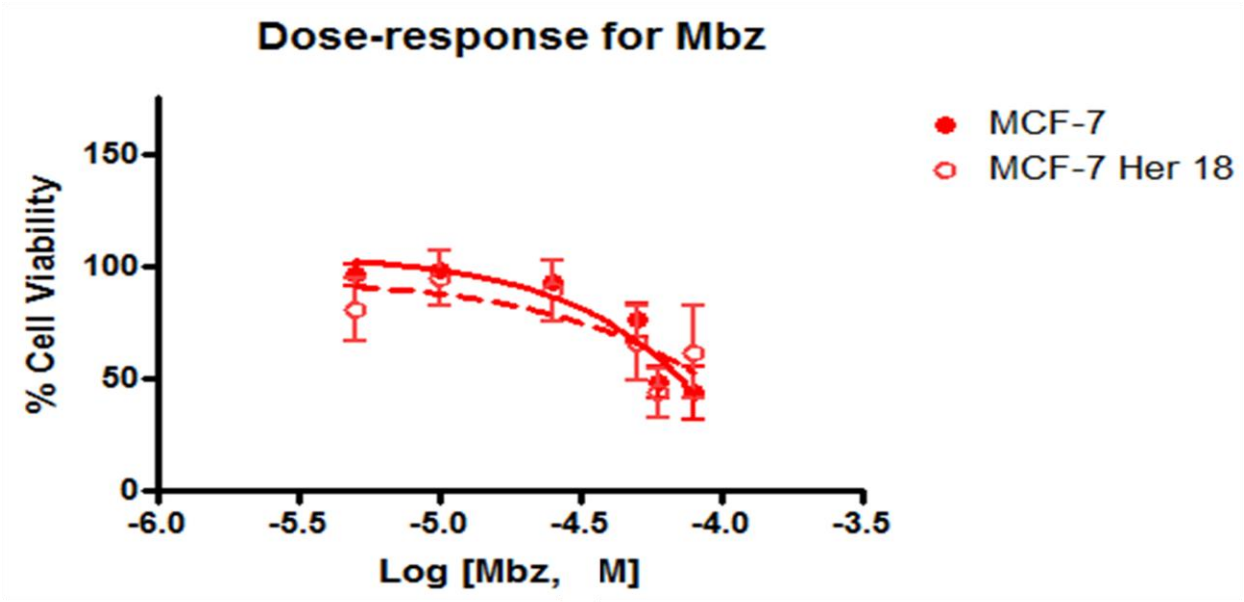

Figure 5-7: In vitro cytotoxicity of Mbz in wild type and HER2 transfected NCF-7 breast cancer cell line. Mbz showed cytotoxicity at a range of (5-80) µM. Values are presented as mean ± standard deviation (N=8 from two independent runs).

5-A-2- Synergistic/additive effect of combined treatment in breast cancer cell lines:

MA and Mbz are toxic in all four breast cancer cell lines investigated. We studied the combination treatment of MA and Mbz in these cell lines taking into consideration the sequence of drug administration. Percent of viable cells was evaluated using the sulforhodamine blue assay. Data was analyzed using the median-effect analysis method, were the measure of synergy/antagonism is defined by the combination index (CI) value calculated using CalcuSyn Biosoft software. A synergistic interaction is defined by a CI<0.9, an additive interaction is defined by a 0.9<CI<1.1 and antagonism is defined by a CI>1.1. Today a more refined scale is recommended for CalcuSyn Biosoft users. We choose to use the CI ranges specified in Table 5-1 when generating our synergy heat map.

5-A-2a- Combined treatment studies at a fixed (1:1) ratio of MA to Mbz in wild type and HER2 transfected MDA-MB-231 and MCF-7 breast cancer cell lines:

We treated both wild-type and HER2 transected MDA-MB-231 and MCF-7 breast cancer cell lines with different concentrations of MA and Mbz at a 1:1 dose ratio. The doses ranged from (0.061-500) μM. The two drugs were given concurrently or sequentially. With concurrent treatment the cells were treated with MA and Mbz for 48 hrs continuously. While with sequential treatment, cells were treated with either MA or Mbz for 24 hrs, then washed with PBS and treated with the other agent for another 24 hrs. Cell viability was measured and CI values were calculated at different concentrations

for all combinations. A synergy heat map was plotted [Figure 5-8] based on the color code given in table 5-1.

Range of Combination Index	Treatment Effect	Color
< 0.1	**Very strong synergism**	
0.1-0.7	**Synergism**	
0.7-0.9	**Slight synergism**	
0.9-1.1	**Additive**	
1.1-3.3	**Slight antagonism**	
3.3-10	**Antagonism**	
>10	**Very strong antagonism**	

Table 5- 1- Range of combination indices describing combination treatment interaction based on CalcuSyn Biosoft software. A color code is used to generate a heat map based on CI values.

Our map depends on drug concentrations with a constant MA to Mbz ratio of 1: 1 at all concentrations. The map revealed two regions of antagonism at low and high concentrations, and a region of synergism in the middle portion. Our results indicate that most combination treatments between the concentrations (3.9 – 125) µM are synergistic

with some exceptions, depending on the cell line and sequence of drug administration. In wild type MCF-7 concurrent treatment was always antagonistic except at the MA and Mbz concentration of 3.9 µM. In MDA-MB-231/ErbB2 cells Mbz 1st treatment was antagonistic at all concentrations except 7.88 and 15.6 µM where synergy was observed. These results show that the final outcome of MA and Mbz combination depends on concentration, sequence of drug administration, and the targeted cells.

Concentration (uM)	MDA-MB-231			MDA-MB-231 /ErbB2			MCF-7			MCF-7/Her 18		
	Mix	MA 1st	Mbz 1st	Mix	MA 1st	Mbz 1st	Mix	MA 1st	Mbz 1st	Mix	MA 1st	Mbz 1st
0.061				0.74						0.02		0.001
0.122				6e8						0.02		0.001
0.244	0.26			7.6 e4						0.283		0.002
0.488	0.51			6.5 e8						220.024		0.006
0.977	0.49			7.9 e10		11.87						0.013
1.95	0.55	0.916	347.47	0.648		9 e9						0.231
3.9	0.68	0.77	0.44	0.046	0.625	2.3 e2	0.44	0.49	1.116	0.142	1.897	0.132
7.81	0.622	82.167	0.089	0.025	0.073	0.251	4.88	1.077	1.198	0.124	0.21	0.115
15.6	0.453	0.002	3.124	0.93	0.025	0.93	6.214	0.92	1.202	0.183	0.01	0.180
31.25	0.75	0.36	6.49 e2	2 e4	0.051	4 e5	4.66	0.557	0.595	0.201	0.016	0.162
62.5	0.69	0.024	0.015	0.523	0.033	47	4.87	0.959	1.093	0.103	0.029	0.129
125	0.566	0.668	0.034	0.514	0.066	1.8	2.596	1.9	1.782	0.447	0.07	0.52
250		169.06	0.196	1.477	0.188	5.06	2.233	4.82	3.564		0.164	6.168
500		1.76 e7	12.9	22.5	0.705	165.8	3.93	178.129	8.536		2.409	143

Figure 5-8- In vitro synergy heat map for (1:1) MA to Mbz combination treatment in wild type and HER2 transfected MDA-MB-231 and MCF-7 breast cancer cell lines. Synergy heat map was first presented by Mayer et al, 2009. Mapping was based on CI values obtained using CalcuSyn Biosoft software. (n=12 from three independent runs).

5-A-2b- Combined treatment studies at different ratios of MA to Mbz in wild type and HER2 transfected MDA-MB-231 and MCF-7 breast cancer cell lines:

Treating cancer cells with concurrent and sequential combinations of MA and Mbz at a ratio of 1:1 at various concentrations showed mixed synergistic and antagonistic effects. The effect observed was concentration dependent. Mayer et al presented data showing that treating cancer cells with various drug1 to drug2 ratios also shows mixed synergistic and antagonistic effects based on the drug1 to drug2 ratio. We studied the combination treatment of MA and Mbz in wild type and HER2 transfected MDA-MB-231 and MCF-7 breast cancer cell lines with different MA to Mbz ratios, taking into consideration the sequence of drug administration. Percent of viable cells was evaluated. Data was analyzed using the median-effect analysis method, were the measure of synergy/antagonism is defined by the combination index (CI) value calculated using CalcuSyn software. We used the CI range and color code presented in table 5-1 to generate the synergy heat map in figure 5-9.

5-A-2b- 1- Synergy map for combined treatment studies at different ratios of MA to Mbz in MCF-7 and MCF-7/Her18 breast cancer cell lines:

We studied the sequential treatment with the combination of MA and Mbz in wild type and HER2 transfected MCF-7 breast cancer cell lines using different MA to Mbz ratios. MA was used at the concentrations (0.5, 2.5, 5, and 10 μM). Mbz concentrations were (0.5, 2.5, 5, 10, 25, and 50 μM). Cells were treated with MA or Mbz for 24 hrs then

washed with PBS and treated with the other agent for another 24 hrs. Percent of viable cells was evaluated using the XTT cell proliferation assay kit. CI values were calculated for the different treatment ratios, and a synergy heat map was plotted [Figure 5-9]. Our map depends on drug concentrations and (MA: Mbz) ratios. This map revealed that both in MCF-7 and MCF-7/Her18 cancer cells treatment with MA 1st gives the exact opposite results compared to Mbz 1st treatment. Regions of synergy in MA 1st treatment contrast with regions of antagonism in Mbz 1st treatment at the same ratio in each cell line, and vice versa. In MCF-7 cells MA 1st treatment was synergistic at low concentration (0.5 µM) and antagonistic with high concentrations (10 µM) regardless of the (MA: Mbz) ratio. In MCF-7/Her18 MA concentrations of 0.5 and 2.5µM were always antagonistic with MA 1st treatment, while a concentration of 10µM was always synergistic, and an MA concentration of 5µM was either synergistic or antagonistic when MA was given first depending on the (MA: Mbz) ratio in both cell lines.

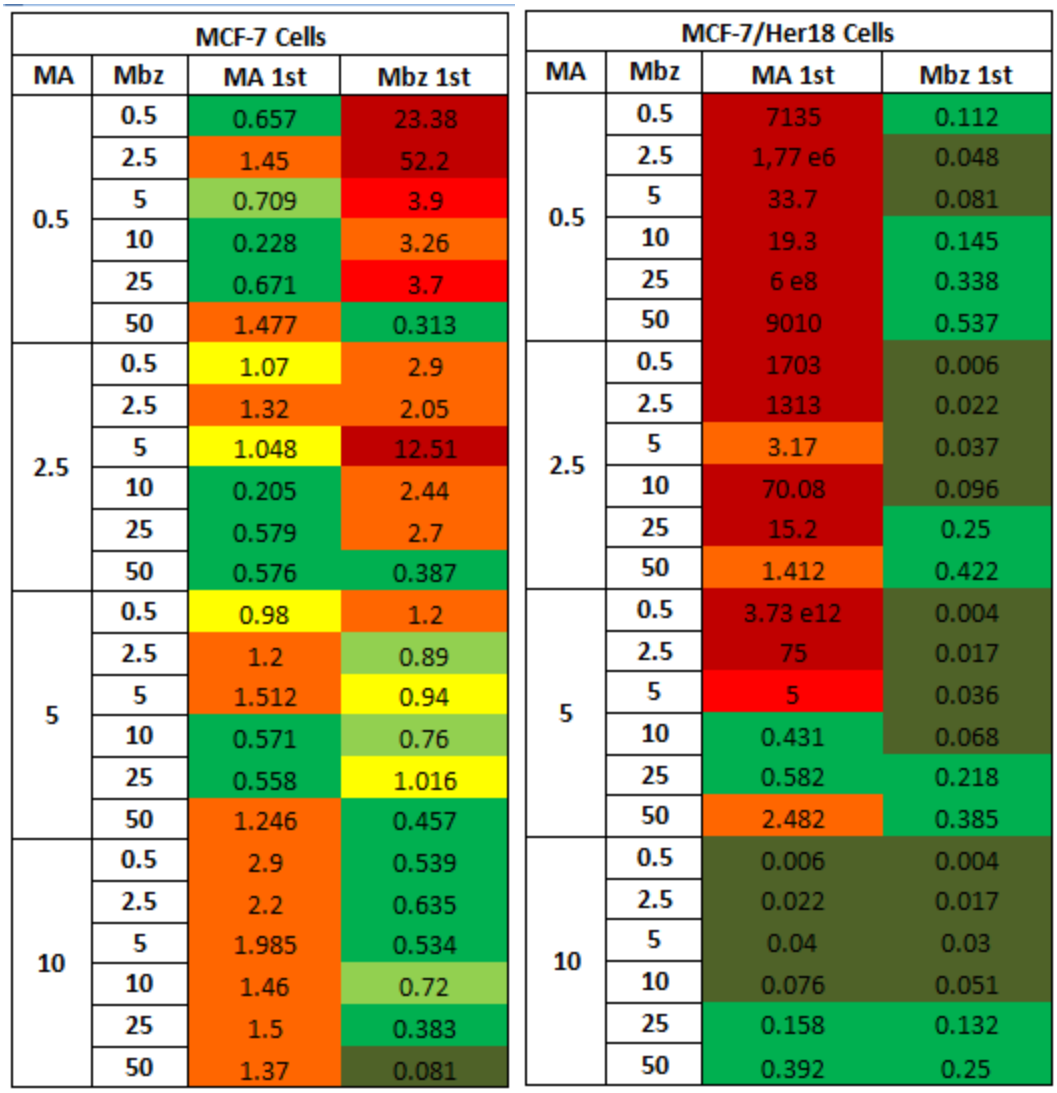

MCF-7 Cells			
MA	Mbz	MA 1st	Mbz 1st
0.5	0.5	0.657	23.38
	2.5	1.45	52.2
	5	0.709	3.9
	10	0.228	3.26
	25	0.671	3.7
	50	1.477	0.313
2.5	0.5	1.07	2.9
	2.5	1.32	2.05
	5	1.048	12.51
	10	0.205	2.44
	25	0.579	2.7
	50	0.576	0.387
5	0.5	0.98	1.2
	2.5	1.2	0.89
	5	1.512	0.94
	10	0.571	0.76
	25	0.558	1.016
	50	1.246	0.457
10	0.5	2.9	0.539
	2.5	2.2	0.635
	5	1.985	0.534
	10	1.46	0.72
	25	1.5	0.383
	50	1.37	0.081

MCF-7/Her18 Cells			
MA	Mbz	MA 1st	Mbz 1st
0.5	0.5	7135	0.112
	2.5	1,77 e6	0.048
	5	33.7	0.081
	10	19.3	0.145
	25	6 e8	0.338
	50	9010	0.537
2.5	0.5	1703	0.006
	2.5	1313	0.022
	5	3.17	0.037
	10	70.08	0.096
	25	15.2	0.25
	50	1.412	0.422
5	0.5	3.73 e12	0.004
	2.5	75	0.017
	5	5	0.036
	10	0.431	0.068
	25	0.582	0.218
	50	2.482	0.385
10	0.5	0.006	0.004
	2.5	0.022	0.017
	5	0.04	0.03
	10	0.076	0.051
	25	0.158	0.132
	50	0.392	0.25

Figure 5-9- In vitro synergy heat map for sequential treatment with different ratios of MA and Mbz in MCF-7 and MCF-7/Her18 breast cancer cell lines. The numbers in the MA and Mbz columns present the concentration of each drug in υM units. Synergy heat map was first presented by Mayer et al, 2007. Mapping was based on CI values obtained using CalcuSyn Biosoft software. (n=8 from two independent runs).

5-A-2b- 2- Comparing single agent to combination treatment with MA and Mbz in wild type and HER2 transfected MDA-MB-231 and MCF-7 breast cancer cell lines:

We treated both wild-type and HER2 transfected MDA-MB-231 and MCF-7 breast cancer cell lines with different concentrations of MA and Mbz at varying dose ratios. The two drugs were given concurrently or sequentially. With concurrent treatment the cells were treated with MA and Mbz for 48 hrs continuously. While with the sequential treatment, cells were treated with either MA or Mbz for 24 hrs, then washed with PBS and treated with the other agent for another 24 hrs. Cell viability was measured using the sulforhodamine blue assay for all combinations and statistical significance of the difference between treatment groups was determined using one way ANOVA followed by Tuckey's test with $p<0.05$, data was presented in bar graphs as mean $\pm$ SD [Figures 5-10-13].

In wild type MDA-MB-231 breast cancer cells [Figure 5-10], concurrent and Mbz 1st treatment groups were not significantly different between each others, nor were they significantly different from treatment with MA or Mbz as single agents regardless of the MA and Mbz concentrations. MA 1st treatment showed higher percent viabilities than all other treatment groups, it was significantly different from concurrent and Mbz 1st treatments at all MA concentrations with Mbz concentrations of 2.5 and 5µM, but not with Mbz concentrations of 8.5 and 17.5 µM . So we conclude that combination treatment produces no additional benefit over single agent treatment in this cell line. This

could be explained when comparing the cell cycle arrest induced by the two drugs. Both MA and Mbz induce G2/M phase cell arrest, thus when giving MA 1st the cells arrest at G2/M phase and are no longer actively dividing, so they are not sensitive to Mbz.

MA1st treatment gave different results in HER2 transfected MDA-MB-231/ErbB2 cells [Figure 5- 11] showing lower percent cell viability than all other treatment groups. The higher the MA and Mbz concentrations the more significantly different the MA1st treatment became compared to the other two combinations.

In the wild type MCF-7 cancer cells the difference in cytotoxicity between the different treatment groups is influenced by MA concentration. At the lower MA concentrations MA 1st is significantly different from concurrent treatment, while at higher MA concentrations MA 1st becomes significantly different from Mbz 1st treatment, and shows no significant difference in cytotoxicity compared to MA alone and concurrent treatments. We conclude that as the MA concentration increases it interferes with Mbz mechanism of action blocking its cytotoxicity.

Mbz 1st treatment group is significantly different from the other two combinations showing higher cell viability. It offers no additional benefit compared to treatment with single agents, thus it is considered antagonistic. It is also observed that when used alone Mbz was less cytotoxic compared to concurrent and MA 1st treatment indicating that the effect of treatment is controlled by MA in these groups [Figure 5-12].

Mbz 1st treatment group in the HER2 transfected MCF-7/Her18 cancer cells gives the lowest percent cell viability compared to all other treatment groups. At MA dose of 60μM, difference between Mbz 1st and MA alone, MA 1st and concurrent treatments is significant. One can conclude that Mbz1st shows additional benefit compared to single agent and other combination treatment groups. CI values presented in the synergy map do indicate that Mbz1st was synergistic in this cell line at different ratios and concentrations of MA and Mbz. [Figure 5-13].

Results obtained from the four cell lines revealed that wild type cells didn't benefit from MA and Mbz combination. HER2 expressing cells did show an improved effect with combination compared to single agent treatment. The optimal combination varied, with MA 1st being superior in MDA-MB-231/ErbB2 and Mbz 1stbeing superior in MCF-7/Her18.

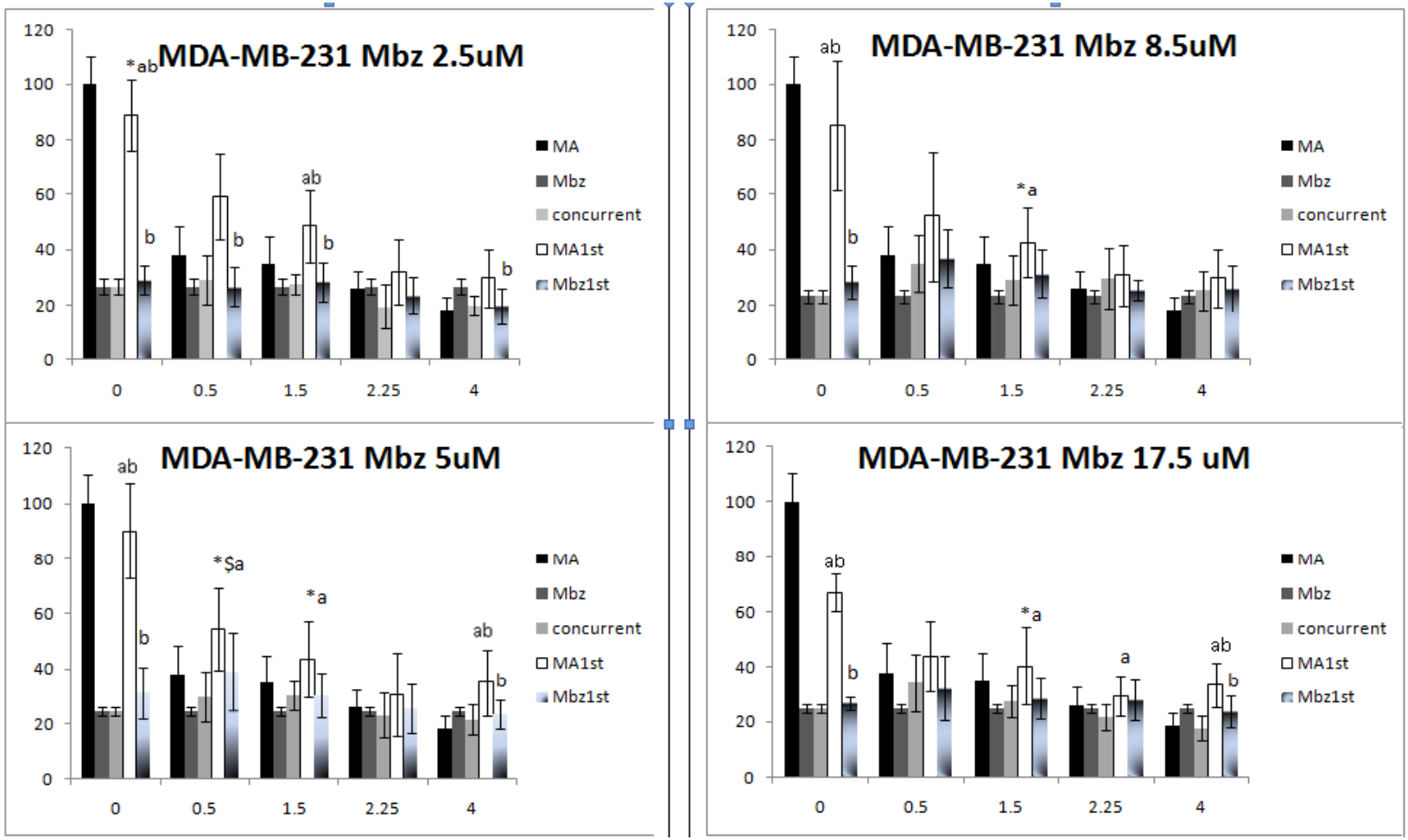

Figure 5-10: In vitro single agent and combination treatment with MA and Mbz in wild type MDA-MB-231 breast cancer cell line; x axis is MA concentration in uM, y axis is percent cell viability determined by sulforhodamine blue (The statistical significance of the difference between treatment groups was determined using one way ANOVA followed by Tuckey's test with $p<0.05$. $: significantly different from MA alone, *: significantly different from Mbz alone, a: significantly different from concurrent, b: significantly different from the other sequence). (n=24 from three independent runs).

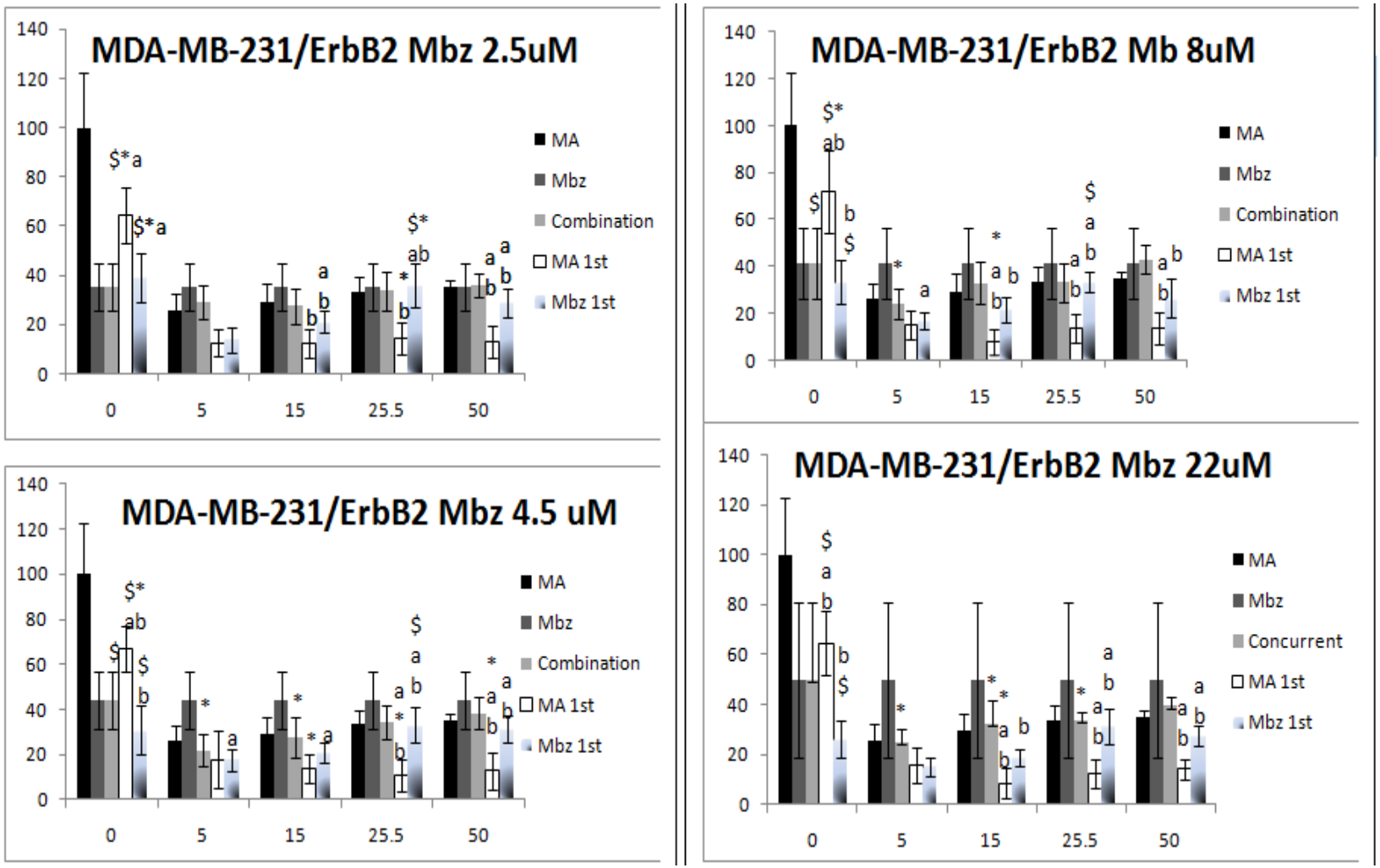

Figure 5-11: In vitro single agent and combination treatment with MA and Mbz in HER2 transfected cells MDA-MB-231/ErbB2 breast cancer cell line; x axis is MA concentration in uM, y axis is percent cell viability determined by sulforhodamine blue (The statistical significance of the difference between treatment groups was determined using one way ANOVA followed by Tuckey's test with $p<0.05$. $: significantly different from MA alone, *: significantly different from Mbz alone, a: significantly different from concurrent, b: significantly different from the other sequence). (n=24 from three independent runs).

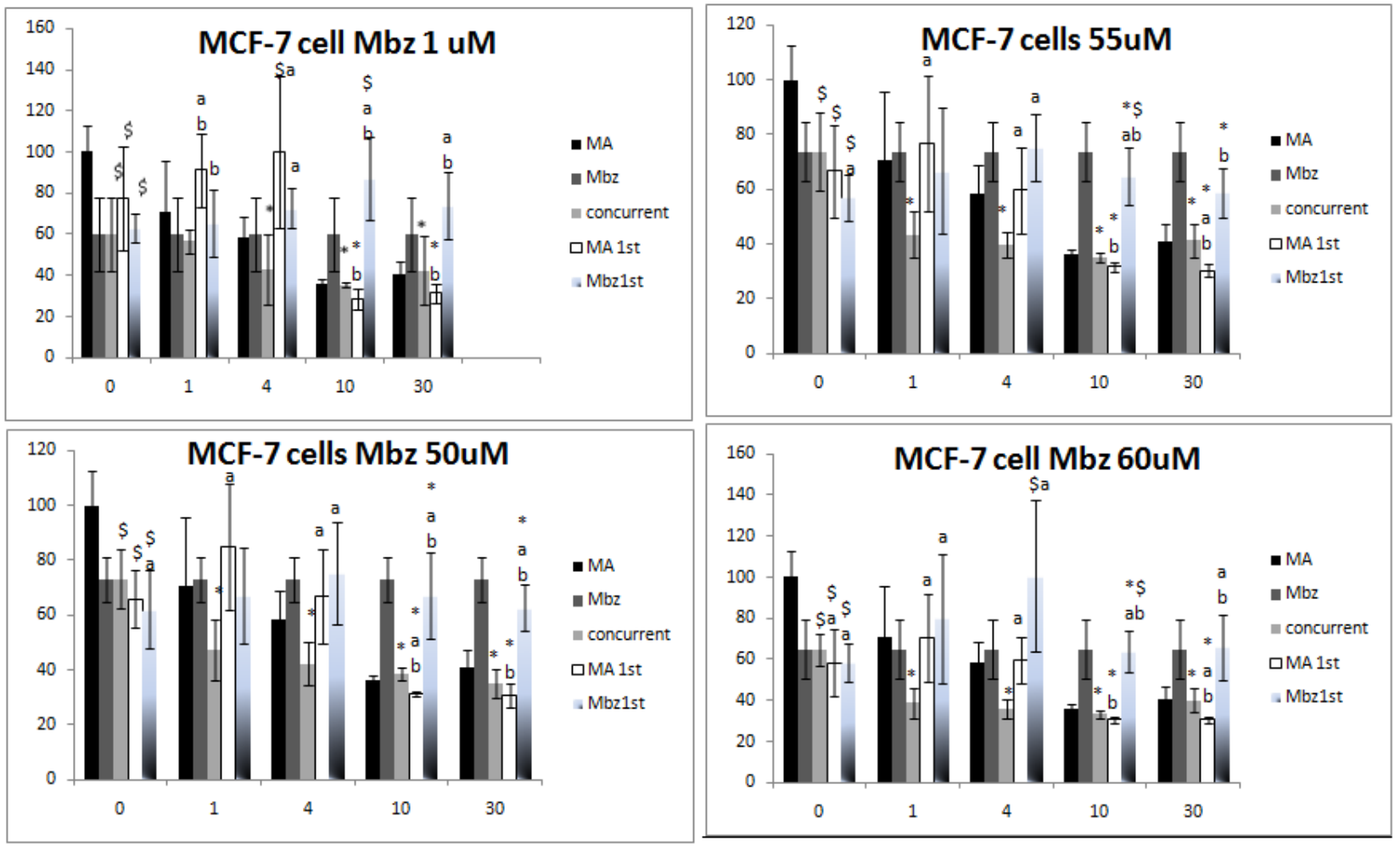

Figure 5- 12: In vitro single agent and combination treatment with MA and Mbz in wild type MCF-7 breast cancer cell line; x axis is MA concentration in uM, y axis is percent cell viability determined by sulforhodamine blue (The statistical significance of the difference between treatment groups was determined using one way ANOVA followed by Tuckey's test with $p<0.05$. $: significantly different from MA alone, *: significantly different from Mbz alone, a: significantly different from concurrent, b: significantly different from the other sequence). (n=24 from three independent runs).

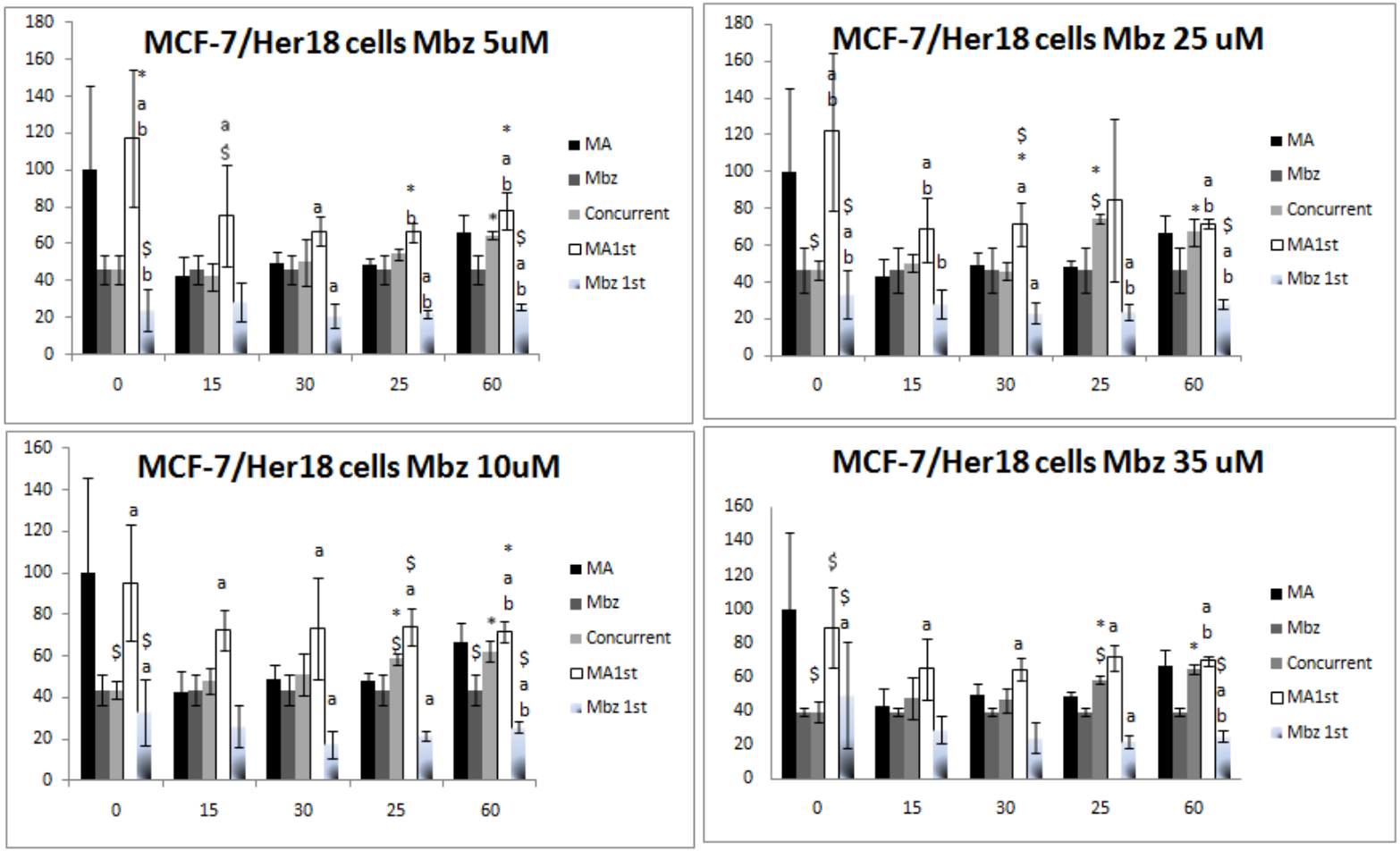

Figure 5-13: In vitro single agent and combination treatment with MA and Mbz in HER2 transfected MCF-7/Her18 breast cancer cell line; x axis is MA concentration in uM, y axis is percent cell viability determined by sulforhodamine blue (The statistical significance of the difference between treatment groups was determined using one way ANOVA followed by Tuckey's test with $p<0.05$. $: significantly different from MA alone, *: significantly different from Mbz alone, a: significantly different from concurrent, b: significantly different from the other sequence). (n=24 from three independent runs).

Cell line	Synergism	Consistent with CalcuSyn
MDA-MB-231	**No synergism**	
MDA-MB-231/ErbB2	**MA** 1^{st}	**yes**
MCF-7	**No synergism**	
MCF-7/Her18	**Mbz**1^{st}	**yes**

Table 5-2- Summary of results for single and combination treatment experiments.

5-B- Assessing the role of cell cycle arrest and apoptosis in the cytotoxicity of combined MA and Mbz treatments in the four breast cancer cell lines:

To explain the observed difference in treatment effect of various MA and Mbz combinations in wild type and HER2 transfected MDA-MB-231 and MCF-7 breast cancer cell lines, we investigated the effect each treatment has on cell cycle and the influence of apoptotic cell death on the final outcome using flow cytometry and western blot.

5-B-1- Flow cytometry to cell cycle arrest and apoptosis:

After treating wild type and HER2 transfected MDA-MB-231 and MCF-7 breast cancer cells with the different treatment groups, the cells were fixed with ethanol and stained with propidium iodide (PI), a nucleic acid dye, to determine the different cell cycle stages and the cell cycle arrest each treatment group has on these cell lines. In another set of experiments, the cells were harvested and stained with Annexin-V-FITC post treatment, to determine the extent of cells undergoing apoptosis.

5-B-1a-Flow Cytometry using propidium iodide staining to determine cell cycle arrest:

Flow cytometry studies using PI showed that Mbz arrests the cells at the G2/M phase in both cell lines [Figures5: 14-17], this is manifested by an increase in the proportion of cells in the G2/M phase following treatment with Mbz alone both in wild type and HER2 transfected cells. MA on the other hand, induced a cell cycle arrest at different phases of the cell cycle in MDA-MB-231 compared to MCF-7 cell lines.

When used alone, MA arrested the wild type and HER2 transfected MDA-MB-231 cells at the G_2/M-phase [Figures 14 & 15]. This is observed as a significant increase in the proportion of cells in the G2/M phase at the expense of the cells in the G1 phase. In both wild type and HER2 transfected cells no significant difference between concurrent and MA alone treatments was observed when comparing cell percentages in the different cell cycle phases. This explains our previous results showing no significant difference in percent viability of cells in these two groups stated above (section 5-A-2b- 2).

In MDA-MB-231 cells an increase in the subdiploid portion was observed with single agent Mbz treatment (20%) compared to all other groups (< 10%). This increase was not statistically significant. Since the subdiploid portion presents apoptotic and necrotic cells, the small percentage of cells in subdiploidy indicates a minimal role for apoptosis in cell killing in all treatment groups in this cell line. Cell cycle analysis of MDA-MB-231/ErbB2 cells show that 20% of cells treated with single agent Mbz or Mbz 1^{st}, 10% of cells treated with MA and Mbz concurrently, and less than 5% of cells treated with single agent MA or MA 1^{st} are in the subdiploid portion. Due to the strong evidence in literature indicating that HER2 inhibits apoptosis we do expect the majority of these cells to be necrotic rather than apoptotic.

Comparing MA 1^{st} treatment group in MDA-MB-231/ErbB2 cells with concurrent and Mbz 1^{st} treatments reveals that MA 1^{st} triggered an increase in S and G2/M phases, while the other two treatments did not affect the percentage of cells in S phase [Figure 15].

In MCF-7 breast cancer cell lines treatment with single agent MA arrested the cells at G_1/S phase, an increase in the proportion of cells in the S phase was observed. The difference in the cell percentage in any of the cell cycle phases in concurrent and MA alone groups was insignificant. MA 1^{st} treatment showed a significant increase in subdiploid portion compared to other treatments. Mbz 1^{st} treatment showed a significant decline in the percentage of cells in the G1 and S phases and a significant increase in the

G2/M phase compared to the other two combinations [Figure 16]. MA arrested the cells at G_1/S phase and increased the proportion of cells in the S phase in MCF-7/Her18 cells.

Our final conclusion obtained from flow cytometry using PI staining is that MA arrests the two breast cancer cell lines MDA-MB-231 and MCF-7 at different stages, yet the expression of HER2 did not have an effect on MA cell cycle arrest. Also due to the low percentage of cells in the subdiploid portion, one can predict that apoptosis does not have a crucial role in cell death with MA and Mbz treatment in wild type and HER2 transfected MDA-MB-231 and MCF-7 breast cancer cell lines.

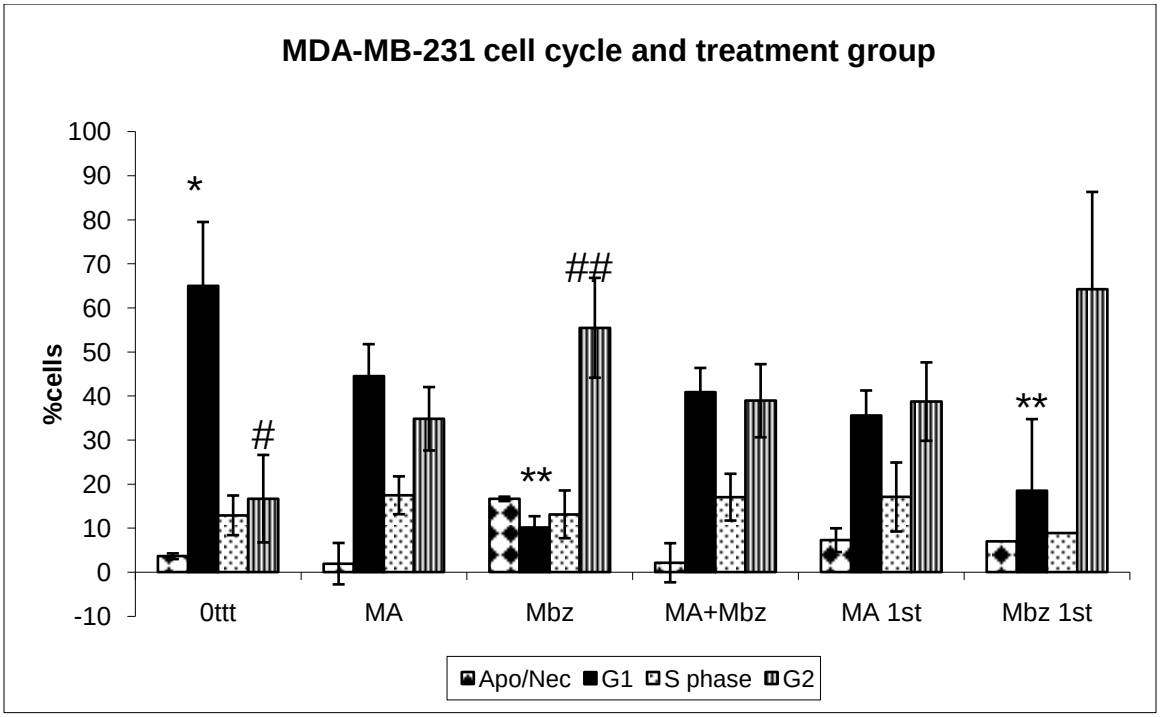

Figure 5-14- Cell cycle analysis in wild type MDA-MB-231 breast cancer cells. Cells were treated with the different treatments at MA concentration of 10uM and Mbz concentration of 5uM. 48hr after treatment cells were fixed with ethanol, stained with propidium iodide and analyzed by flow cytometry. The percentage of cells in each cell cycle stage is presented as mean $\pm$ SD from four independent runs. Data was analyzed using one-way ANOVA followed by Tukey's test at $p < 0.05$. (n=4 for each treatment group).

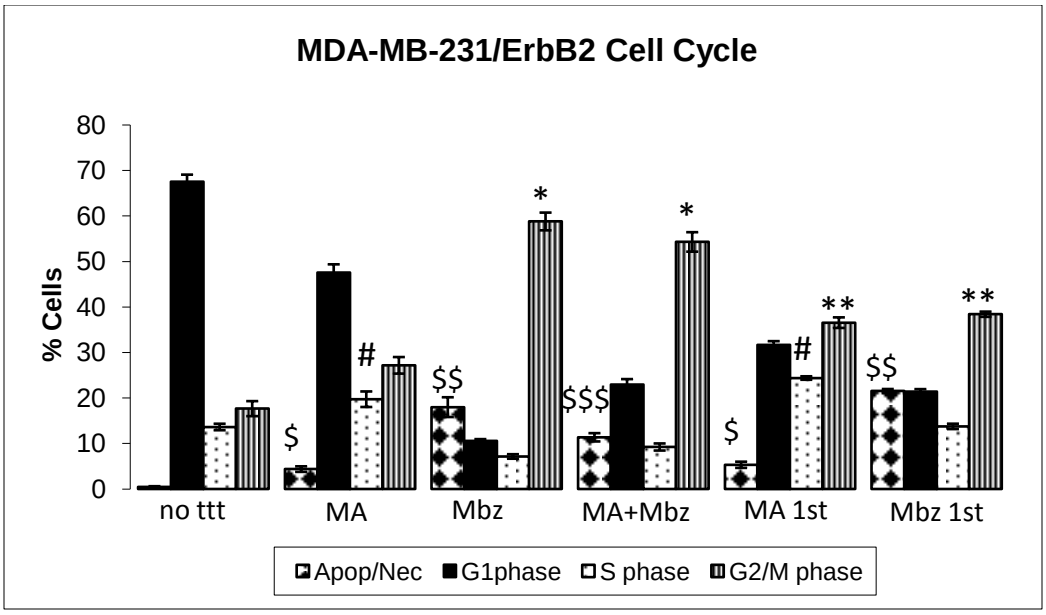

Figure 5- 15- Cell cycle analysis in MDA-MB-231/ErbB2 breast cancer cells. Cells were treated with the different treatments at MA concentration of 5uM and Mbz concentration of 1.25uM. 48hr after treatment cells were fixed with ethanol, stained with propidium iodide and analyzed by flow cytometry. The percentage of cells in each cell cycle stage is presented as mean $\pm$ SD from three independent runs. Data was analyzed using one-way ANOVA followed by Tukey's test at $p < 0.05$. (n=3 for each treatment group).

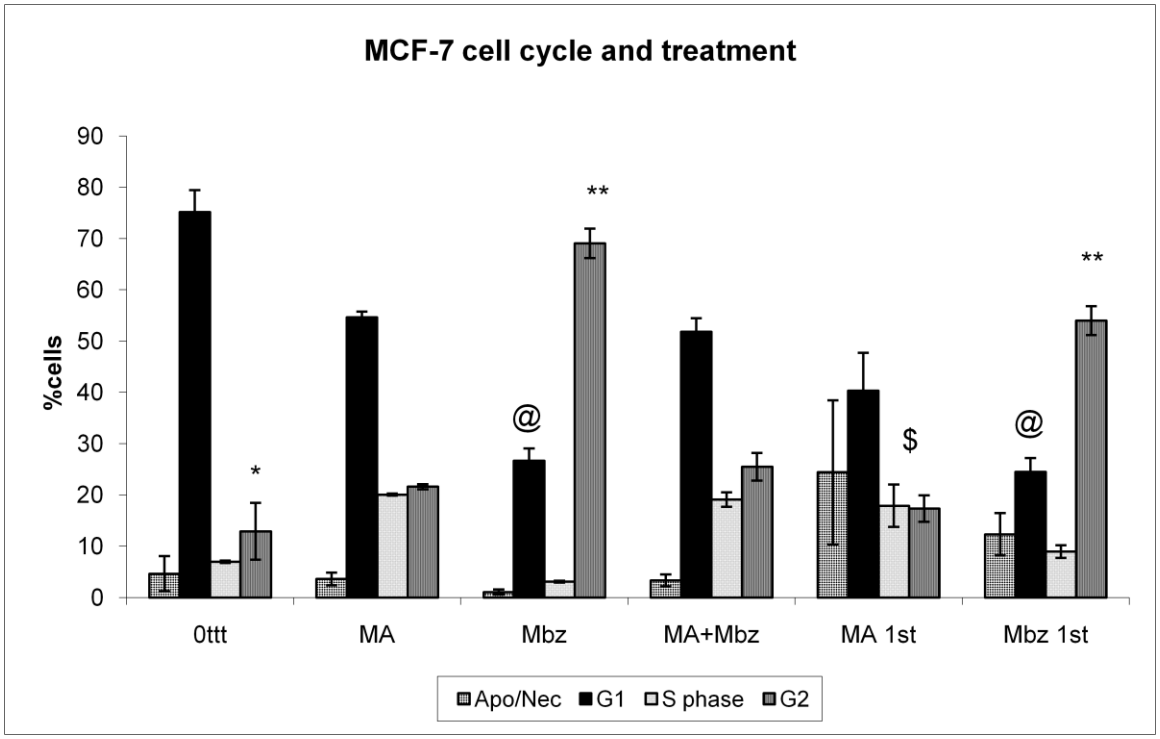

Figure 5-16- Cell cycle analysis in wild type MCF-7 breast cancer cells. Cells were treated with the different treatments at MA concentration of 10uM and Mbz concentration of 5uM. 48hr after treatment cells were fixed with ethanol, stained with propidium iodide and analyzed by flow cytometry. The percentage of cells in each cell cycle stage is presented as mean $\pm$ SD from four independent runs. Data was analyzed using one-way ANOVA followed by Tukey's test at $p< 0.05$. (n=4 for each treatment group).

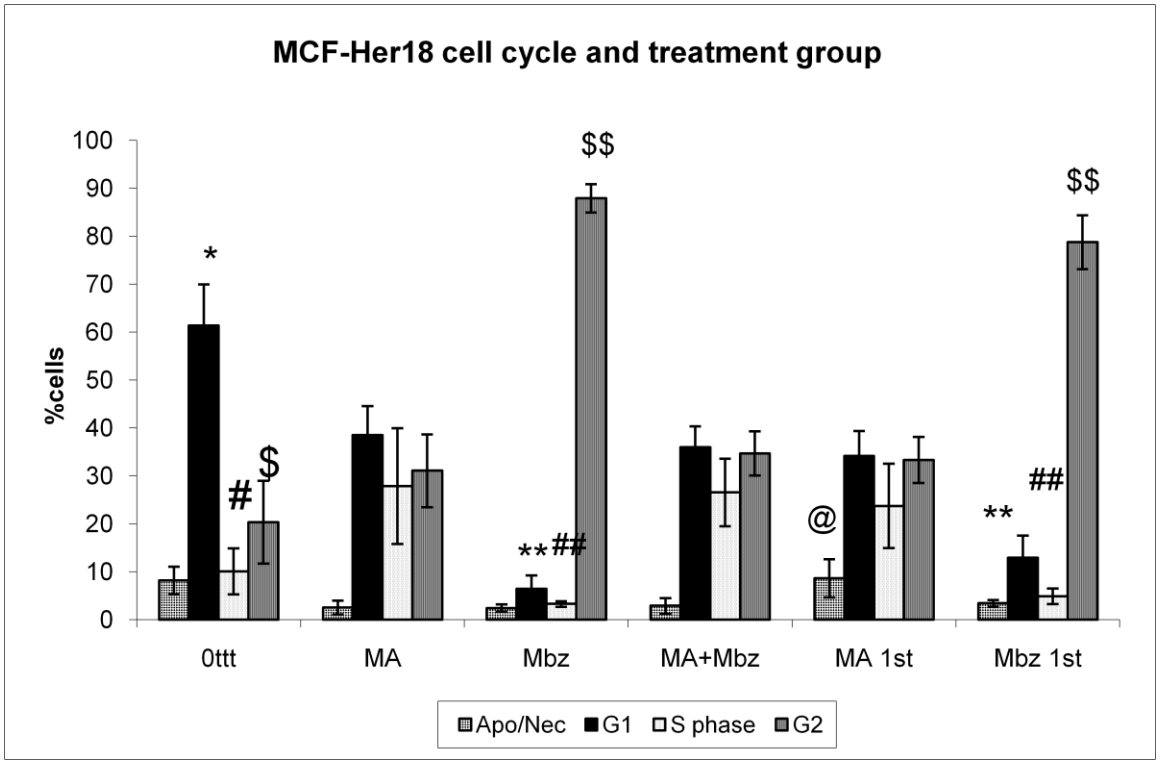

Figure 5-17- Cell cycle analysis in MCF-7/Her18 breast cancer cells. Cells were treated with the different treatments at MA concentration of 10uM and Mbz concentration of 5uM. 48hr after treatment cells were fixed with ethanol, stained with propidium iodide and analyzed by flow cytometry. The percentage of cells in each cell cycle stage is presented as mean $\pm$ SD from four independent runs. Data was analyzed using one-way ANOVA followed by Tukey's test at $p< 0.05$. (n=4 for each treatment group).

5-B-1b- Flow cytometry using Annexin-V-FITC staining to detect apoptosis:

Since MA 1st treatment was superior to other treatment groups in MDA-MB-231/ErbB2 breast cancer cells we wanted to evaluate the role of apoptosis in enhancing cytotocixity in this combination and to compare it to other treatment groups. Cells were treated with single agent MA (5µM), single agent Mbz (1.25µM) or one of the combinations. Cells were harvested 12 or 24 hours after treatment, then stained by Annexin V-FITC and PI for flow cytometry analysis. No significant difference in Annexin staining was observed among the different treatment groups, indicating that apoptosis did not occur neither at 12 nor 24 hours of treatment [Figures 5- 18].

We chose the MCF-7 cells pair to study the difference in the level of apoptotic cell death between wild type and HER2 transfected cells. Both wild type and HER2 transfected MCF-7 cancer cells were treated with MA (10µM), Mbz (5µM) or one of the combinations. Cells were harvested 12 or 24 hours after treatment, then were stained Annexin V-FITC and PI for flow cytometry analysis. Data did not show any significant difference in the staining with Annexin among the different treatment groups, indicating that apoptosis did not occur neither at 12 nor 24 hours of treatment [Figures 5-19 and 20]. The expression of HER2, a pro-proliferation protein, inhibits apoptosis, thus this result is expected.

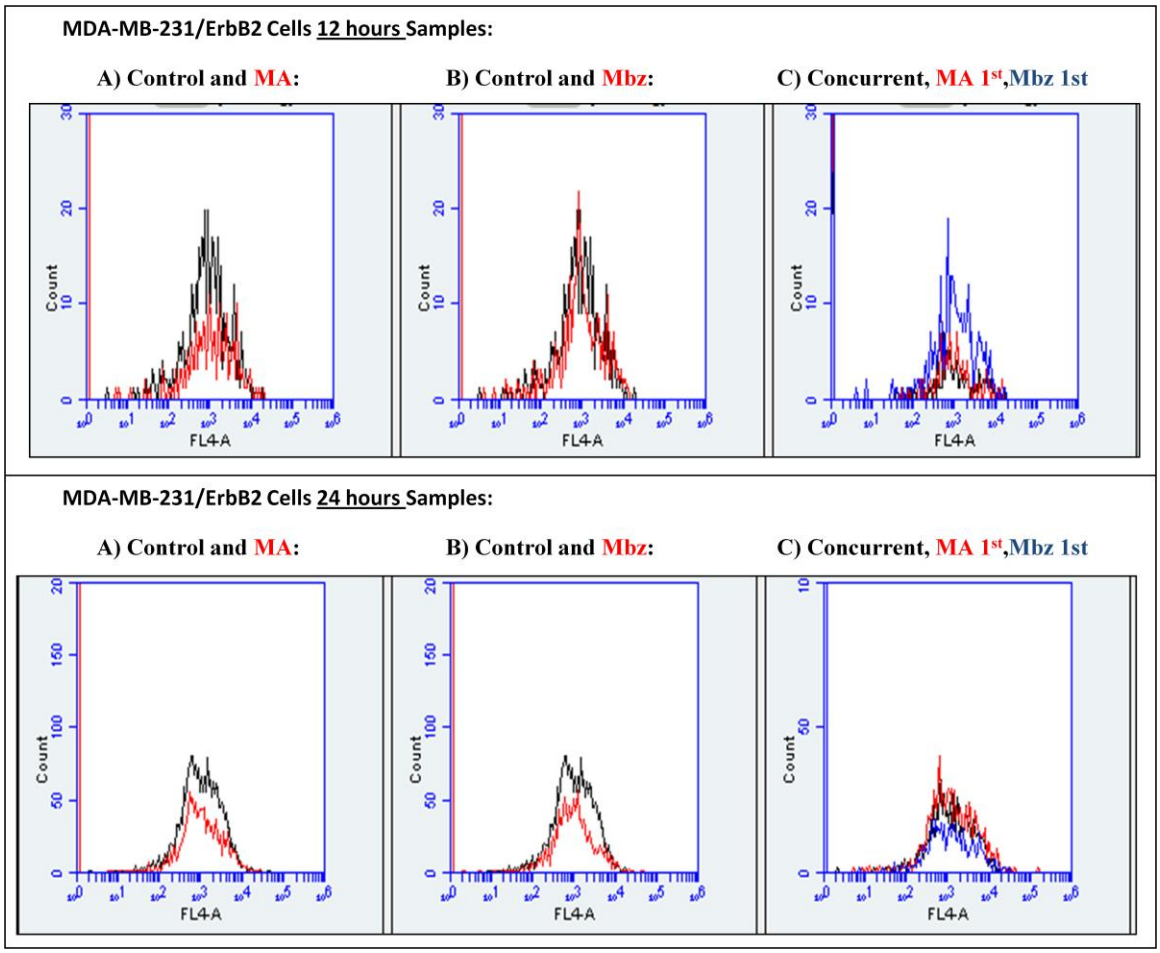

Figure 5-18: HER2 transfected MDA-MB-231/ErbB2 breast cancer cell lines. Cells were treated and harvested 12 (upper panel) or 24 (lower panel) hours after treatment then stained with Annexin V-FITC and PI for flow cytometry. A) visual gain data for control (black) and single agent MA (red) treatment. B) visual gain data for control (black) and single agent Mbz (red) treatment. C) visual gain data for Concurrent (black), MA 1st (red) and Mbz 1st (blue) treatments. No difference was observed between treatment groups. Data presented is from one sample, all four samples gave similar results (n=4 from two independent runs).

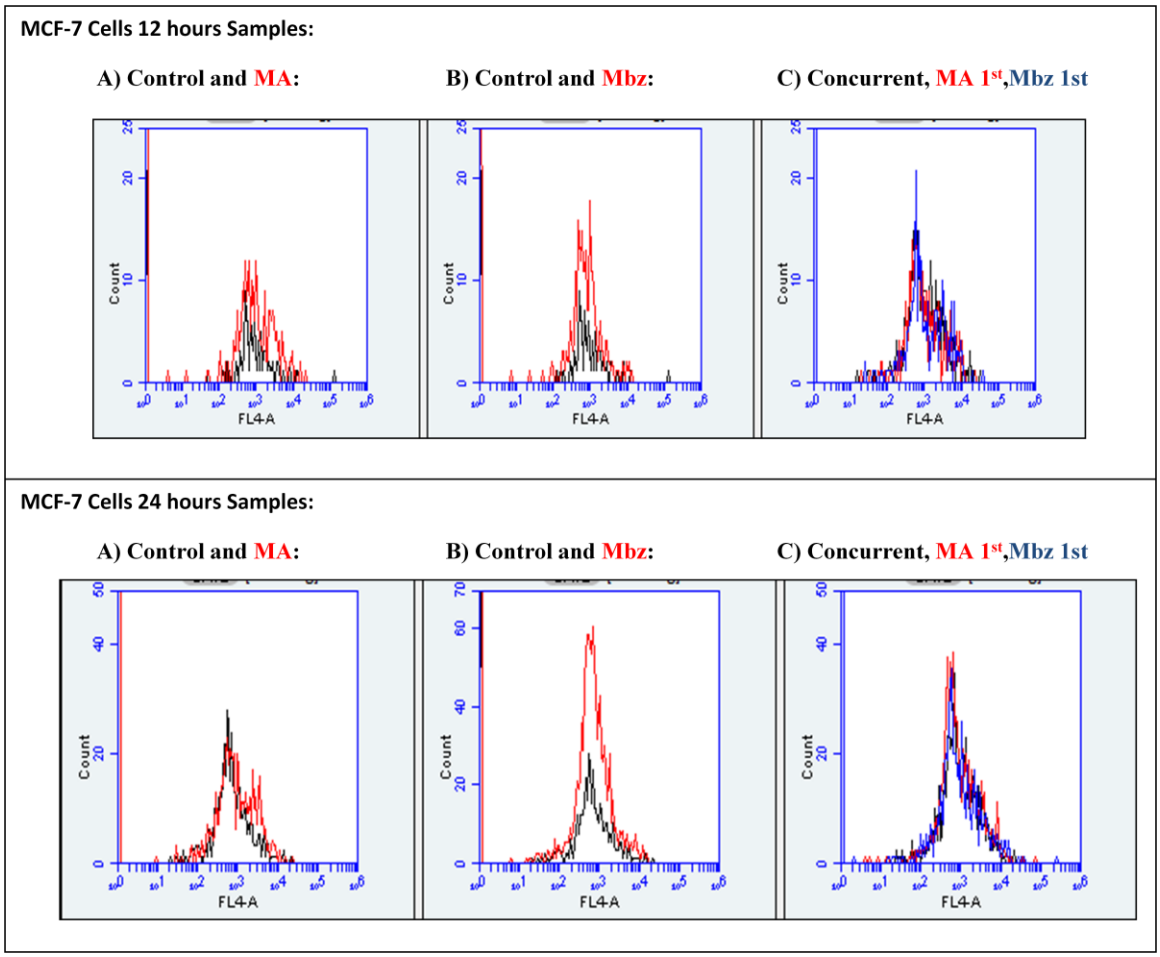

Figure 5-19: Wild type MCF-7 breast cancer cell lines. Cells were treated and harvested 12 (upper panel) or 24 (lower panel) hours after treatment then stained with Annexin V-FITC and PI for flow cytometry. A) visual gain data for control (black) and single agent MA (red) treatment. B) visual gain data for control (black) and single agent Mbz (red) treatment. C) visual gain data for Concurrent (black), MA 1st (red) and Mbz 1st (blue) treatments. No difference was observed between treatment groups. Data presented is from one sample, all four samples gave similar results (n=4 from two independent runs).

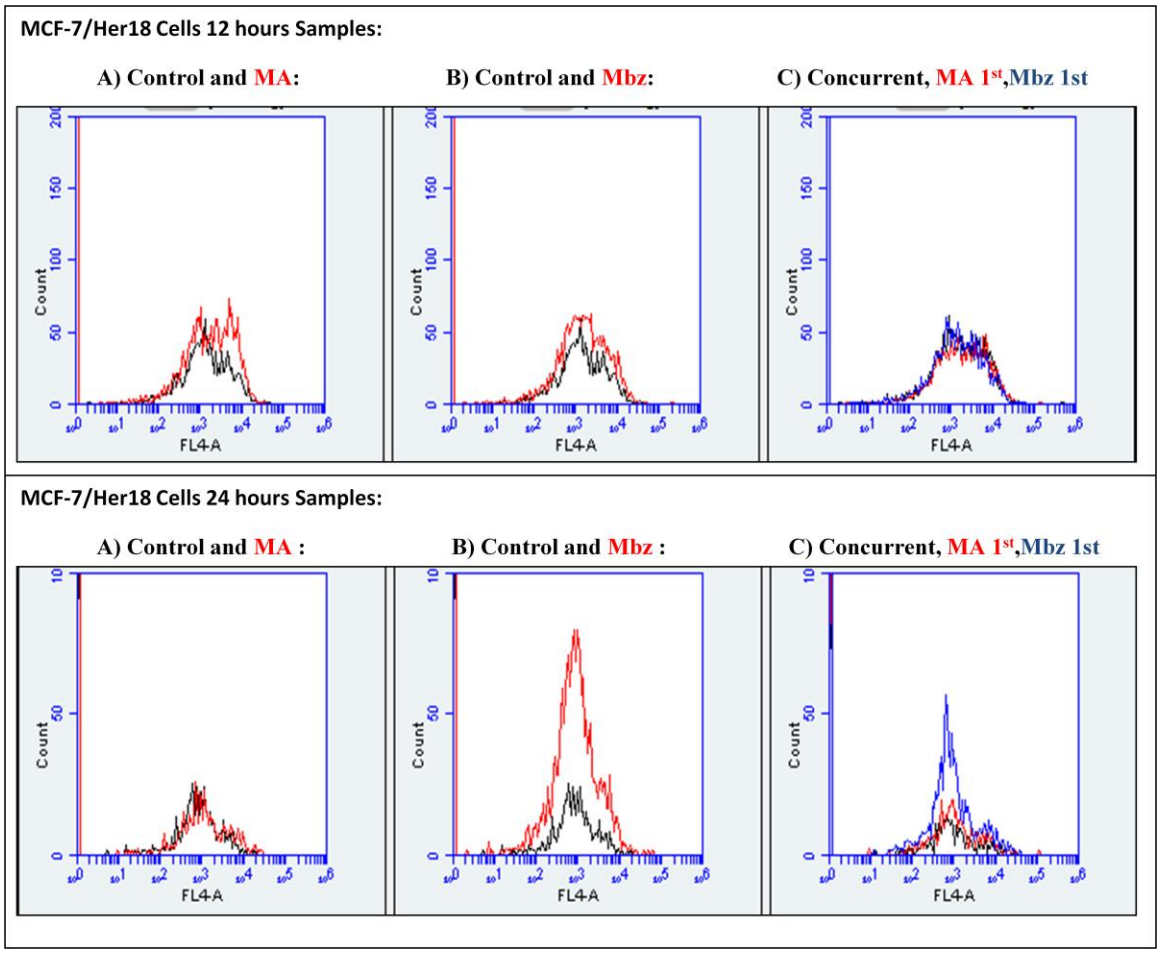

Figure 5-20: HER2 transfected MCF-7/Her18 breast cancer cell lines. Cells were treated and harvested 12 (upper panel) or 24 (lower panel) hours after treatment then stained with Annexin V-FITC and PI for flow cytometry. A) visual gain data for control (black) and single agent MA (red) treatment. B) visual gain data for control (black) and single agent Mbz (red) treatment. C) visual gain data for Concurrent (black), MA 1st (red) and Mbz 1st (blue) treatments. No difference was observed between treatment groups. Data presented is from one sample, all four samples gave similar results (n=4 from two independent runs).

5-B-2- Western blotting for cleaved PARP, Cyclin E, and Cyclin B to determine the role of apoptosis and cell cycle arrest in MA and Mbz cytotoxicity in single and combination treatment:

To evaluate the role of cell cycle arrest and apoptosis in MA and Mbz cytotoxicity, wild type and HER2 transfected MDA-MB-231 and MCF-7cells were treated with MA and Mbz as single agents or in combination. The cells were harvested at different time points. A thorough literature review revealed that the proteins probed for (cleaved PARP, Cyclin E and Cyclin B) are detected within 12-18hrs after treatment with agents that induce apoptosis or cell cycle arrest. Cells were harvested at 6, 12 and 24 hours after treatment. Sequential treatment groups were treated with MA or Mbz for half the duration, then washed with PBS and treated with the second agent for the other half. Cells were harvested, lysed and protein levels assayed. Then the samples were electrophoresed and transferred to nitrocellulose membranes and probed for proteins according to the protocol described in methods section (4-B-2b). Protein bands' density was quantified using the FluorChem8900 software from Alpha Ease, and was normalized in reference to β-actin. The samples were blotted in triplicates and presented as mean of fold increase compared to no treatment $\pm$ SD.

According to our flow cytometry analysis both wild type and HER2 transfected MDA-MB-231 cells undergo G2/M phase cell cycle arrest after treatment with single agent MA or Mbz or the combination. Our flow cytometry analysis show that both wild

type and HER2 transfected MCF-7 cells undergo G1/S phase and G2/M phase cell cycle arrest after treatment with single agent MA, and single agent Mbz, respectively. To better understand the effect of combination treatment on cell cycle progression, we probed for cyclins E and B. We do expect an increase in the levels of cyclin B in treatment groups compared to control in MDA-MB-231 cells, and an increase in cyclin E with MA treatment and cyclin B with Mbz treatment in MCF-7 cells. Probing for cyclin B gave one band at 50kDa, while probing for cyclin E we got two bands, one at 46kDa presenting cyclin E and an additional band at 64kDa which we believe presents bi-ubiquitinated cyclin E. The density of the cyclin E band observed just below the 50kDa marker band will be measured and presented.

As concluded in our flow cytometry studies, apoptosis did not play a major role in MA and Mbz cytotoxicity in the studied cell lines at the concentrations used for treatment. To further support our observation we probed for the cleaved 89kDa PARP, an indicator of apoptosis. We do not expect to detect high levels of cleaved PARP at 89 kDa.

Samples for 6, 12 and 24 hour treatments were blotted to determine the change in protein levels [Data not shown]. Twelve and twenty four hour samples were run in triplicates, data is presented as mean $\pm$ standard deviation and statistical analysis for all western blot data was done using one-way ANOVA followed by Tukey's test at $p < 0.05$ [Figures 5: 21-29].

5-B-2a- MDA-MB-231 Breast Cancer Cells:

We probed for 89kDa PARP, which results from the cleavage of full length PARP (116 kDa) by caspases 3 and 7 in the final step leading to apoptosis. We detected a band at 47kDa but no band was observed at 89kDa. The 47kDa PARP band is characteristic of necrotic cell death. At 12 hours only Mbz 1st treatment showed statistically significant increase in 47kDa PARP compared to single agent treatment groups [Figure 5-21]. At 24 hours both concurrent and Mbz 1st treatments were different from MA single agent. Mbz 1st had a 3 fold increase compared to control, and 3.5 fold increase compared to MA single agent. These observations further support our conclusion that apoptosis does not play a role in cytotoxicity of both MA and Mbz in wild type MDA-MB-231 breast cancer cell line. Yet, we did not study the specificity of the bands at the 47kDa to confirm that they present PARP.

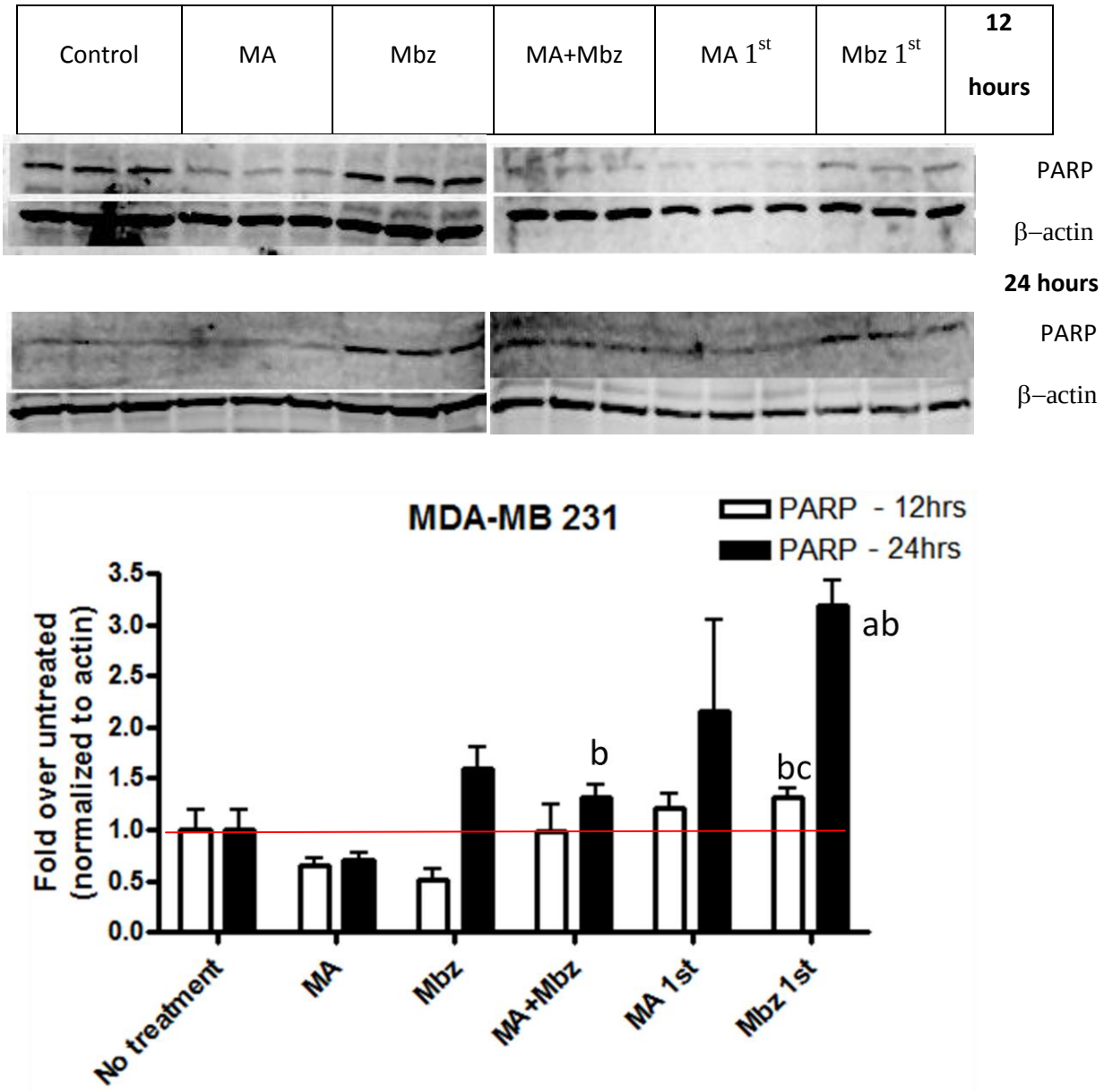

Figure 5-21- PARP in wild type MDA-MB-231 breast cancer cells detected at 47kDa. The 47kDa PARP band is detected when cells undergo secondary necrosis. Cells were treated with MA (10uM) or Mbz (5uM) or one of the combinations, samples were harvested at different time points. Samples blotted were normalized to beta actin, the fold increase over untreated cells was calculated and presented as mean $\pm$ SD. Data was analyzed using one-way ANOVA followed by Tukey's test at $p < 0.05$ (n=3).

At 12 hours Mbz 1st treatment showed a statistically significant increase in cyclin B compared to control, MA single agent and concurrent treatment groups. It was not statistically different from Mbz alone or MA 1st. Cyclin B was statistically higher in MA 1st compared to MA single agent. MA single agent had lower levels of cyclin B compared to control. At 24 hours both Mbz single agent and Mbz 1st treatments had higher levels of cyclin B compared to control, yet there was no statistical significance in the difference among the three combination treatment groups. Notice that the increase in cyclin B was observed at 12 hours with Mbz1st treatment, and only at 24 hours in Mbz single treatment [Figure 5-22].

At 12 hours cyclin E was quantifiable in control, single agent, and concurrent treatment groups. Treatment with single agent MA or Mbz reduced levels of cyclin E significantly compared to control, an indication that treatment with MA or Mbz increased cell cycle progression through G1 and S phase reflected as a decrease in cyclin E. Concurrent treatment induced a 2.5 fold increase in cyclin E levels indicating that combining MA and Mbz blocked the effectobserved with single agents on cell cycle. At 24 hours cyclin E was detected in all treatment groups. Mbz 1st was the only group different from control. Both concurrent and Mbz 1st had higher levels compared to MA single agent. The two sequential groups were statistically different. Concurrent and MA 1st were not statistically different from MA single agent, this indicates that MA is blocking any further effect of Mbz in these treatment groups [Figures 5-23].

In conclusion data obtained from cyclins B and E reveal that Mbz induced G2/M phase arrest within the first 24 hours of treatment. This effect was not observed with concurrent and MA 1st indicating that MA interferes with Mbz effect on cell cycle in wild-type MDA-MB-231 breast cancer cells.

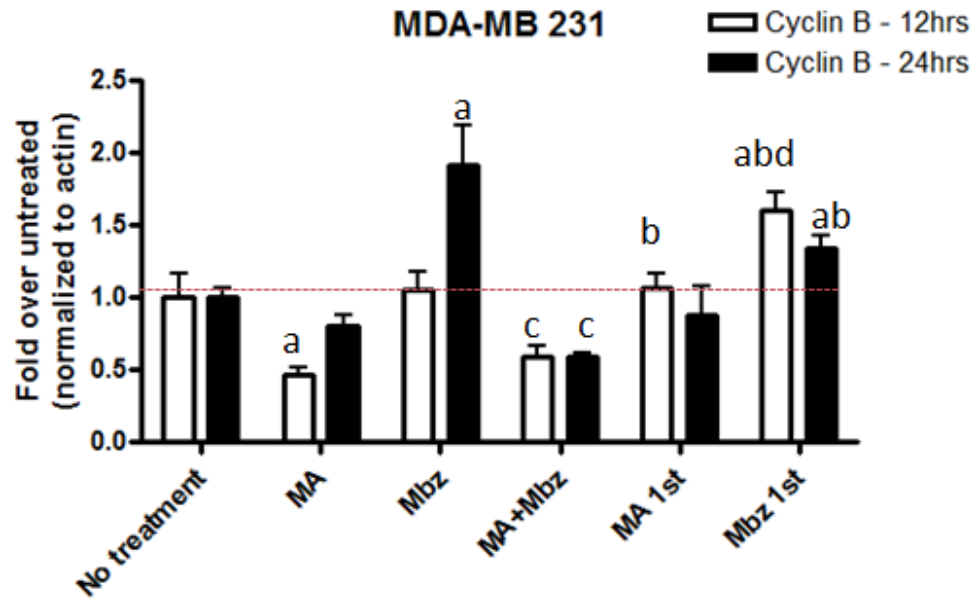

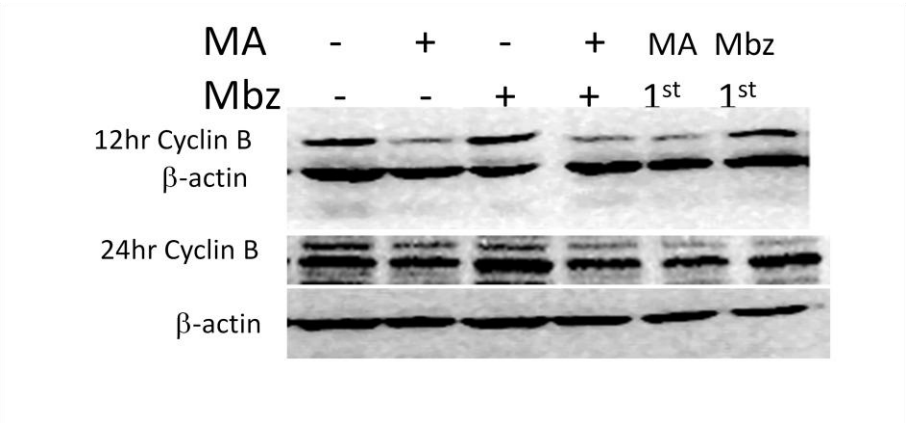

Figure 5-22- Cyclin B in wild type MDA-MB-231 breast cancer cells detected at 55 kDa. Cells were treated with MA (10uM) or Mbz (5uM) or one of the combinations, samples were harvested at different time points. Samples blotted were normalized to beta actin, the fold increase over untreated cells was calculated and presented as mean ± SD. Data was analyzed using one-way ANOVA followed by Tukey's test at $p < 0.05$ (n=3).

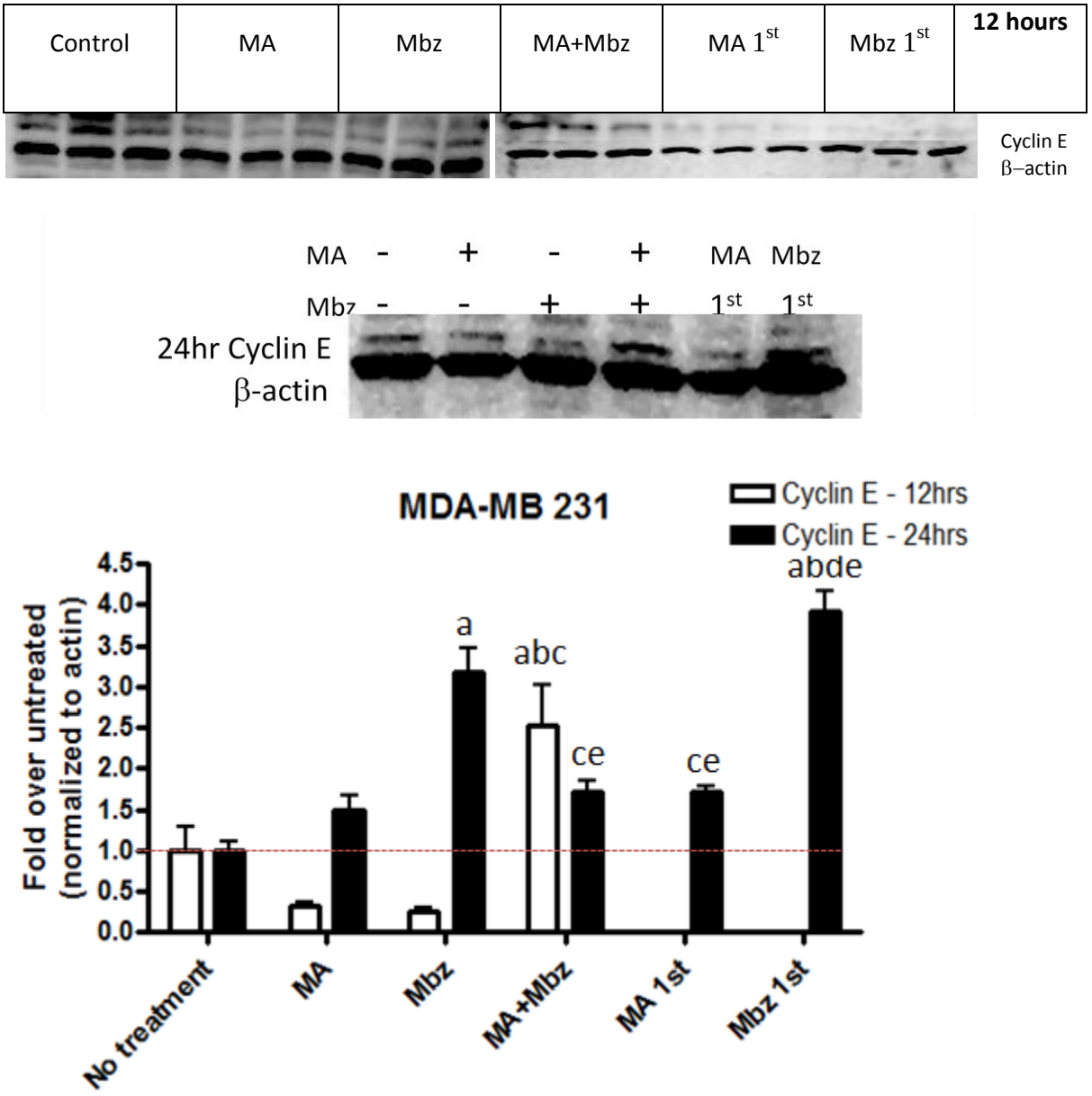

Figure 5-23- Cyclin E in wild type MDA-MB-231 breast cancer cells detected at 55 kDa. Cells were treated with MA (10uM) or Mbz (5uM) or one of the combinations, samples were harvested at different time points. Samples blotted were normalized to beta actin, the fold increase over untreated cells was calculated and presented as mean $\pm$ SD. Data was analyzed using one-way ANOVA followed by Tukey's test at $p < 0.05$ (n=3).

Immunoblots at 12 and 24 hour samples for HER-2 transfected MDA-MB-231/ErbB2 cells are presented in [Figures 5: 24 and 25]. No bands were detected after overnight incubation with anti PARP antibody. At 12 hours all treatment groups did not show any statistically significant difference in cyclin B levels except for Mbz 1st which expressed a 2 fold increase in cyclin B levels compared to control. At 24 hours both concurrent and Mbz 1st treatments showed a 3 and 4.5 fold increases in cyclin B compared to control. At 24 hours, cyclin B levels were statistically higher in concurrent and Mbz 1st groups compared to single agent and MA 1st treatments. Single agent and MA 1st treatment groups were not statistically different from control. There was no significant difference between concurrent and Mbz 1st treatments.

Only MA single agent treatment showed an increase in cyclin E levels at 12 hours. A 4.5 fold increase was observed in MA single agent compared to control. At 24 hours, there was no statistically significant difference in cyclin E levels in all treatment groups compared to control. This indicates that the effect of MA on cell cycle is blocked in the presence of Mbz in concurrent treatment. Since the increase in cyclin E observed with MA single agent is absent in MA 1st treatment and there was no difference in cyclin B levels we speculate that the enhanced cytotoxicity observed with MA 1st compared to all other treatment groups is not mediated by synergy in cell cycle arrest.

Comparing wild type to HER-2 transfected MDA-MB-231 cells revealed the following difference:

i. No PARP was detected in MDA-MB-231/ErbB2 cells contrary to the wild type.

ii. The increase in cyclin B was observed as early as 12 hours in MDA-MB-231 cells but not in MDA-MB-231/ErbB2 cells (increased at 24 hours).

iii. At 12 hours cyclin E levels were 4.5 fold higher than control in MDA-MB-231/ErbB2 cells but were lower than control in MDA-MB-231 cells in MA single agent group.

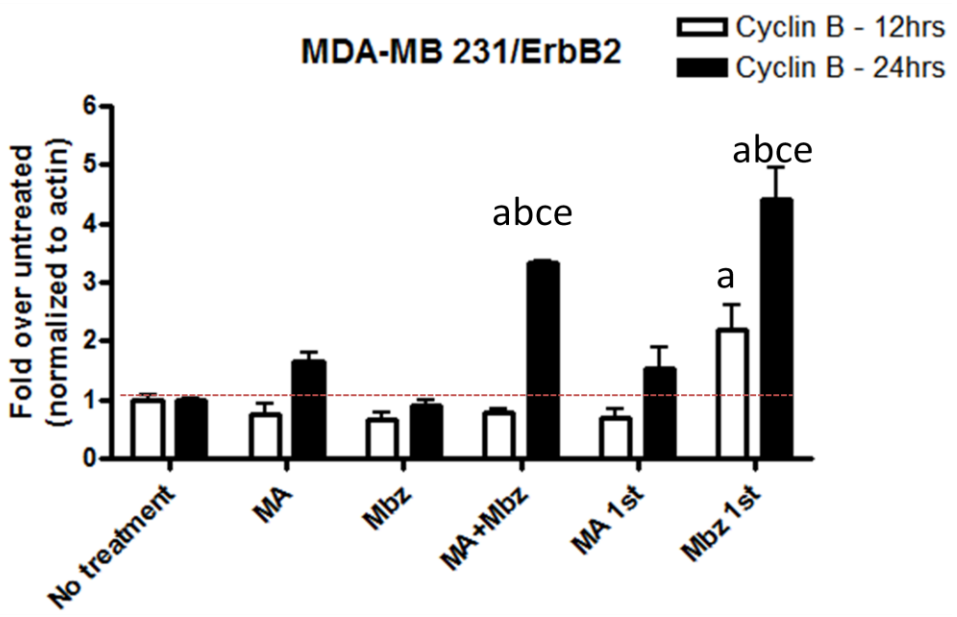

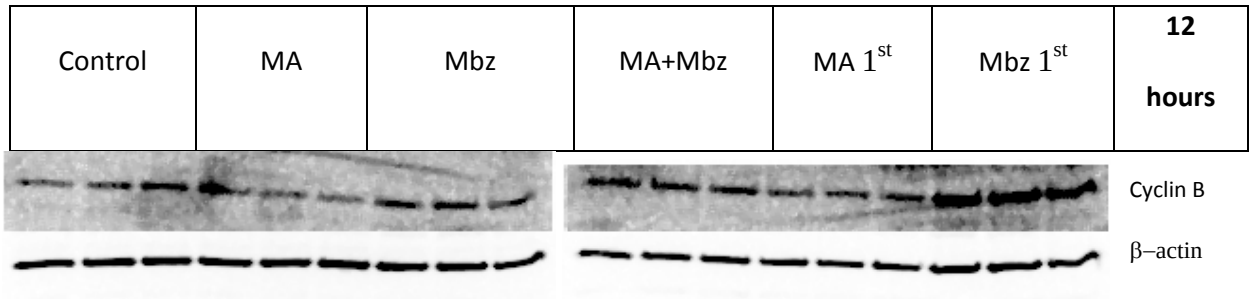

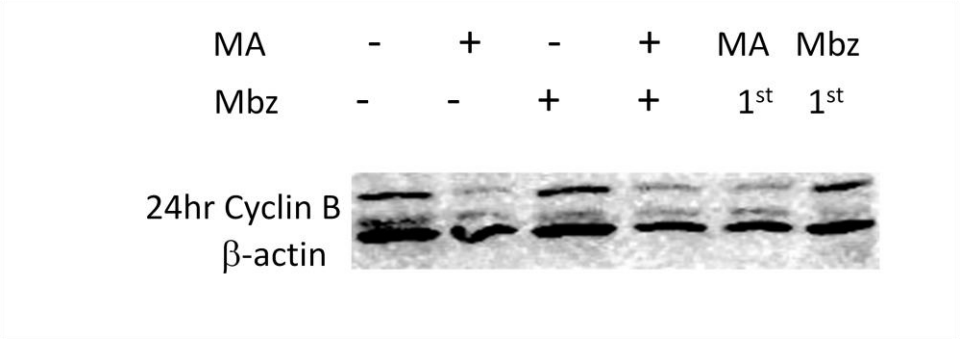

Figure 5-24- Cyclin B in HER-2 transfected MDA-MB-231/ErbB2 breast cancer cells detected at 55 kDa. Cells were treated with (5uM) MA or (1.25uM) Mbz or the combination. Band densities were normalized to β–actin and are presented as mean ± SD. Mbz 1st treatment is statistically different from control. There was no significant difference among the other treatment groups. Data was analyzed using one-way ANOVA followed by Tukey's test at $p < 0.05$ (n=3).

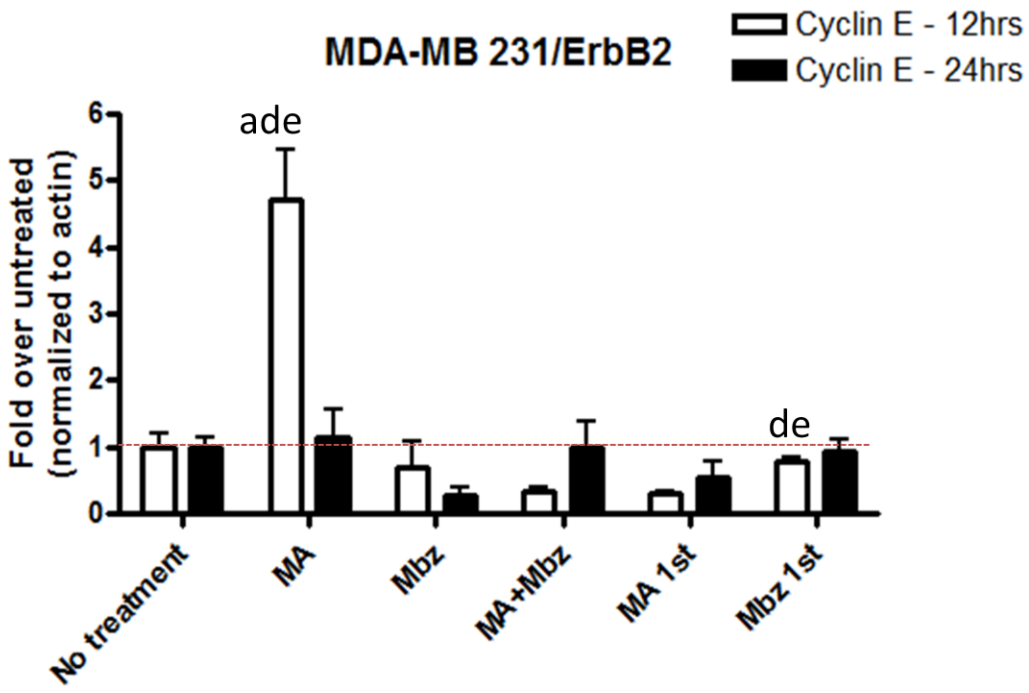

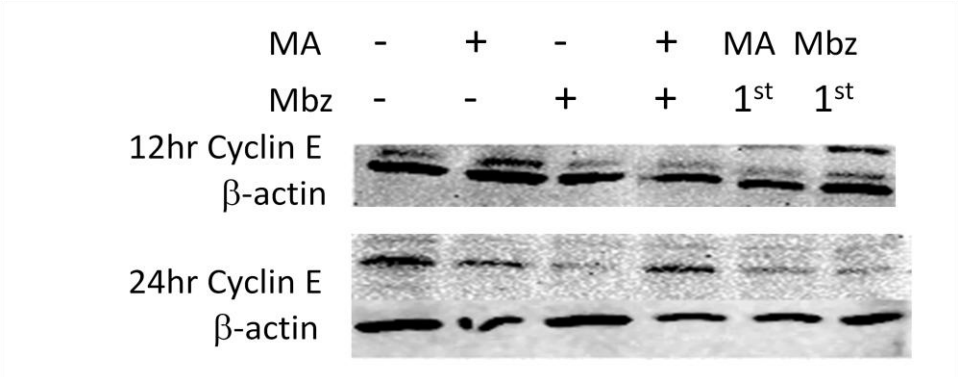

Figure 5-24- Cyclin E in HER-2 transfected MDA-MB-231/ErbB2 breast cancer cells detected at 50 kDa. Cells were treated with (5uM) MA or (1.25uM) Mbz or the combination. Band densities were normalized to β–actin and are presented as mean ± SD. Mbz 1st treatment is statistically different from control. There was no significant difference among the other treatment groups. Data was analyzed using one-way ANOVA followed by Tukey's test at $p < 0.05$ (n=3).

5-B-2b- MCF-7 Breast cancer cells:

Western blots for wild type MCF-7 cells did not show PARP bands. Cyclin B levels were only elevated in Mbz single agent treatment at 12 hours. At 24 hours Mbz single agent, concurrent and Mbz 1st treatment expressed higher levels of cyclin B compared to control. Both Mbz 1st and Mbz single agent treatments had statistically higher levels of cyclin B compared to MA single agent. Mbz 1st treatment showed 2.5 folds increase in cyclin B compared to MA 1st treatment. This could be a result of MA blocking Mbz effect when given first. We were not able to quantify cyclin E bands as very faint bands were observed [Figure 5-25].

MCF-7/Her18 cells showed PARP band at 40kDa. This band was detected in control and single treatment but not in any of the combination treatments at 12 hours. PARP levels were lower than control in both MA and Mbz single agent treatment groups. At 24 hours, we observed the bands in all treatment groups. Mbz single treatment had higher levels (1.5 folds) compared to control. All other treatment groups were not statistically different from control [Figure 5-26]. Yet, we did not determine the specificity of this band to ensure that it presents PARP. At 24 hours Mbz 1st treatment showed a 2.5 folds increase in cyclin B compared to all other treatment groups [Figure 5-27]. Levels of cyclin E were higher in control and single agent treatments at 12 hours. Both concurrent and Mbz 1st treatments showed an increase in cyclin E levels at 24 hours compared to control and MA single agent [Figure 5-28].

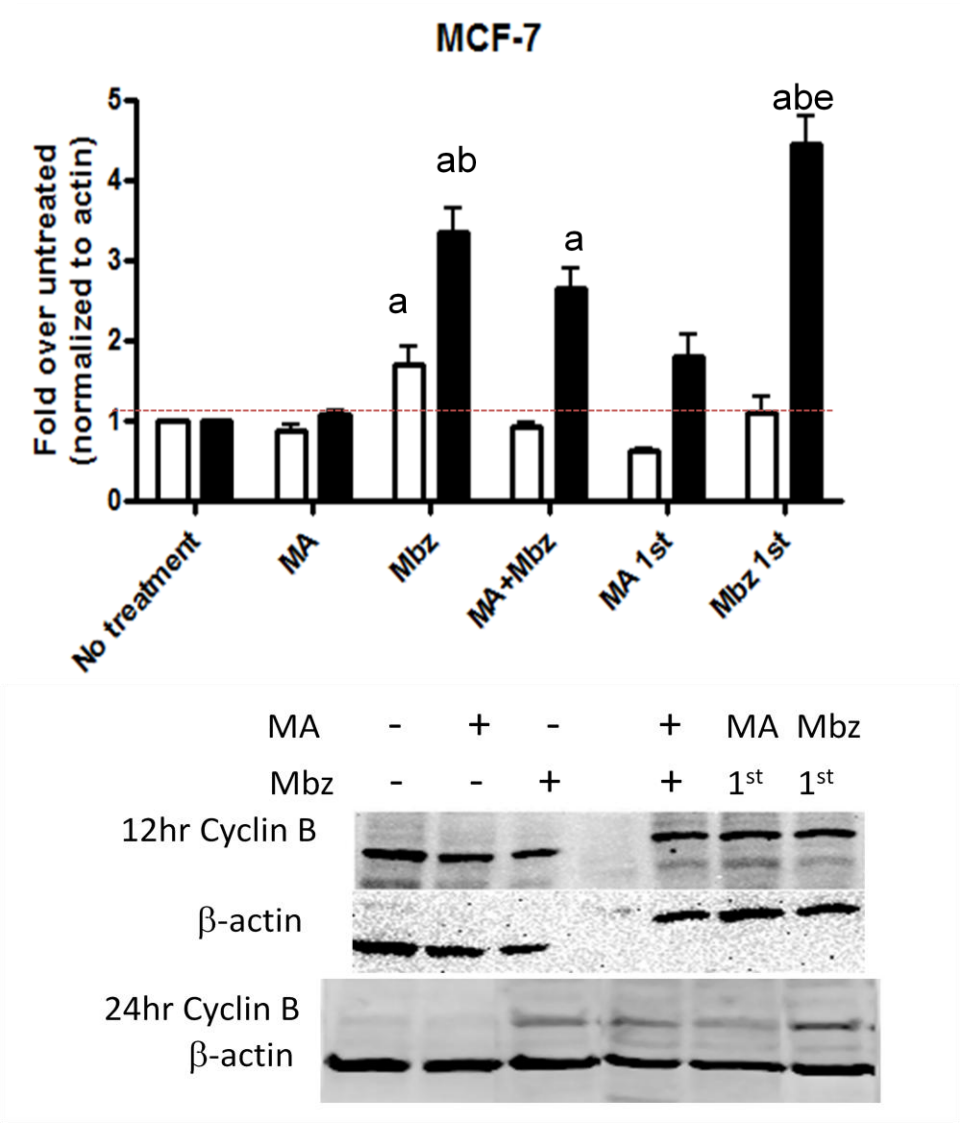

Figure 5-25- Cyclin B in MCF-7 breast cancer cells detected at 55 kDa. Cells were treated with (10uM) MA or (5uM) Mbz or the combination. Band densities were normalized to β–actin and are presented as mean of fold increase compared to control $\pm$ SD. Data was analyzed using one-way ANOVA followed by Tukey's test at $p < 0.05$ (n=3).

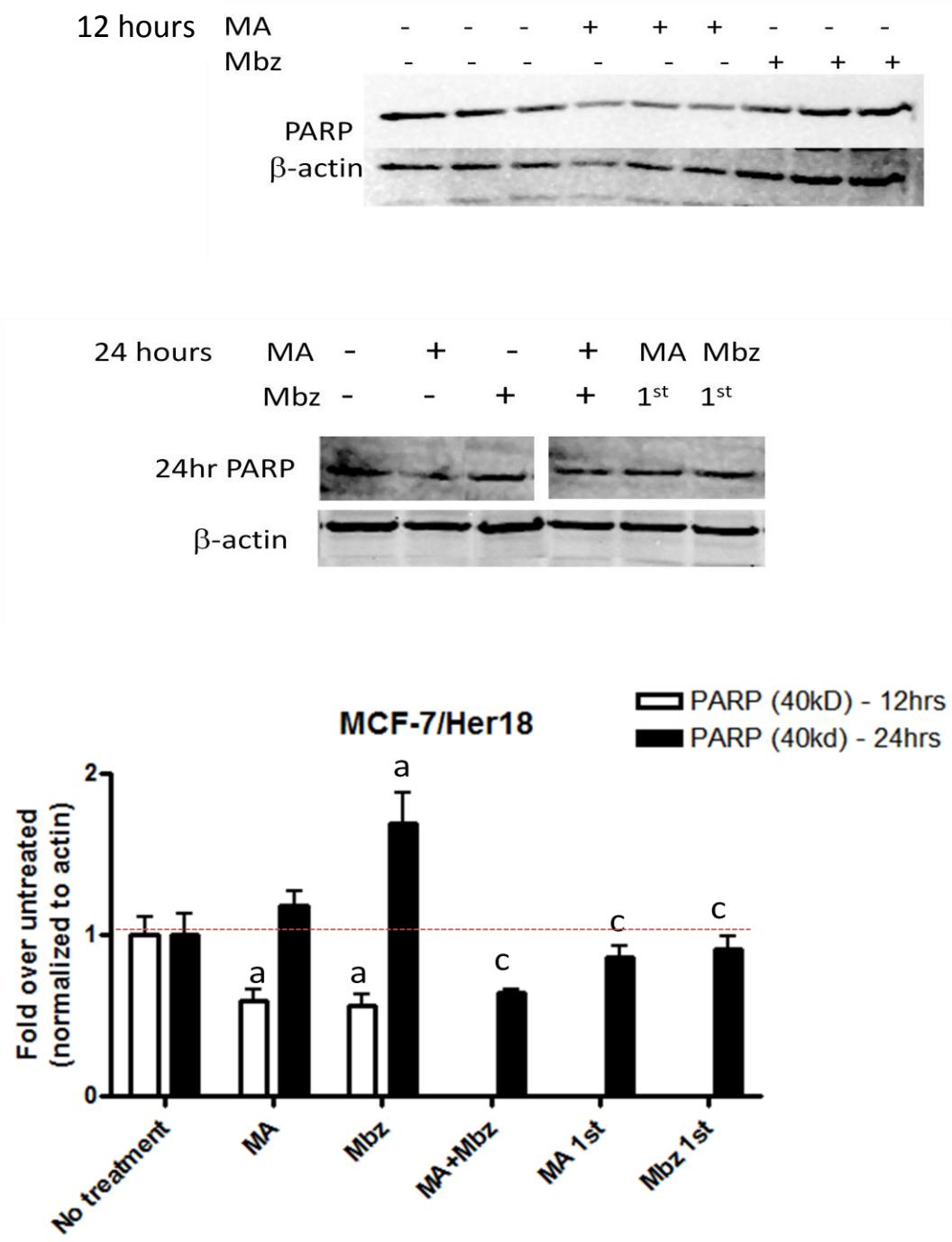

Figure 5-26- PARP in MCF-7/Her18 breast cancer cells detected at 40 kDa. Cells were treated with (10uM) MA or (5uM) Mbz or the combination. No bands were observed in combination treatment groups at 12 hours. Band densities were normalized to β–actin and are presented as mean of fold increase compared to control ± SD. Data was analyzed using one-way ANOVA followed by Tukey's test at $p < 0.05$ (n=3).

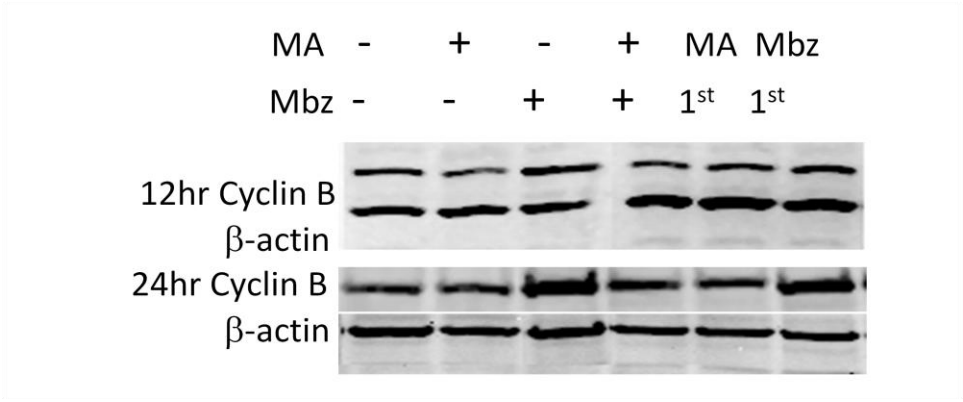

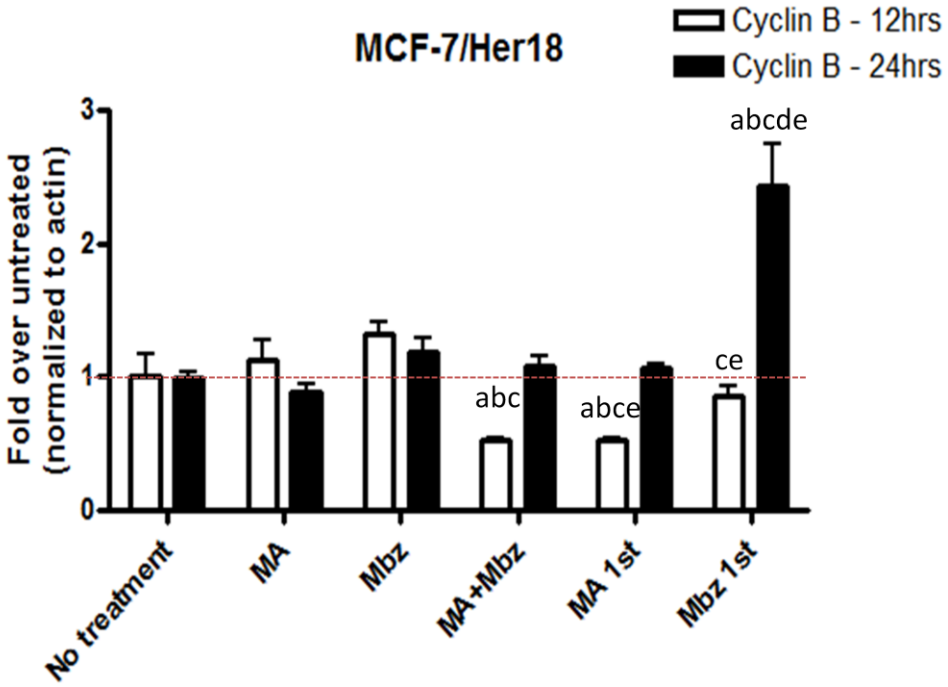

Figure 5-27- Cyclin B in MCF-7/Her18 breast cancer cells detected at 55 kDa. Cells were treated with (10uM) MA or (5uM) Mbz or the combination. Band densities were normalized to β−actin and are presented as mean of fold increase compared to control ± SD. Data was analyzed using one-way ANOVA followed by Tukey's test at $p < 0.05$ (n=3).

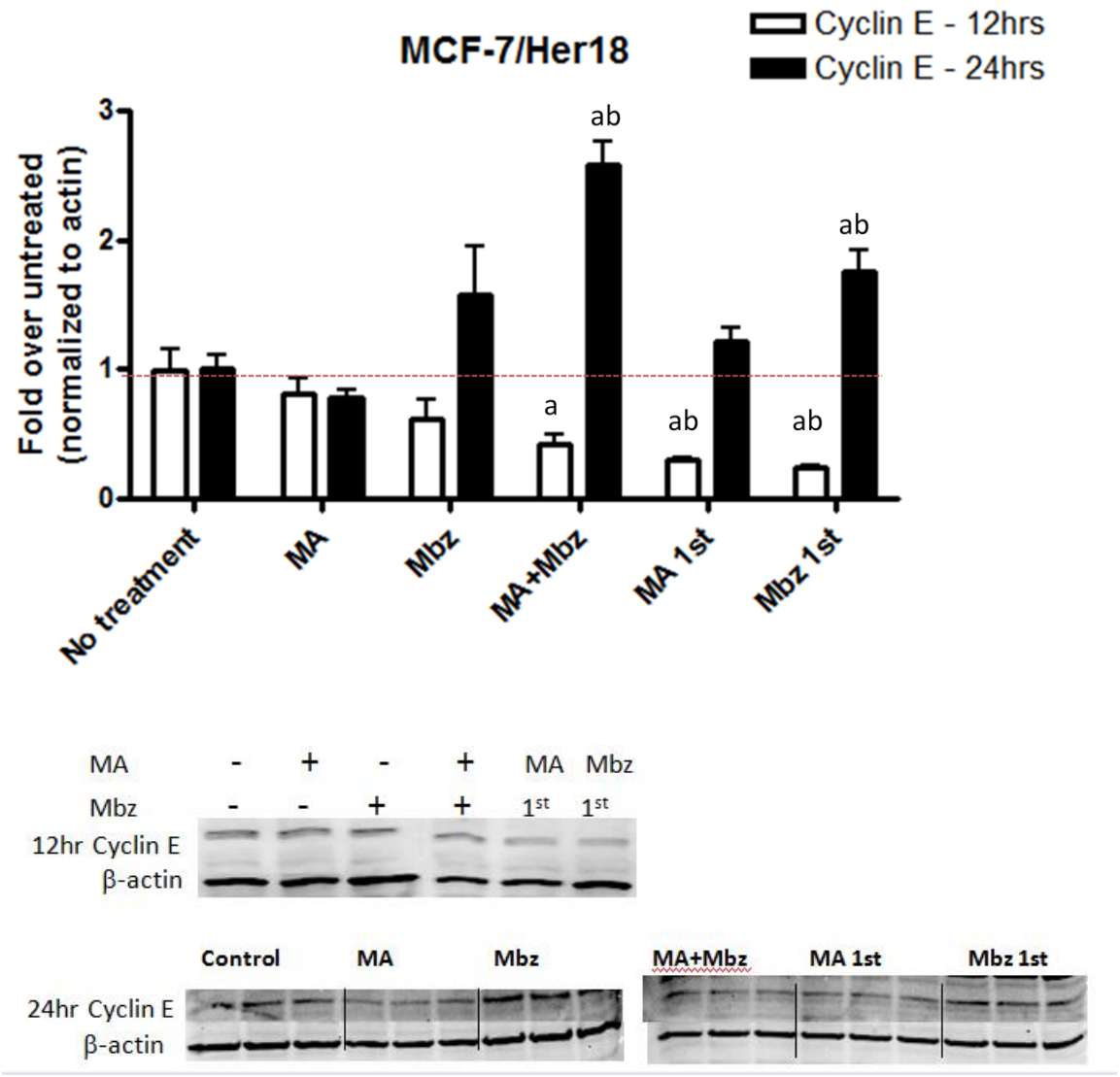

Figure 5-28- Cyclin E in MCF-7/Her18 breast cancer cells detected slightly below the 50 kDa molecular weight marker band. Cells were treated with (10uM) MA or (5uM) Mbz or the combination. Band densities were normalized to β–actin and are presented as mean of fold increase compared to control ± SD. Data was analyzed using one-way ANOVA followed by Tukey's test at $p < 0.05$ (n=3).

5-C-To determine the in vivo effect of MA and Mbz treatment using wild type and HER-2 transfected MDA-MB-231 breast cancer xenografts in nu/nu Swiss background nude mice:

5-C-1- Determining the best dose of MA and Mbz for combination therapy in vivo (dose response study in nu/nu Swiss background athymic mice):

We studied the effect of MA and Mbz as single agents against wild type and HER2 transfected MDA-MB-231 breast cancer cells in vivo. Tumor cells were inoculated subcutaneously into the mice as described in section (4-B-3) in methodology. The tumors were allowed to grow to a volume of 250-400 mm^3. Mice were randomized into groups based on their body weight and tumor size using the Microsoft FoxPro 7 randomization program.

5-C-1a- Dose response study for wild type MDA-MB-231 cells:

For the dose response study four groups of MA and five groups of Mbz were studied for the wild type MDA-MB-231 breast cancer cells. The groups for MA were 1mg/kg, 2.5 mg/kg, 5 mg/kg, and 7.5 mg/kg and for Mbz were 0.5mg/kg, 1 mg/kg, 2.5mg/kg, 5mg/kg and 33.3 mg/kg. The two drugs were dosed intraperitonealy, drug solutions with different concentrations were prepared with 2.5% DMSO tissue culture media, except for the 33.3 mg/kg Mbz dose where the drug was prepared as 10 mg/ml in

DMSO and dosed as 100 µl ip. With all other groups a constant volume of 200µl was given to each animal at each dose. There was one control group for MA and Mbz. The control group received 200 µl of drug free 2.5% DMSO tissue culture media. The drug was dosed twice weekly for a total of 8 doses.

Tumor volume was measured on the first day of dosing and twice weekly before each dose for 29 days. The volume was recorded as (V=L.W. H). The efficacy was expressed as the volume on day of measurement divided by the volume on first day of dosing V/Vo. The survival duration was expressed as the period between the day of sacrifice or death and the first day of treatment. Toxicity was expressed as body weight loss greater than 15%. Mice were sacrificed if the tumor volume exceeded 7000 mm^3 or the body weight loss was greater than 15%.

1- MA dose response efficacy:

The tumor growth ratio (V/V0) versus time in days for MA treatment groups is shown in [Figure 5: 29 and 30 (log Scale)]. The lowest growth rate was achieved with 2.5 mg/kg MA treatment. Compared to control the difference in growth rate was statistically significant. On day 29 there was statistical significance in the difference in growth rates between 2.5mg/kg and 5 mg/ kg treatment groups ($p< 0.1$). Table 5-3 summarizes the growth rates for MA treatment groups. Growth rate was calculated by dividing either V/V0 or tumor weight on day of sacrifice by the duration from first dose until the day of sacrifice. The growth rates in day^{-1} were 0.17 ± 0.064 without MA treatment, 0.13 ± 0.053

for 1mg/kg, 0.05 ± 0.06 for 2.5 mg/kg, 0.11± 0.065 for 5mg/kg, and 0.14 ± 0.08 for 7.5 mg/kg group. The growth rates in gram/day were 0.0145± 0.006 without MA treatment, 0.0117± 0.0046 for 1mg/kg, 0.005 ± 0.005 for 2.5 mg/kg, 0.0117± 0.01 for 5mg/kg, and 0.0145 ± 0.005 for 7.5 mg/kg group [Figure 5-31]. The difference between growth rates of control and the 2.5 mg/kg MA treatment group was statistically significant when using V/V0 but was not significant with tumor weight.

The tumor regression ratio was calculated by dividing the mean growth rate of each treatment group by that of control at day 29 (T/C) and is presented in [Figure 5-32]. The T/C values for MA treatment groups were 0.753 for 1mg/kg, 0.311 for 2.5mg/kg, 0.649 for 5mg/kg and 0.821 for 7.5mg/kg.

Kaplan Meier Survival analysis is a pictorial representation of the observed animal survival. To detect the statistical difference between survival curves in different treatment groups we will use log-rank test that identifies the chance of a surviving subject in group A to die compared to a surviving subject in group B at a time point t. Log-rank test gives equal weight for all deaths occurring during the length of experiment, compared to Wilcoxon test which attaches more significance to deaths occurring early in the experiment. We will present both Log-rank and Wilcoxon p-values.

Kaplan Meier Survival analysis showed no difference among different MA treatment groups since the survival rate was 100% for all groups, except for 5mg/kg MA where one

animal was sacrificed on day 18 due to an ulcerated tumor. The log-rank P-value was less than 0.317 when compared to placebo indicating no significant difference [Figure 5-33].

The average body weight and ratio of body weight at each time point compared to initial body weight (W/W0) are presented in [Figures 5- 34 and 35]. Loss in body weight is considered an indication of MA toxicity. A loss greater than 15% body weight is an indication for sacrificing the animals. All groups showed controlled and stable average body weight. Using (W/W0) reveals that 7.5 mg/kg MA treatment showed a 10% drop in body weight that reached the maximum at day 14 but stabilized after that with no further decrease.

Animals were sacrificed on day 29 and tumors were harvested and weighed. The average tumor weight in grams is presented in [Figure 5-36]. The average tumor weight reflected the average tumor volume where 2.5 mg/kg had the lowest tumor volume and weight. Using one way ANOVA followed by Tukeys post hoc showed no statistical significance in the difference among the different groups ($p<0.05$).

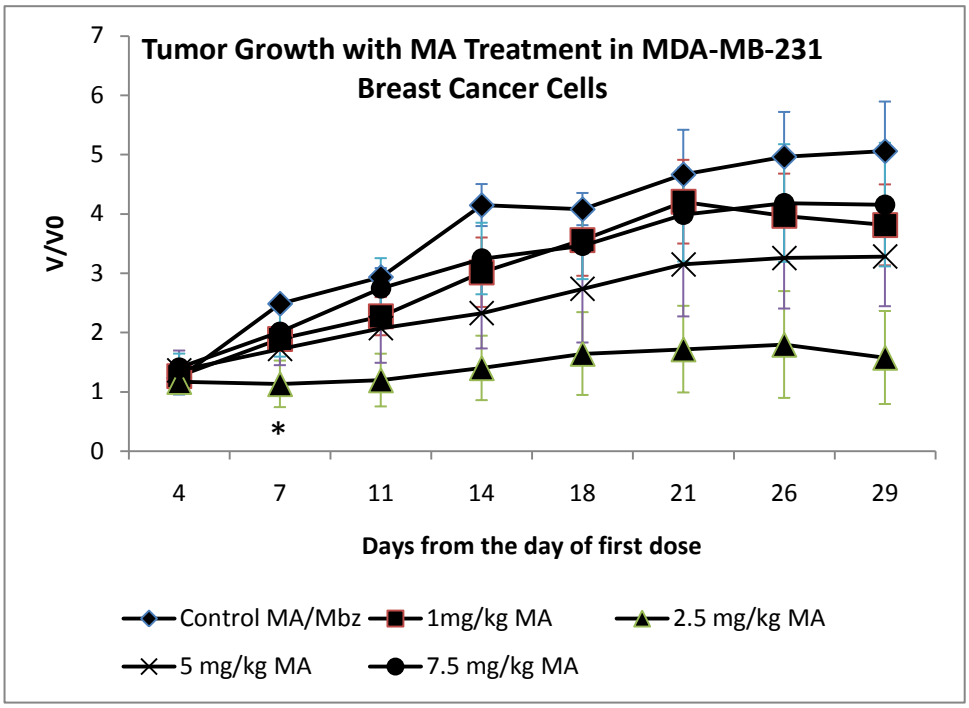

Figure 5-29: Tumor growth versus time for MDA-MB-231 breast cancer cell xenografts with MA treatment. Tumor growth of xenografts expressed as tumor volume on day of measurement divided by initial tumor volume on the day of first dose. Tumors were assessed twice weekly before treatment (n=5). 2.5mg/kg significantly different from control and at day 29 2.5mg/kg was significantly different from 5mg/kg. Data is presented as mean $\pm$ SE.

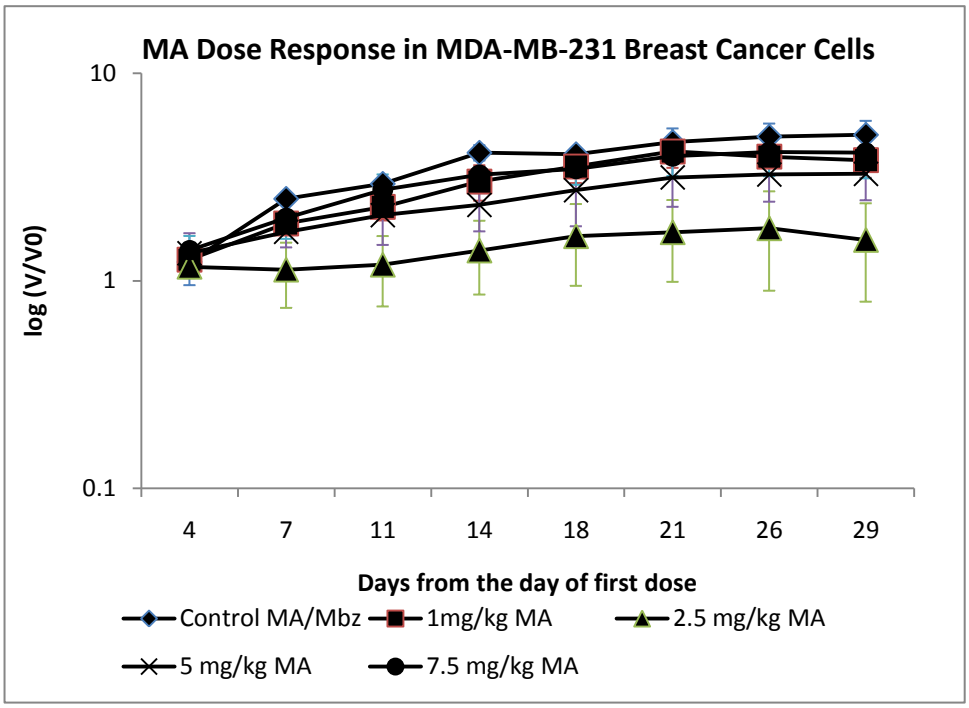

Figure 5-30: Tumor growth versus time on log scale for MDA-MB-231 breast cancer cell xenografts with MA treatment. Tumor growth of xenografts expressed as tumor volume on day of measurement divided by initial tumor volume on the day of first dose. Tumors were assessed twice weekly before treatment (n=5). Data is presented as mean ± SE.

MA Dose (mg/kg)	Growth Rate (day^{-1})	Growth Rate (gram/day)
Control (0mg/kg)	0.17 ± 0.064	0.0145 ± 0.006
1	0.13 ± 0.053	0.0117 ± 0.0046
2.5	0.05* ± 0.06	0.005 ± 0.005
5	0.11 ± 0.065	0.0117 ± 0.01
7.5	0.14 ± 0.08	0.0145 ± 0.005

Table 5- 3: The growth rates of MDA-MB-231 xenografts in nude mice were calculated as last (V/V0) or tumor weight on day of sacrifice divided by the day of last V (day of sacrifice or death). No statistical significance was observed among the different doses, yet only the 2.5mg/kg group was significantly different from the control group. * signifies statistical difference at $p < 0.05$ when 2.5mg/kg was compared to control group using one way ANOVA followed by Tukey's post hoc. (n=5).

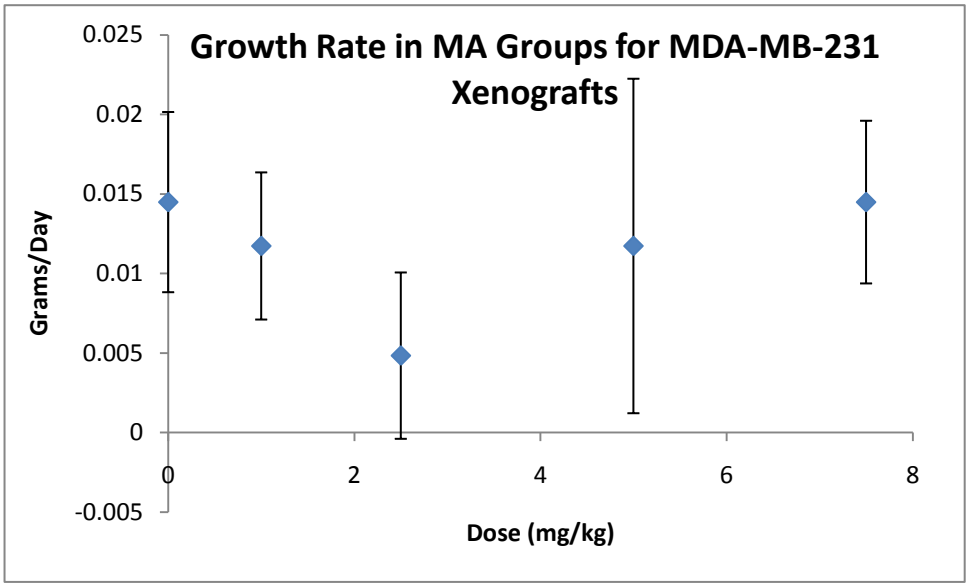

Figure 5- 31- Growth rate calculated as tumor weight in grams at day of sacrifice divided by the number of days from first dose till day of sacrifice. Data is presented as mean ± SD. (n=5)

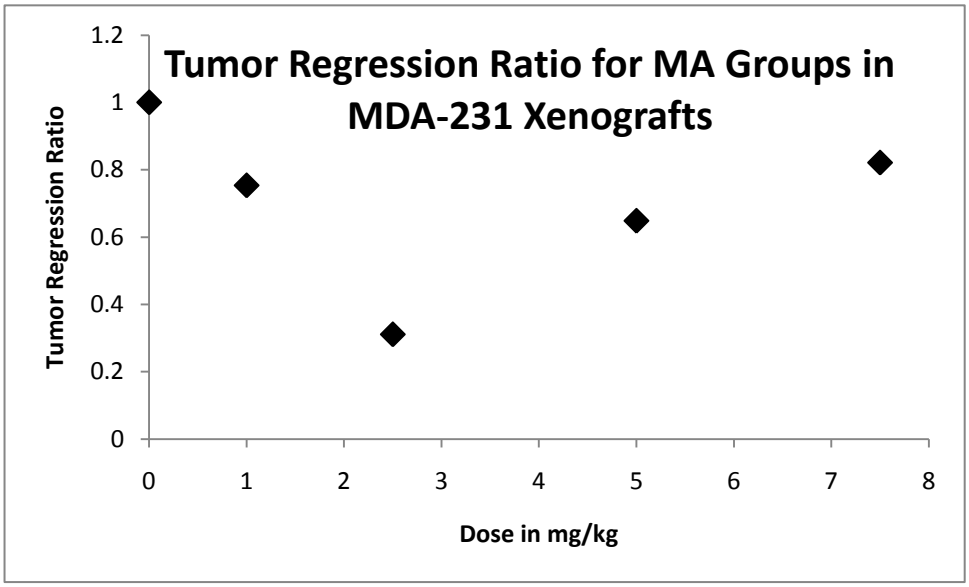

Figure 5-32- Tumor regression ratio determined by dividing the mean of final tumor volume of each treatment group by the mean of final tumor volume of the control group.

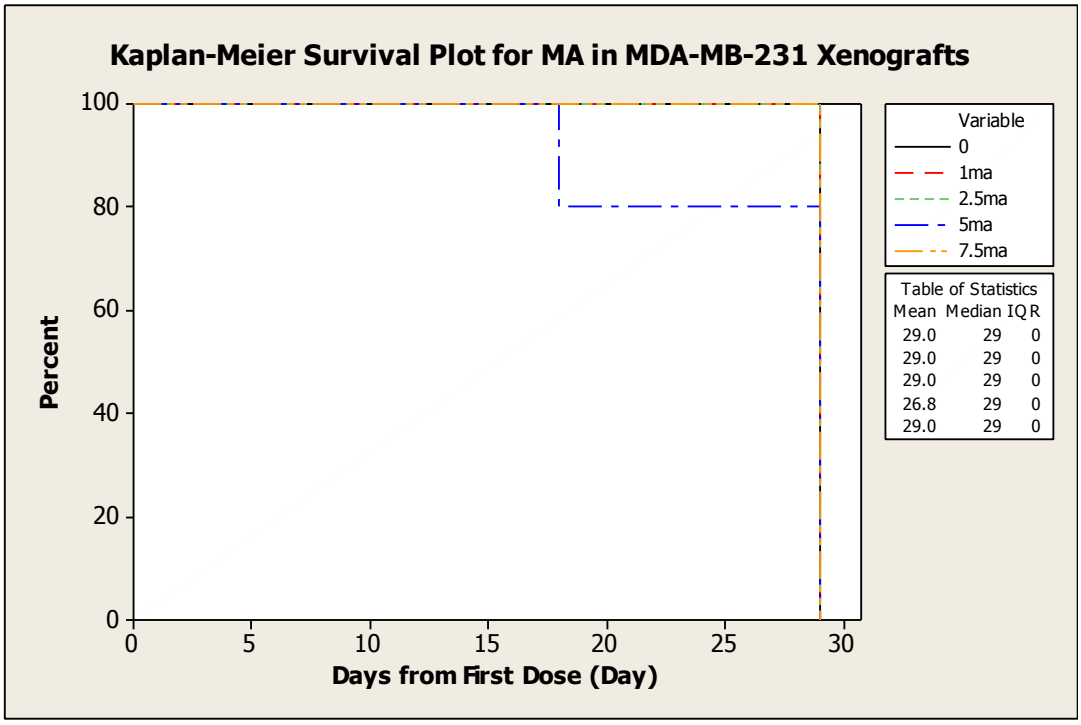

Figure 5-33- Survival of animals in MA treatment groups over time in days from the day of first dose. Survival is expressed as percentage of animals surviving from the original number at day of first dose. All groups had 100% survival all through the experiment, except for 5 mg/kg dose where one animal was sacrificed due to bleeding tumor ulcer. Using Kaplan-Meier statistical method the log rank and wilcoxon p-values are < 0.317 comparing placebo to 5mg/kg MA group showing no significance in the difference in survival rates.

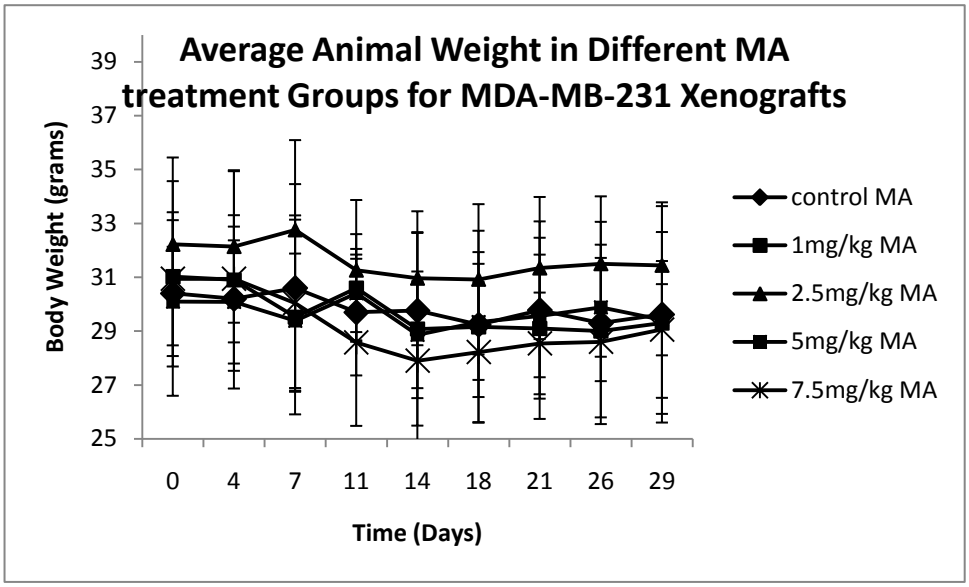

Figure 5- 34- Average body weight (grams) for animals in different MA treatment groups versus time (day) starting at the first dose. (n=5). Data is presented as mean ± SD.

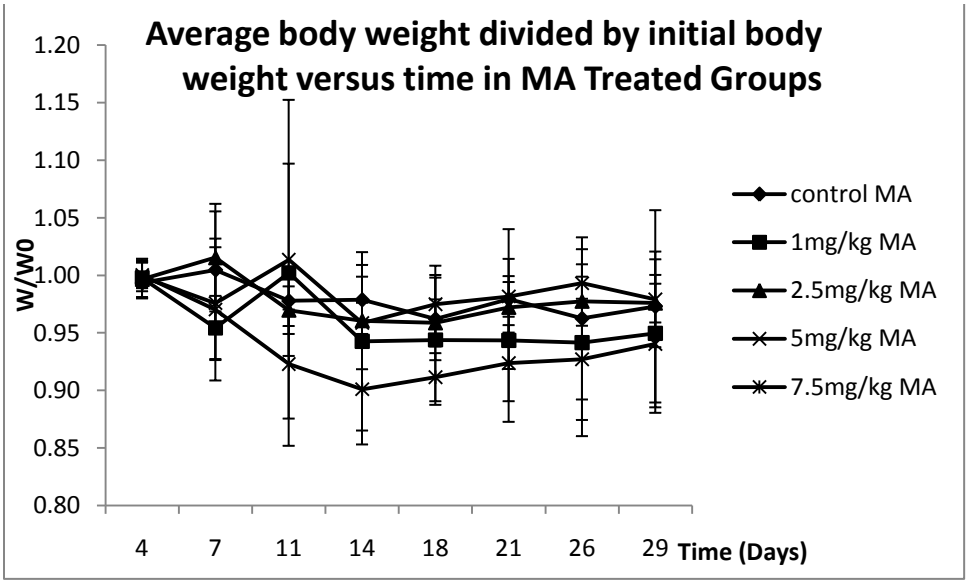

Figure 5- 35- Average body weight divided by initial body weight before first dose (W/W0) versus time in different MA treatment groups as an assessment of MA toxicity in the dose range of 0-7.5 mg/kg given twice weekly for a total of 8 doses. A W/W0 value of 0.85 indicates 15% body weight loss, and is considered an indication of toxicity. (n=5) Data is presented as mean ± SD.

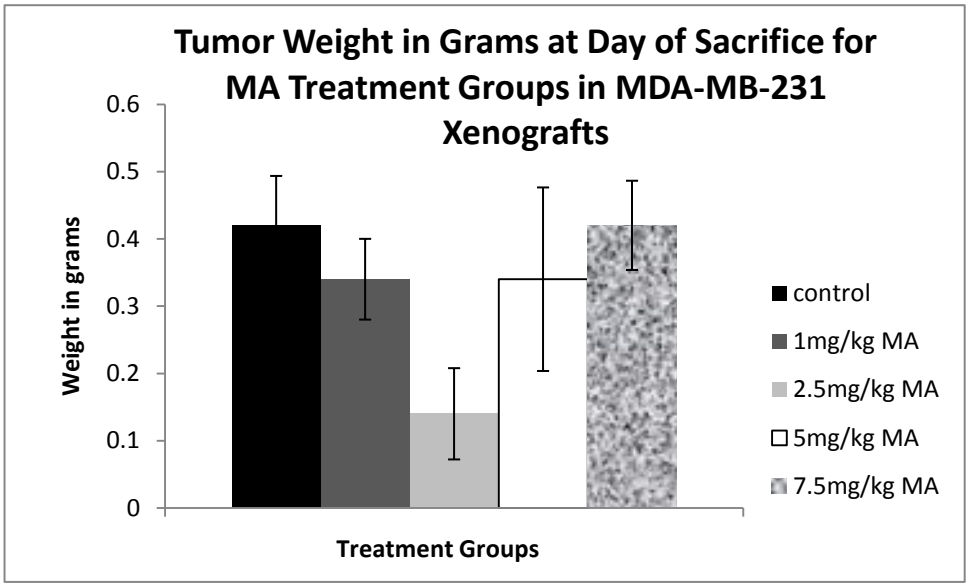

Figure 5-36- Average Tumor Weight at Day of Sacrifice in Different MA Treatment Groups. Animals were sacrificed on day 29 after first dose. One way ANOVA followed by Tukey's post hoc at $p<0.05$ showed no significant difference among the different treatment groups. Data is presented as mean $\pm$ SD.

2- Mbz dose response efficacy:

The tumor growth ratio (V/V0) versus time in days for Mbz treatment groups is shown in [Figure 5-37 and 38 (log Scale)]. There was no statistical difference among the different treatment groups, at any time point. The drop in growth rate observed with 2.5 mg/kg Mbz treatment after day 21 was not statistically different from the other groups including control ($p< 0.1$). Table 5- 4 summarizes the growth rates for Mbz treatment groups. Growth rate was calculated by either dividing V/V0 or weight of tumor on day of

sacrifice by the duration from first dose until the day of sacrifice. Growth rates in day^{-1} were 0.17± 0.064 without treatment, 0.18± 0.08 for 0.5mg/kg, 0.15± 0.1 for 1mg/kg, 0.08 ± 0.06 for 2.5 mg/kg, 0.1± 0.103 for 5mg/kg, and 0.13 ± 0.09 for 33.3 mg/kg group [Figure 5-39a]. Growth rates in day^{-1} were 0.0145 ± 0.006 without treatment, 0.0172± 0.0049 for 0.5mg/kg, 0.018± 0.01 for 1mg/kg, 0.009 ± 0.006 for 2.5 mg/kg, 0.0147± 0.011 for 5mg/kg, and 0.0117 ± 0.008 for 33.3 mg/kg group [Figure 5-39b]. There was no statistical significance in the difference between growth rates among the different Mbz treatment groups.

The tumor regression ratio was calculated by dividing the mean growth rate of each treatment group by that of control at day 29 (T/C) and is presented in [Figure5- 40]. The T/C values for Mbz treatment groups were 1.05 for 0.5mg/kg, 0.857 for 1mg/kg, 0.57 for 2.5mg/kg, 0.752 for 5mg/kg and 0.772 for 33.3 mg/kg.

Kaplan Meier Survival analysis showed no difference among different Mbz treatment groups. All groups had 100% survival all through the experiment, except for 2.5 mg/kg and 5 mg/kg groups where one animal from each group was sacrificed at day 11 due to bleeding tumor ulcers. The log- rank and Wilcoxon p-values are < 0.317 when comparing placebo to 2.5 or 5mg/kg Mbz groups showing no significance in the difference in survival rates [Figure 5-41].

The average body weight and ratio of body weight at each time point compared to initial body weight (W/W0) are presented in [Figures 5- 42 and 43]. Loss in body weight

is considered an indication of Mbz toxicity. A loss greater than 15% body weight is an indication for sacrificing the animals. All groups showed controlled and stable average body weight, (W/W0) versus time reveals controlled body weight during the experiment. There was no statistical difference between treatment groups in average body weight.

Animals were sacrificed on day 29 and tumors were harvested and weighed. The average tumor weight in grams is presented in [Figure 5-44]. Using one way ANOVA followed by Tukeys post hoc showed no statistical significance in the difference among the different groups ($p<0.05$).

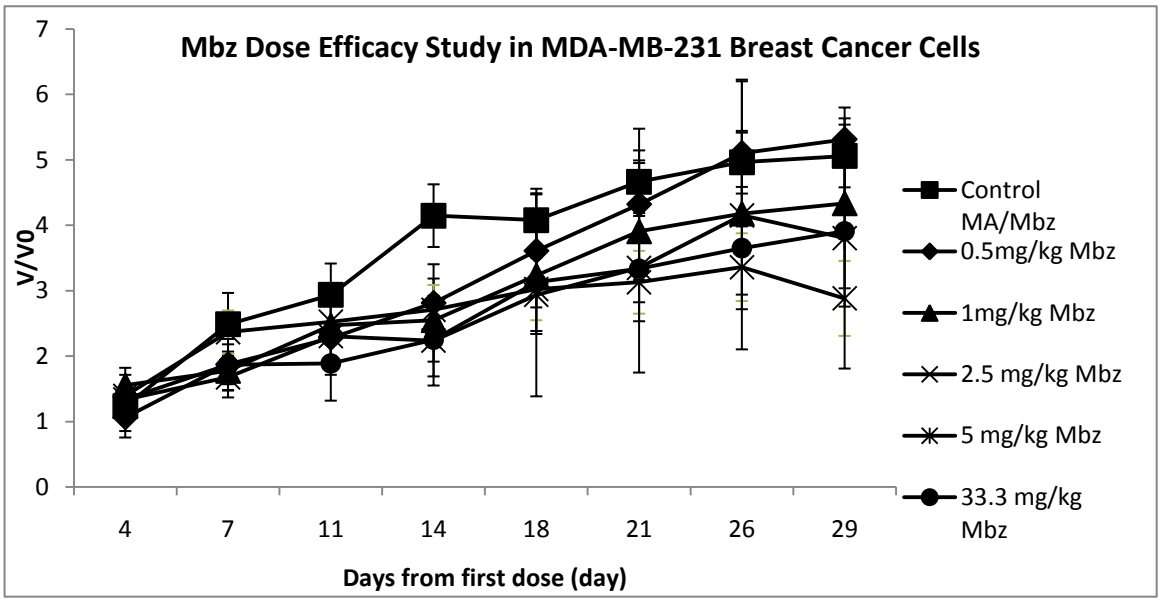

Figure 5-37- Tumor growth versus time for MDA-MB-231 breast cancer cell xenografts with Mbz treatment. Tumor growth of xenografts expressed as tumor volume on day of measurement divided by initial tumor volume on the day of first dose. Tumors were assessed twice weekly before treatment (n=5). Using ANOVA followed by Tukey's post hoc $p<0.1$ there was no statistical significance in the difference between different treatment groups. Data is presented as mean $\pm$ SE.

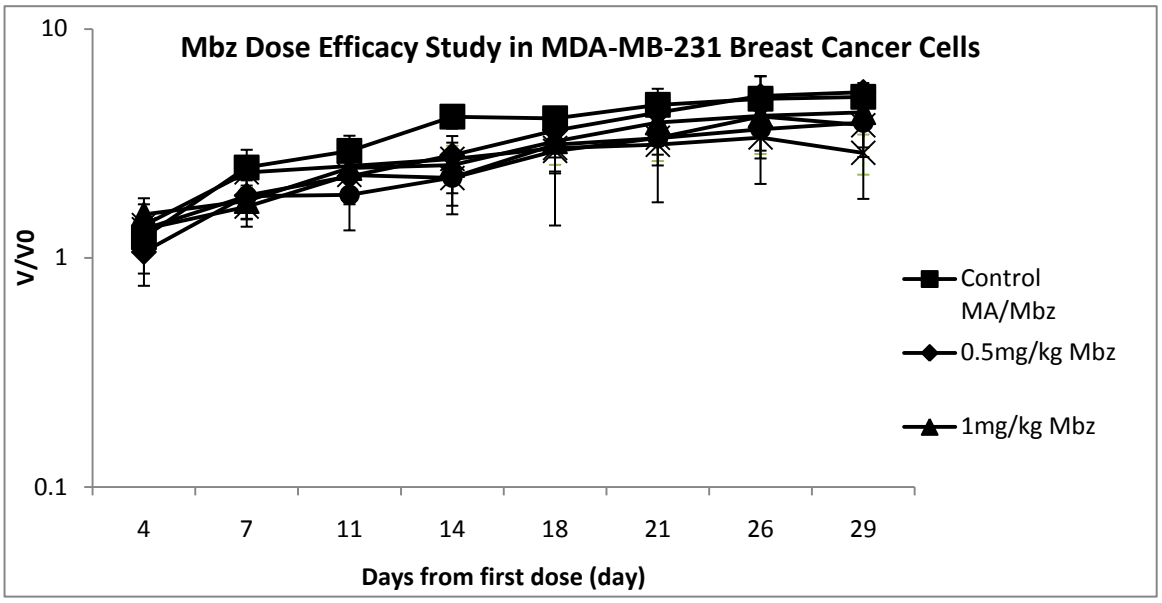

Figure 5- 38- Tumor growth versus time on log scale for MDA-MB-231 breast cancer cell xenografts with Mbz treatment. Tumor growth of xenografts expressed as tumor volume on day of measurement divided by initial tumor volume on the day of first dose. Tumors were assessed twice weekly before treatment (n=5). Data is presented as mean $\pm$ SE.

Mbz Dose (mg/kg)	Growth Rate (day^{-1})	Growth Rate (gram/day)
Control (0 mg/kg)	0.17$\pm$ 0.064	0.0145 $\pm$ 0.006
0.5	0.18 $\pm$ 0.08	0.0172 $\pm$ 0.0049
1	0.15 $\pm$ 0.1	0.018 $\pm$ 0.01
2.5	0.08 $\pm$ 0.059	0.009 $\pm$ 0.006
5	0.1 $\pm$ 0.103	0.0147 $\pm$ 0.011
33.3 (1mg total dose)	0.13 $\pm$ 0.09	0.0117 $\pm$ 0.008

Table 5-4- The growth rates of MDA-MB-231 xenografts in nude mice were calculated as last (V/V0) divided by the day of last V (day of sacrifice or death) or as weight of tumor divided by day of sacrifice. No statistical significance was observed among the different treatment groups using one way ANOVA followed by Tukey's post hoc at $p< 0.1$.

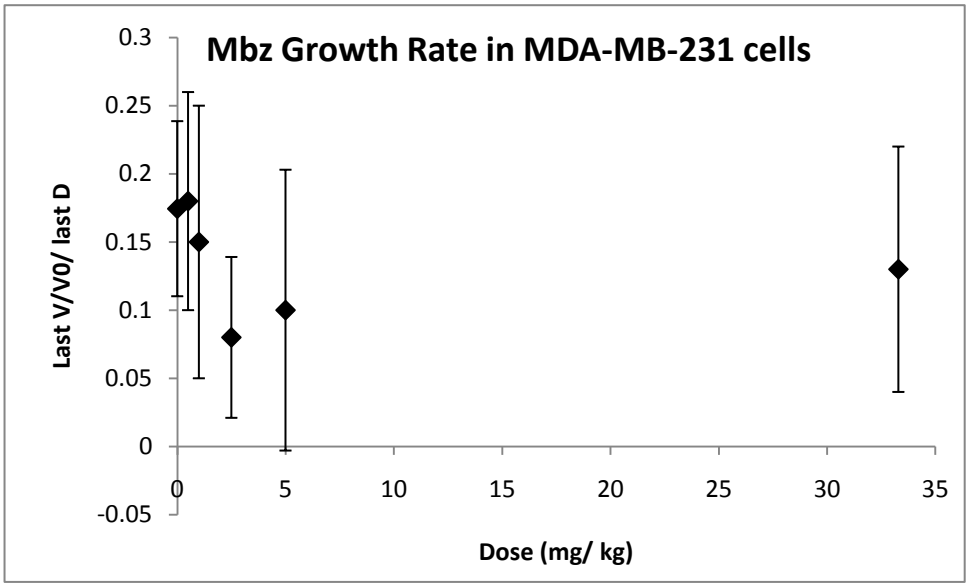

Figure 5- 39a- The growth rate in V/V0 divided by number of days between first dose and day of sacrifice in day^{-1} versus Mbz dose in mg/kg with n=5 in each group. No statistical difference among the treatment groups using ANOVA Tukey's post hoc $p< 0.1$. Data is presented as mean $\pm$ SD.

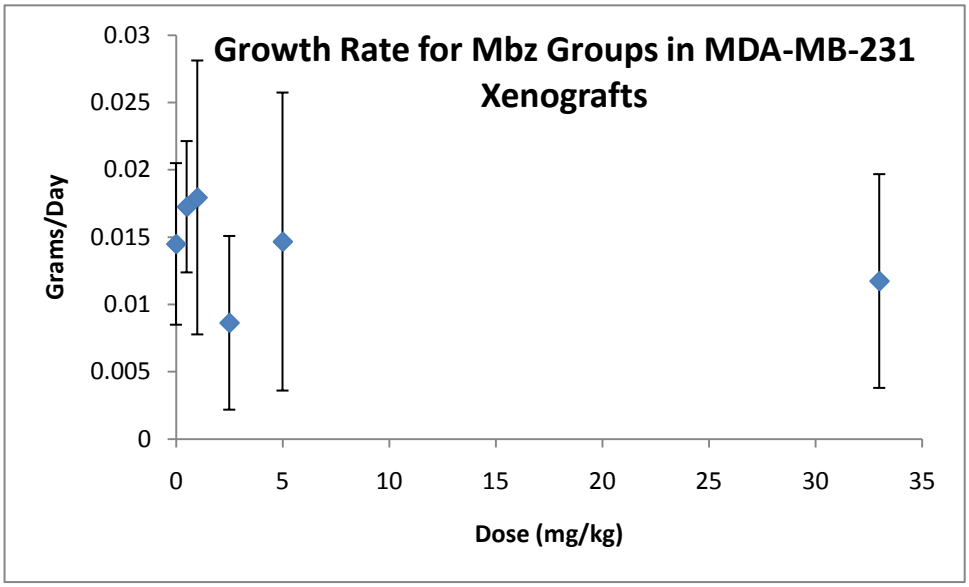

Figure 5- 39b- The growth rate in tumor weight on day of sacrifice divided by number of days between first dose and day of sacrifice in gram/day versus Mbz dose in mg/kg with n=5 in each group. No statistical difference among the treatment groups using ANOVA Tukey's post hoc $p< 0.1$. Data is presented as mean $\pm$ SD.

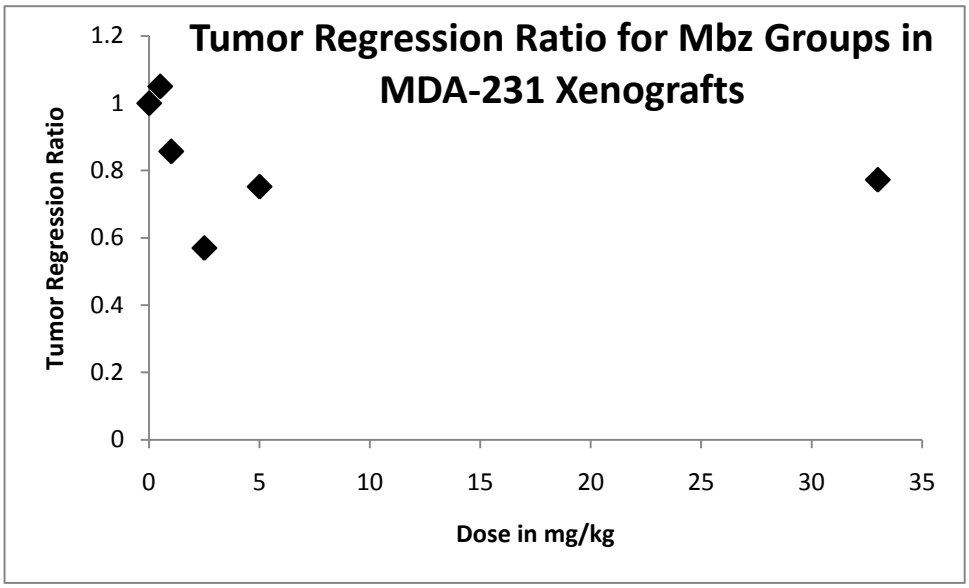

Figure 5- 40- Tumor regression ratio determined by dividing the mean of final tumor volume of each treatment group by the mean of final tumor volume of the control

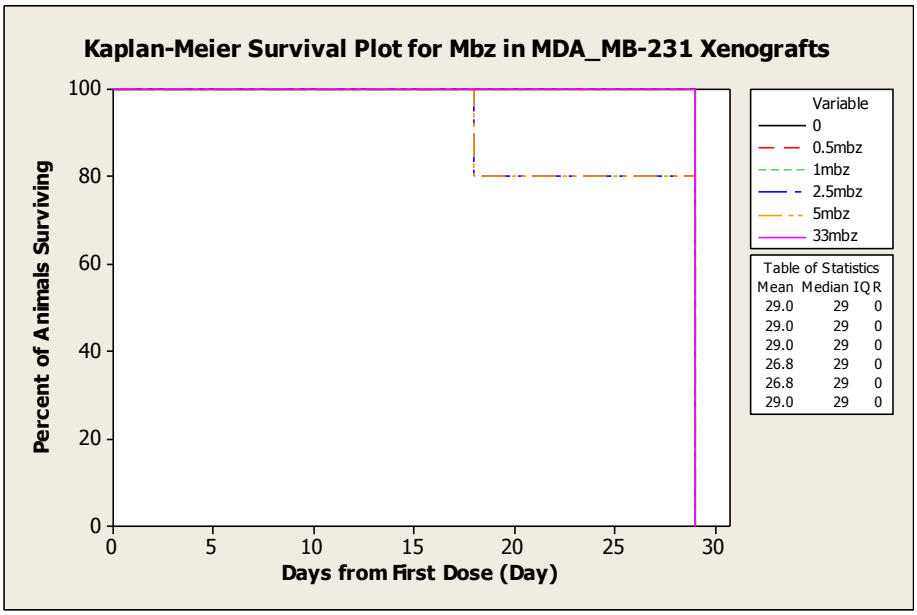

Figure 5-41- Survival of animals in Mbz treatment groups over time in days from the day of first dose. Survival is expressed as percentage of animals surviving from the original number at day of first dose. All groups had 100% survival all through the experiment, except for 2.5 mg/kg and 5 mg/kg dose where one animal was sacrificed at day 11 due to bleeding tumor ulcers. Using Kaplan-Meier statistical method the log rank and wilcoxon p-values are < 0.317 comparing placebo to 2.5 or 5mg/kg Mbz groups showing no significance in the difference in survival rates.

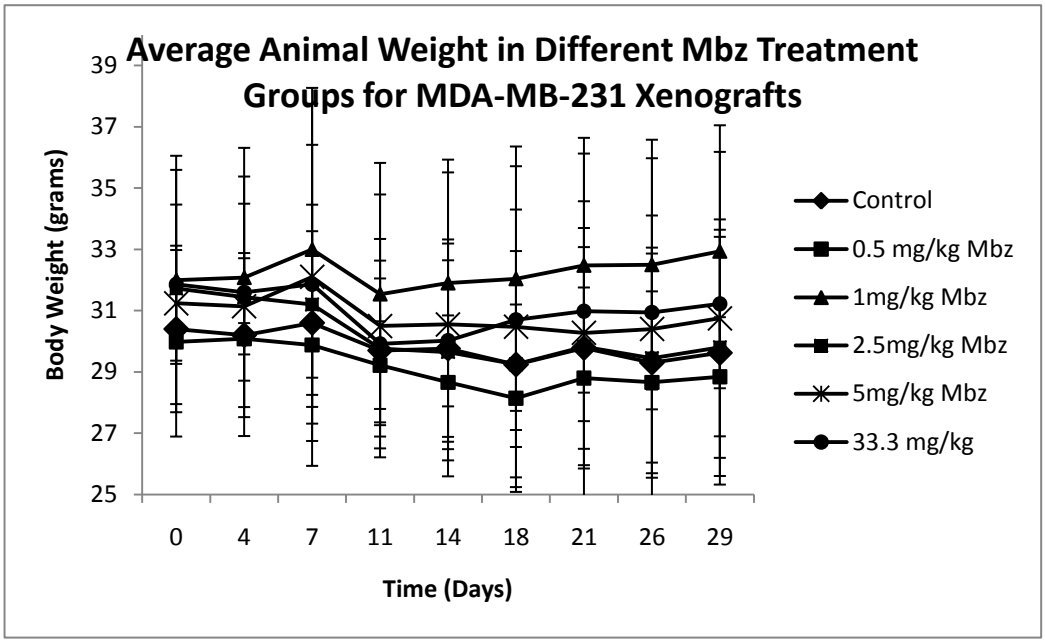

Figure 5-42- Average body weight (grams) for animals in different Mbz treatment groups versus time (day) starting at the first dose. (n=5 for all groups and n= 4 for 2.5 and 5mg/kg starting at day 11 till day 29). Data is presented as mean ± SD.

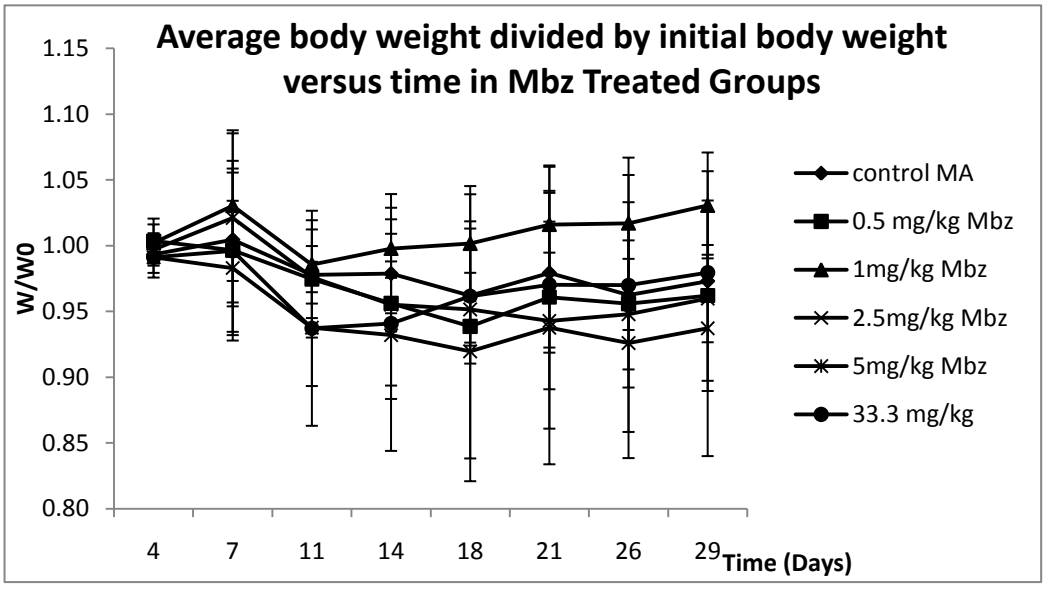

Figure 5-43- Average body weight divided by initial body weight before first dose (W/W0) versus time in different Mbz treatment groups as an assessment of Mbz toxicity in the dose range of 0-33 mg/kg given twice weekly for a total of 8 doses. A W/W0 value of 0.85 indicates 15% body weight loss, and is considered an indication of toxicity. (n=5 for all groups and n= 4 for 2.5 and 5mg/kg starting at day 11 till day 29). Data is presented as mean ± SD.

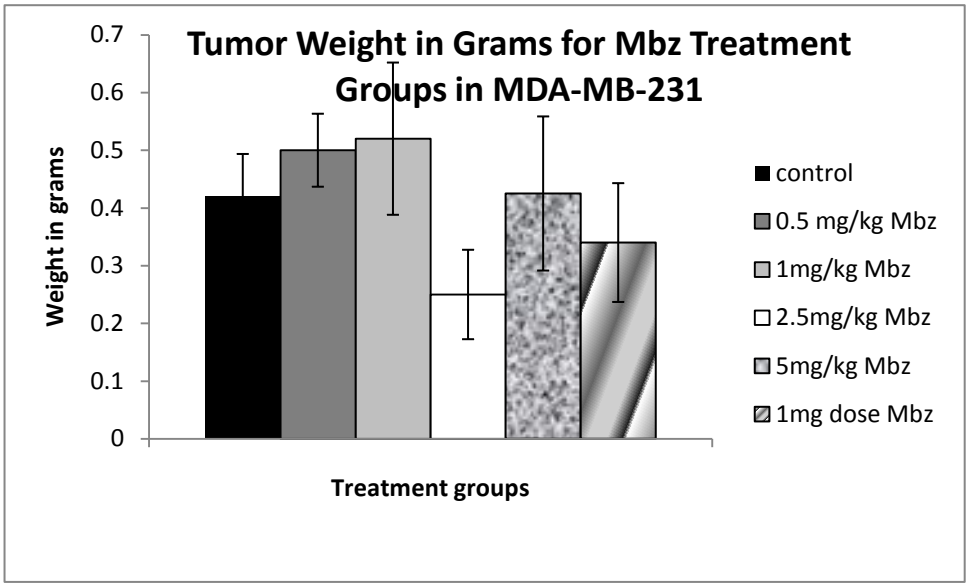

Figure 5-44- Average Tumor Weight at Day of Sacrifice in Different Mbz Treatment Groups. Animals were sacrificed on day 29 after first dose. There was no significant difference among the treatment groups using one way ANOVA followed by Tukey's post hoc at $p<0.1$. (n=5 for control, 0.5, 1 and 33mg/kg groups and n= 4 for 2.5 and 5mg/kg). Data is presented as mean $\pm$ SD.

5-C-1b- Dose response study for HER-2 transfected MDA-MB-231 (MDA-MB-231/ErbB2) cells:

For the dose response study five groups of MA and four groups of Mbz were studied for the HER-2 transfected MDA-MB-231/ErbB2 breast cancer cells. The groups for MA were control, 1mg/kg, 1.5 mg/kg, 2.5 mg/kg, and 5 mg/kg. For Mbz treatment groups were control, 2.5mg/kg, 5mg/kg and 33.3 mg/kg. The two drugs were dosed intraperitonealy, MA drug solutions with different concentrations were prepared in 2.5%

DMSO tissue culture media, Mbz was prepared as a microemulsion at a concentration of 1mg/ml except for the 33.3 mg/kg Mbz, where the drug was prepared as 10 mg/ml in DMSO and dosed as 100 µl ip. With all MA treatment groups a constant volume of 200ul was administered ip to each animal at each dose. Mbz was given at various volumes ranging from 50-250 µl depending on the dose and animal body weight. There were two control groups; for MA the control group received 200 µl of drug free 2.5% DMSO tissue culture media, while for Mbz control group received 250 µl of drug free microemulsion. The drugs were dosed twice weekly for a total of 8 doses.

The tumor volume was measured on the first day of dosing and twice weekly before each dose for 29 days. The volume was recorded as (V=L.W. H). The efficacy was expressed as the volume on day of measurement divided by the volume on first day of dosing V/Vo. The survival duration was expressed as the period between the day of sacrifice or death and the first day of treatment. Toxicity was expressed as body weight loss greater than 15%. Mice were sacrificed if the tumor volume exceeded 7000 mm^3 or the body weight loss was greater than 15%.

1-MA dose response efficacy:

The tumor growth ratio (V/V0) versus time in days for MA treatment groups is shown in [Figure 5: 45 and 46 (log Scale)]. The growth rate in the 1mg/kg MA treatment group was significantly higher than all other groups including the control starting day 18 and continuing until day 29 ($p<0.1$). This could be either a result of a proliferative effect

of MA or the failure of the control group. Compared to control the difference in growth rate in all other treatment groups was not statistically significant neither did we see any statistical significance when comparing the treatment groups with one another. Table 5-5 summarizes the growth rates for MA treatment groups. Growth rate was calculated either by dividing V/V0 or tumor weight on day of sacrifice by the duration from first dose until the day of sacrifice. The growth rates in day^{-1} were 0.1$\pm$ 0.05 without MA treatment, 0.36$\pm$ 0.015 for 1mg/kg, 0.26 $\pm$ 0.07 for 1.5 mg/kg, 0.19$\pm$ 0.081 for 2.5mg/kg, and 0.16 $\pm$ 0.072 for 5 mg/kg group [Figure 5-47a]. The growth rates in gram/day were 0.0264$\pm$ 0.0121 without MA treatment, 0.07$\pm$ 0.047 for 1mg/kg, 0.029 $\pm$ 0.006 for 1.5 mg/kg, 0.0466$\pm$ 0.052 for 2.5mg/kg, and 0.0259 $\pm$ 0.0143 for 5 mg/kg group [Figure 5-47b]. The difference between growth rates of 1 mg/kg and control groups was statistically significant when using V/V0 to calculate growth rate.

The tumor regression ratio was calculated by dividing the mean growth rate of each treatment group at day 21 by that of control at day 21 (T/C) and is presented in [Figure 5-48]. The T/C values for MA treatment groups at day 21 were 1.97 for 1mg/kg, 1.01 for 1.5mg/kg, 0.637 for 2.5mg/kg and 0.615 for 5mg/kg.

Kaplan Meier Survival analysis showed no difference among different MA treatment groups [Figure 5-49]. The survival rate was 100% for 1.5 and 2.5 mg/kg MA groups, 80% for 5mg/kg, and 60% for 1mg/kg and control groups. All animals except one were sacrificed because of their ulcerated tumors. The animal in 5mg/kg MA group was

sacrificed due to swelling where the animal's body weight increased from 33 grams on day 14 to 43.3 grams on day 18 when it was sacrificed. The log-rank and Wilcoxon p-values are presented in table 5-6.

The average body weight and ratio of body weight at each time point compared to initial body weight (W/W0) are presented in [Figures 5-50 and 51]. Loss in body weight is considered an indication of MA toxicity. A loss greater than 15% body weight is an indication for sacrificing the animals. All groups showed controlled and stable average body weight during the 29 days. MA 7.5mg/kg dose was initiated at the beginning of treatment, but was discontinued at day11 due to loss in body weight. The different readings of body weight are presented in table 5- 7.

Animals were sacrificed on day 29 and tumors were harvested and weighed. The average tumor weight in grams is presented in [Figure 5- 52. Using one way ANOVA followed by Tukeys post hoc showed no statistical significance in the difference in tumor weight among the different groups ($p<0.1$).

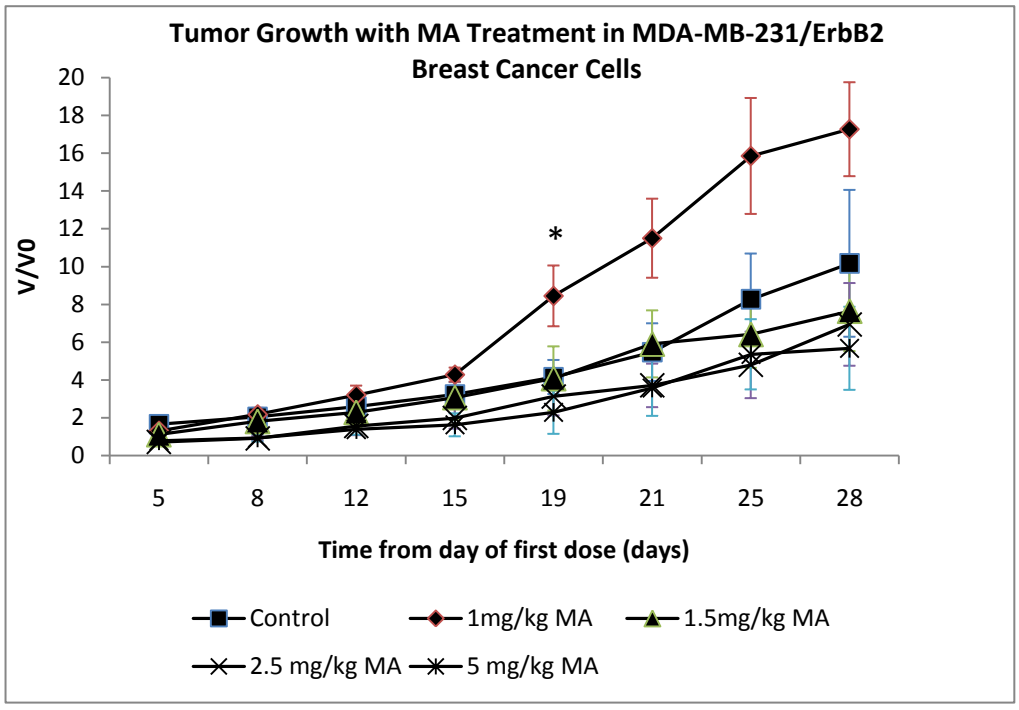

Figure 5-45- Tumor growth versus time for MDA-MB-231/ErbB2 breast cancer cell xenografts with MA treatment. Tumor growth of xenografts expressed as tumor volume on day of measurement divided by initial tumor volume on the day of first dose. Tumors were assessed twice weekly before treatment (n=5). Using ANOVA followed by Tukey's post hoc $p<0.1$ there was no statistical significance in the difference between different treatment groups except with MA 1mg/kg. this group was significantly different from all other groups on days 18, 21, 26 and 29, this group was not different from other treatments earlier than day 18. Data is presented as mean $\pm$ SE.

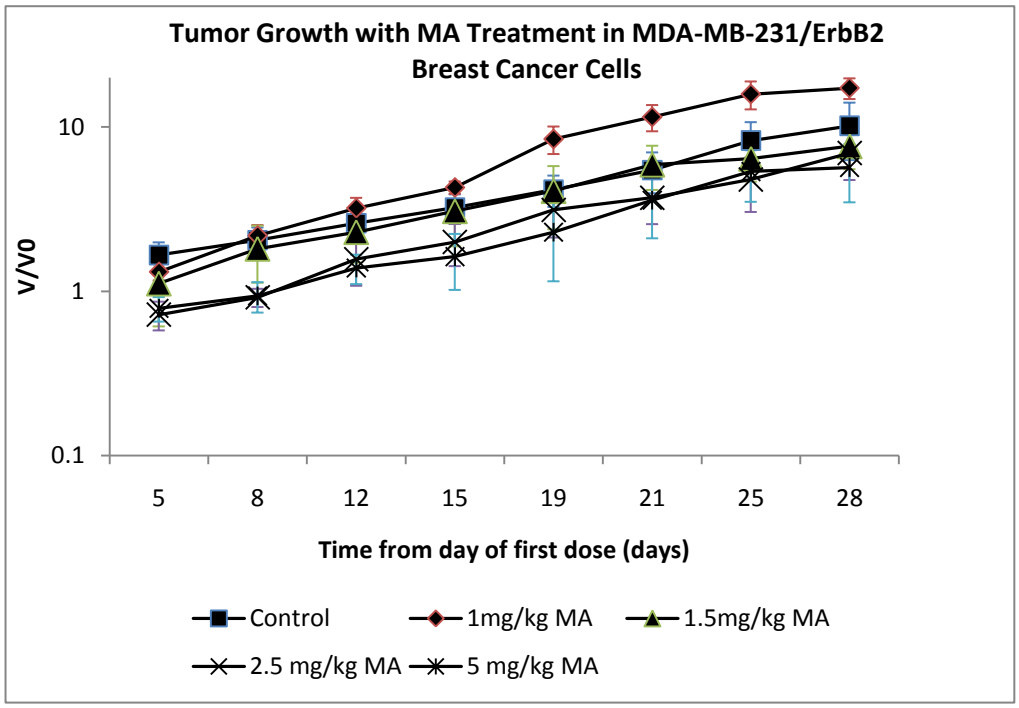

Figure 5-46- Tumor growth versus time on log scale for MDA-MB-231/ErbB2 breast cancer cell xenografts with MA treatment. Tumor growth of xenografts expressed as tumor volume on day of measurement divided by initial tumor volume on the day of first dose. Tumors were assessed twice weekly before treatment (n=5). Data is presented as mean ± SE.

MA Dose (mg/kg)	Growth Rate (day^{-1})	Growth Rate (grams/day)
Control (0mg/kg)	0.1 ± 0.05	0.0264 ± 0.0121
1	0.36 *± 0.015	0.07 ± 0.0475
1.5	0.26 ± 0.07	0.029 ± 0.006
2.5	0.19 ± 0.081	0.0466 ± 0.052
5	0.16 ± 0.072	0.0259 ± 0.0143

Table 5-5- The growth rates of MDA-MB-231/ErbB2 xenografts in nude mice were calculated as last (V/V0) or tumor weight on day of sacrifice divided by the day of last V (day of sacrifice or death). The 1mg/kg MA treatment group was significantly different from control. No statistical significance was observed among the other treatment groups using one way ANOVA followed by Tukey's post hoc at $p< 0.1$. (n=5 for 1.5 and 2.5mg/kg, n=4 for 5mg/kg, and n= 3

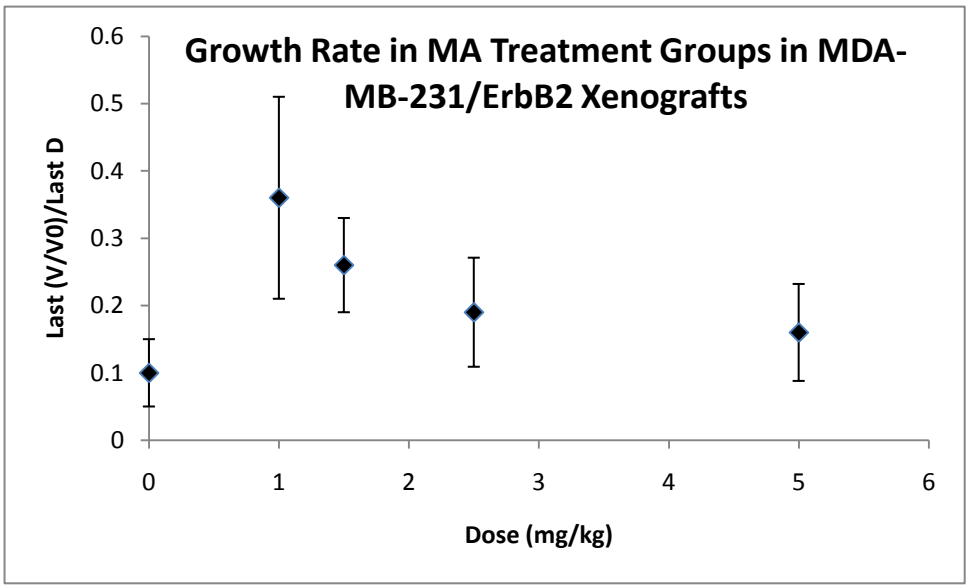

Figure 5- 47a- The growth rate in V/V0 divided by number of days between first dose and day of sacrifice in day^{-1} versus MA dose in mg/kg (n=5 for 1.5 and 2.5mg/kg, n=4 for 5mg/kg, and n= 3 for control and 1mg/kg).

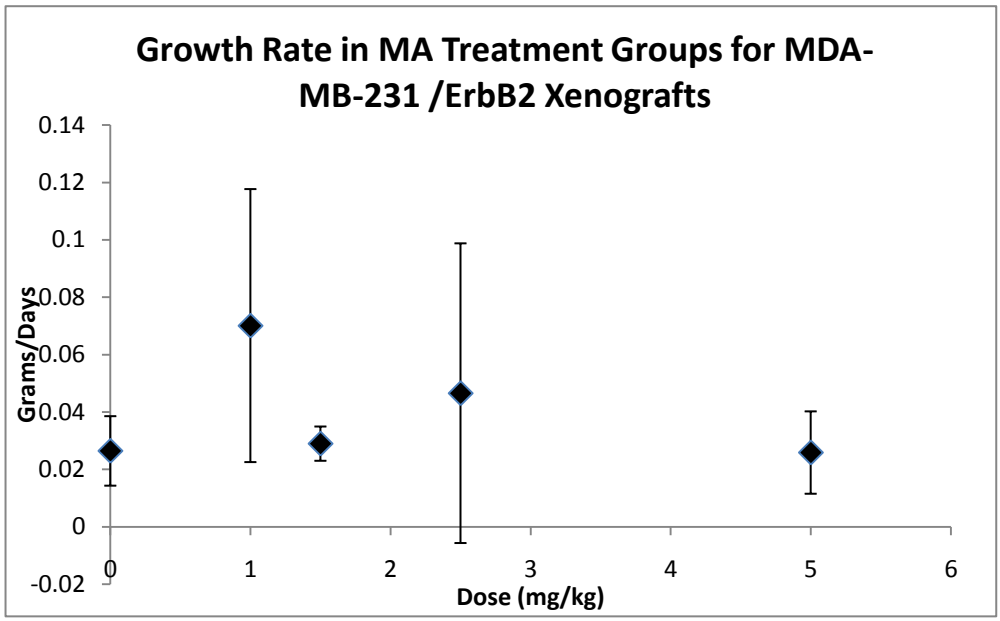

Figure 5- 47b- The growth rate in Tumor weight on day of sacrifice divided by number of days between first dose and day of sacrifice in grams/day versus MA dose in mg/kg (n=5 for 1.5 and 2.5mg/kg, n=4 for 5mg/kg, and n= 3 for control and 1mg/kg).

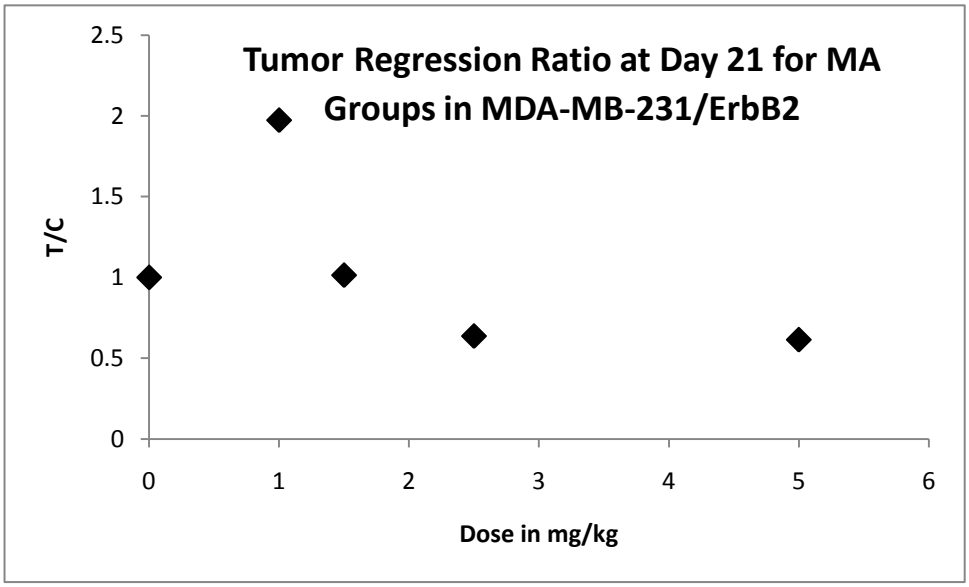

Figure 5-48- Tumor regression ratio determined by dividing the mean of final tumor volume of each treatment group by the mean of final tumor volume of the control group. We chose day 21 as the average of tumor volume represents four animals.

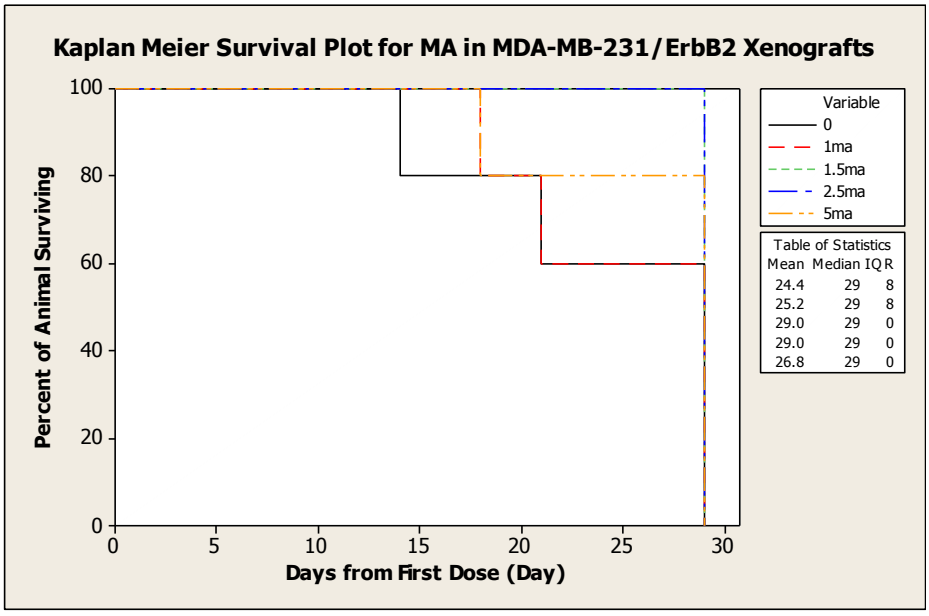

Figure 5-49- Survival of animals in MA treatment groups over time in days from the day of first dose. Survival is expressed as percentage of animals surviving from the original number at day of first dose. The 1.5 and 2.5mg/kg groups had 100% survival, in 5 mg/kg dose one animal was sacrificed due swelling, and 1mg/kg group had a 60% survival with two animals sacrificed due to tumor ulceration while the control group had a 60% survival with one animal sacrificed due to sever drop in body weight and one sacrificed due to tumor ulceration. Ten way comparison using Kaplan-Meier Survival analysis gave a log-rank $p<0.315$ and wilcoxon $p< 0.324$, indicating no statistical difference in survival rate among the different treatment groups.

Groups compared	Log-Rank P-value	Wilcoxon P-value
Placebo - 1mg/kg MA	**0.954** not significantly different	**0.906**
Placebo - 1.5mg/kg MA	**0.134** not significantly different	**0.136**
Placebo - 2.5mg/kg MA	**0.134** not significantly different	**0.136**
Placebo - 5mg/kg MA	**0.52** not significantly different	**0.522**
Placebo - 2.5 Mbz	**0.317** not significantly different	**0.317**
Placebo - 5 Mbz	**0.317** not significantly different	**0.317**
Placebo - 33 Mbz	**0.459** not significantly different	**0.439**

Table 5-6- Kaplan-Meier Survival Analysis showed no statistically significant difference in survival when comparing each group to placebo.

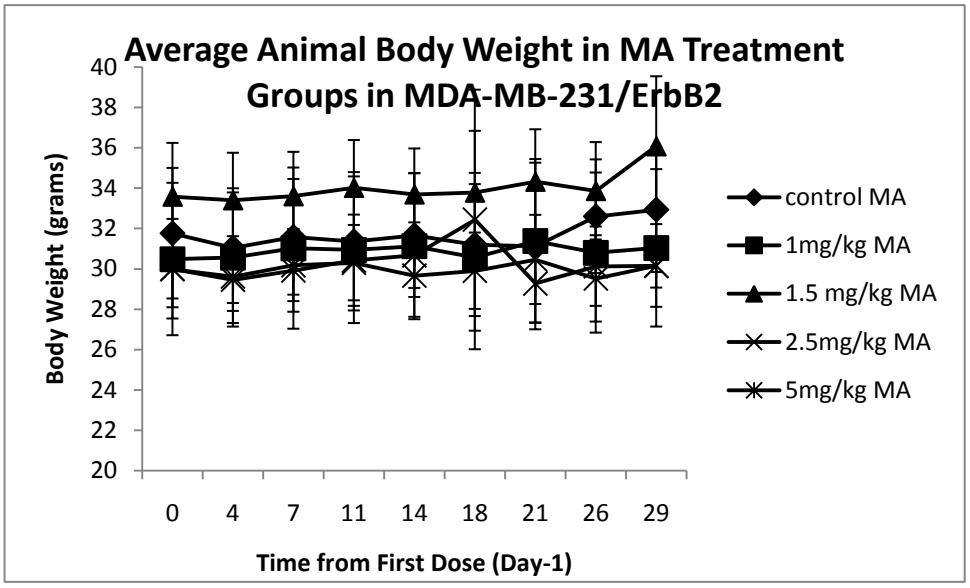

Figure 5-50- Average body weight (grams) for animals in different MA treatment groups versus time (day) starting at the first dose. (n=5 for 1.5 and 2.5mg/kg groups, and n= 4 for 5mg/kg starting at day 18 and n=3 for control and 1mg/kg groups starting day 21). Data is presented as mean $\pm$ SD.

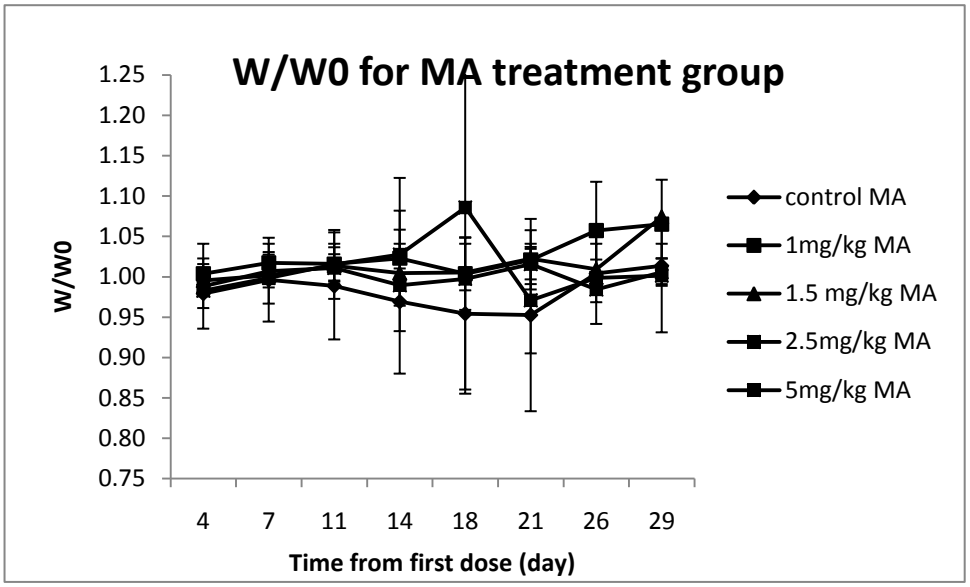

Figure 5-51- Average body weight divided by initial body weight before first dose (W/W0) versus time in different MA treatment groups as an assessment of MA toxicity in the dose range of 0-5 mg/kg given twice weekly for a total of 8 doses. A W/W0 value of 0.85 indicates 15% body weight loss, and is considered an indication of toxicity. (n=5 for 1.5 and 2.5mg/kg groups, and n= 4 for 5mg/kg starting at day 18 and n=3 for control and 1mg/kg groups starting day 21). Data is presented as mean $\pm$ SD.

Animal	Day 0	Day 4	Day 7	Day 11
1	32.8	32	32	33.1
2	27.5	26	25.4	27.3
3	38	36.2	35	34.6
4	27.4	27	26	37
5	30	29	28.5	27.9

Table 5- 6-Animal body weight readings for 7.5mg/kg MA treatment group animals, a decline in body weight was observed in three of the animals, and the treatment was stopped after the third dose.

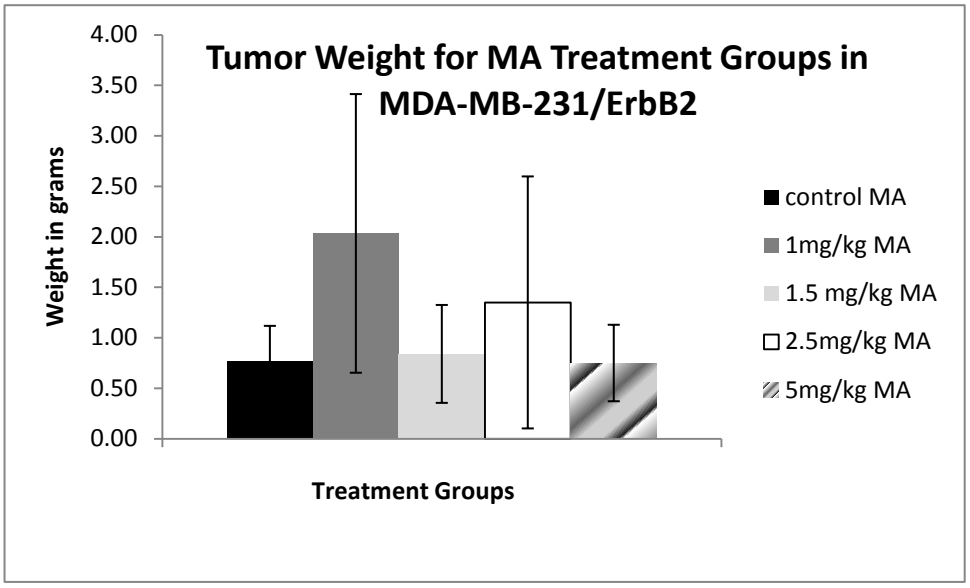

Figure 5- 52- Average Tumor Weight at Day of Sacrifice in Different MA Treatment Groups. Animals were sacrificed on day 29 after first dose. One way ANOVA followed by Tukey's post hoc at $p<0.05$ showed no significant difference among the different treatment groups. Data is presented as mean $\pm$ SD.

2-Mbz dose response efficacy:

The tumor growth ratios (V/V0) versus time in days for Mbz treatment groups are shown in [Figures 5- 53 and 54 (log Scale)]. There was no statistical difference among the different treatment groups at any time point ($p< 0.1$). Table 5- 8 summarizes the growth rates for Mbz treatment groups. Growth rate was calculated either by dividing V/V0 or tumor weight on day of sacrifice by the duration from first dose until day of sacrifice. The growth rates in day^{-1} were 0.2 ± 0.056 without treatment, 0.32 ± 0.07 for 2.5mg/kg, 0.16 ± 0.076 for 5mg/kg, and 0.21 for 33 mg/kg group [Figure 5-55a]. The growth rates in gram/day were 0.066 ± 0.013 without treatment, 0.085 ± 0.011 for

2.5mg/kg, 0.0529 ± 0.014 for 5mg/kg, and 0.0586 ± 0.0345 for 33 mg/kg group [Figure 5-55b]. There was no statistical significance in the difference between growth rates among the different Mbz treatment groups. Increasing the dose from 5mg/kg to 33 mg/kg did not affect the growth rate. Mbz was given as a microemulsion with the 5mg/kg dose, and dissolved in DMSO with the 33mg/kg dose.

The tumor regression ratio was calculated by dividing the mean growth rate of each treatment group by that of control at day 29 (T/C) and is presented in [Figure 56]. The T/C values for Mbz treatment groups were 1.267 for 2.5mg/kg, 0.632for 5mg/kg, and 0.545 for 33.3 mg/kg.

Kaplan Meier Survival analysis showed no difference among different Mbz treatment groups. Survival of animals in Mbz treatment groups over time in days from the day of first dose is presented in [Figure 5- 57]. Survival is expressed as percentage of animals surviving from the original number at day of first dose. The 2.5mg/kg and 5 mg/kg groups had 100% survival, 33.3mg/kg group had a 60% survival with one animal sacrificed due to tumor ulceration and one died of unknown cause. Control group had 80% survival with one animal sacrificed due to tumor ulceration. Kaplan-Meier Survival analysis gave a log-rank p-value <0.220 and Wilcoxon p< 0.217, indicating no statistical difference in survival rate among the different treatment groups.

The average body weight and ratio of body weight at each time point compared to initial body weight (W/W0) are presented in [Figures 5- 58 and 59]. Loss in body weight

is considered an indication of Mbz toxicity. A loss greater than 15% body weight is an indication for sacrificing the animals. All groups showed controlled and stable average body weight. There was no statistical difference between treatment groups in average body weight.

Animals were sacrificed on day 29 and tumors were harvested and weighed. The average tumor weight in grams is presented in [Figure 60]. Using one way ANOVA followed by Tukey's post hoc there was no statistical significance in the difference among the different groups ($p<0.1$).

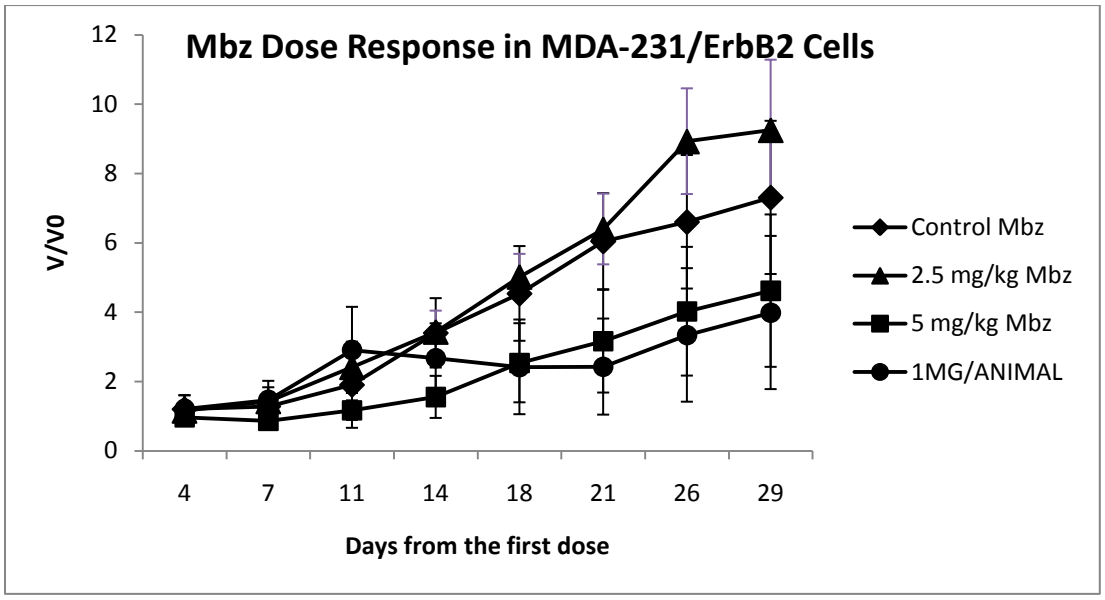

Figure 5- 53- Tumor growth versus time for MDA-MB-231/ErbB2 breast cancer cell xenografts with Mbz treatment. Tumor growth of xenografts expressed as tumor volume on day of measurement divided by initial tumor volume on the day of first dose. Tumors were assessed twice weekly before treatment (n=5). Using ANOVA followed by Tukey's post hoc $p<0.1$ there was no statistical significance in the difference between different treatment groups. Data is presented as mean $\pm$ SE.

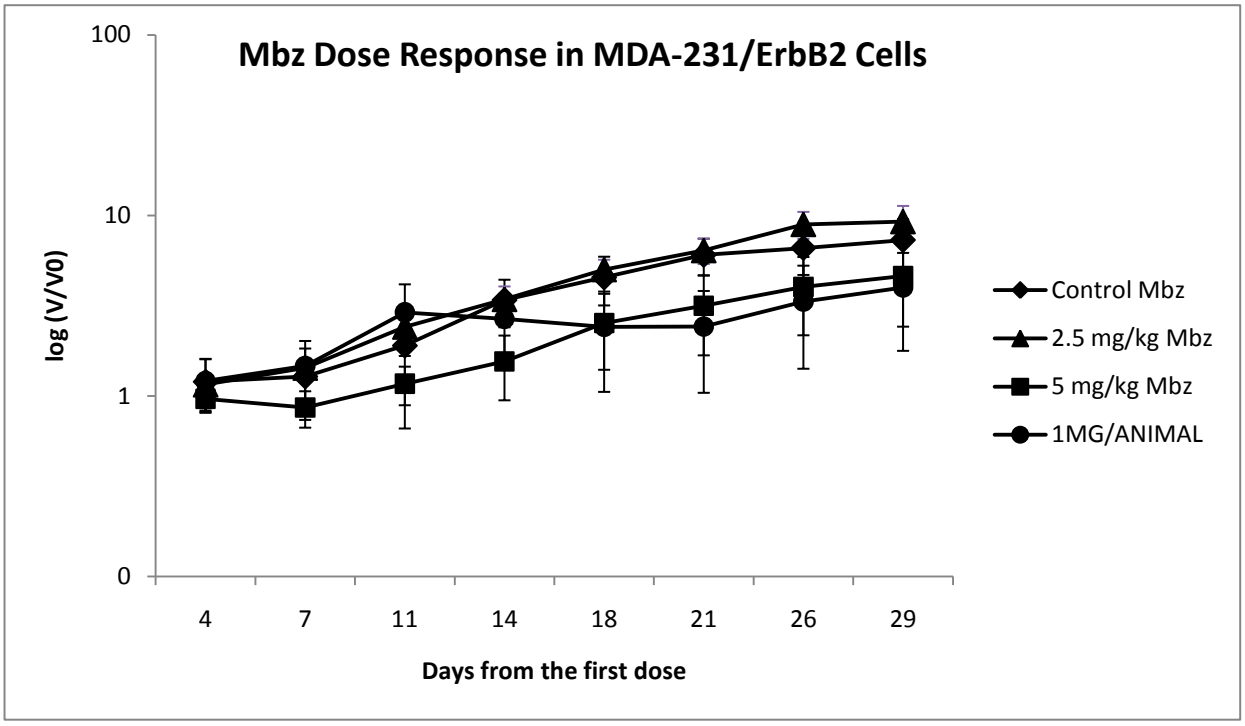

Figure 5- 54- Tumor growth versus time on log scale for MDA-MB-231/ErbB2 breast cancer cell xenografts with Mbz treatment. Tumor growth of xenografts expressed as tumor volume on day of measurement divided by initial tumor volume on the day of first dose. Tumors were assessed twice weekly before treatment (n=5). Data is presented as mean $\pm$ SE.

Mbz Dose (mg/kg)	Growth Rate (day^{-1})	Growth Rate (gram/day)
Control	0.2 $\pm$ 0.056	0.066 $\pm$ 0.013
2.5	0.32 $\pm$ 0.07	0.085 $\pm$ 0.011
5	0.16 $\pm$ 0.076	0.0529 $\pm$ 0.014
33.3 The average of 2 readings	0.21	0.0586

Table 5-7- The growth rates of MDA-MB-231/ErbB2 xenografts in nude mice were calculated as last (V/V0) divided by the day of last V (day of sacrifice or death). No statistical significance was observed among the different treatment groups using one way ANOVA followed by Tukey's post hoc at $p < 0.1$. (n=5 for 5 and 2.5mg/kg, n=4 for control, and n= 2 for 33.3 mg/kg).

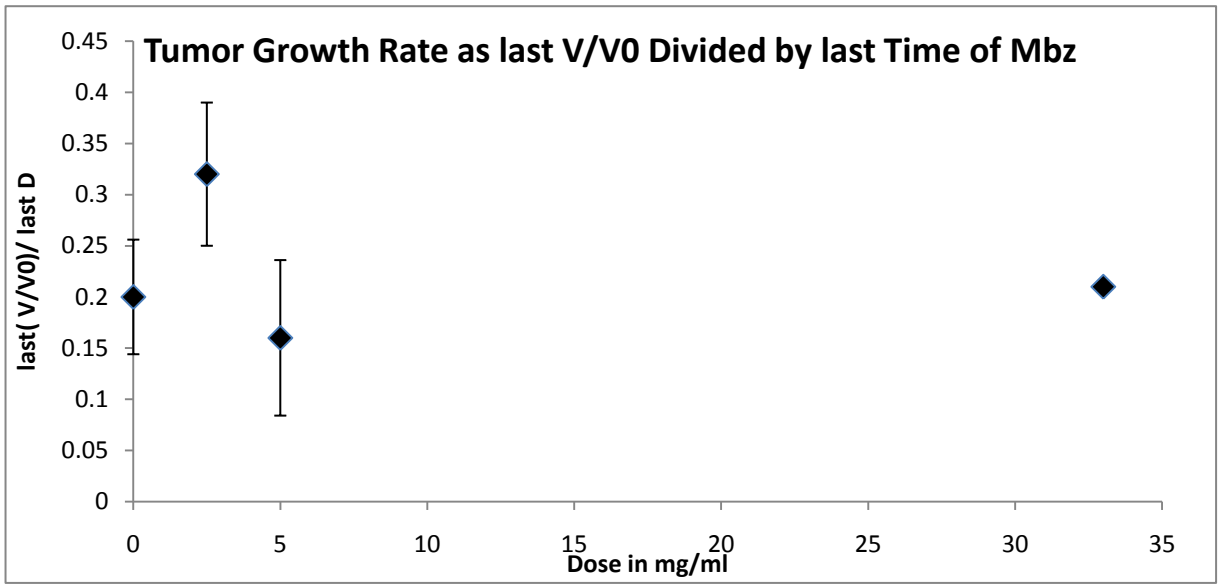

Figure 5- 55a- The growth rate in V/V0 divided by number of days between first dose and day of sacrifice in day^{-1} versus Mbz dose in mg/kg (n=5 for 5 and 2.5mg/kg, n=4 for control and n=2 for 33mg/kg).

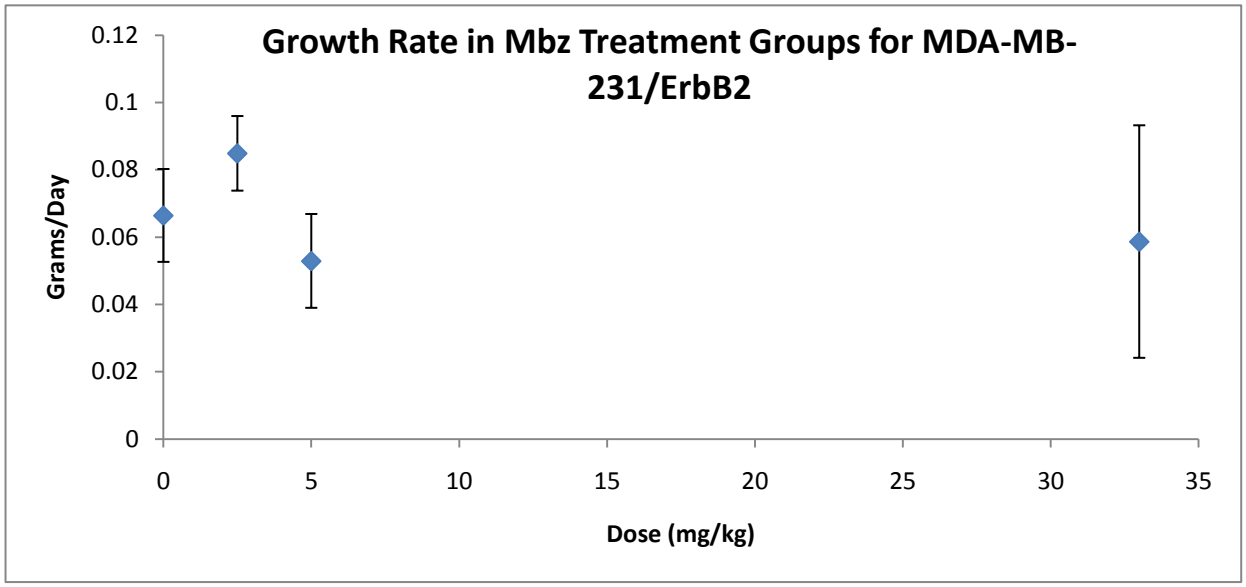

Figure 5- 55b- The growth rate in tumor weight divided by number of days between first dose and day of sacrifice in gram/day versus Mbz dose in mg/kg (n=3for control, 2.5 and 5mg/kg and n=2 for 33mg/kg).

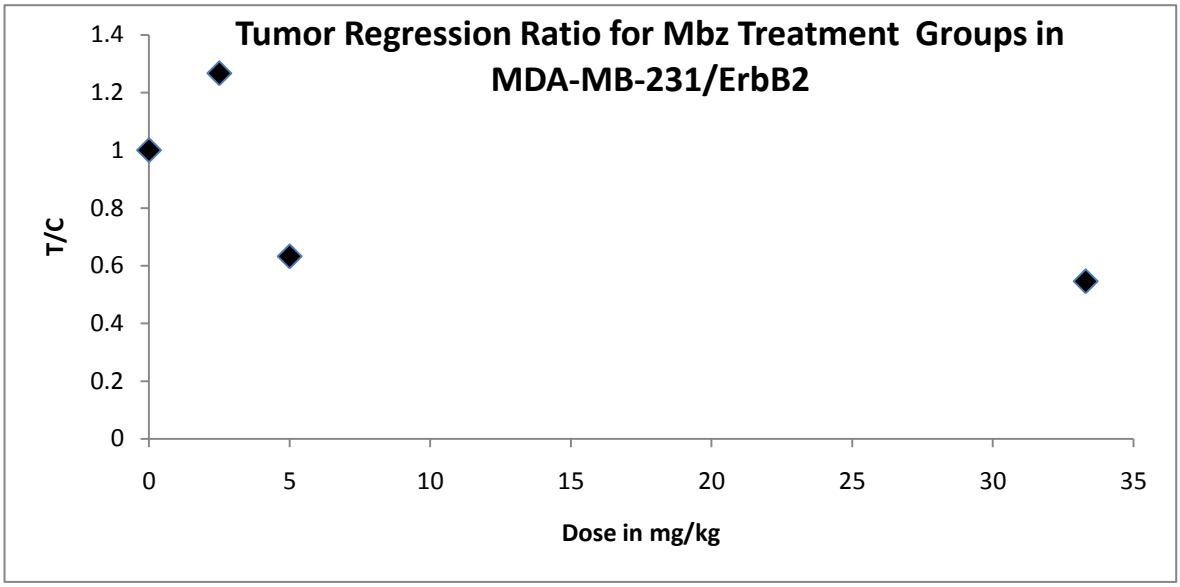

Figure 5- 56- Tumor regression ratio determined by dividing the mean of final tumor volume of each treatment group by the mean of final tumor volume of the control group.

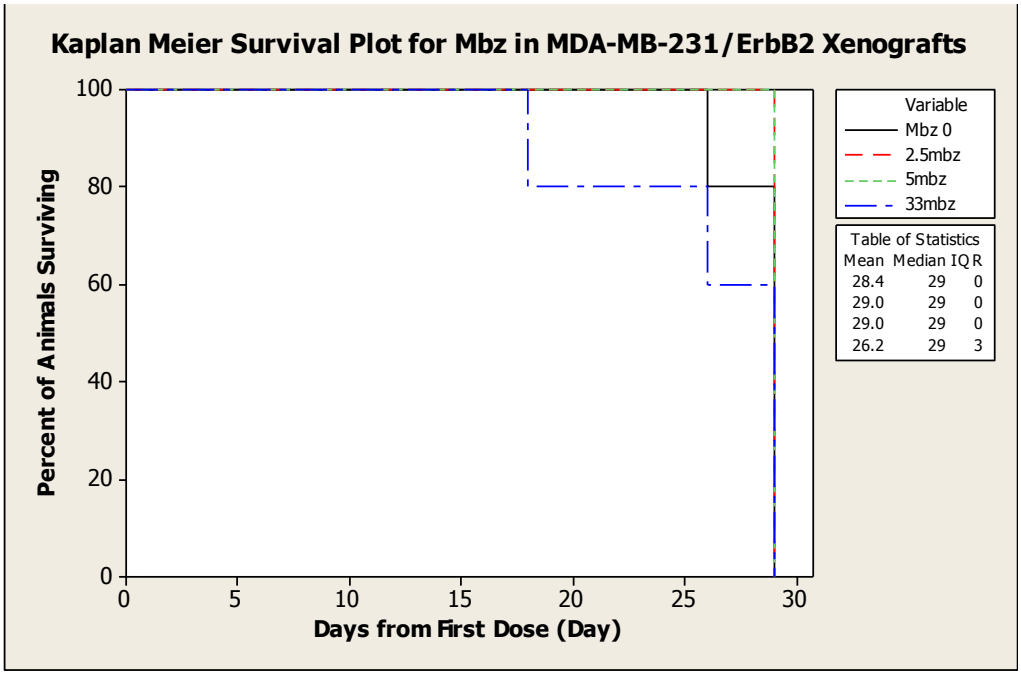

Figure 5- 57- Survival of animals in Mbz treatment groups over time in days from the day of first dose. Survival is expressed as percentage of animals surviving from the original number at day of first dose. The 2.5mg/kg and 5 mg/kg groups had 100% survival, 33.3mg/kg group had a 60% survival with one animal sacrificed due to tumor ulceration and one died of unknown cause. Control group had 80% survival with one animal sacrificed due to tumor ulceration. Kaplan-Meier Survival analysis gave a log-rank $p<0.220$ and wilcoxon $p< 0.217$, indicating no statistical difference in survival rate among the different treatment groups.

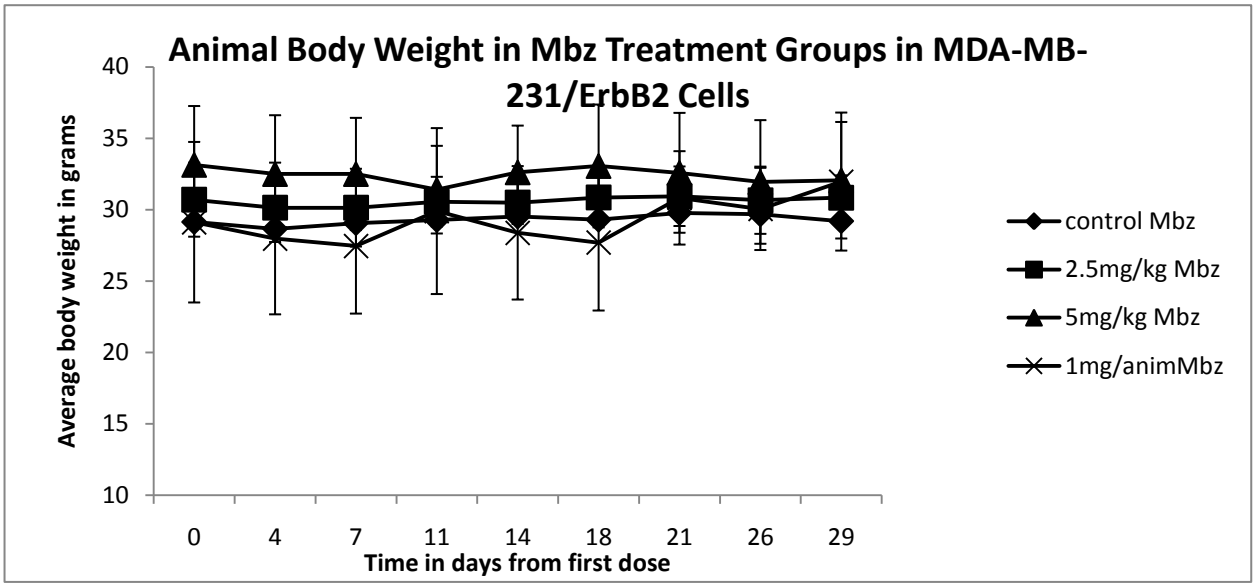

Figure 5-58- Average body weight (grams) for animals in different Mbz treatment groups versus time (day) starting at the first dose. Data is presented as mean + SD.

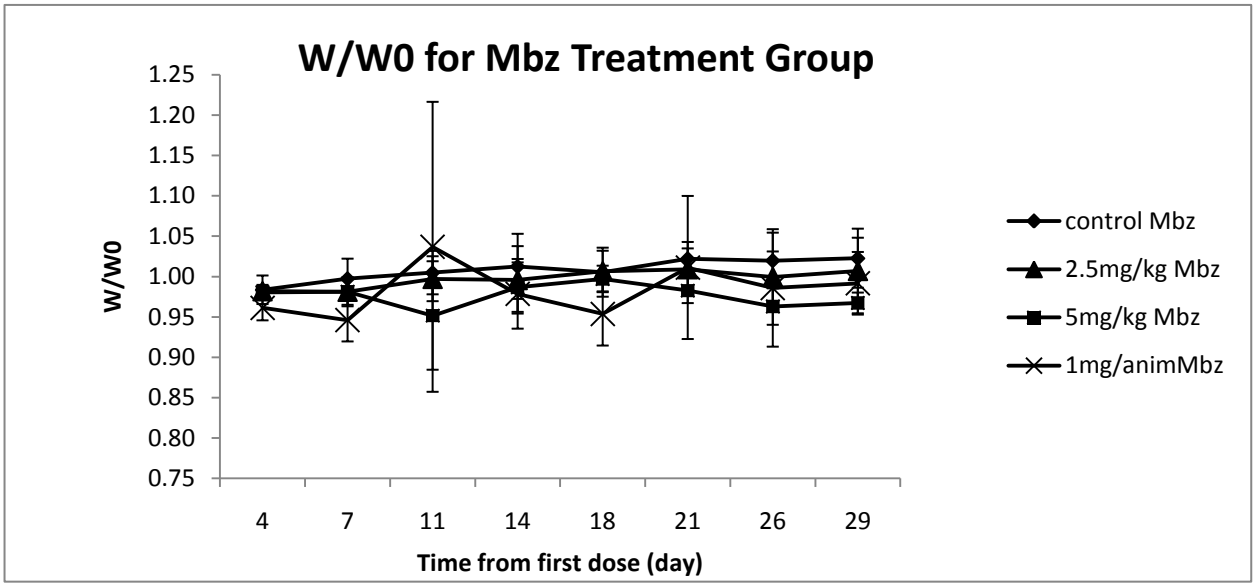

Figure 5- 59- Average body weight divided by initial body weight before first dose (W/W0) versus time in different Mbz treatment groups as an assessment of Mbz toxicity in the dose range of 0-33 mg/kg given twice weekly for a total of 8 doses. A W/W0 value of 0.85 indicates 15% body weight loss, and is considered an indication of toxicity. Data is presented as mean $\pm$ SD.

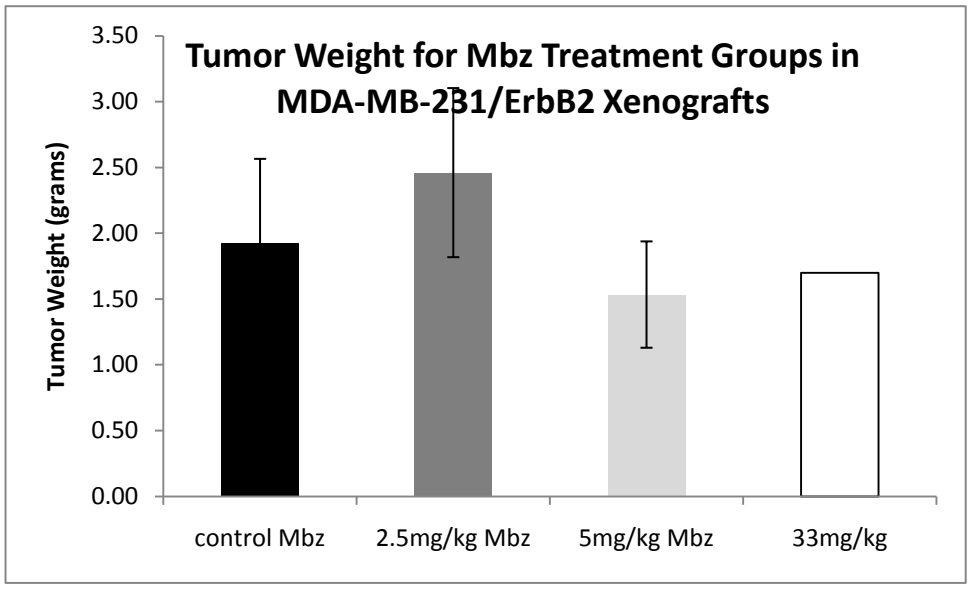

Figure 5-60- Average Tumor Weight at Day of Sacrifice in Different Mbz Treatment Groups. Animals were sacrificed on day 29 after first dose. One way ANOVA followed by Tukey's post hoc at $p<0.1$ showed no significant difference among the different treatment groups. Data is presented as mean $\pm$ SD.

5-C-2- Efficacy experiments for MA and Mbz combination treatments in nu/nu athymic mice:

The dose for MA and Mbz was chosen from the dose efficacy study in (5-C-1), where 2.5mg/kg MA was used in both experiments. There was no need to use a higher dose as there was no statistical significance in tumor volume difference between 2.5 and 5 mg/kg doses in MDA-MB-231/ErbB2 cells, and doses higher than 2.5mg/kg were less effective in MDA-MB-231 cells. MA was prepared as 2.5% DMSO cell culture media solution. One hundred microliters were administered i.p. to animals receiving the drug.

Mbz was given at a dose of 1mg/kg to animals with wild type MDA-MB-231 xenografts and 5mg/kg to animals with MDA-MB231/ErbB2 xenografts. In wild type cells there was no statistical difference among the different Mbz doses in the range of 1-33mk/kg so we decided to use the lowest dose. Mbz was prepared as a microemulsion as described earlier and was administered i.p. in the volume range of 50-200µl depending on the dose and animal body weight. For the MA and Mbz single agent treatments a total of 8 doses of either drug were administered. The concurrent treatment group received both MA and Mbz at each dose for a total of 8 doses, while sequential treatment groups alternated between MA and Mbz at each dose for a total number of 8 doses. The animals were monitored for three weeks following the last dose to observe any change in tumor size and tumor growth rate. Animals were sacrificed after the last measurement and the tumors were weighed. Following are the results for the efficacy study of MA and Mbz combination therapy in wild type and HER-2 transfected MDA-MB-231 xenografts.

5-C-2a- Efficacy Study for MA and Mbz Combination Therapy in MDA-MB-231 Breast Cancer Cells:

Sample size and power calculation:

Ten mice were used in each treatment group. To calculate the power for this experiment we used MiniTab software using data obtained from combination efficacy study for MDA-MB-231 xenografts.

```
Calculating power for mean = null + difference
Alpha = 0.05  Assumed standard deviation = 7.58


            Sample
Difference    Size     Power
         9      10  0.915011
```

The difference was obtained by subtracting the smallest value for (V/V0) at day 47 from the largest value (13.6 - 4.68). Standard deviation used was the largest intergroup value of standard deviation observed for all treatment groups excluding the control group, the largest values for SD in each group were (2.95, 3.26, 3.48, 5.49, and 7.58). The largest value for SD in control was 23.3 Using (23.3) as the standard deviation our power calculation yield:

```
Alpha = 0.05  Assumed standard deviation = 23.3


            Sample
Difference    Size     Power
         9      10  0.194483
```

In this case the proper sample size that will give a power of 80% would be 55 for each group.

```
Alpha = 0.05  Assumed standard deviation = 23.3


            Sample  Target
Difference    Size   Power  Actual Power
         9      55     0.8      0.803275
```

Tumor volume ratio (V/V0) versus time in days for all control and treatment groups in mice with MDA-MB-231 xenografts is shown in [Figures 5- 61 and 62 (log

Scale)]. Using repeated measures one-way ANOVA (mixed design) followed by Tukey's post hoc at $p<0.05$ showed no statistical significance in the difference in tumor volume ratios (V/V0) between the different groups. The repeated measures ANOVA p-value was (0.1633). The Tukey's multiple comparison test yielded p-value > 0.05 in all group comparisons.

Table 5- 9 summarizes the growth rates for MDA-MB-231 xenografts. Growth rate was calculated by dividing either tumor weight at day of sacrifice or V/V0 by the duration from first dose until the day of sacrifice. The growth rates in (day^{-1}) are presented in [Figure 5-63] and are 0.23$\pm$ 0.063 for MA control, 0.29 $\pm$ 0.5 for Mbz control, 0.11 $\pm$ 0.074 for MA single agent, 0.15 $\pm$ 0.21for Mbz single agent, 0.1 $\pm$ 0.0.072 for concurrent, 0. 2 $\pm$ 0.16 for MA 1^{st}, and 0.15 $\pm$ 0.11 for Mbz 1^{st} treatment groups. The growth rates in (gram/day) are presented in [Figure 5-64] and are 0.0197 $\pm$ 0.006 for MA control, 0.0042 $\pm$ 0.000 for Mbz control, 0.0077 $\pm$ 0.006 for MA single agent, 0.0061 $\pm$ 0.006 for Mbz single agent, 0.0097 $\pm$ 0.007 for concurrent, 0.0132 $\pm$ 0.010 for MA 1^{st}, and 0.0113 $\pm$ 0.009 for Mbz 1^{st} treatment groups. There was no statistical significance in the difference between growth rates among the different treatment groups.

Kaplan Meier Survival analysis showed no difference in survival rates among the different groups. Survival of animals in control and treatment groups over time in days from the day of first dose is presented in [Figure 5-65]. Survival is expressed as percentage of animals surviving from the original number at day of first dose. MA and

Mbz single agent and MA 1st treatment groups had 100% survival. One animal was sacrificed from control MA (D23) concurrent (D19) and Mbz 1st (D26) groups due to weight loss (16%), swelling caused by liver failure, and tumor ulceration, respectively. In the control Mbz group one animal died of unknown reason (D16) and another was sacrificed due to tumor ulceration (D26). The log-rank p-value was <0.204 and Wilcoxon p-value was < 0.195 indicating no statistical difference in survival rates among the different treatment groups.

The average body weight and ratio of body weight at each time point compared to initial body weight (W/W0) are presented in [Figures 5- 66 and 67]. A loss greater than 15% body weight is an indication of toxicity. All groups showed controlled and stable average body weight. There was no statistical difference between treatment groups in average body weight. One animal showed a decrease of 16% of its body weight (W0=35.8 and W= 30.1 grams). This was an exclusive case that did not indicate treatment toxicity.

Animals were sacrificed on day 47 and tumors were harvested and weighed. The average tumor weight in grams is presented in [Figure 5-68]. Using one way ANOVA followed by Tukey's post hoc ($p<0.1$) showed that control Mbz and both single agent treatment groups were statistically different compared to control MA giving a p-value of 0.071.

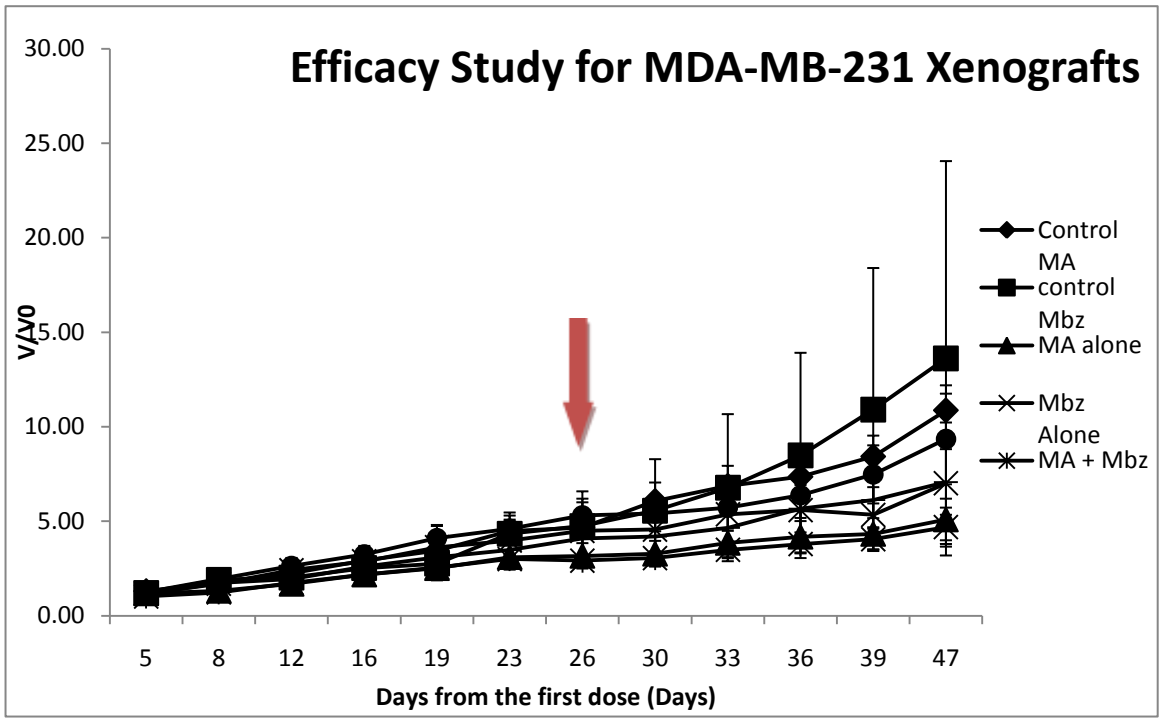

Figure 5-61- Tumor growth versus time for MDA-MB-231 breast cancer cell xenografts with different treatment groups. MA was administered ip at a dose of 2.5mg/kg and Mbz microemulsion was given ip at a dose of 1mg/kg. Tumor growth expressed as tumor volume on day of measurement divided by initial tumor volume on the day of first dose (V/V0) versus days from first dose. Tumors were assessed twice weekly before treatment (n=10 for treatment and 5 for control groups). Last dose was administered on day 26. Analysis was done using repeated measures ANOVA (mixed model) followed by Tukey's post hoc $p<0.05$. Data is presented as mean $\pm$ SE.

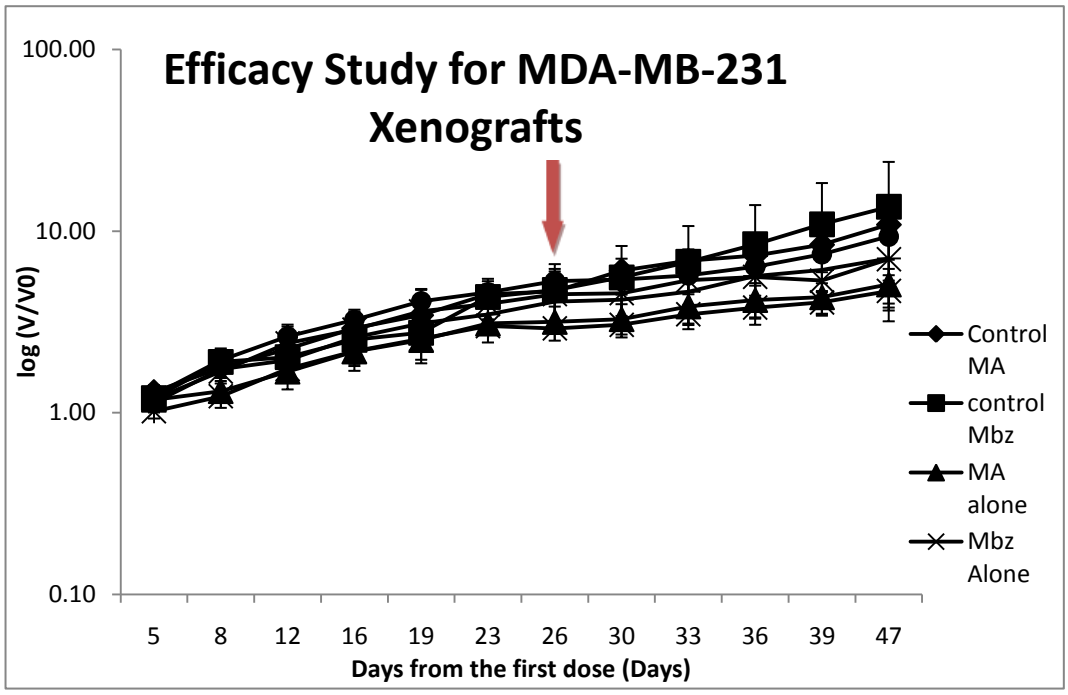

Figure 5-62- Log (V/V0) versus time for MDA-MB-231 breast cancer cell xenografts with different treatment groups. Last dose was administered on day 26. Analysis was done using repeated measures ANOVA (mixed model) followed by Tukey's post hoc $p<0.05$. Data is presented as mean $\pm$ SE. (n=10 for treatment and 5 for control groups).

Treatment Group	Growth Rate (day^{-1})	Growth Rate (gram/day)
Control MA	0.23± 0.063	0.0197 ± 0.006
Control Mbz	0.29 ± 0.5	0.0042 ± 0.000
MA Single Agent	0.11 ± 0.074	0.0077 ± 0.006
Mbz Single Agent	0.15 ± 0.21	0.0061 ± 0.006
Concurrent	0.1 ± 0.0.072	0.0097 ± 0.007
MA 1^{st}	0.2 ± 0.16	0.0132 ± 0.010
Mbz 1^{st}	0.15 ± 0.11	0.0113 ± 0.009

Table 5-9- The growth rates of MDA-MB-231 xenografts in nude mice were calculated as last (V/V0) divided by the day of last V (day of sacrifice or death) or as weight of tumor divided by day of sacrifice. No statistical significance was observed among the different treatment groups using one way ANOVA followed by Tukey's post hoc at $p< 0.05$. Values are presented as mean ± SD.

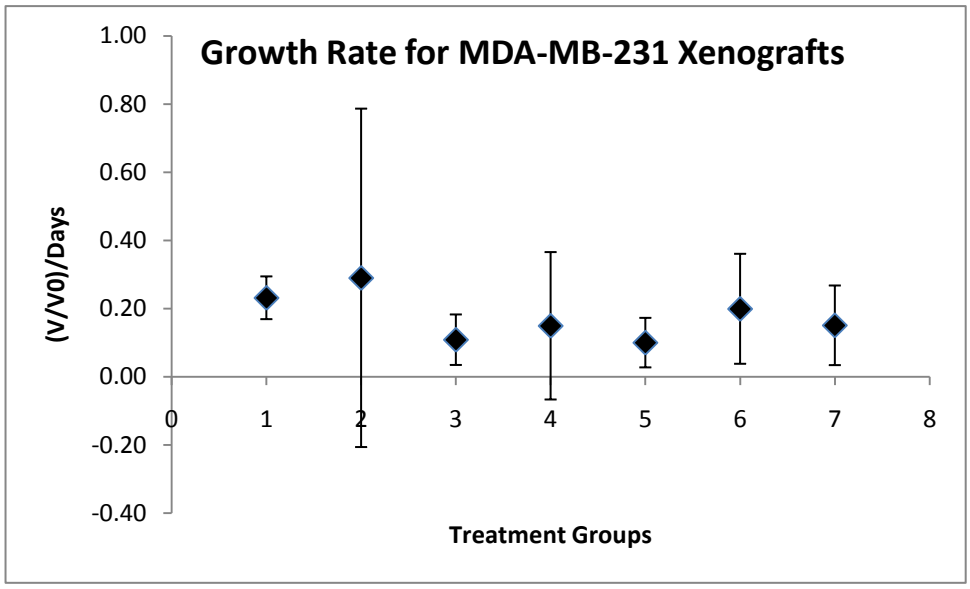

Figure 5-63- Growth rate for MDA-MB-231 xenografts with different treatments calculated using V/V0 on day of sacrifice divided by day of sacrifice (day). Animals were sacrificed on day 47 after first dose. 1 is MA control, 2 is Mbz control, 3 is MA single agent, 4 is Mbz single agent, 5 is concurrent, 6 is MA 1^{st} and 7 is Mbz 1^{st} treatment. There was no statistical significance in the difference between groups. Analysis was done using one-way ANOVA followed by Tukey's post hoc $p<0.05$. Data is presented as mean ± SD. (n=10 and 5 for control groups).

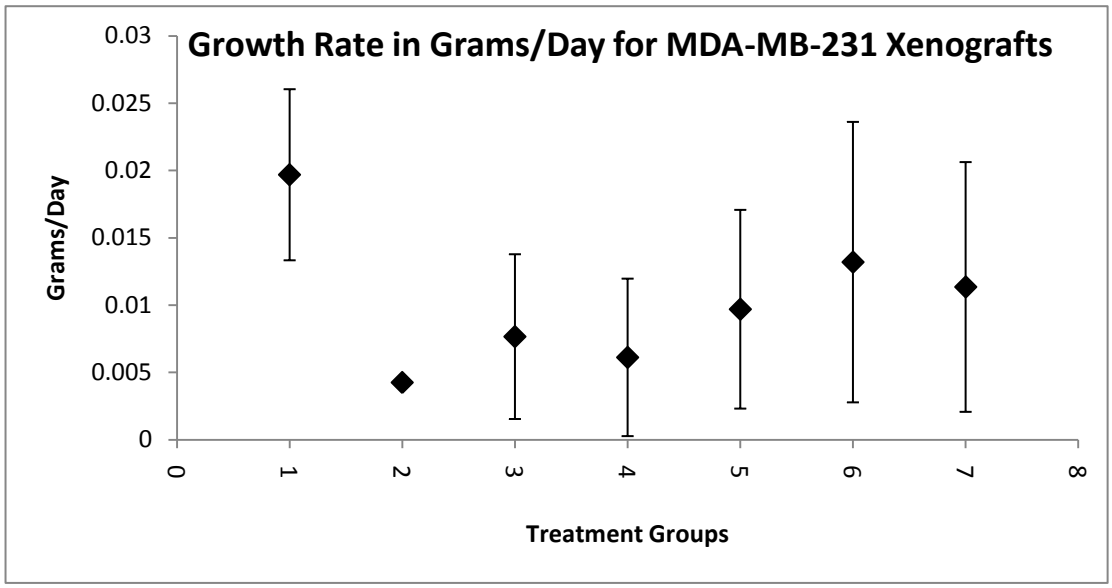

Figure 5-64- Growth rate for MDA-MB-231 xenografts with different treatments calculated using **t**umor weight on day of sacrifice (grams) divided by day of sacrifice (day). Animals were sacrificed on day 47 after first dose. 1 is MA control, 2 is Mbz control, 3 is MA single agent, 4 is Mbz single agent, 5 is concurrent, 6 is MA 1st and 7 is Mbz 1st treatment. There was no statistical significance in the difference between groups. Analysis was done using one-way ANOVA followed by Tukey's post hoc $p<0.05$. Data is presented as mean $\pm$ SD. (n=10 and 5 for control groups).

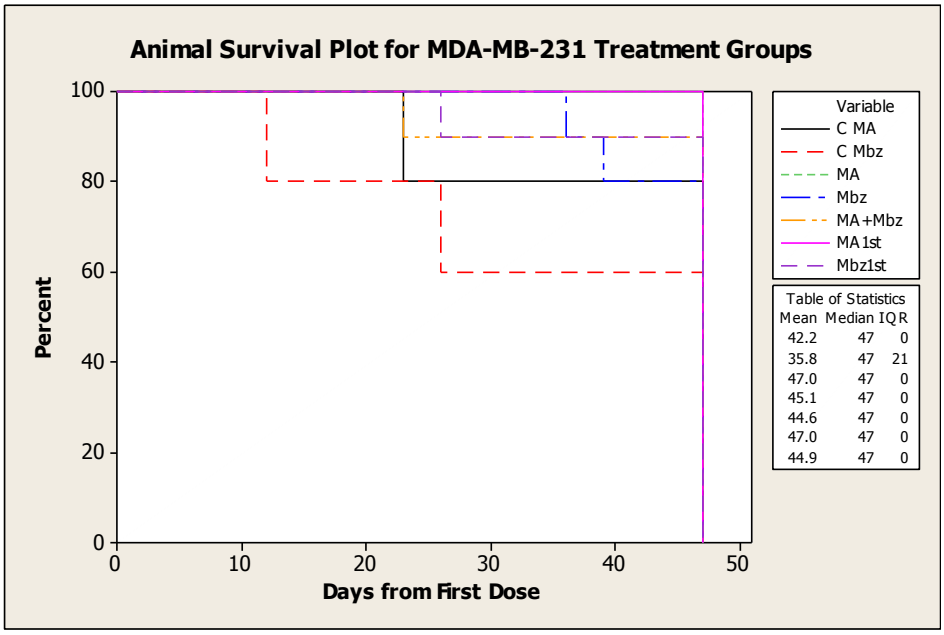

Figure 5-65- Survival of animals with MDA-MB-231 xenografts. Survival is expressed as percentage of animals surviving from the original number at day of first dose. MA single agent and MA1st groups had 100% survival, MA control, concurrent and Mbz 1st had 90% survival, Mbz control and Mbz single agent had 80%. Using Kaplan-Meier statistical method the log rank and wilcoxon p-values are < 0.204 and 0.195 respectively. There was no significant difference in survival rates between different groups.

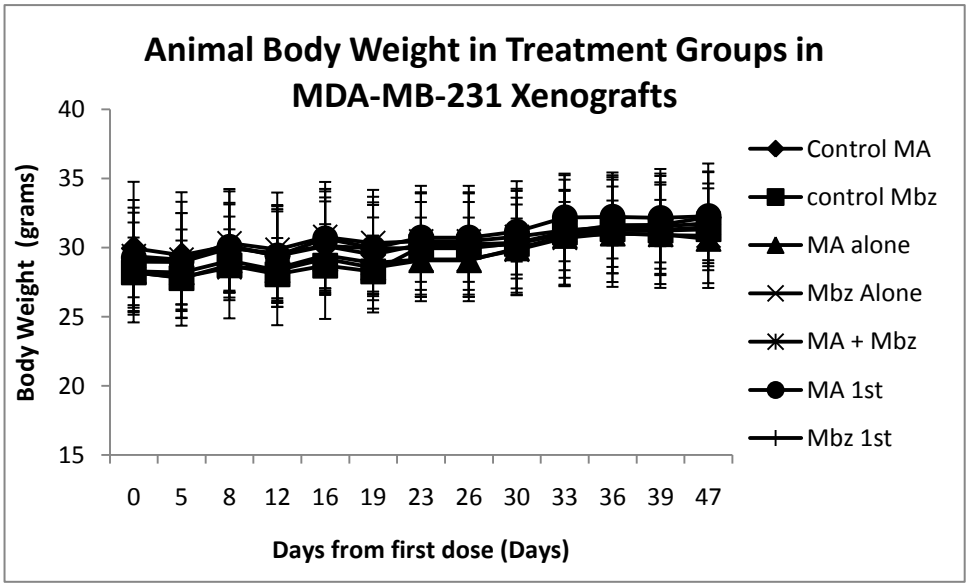

Figure 5-66- Average animal body weight in mice with MDA-MB-231 xenografts. There was no significant difference in body weight between different groups. Average animal body weight was stable during the time of the experiment.

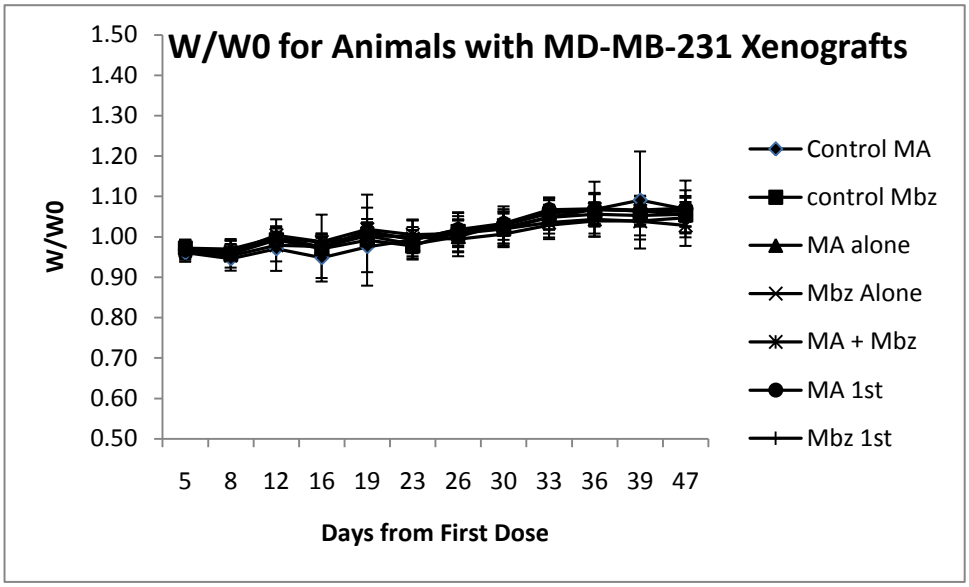

Figure 5-67- Body weight ratio in mice with MDA-MB-231 xenografts. There was no significant difference in body weight ratio between different groups. This indicates that average body weight was stable during the time of the experiment.

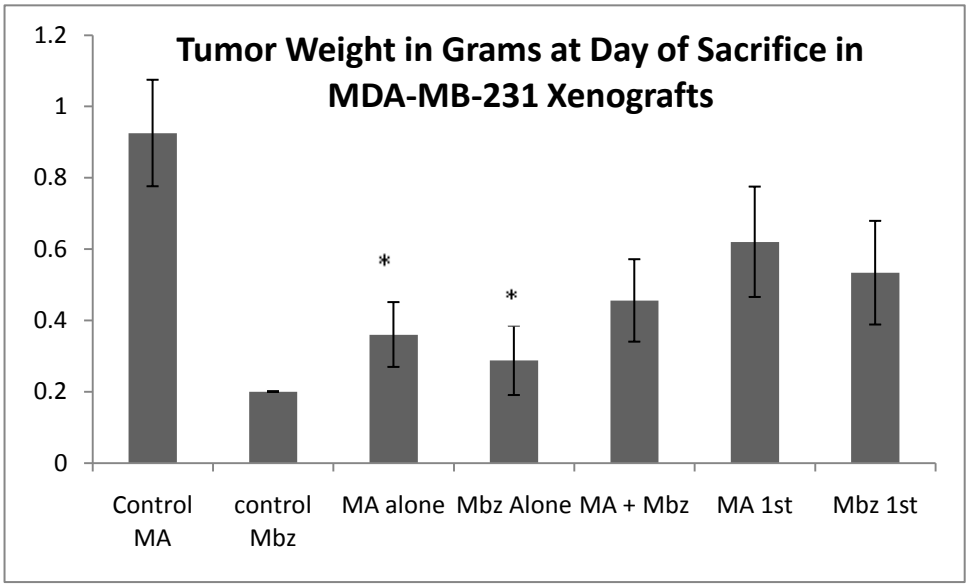

Figure 5-68-Tumor weight in grams on day of sacrifice for different treatment groups in MDA-MB-231 breast cancer cell xenografts. Animals were sacrificed on day 47 after first dose. Last dose was administered on day 26. * indicates statistical significance (p-value= 0.071) compared to control MA. Analysis was done using one-way ANOVA followed by Tukey's post hoc $p<0.1$. Data is presented as mean $\pm$ SD. (n=10 for MA and MA1st, n=9 for concurrent and Mbz 1st, 8 for Mbz treatment and 5 for control groups).

5-C-2b- Efficacy Study for MA and Mbz Combination Therapy in MDA-MB-231/ErbB2 Breast Cancer Cells:

The tumor volume ratio (V/V0) versus time in days for all control and treatment groups is shown in [Figures 5- 69 and 70 (log Scale)]. Using repeated measures one-way ANOVA with Tukey's post hoc ($p< 0.05$) concurrent treatment was statistically different from control MA and Mbz 1st treatments with a p-value <0.001. MA single agent was significantly different from control MA ($p<0.01$) and Mbz 1st ($p<0.05$). Concurrent treatment gave the lowest and Mbz 1st treatment gave the highest tumor volume ratios.

Table 5- 10 summarizes the growth rates for MDA-MB-231/ErbB2 xenografts. Growth rate was calculated by dividing either tumor weight at day of sacrifice or V/V0 by the duration from first dose until the day of sacrifice. The growth rates in (day^{-1}) are presented in [Figure 5-71] and are 0.74$\pm$ 0.44 for MA control, 0.24 $\pm$ 0.115 for Mbz control, 0.40 $\pm$ 0.24 for MA single agent, 1.03 $\pm$ 1.13 for Mbz single agent, 0.19 $\pm$ 0.0.13 for concurrent, 0.48 $\pm$ 0.52 for MA 1st, and 0.75 $\pm$ 0.6 for Mbz 1st treatment groups. The growth rates in (gram/day) are presented in [Figure 5-72] and are 0.056 $\pm$ 0.03 for MA control, 0.02 $\pm$ 0.009 for Mbz control, 0.047 $\pm$ 0.039 for MA single agent, 0.064 $\pm$ 0.04 for Mbz single agent, 0.0292 $\pm$ 0.0168 for concurrent, 0.046 $\pm$ 0.032 for MA 1st, and 0.0577 $\pm$ 0.027 for Mbz 1st treatment groups. There was no statistical significance in the difference between growth rates among the different treatment groups.

Kaplan Meier Survival analysis showed no difference among the different groups. Survival of animals in control and treatment groups over time in days from the day of first dose is presented in [Figure 5-73]. Survival is expressed as percentage of animals surviving from the original number at day of first dose. Survival rates and cause of death are summarized in [Table 5-11]. Tumor ulceration was the reason for the majority of animal sacrifices. The log-rank p-value was <0.539 and Wilcoxon p-value was < 0.467, indicating no statistical difference in survival rate among the different treatment groups.

The average body weight and ratio of body weight at each time point compared to initial body weight (W/W0) are presented in [Figures 5- 74 and 75]. Loss in body weight is considered an indication of treatment toxicity. A loss greater than 15% body weight is an indication for sacrificing the animals. All groups showed controlled and stable average body weight. There was no statistical difference between treatment groups in average body weight. One animal had a 24% drop in body weight, this was an individual case and not related to treatment toxicity.

Animals were sacrificed on day 47 and tumors were harvested and weighed. The average tumor weight in grams is presented in [Figure 5-76]. Using one way ANOVA followed by Tukey's post hoc ($p<0.05$) showed no statistical significance between groups. Harvested tumor of one animal (with the tumor volume closest to the mean) was chosen from each group [Picture 5-1]. The original volumes, tumor volumes along the duration of the experiment and tumor weight are all summarized in [Table 5-12].

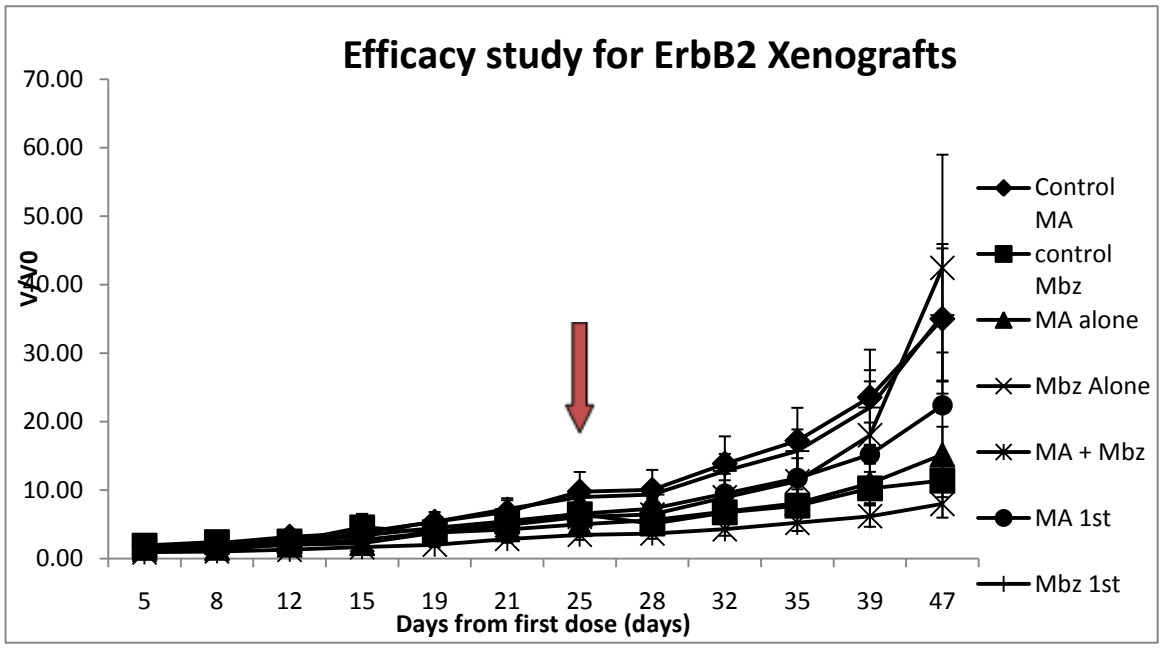

Figure 5-69- Tumor growth versus time for MDA-MB-231/ErbB2 breast cancer xenografts with different treatment groups. MA was administered ip at a dose of 2.5mg/kg and Mbz microemulsion was given ip at a dose of 5mg/kg. Tumor growth expressed as tumor volume on day of measurement divided by initial tumor volume on the day of first dose (V/V0) versus days from first dose. Tumors were assessed twice weekly before treatment. Last dose was administered on day 25. Concurrent treatmentwas significantly better than control MA and Mbz 1st. Analysis was done using repeated measures ANOVA (mixed model) followed by Tukey's post hoc $p<0.05$. Data is presented as mean $\pm$ SE. (n=10 for treatment and 5 for control groups).

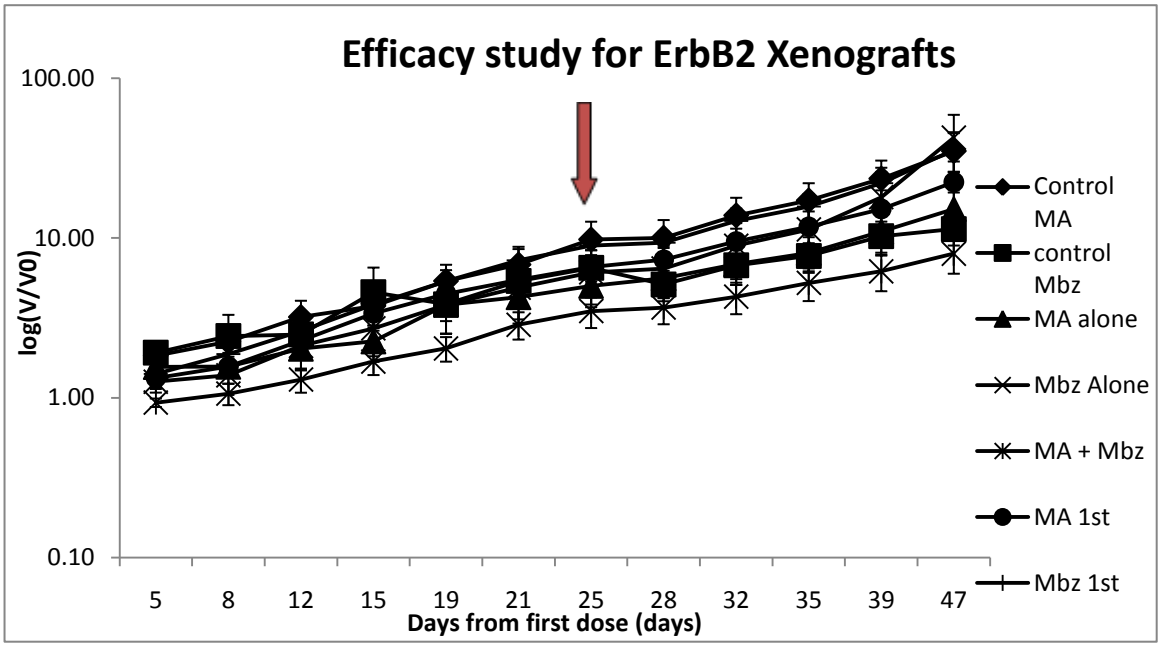

Figure 5-70- Log (V/V0) versus time for MDA-MB-231/ErbB2 breast cancer cell xenografts with different treatment groups. Last dose was administered on day 25. Analysis was done using repeated measures ANOVA (mixed model) followed by Tukey's post hoc $p<0.05$. Data is presented as mean $\pm$ SE. (n=10 for treatment and 5 for control groups).

Treatment Group	Growth Rate (day^{-1})	Growth Rate (gram/day)
Control MA	0.74$\pm$ 0.44	0.056 $\pm$ 0.03
Control Mbz	0.24 $\pm$ 0.115	0.02 $\pm$ 0.009
MA Single Agent	0.40 $\pm$ 0.24	0.047 $\pm$ 0.039
Mbz Single Agent	1.03 $\pm$ 1.13	0.064 $\pm$ 0.04
Concurrent	0.19 $\pm$ 0.0.13	0.0292 $\pm$ 0.0168
MA 1^{st}	0.48 $\pm$ 0.52	0.046 $\pm$ 0.032
Mbz 1^{st}	0.75 $\pm$ 0.6	0.0577 $\pm$ 0.027

Table 5-10- The growth rates of MDA-MB-231/ErbB2 xenografts in nude mice were calculated as last (V/V0) divided by the day of last V (day of sacrifice or death) or as weight of tumor divided by day of sacrifice. No statistical significance was observed among the different treatment groups using one way ANOVA followed by Tukey's post hoc at $p< 0.05$. Values are presented as mean $\pm$ SD.

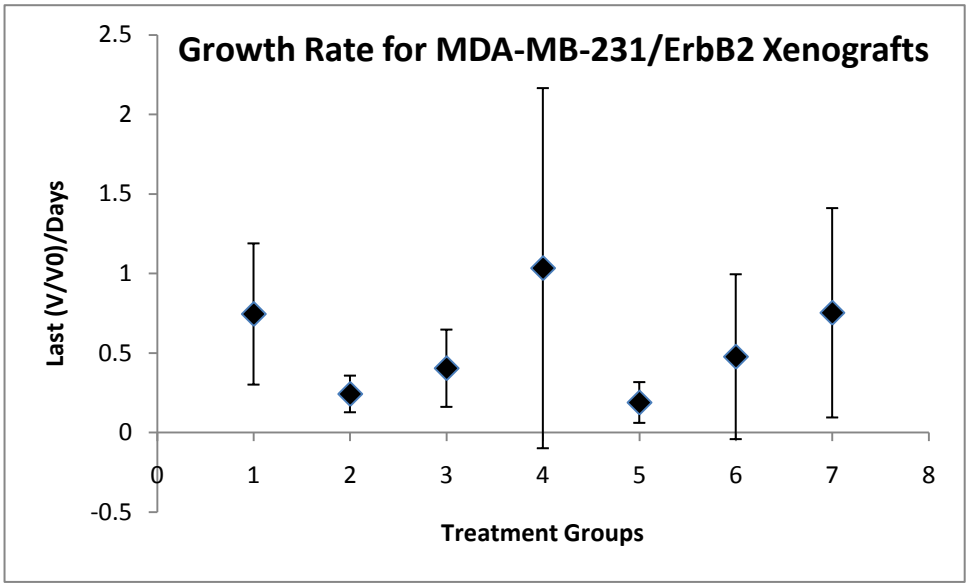

Figure 5-71- Growth rate for MDA-MB-231/ErbB2 xenografts with different treatments calculated using V/V0 on day of sacrifice divided by day of sacrifice (day). Animals were sacrificed on day 47 after first dose. 1 is MA control, 2 is Mbz control, 3 is MA single agent, 4 is Mbz single agent, 5 is concurrent, 6 is MA 1st and 7 is Mbz 1st treatment. There was no statistical significance in the difference between groups. Analysis was done using one-way ANOVA followed by Tukey's post hoc $p<0.05$. Data is presented as mean $\pm$ SD. (n=10 and 5 for control groups).

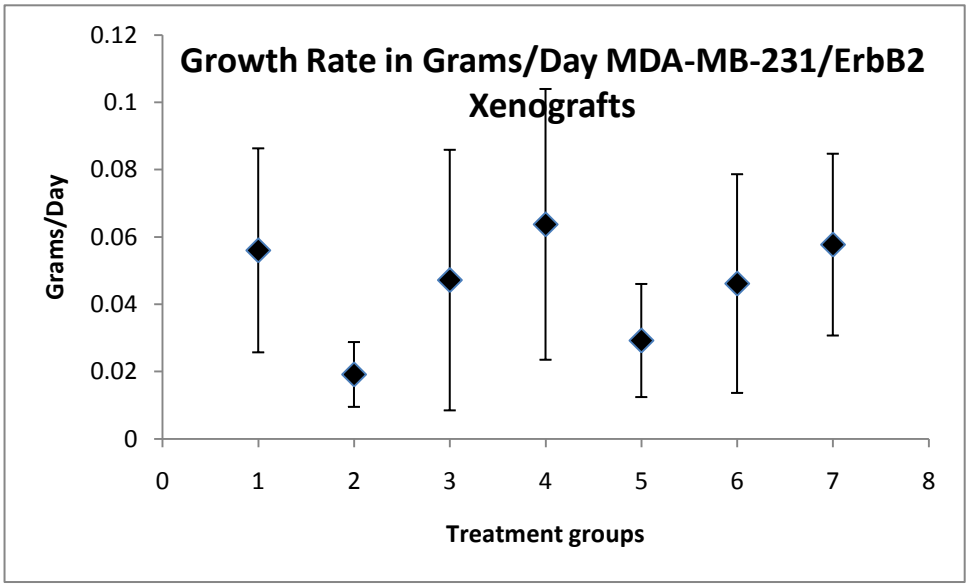

Figure 5-72- Growth rate for MDA-MB-231/ErbB2 xenografts with different treatments calculated using **t**umor weight on day of sacrifice (grams) divided by day of sacrifice (day). Animals were sacrificed on day 47 after first dose. 1 is MA control, 2 is Mbz control, 3 is MA single agent, 4 is Mbz single agent, 5 is concurrent, 6 is MA 1st and 7 is Mbz 1st treatment. There was no statistical significance in the difference between groups. Analysis was done using one-way ANOVA followed by Tukey's post hoc $p<0.05$. Data is presented as mean $\pm$ SD. (n=10 and 5 for control groups).

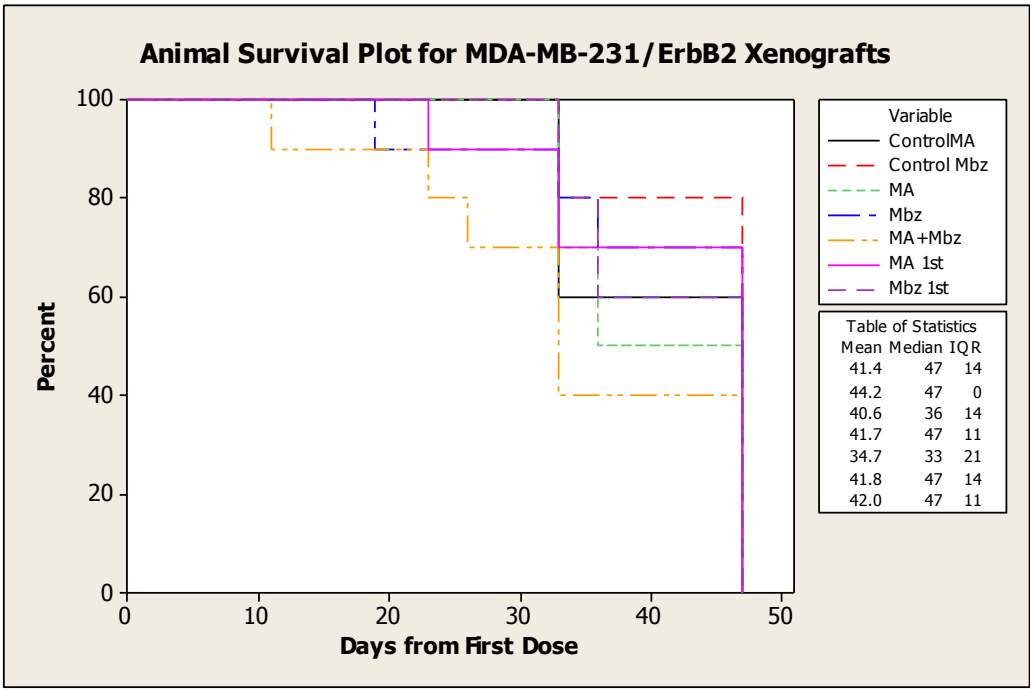

Figure 5-73- Survival of animals with MDA-MB-231/ErbB2 xenografts. Survival is expressed as percentage of animals surviving from the original number at day of first dose. Using Kaplan-Meier statistical method the log rank and wilcoxon p-values are < 0.539 and 0.467 respectively. There was no significant difference in survival rates between different groups.

Treatment	Tumor Ulceration		Swelling		Large Tumor		Weight Loss		Unknown		Survival
	Animal	Day	Animal	Day	Animal	Day	Animal	Day	Animal	Day	day 47
Control MA	1	32					1	32			60%
Control Mbz	1	32									80%
MA	2/1	32/ 35									70%
Mbz	1	32			1/1	32 / 35					70%
Concurrent	1/2	21 / 32	2/1	18 /32					1	11	30%
MA 1st	2	32	1	18							70%
Mbz 1st	2	32			1	35					70%

Table 5- 11- Summary of reasons for animal sacrifice before the end of the experiment. Animal represents the number of animals sacrificed, day represent the day from first dose on which the animal was sacrificed. The most common reason for sacrifice was tumor ulceration, followed by swelling.

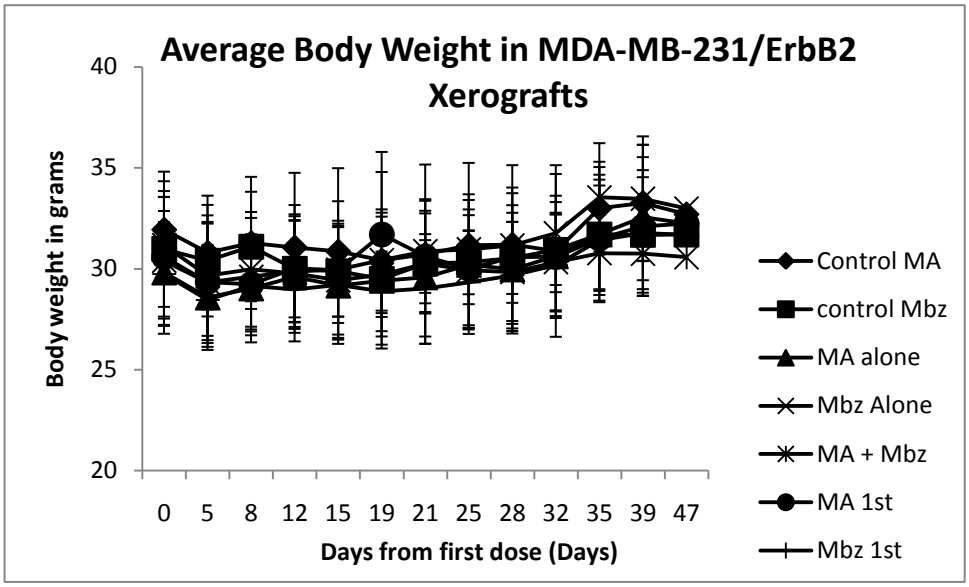

Figure 5-74- Average animal body weight in mice with MDA-MB-231/ErbB2 xenografts. There was no significant difference in body weight between different groups. Average animal body weight was stable during the time of the experiment.

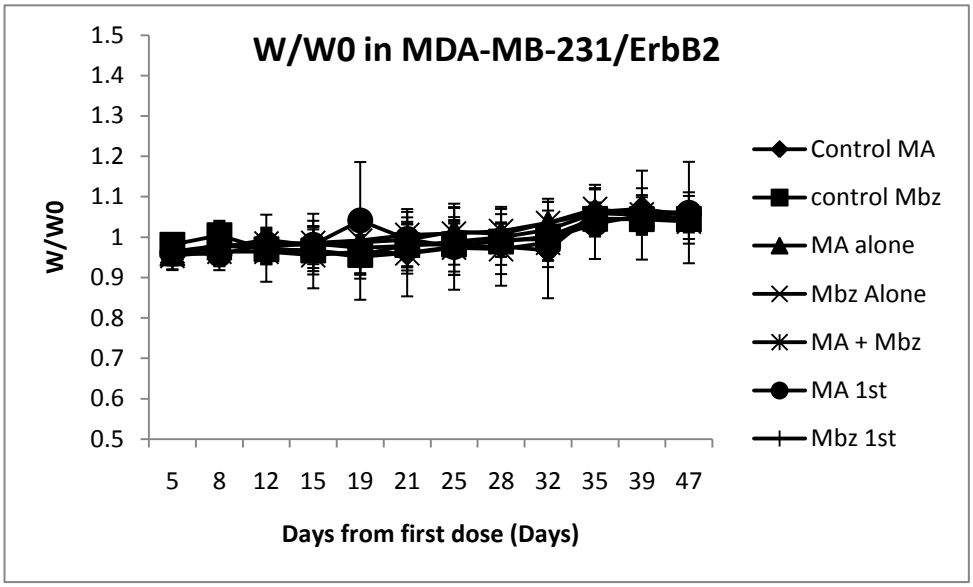

Figure 5-75- Body weight ratio in mice with MDA-MB-231/ErbB2 xenografts. There was no significant difference in body weight ratio between different groups. This indicates that average body weight was stable during the time of the experiment.

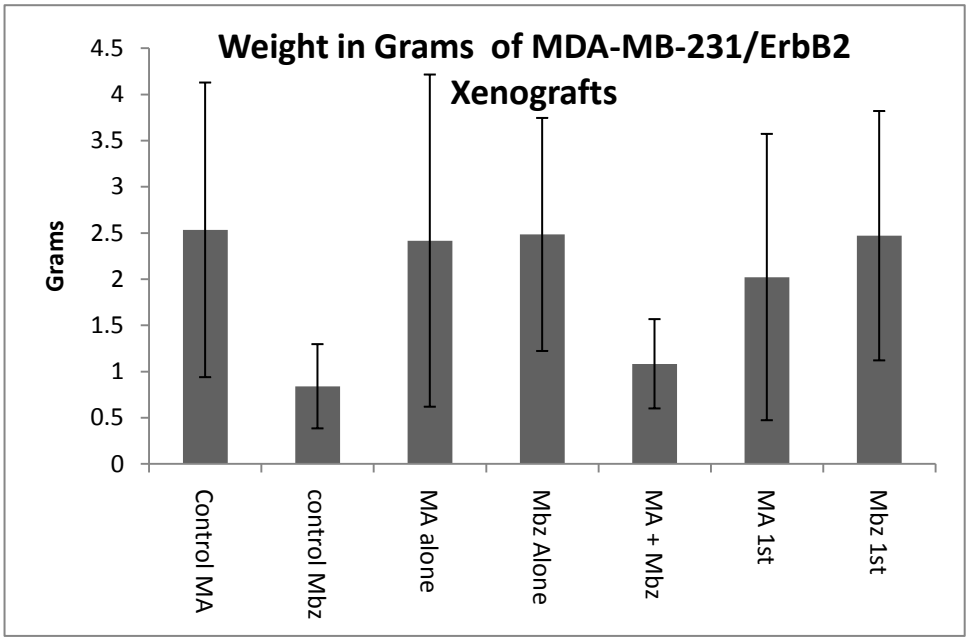

Figure 5-76-Tumor weight in grams on day of sacrifice for different treatment groups in MDA-MB-231/ErbB2 breast cancer xenografts. Animals were sacrificed on day 47 after first dose. Last dose was administered on day 25. There was no statistical significance in the difference between groups. Analysis was done using one-way ANOVA followed by Tukey's post hoc $p<0.05$. Data is presented as mean $\pm$ SE. (n=10 and 5 for control groups).

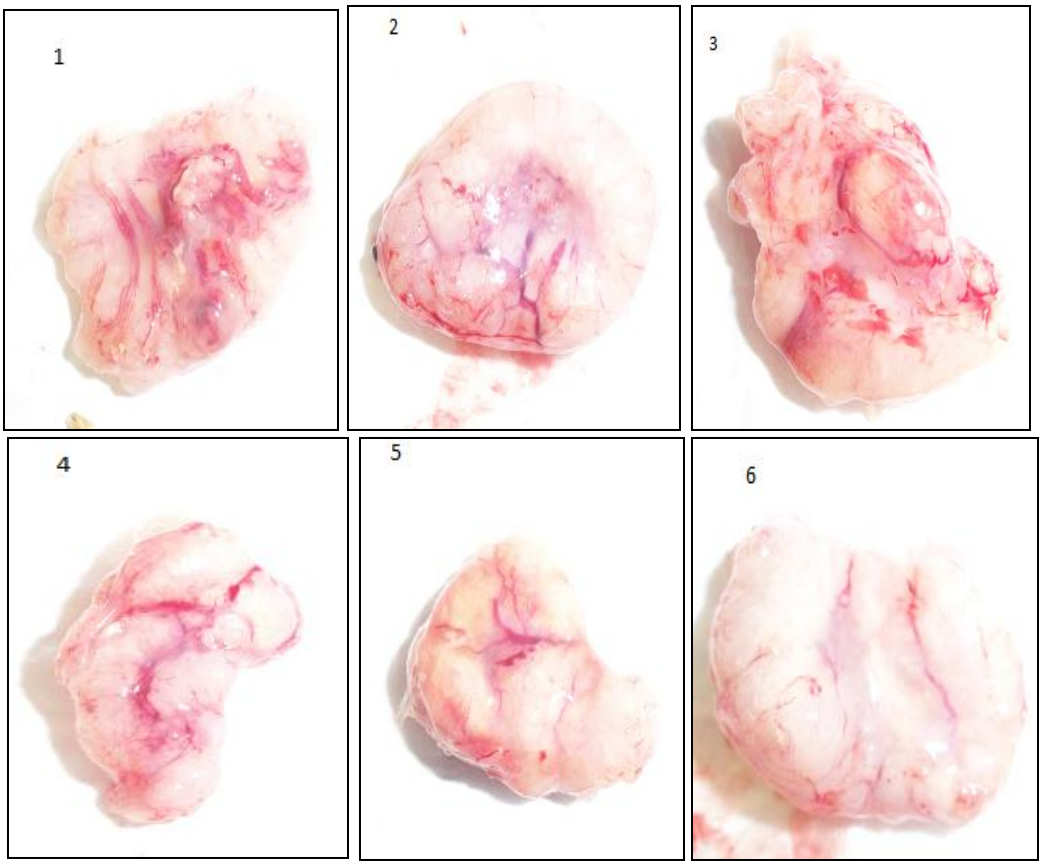

Picture 5-1- Harvested tumors from MDA-MB-231/ErbB2 xenografted mice. 1 is control MA, 2is MA, 3 is Mbz, 4 is concurrent, 5 is MA1st and 6 is Mbz 1st treatment groups.

Animal #	Treatment	Volume D0 (mm3)	Volume D5	Volume D8	Volume D12	Volume D15	Volume D19	Volume D21	Volume D25	D29 last Dose	Volume D33	Volume D36	Volume D39	Volume D47	TumorWeight grams
228	Control	**185.33**	312	315	542	685	926	1421	1919	2746	3694	4396	6437	9829	**3.6**
217	MA alone	**256.50**	223	335	376	534	874	1137	1448	2058	2334	2547	3958	6619	**3.3**
210	Mbz alone	**417.60**	358	464	663	722	1119	1470	1868	2596	2669	3809	4032	6196	**2.9**
242	MA +Mbz	**316.91**	306	523	577	846	924	1685	1275	1556	1964	2143	2321	2798	**1.2**
233	MA 1st	**369.38**	365	471	762	937	1061	1320	1877	1825	2765	2958	3126	4214	**2**
205	Mbz 1st	**617.70**	712	879	903	1484	2023	2772	2120	2241	2614	2839	2845	5935	**3.1**

Table 5- 12- Summary of tumor sizes and weight for tumorsg in Picture 1. Table presents initial tumor volumes (mm^3), volume measurements during the experiment and final tumor weight in grams.

5-C-2c- Variation in response to MA and Mbz combination treatment due to gender:

Upon harvesting the tumors from MDA-MB-231 xenografted mice, we noticed a great variation in tumor size and weight in Mbz 1st treatment group. Tumors obtained from male mice were smaller than those obtained from females [Picture 5-2]. Data from all treatment groups was segregated into female and male readings (we started with 5 male and 5 female mice in each group), we noticed that the variation between male and female tumors was only obvious in the Mbz single agent and Mbz 1st groups [Figure 5-77]. Comparing tumor weight in grams using one way ANOVA followed by Tukey's post hoc ($p<0.05$) revealed that this gender related difference is statistically significant with p-value of 0.013 in Mbz 1st treatment but not with Mbz single agent group. Tumor volumes in the Mbz 1st and Mbz single agent treatment groups were plotted for male and female mice [Figure 5-78 and 79].

Data from MDA-MB-231/ErbB2 xenografts was also analyzed to determine any gender related variation. This variation was seen with concurrent treatment and Mbz single agent. Mbz single agent yield larger tumors compared to concurrent treatment in female mice [Figure 5-80]. No statistical significance was observed when comparing these groups using one-way ANOVA with Tukey's post hoc ($p<0.05$). The lack of statistical significance is thought to be due to the small sample size. Mbz single agent and concurrent treatments did not vary in male mice. Profile was only plotted for 28 days due to the need to sacrifice 5 animals from concurrent treatment on day 32.

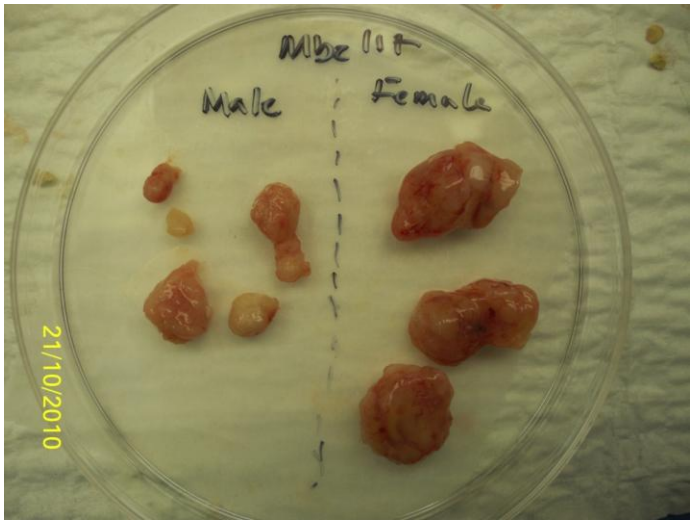

Picture 5-2- Harvested tumors at day 47 after first dose from mice with MDA-MB-231 xenografts treated with Mbz 1st treatment. Male mice had noticeably smaller tumors compared to female mice.

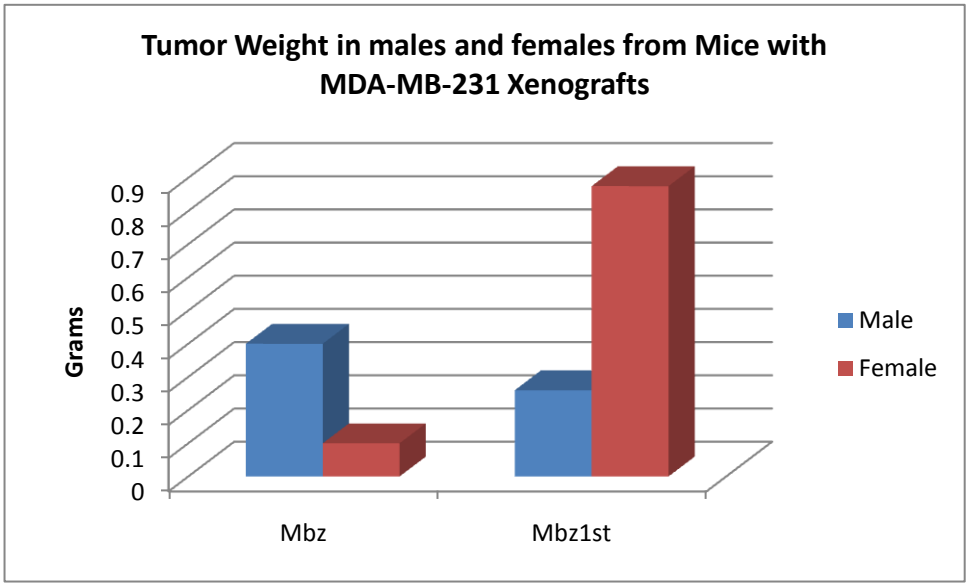

Figure 5-77-Tumor weight after sacrificing the animals in male compared to female mice after treatment with Mbz single agent and Mbz1st in MDA-MB-231 breast cancer xenografts. Animals were sacrificed on day 47 after first dose. Using one-way ANOVA with Tukey's post hoc shows a statistically significant difference in tumor weight with Mbz 1st treatment but not in Mbz treatment p-value =0.013. (n=5 in male mice, 4 in Mbz 1st treatment and 3 in Mbz treatment in females).

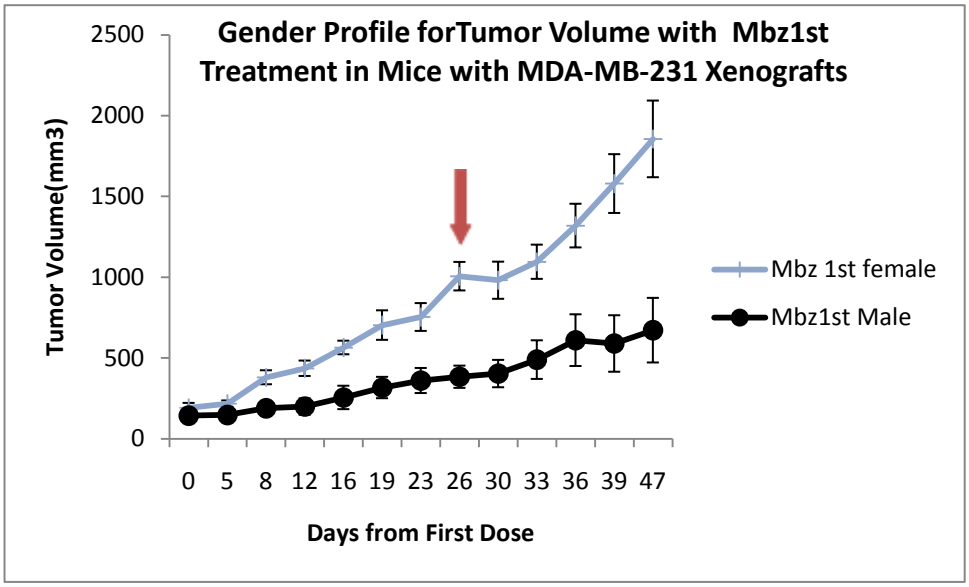

Figure 5-78-Tumor volumes in male mice compared to female mice after treatment with Mbz1st in MDA-MB-231 breast cancer xenografts. Animals were sacrificed on day 47 after first dose. Last dose was administered on day 26.

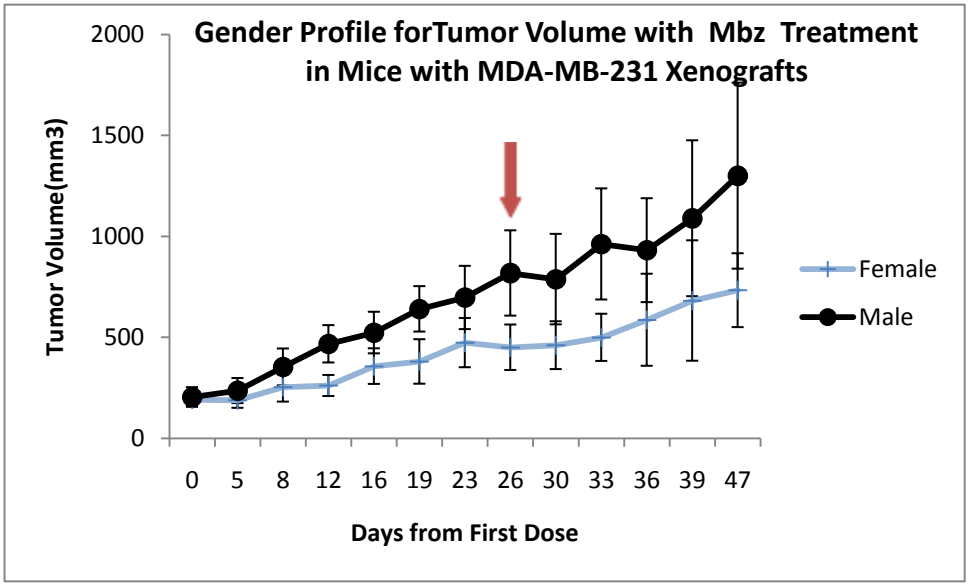

Figure 5-79-Tumor volumes in male mice compared to female mice after treatment with Mbz single agent in MDA-MB-231 breast cancer xenografts. Animals were sacrificed on day 47 after first dose. Last dose was administered on day 26.

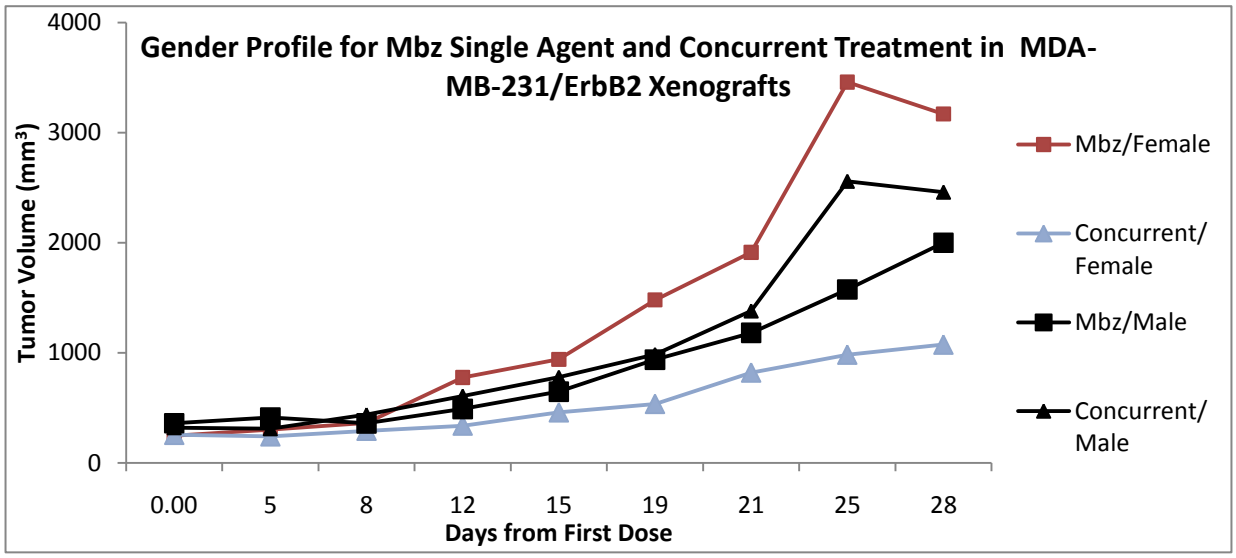

Figure 5-80-Tumor volumes in male mice compared to female mice after treatment with Mbz single agent and concurrent treatment in MDA-MB-231/ErbB2 breast cancer xenografts. Animals were sacrificed on day 47 after first dose. Last dose was administered on day 25. We can clearly see how Mbz and concurrent treatments are super imposed in male mice (two black lines). Mbz single agent yield larger tumors compared to concurrent treatment in female mice (orange and blue lines). No statistical significance was observed when comparing these groups using repeated measures one-way ANOVA with Tukey's post hoc ($p<0.05$) this is thought to be due to the small sample size. Profile was only plotted for 28 days due to the need to sacrifice 5 animals from concurrent treatment on day 32.

CHAPTER-6- DISCUSSION

6-A-The effect of single and combination treatment with MA and Mbz in all four breast cancer cell lines:

FTIs were first introduced to target FTase and inhibit ras activation. Bench work and clinical trials on these agents later revealed that they produce their cytotoxic effect by altering the farnesylation of proteins other than ras and by mechanisms independent of the FTase pathway. Due to their cytostatic effect, clinical trials were concluded to recommend their use as adjuvant rather than single agent chemotherapies. FTIs were used in a number of combinations. The most effective combination was FTIs and taxanes. Today we know that FTIs interfere with HDAC6 function and increase microtubule acetylation and stability, this is thought to augment the effect of taxanes leading to the synergism of the combination. Another point of interaction is through apoptosis. Apoptosis increased with combination treatment compared to single agents MA and Paclitaxel. All reported studies focused on FTIs and the microtubule stabilizing rather than destabilizing agents.

In our study we evaluate the combination of the FTI, MA, and the microtubule destabilizing drug, Mbz. Mbz is effective in a number of ovarian, breast, and lung cancers. It binds to colchicine binding site on the microtubules altering their equilibrium and destabilizing them by halting the continuous addition of β–tubulin to the C- terminus.

Due to the role anti-microtubule drugs play in breast cancer treatment, we chose to study this combination in human breast cancer cell lines. Breast cancers are very diverse; this increases the complexity of their treatment. We chose two human breast cancer cell lines that are very diverse in their origin and genetic composition. Regardless of the aggressiveness and drug resistance of HER2 expressing tumors, tumors overexpressing HER2 benefited from the addition of taxanes to the chemotherapeutic regimen. Johnson et al reported that in breast cancer most of the responses with FTIs occurred in HER2/neu positive cancers [Mazieres et al, 2004]. We evaluated the effect of HER2 overexpression on the final outcome of MA and Mbz combination. We studied the wild type and HER2 transfected MDA-MB-231 and MCF-7 human breast cancer cell lines.

Both MA and Mbz were evaluated as single agents in breast cancer tumor cells and showed activity. We found no report regarding their activity in the fore mentioned cell-lines, so we started our study by evaluating the cytotoxicity of single agent MA and Mbz in the four cell-lines.

MA dose response curves for wild type and HER2 transfected MDA-MB-231 and MCF-7 breast cancer cell lines revealed that the expression of HER2 does not affect the sensitivity of cells to MA. MA inhibited cell growth in all four cell lines showing the same potency in wild type and HER2 transfected cells. We did not observe any difference in sensitivity to MA between the two cell line pairs (MDA-MB-231 and MCF-7) [Figure 5-1, 2, and 3].

In MCF-7/Her18 cells, MA dose response curve present cell viabilities higher than 100% compared to control. This warranted further investigation to determine whether the increase in cell viability is true or is an artificial. Cell viabilities for dose response experiments were obtained using the XTT assay, we regenerated the curve using the SRB assay, and found that cell viabilities obtained using this method did not exceed 100% [Figure 5-4]. The Log EC_{50} value for MA dose response obtained by SRB was (- 5.434 $\pm$ 0.04723) M compared to (- 4.498 $\pm$ 0.04539) M with XTT.

XTT based assay is a colorimetric quantification method of cell proliferation and viability. The yellow tetrazolium salt XTT is cleaved to form an orange water soluble formazan dye by metabolically active cells via mitochondrial dehydrogenases, a conversion that occurs only in viable cells. An increase in the number of living cells results in an increase in the overall metabolic activity reflected by an increase in color intensity. Evidence of tetrazolium reduction by constituents of culture media like antioxidants and FBS was recently described. Both bovine and human serum albumins led to a serum concentration dependent increase in XTT signals [Frei et al 2007]. MA induces ROS formation which could be the reason for the artificial increase in cell viability of MCF-7/Her18 cells when MA dose response curve was assayed by XTT compared to SRB. Cell proliferation, measured as total protein synthesis, is a very sensitive toxicology marker. SRB is an anionic dye that binds electrostatically to cellular proteins. SRB binds to protein components of cells that have been fixed to tissue culture plates by trichloroacetic acid. Binding of SRB is stoichometric and the final absorption of

the extracted SRB is directly proportional to the cell mass. This method has the advantage of being independent of cell metabolic activity and minimal interference with culture media [Vichai and Kirtikara 2006].

Based on the previous findings and discussion we decided to use the SRB for further treatment assessment of MA and Mbz single and combination treatments.

The cytotoxicity of Mbz was tested on wild type and HER2 transfected MDA-MB-231 and MCF-7 breast cancer cell lines in vitro. Mbz inhibited the growth of all four cell lines with higher potency in the MDA-MB-231 cell pair [Figure 5-5]. Again the expression of HER2 did not affect cell sensitivity to Mbz [Figures 5-6, and 7].

Single agent treatment with MA or Mbz showed cytotoxicity in wild type and HER2 transfected MDA-MB-231 and MCF-7 breast cancer cell lines. This drove us to investigate the use of MA as a FTI in combination with Mbz as a microtubule destabilizing agent in these cell lines.

The final outcome of anticancer-drug combinations is synergism, additivity, or antagonism. The effect of the MA- Mbz combination treatment on the four breast cancer cell lines showed all three outcomes. Our study correlates these varying outcomes to drug concentration, MA to Mbz dose ratio, sequence of drug administration and cellular composition. The effect of MA and Mbz was evaluated first by using a constant MA to Mbz (1:1) ratio approach to test for the effect of concentration on treatment outcome. The median effect analysis was performed using CalcuSyn Biosoft software, and the CI

values were calculated and presented in a synergy heat map [Figure 5-8]. We noticed an antagonistic activity at high MA and Mbz doses which could be a result of drug-drug interactions that are bypassed at lower concentrations. Many drugs have different pharmacological targets at different concentrations [Mayer et al 2006]. MA inhibited ras farnesylation completely at a concentration of 10 uM in medulloblastoma cells, at higher concentrations MA showed increased cytotoxicity indicating that it had targets other than FTase [Wang and Macaulay 1999]. Mbz is known to bind to the colchicine binding site on the microtubules. Microtubules in a protofilament are stabilized through lateral and longitudinal interactions, any interference with these interactions destabilize microtubules. Cochicine has a dose related effect on microtubules. At low TC-complex (Tubulin-Colchicine complex) concentrations, the complex gets incorporated into microtubules affecting lateral interactions only, this interference is minimal so the microtubule remains intact but can no longer be in a straight conformation. As the concentration of colchicine increases the concentration of TC-complex increase, and its incorporation into the microtubule affects both lateral and longitudinal binding and leads to the disassembly of microtubules [Bhattacharya et al 2008]. The activity of FTase is required for HDAC6 mediated microtubule deacetylation, where both FTase and HDAC6 bind to microtubules to facilitate deacetylation. MA and colchicine interfere with this interaction. MA inhibits FTase this decreases deacetylation and increases microtubules stability. Only at high doses does colchicine interfere with the FTase and HDAC6 binding to microtubules [Zhou et al, 2009]. Thus we do speculate that the binding of Mbz

to the colchicine binding site on the microtubules at a high concentration will also interfere with FTase and HDAC6 interaction, and at low doses Mbz will destabilize the microtubules without interfering with HDAC6.

At a fixed concentration of MA and Mbz different cell lines reacted differently to combination treatment. Charafe-Jauffret et al profiled gene expression in 31 breast cancer cell lines. They concluded that the molecular heterogeneity of breast cancers influence the final treatment outcome. Their research emphasized the difference in gene and protein expression between the mesenchymal like MDA-MB-231 cells that are ER and PR negative and the luminal like MCF-7 cells that are ER and PR positive [Charafe-Jauffret et al 2006]. The effect of the antifungal resveratrol on MDA-MB-231 and MCF-7 was studied. The two cell lines responded differently to treatment with MDA-MB-231 cells undergoing non-apoptotic cell death and MCF-7 cells showing evidence of apoptosis [Salguero et al 2002]. This support our results showing that MCF-7 and MDA-MB-231 cells responded differently to MA and Mbz combination. We did show that MA induced a G1/S and G2/M phase arrest in MCF-7 and MD-MB-231 cells, respectively. This difference is attributed to the expression of wild type p53 in MCF-7 and a mutant p53 in MDA-MB-231 cell line [Mazierel et al 2004]. Again, this emphasizes the role targeted cell characteristics have on final outcome of treatment.

Schedule-dependent synergism was observed with a number of combinations in clinical trials. Thus we evaluated both sequential and concurrent treatments comparing the three

different MA and Mbz combination treatments for each cell line (concurrent,MA1st and Mbz 1st), we can clearly see that the final outcome of treatment depends on sequence of drug administration. Goldie and Coldman et al. suggested a mathematical model for cancer treatment stating that "*to avoid selection of doubly resistant mutants, multiple non-cross-resistant drugs should be used together rather than sequentially*." On the other hand, Norton et al. recommended "*individual drugs, not multiple drugs, should be given sequentially at their highest possible dose to treat cancers."* [Norton et al, 1998]. Norton et al. conducted a clinical trial based on their model. Sequential cyclophosphamide, doxorubicin and paclitaxel were evaluated in women diagnosed with primary breast cancer with four or more positive lymph nodes. Outstanding results were observed, with 80% 4-year disease free survival compared to 50% relapse rate at 4 years with the standard therapy of cyclophosphamide plus doxorubicin [Hudis et al, 1999]. Our heat map reveals that the sequence of drug administration contributes to the final outcome. Targeted cancer cells determine which combination, sequential or concurrent, gave the favorable outcome. Since antagonism persists at high doses of MA and Mbz, we contradict the Goldie and Coldman model.

Our in vitro experiment led us to conclude that no one-size fits all in cancer treatment, and that the genetic composition of the targeted cells, drug concentration and sequence of drug administration determines the final outcome of MA and Mbz combination treatment.

To evaluate the role of HER2 expression and MA to Mbz ratio on the final treatment effect, we studied the MA and Mbz combination in MCF-7 and MCF-7/Her18 cells using varying MA to Mbz concentration ratios. The results were presented in a synergy heat map [Figure 5-9]. HER2 expression didn't alter the effect of MA and Mbz Single treatment on the studied breast cancer cell lines. Comparing wild type to HER2 expressing MCF-7 cells we observed different reactions to combination treatment in the two cells. HER 2 expression rendered Mbz 1st treatment synergistic at all MA to Mbz ratios and concentrations. The role of MA to Mbz ratio was more obvious in wild type MCF-7 cells. When MA to Mbz ratio was 1:10, MA 1st treatment was synergistic at MA concentrations of 0.5 and 2.5 µM, and antagonistic at MA concentration of 5 µM, the final outcome was reversed with Mbz 1st treatment. So we conclude that for MA and Mbz combination the ratio of MA to Mbz does affect the final outcome of treatment. HER2 expression is another factor influencing combination cytotoxicity. In MCF-7/Her18 MA concentrations of 0.5 and 2.5µM were always antagonistic with MA 1st treatment, while a concentration of 10µM was always synergistic, and an MA concentration of 5µM was either synergistic or antagonistic when MA was given first depending on the (MA: Mbz) ratio. Again this observation reveals that in addition to the ratio, the actual concentration of drugs used influence the final outcome in combination therapy.

To our knowledge we are the first to construct a synergy map for sequential combination treatment as Mayer et al investigated concurrent treatments only and raised the question whether this will apply to sequential therapy as well. It is not in the scope of our study to investigate the mechanisms leading to synergy and antagonism at the different concentration ratios. Yet, this worthwhile observation can influence future drug formulations of MA and Mbz. We do suggest putting this newly defined principle of drug-ratio antagonism into use by generating clinical synergy heat maps for existing chemotherapy combinations. Clinical heat maps should be based on drug ratios in blood samples obtained from responsive and non-responsive cancer patients to help improve treatment and enhance response to chemotherapy by maintaining blood levels at synergistic ratios observed in responsive patients. This speculation is based on the dissimilarity in pharmacokinetics and pharmacodynamics of drugs between individuals, which leads to variation in drug concentrations and ratios after systemic administration of the same dose to different individuals. Drugs in a combination should be introduced to the body in a form that coordinates drug release with pharmacokinetics and biodistribution to ensure that drugs are delivered to the tumor at a synergistic ratio. We did observe the effect of PK/PD in our in vivo studies, where female mice showed antagonism male mice showed synergism with Mbz 1st in MDA-MB-231 xenografted mice. We attribute this to the difference in drug metabolism in females leading to a different MA to Mbz ratio than that in male mice.

MA and Mbz combination treatment did not show any additional benefit over treatment with single agents in wild type MDA-MB-231 and MCF-7 breast cancer cells. HER2 overexpression increased sensitivity to sequential combination treatment in both cell lines. The optimal sequence of drug administration was different in the two HER2 positive cell lines. MA 1^{st} and Mbz 1^{st} treatment were superior in MDA-MB-231/ErbB2 and MCF-7/Her18 cells, respectively. The outcome of treatment with MA and Mbz is influenced by HER2 overexpression.

When comparing the two cells in each pair we observe that the only difference between the two cell lines in each pair is HER2 overexpression, thus we will try to discuss our data in reference to HER2 according to the model proposed by Wilson et al [Figure 6-1]. Wilson et al studied the effect of HER2 expression on the TGF-β signaling by gene microarray both in MCF-7 and MDA-MB-231 cells. They proposed a model in which two major branches of TGF-β responses exist; one that is inhibited by ER signaling and the other by constitutively active ras. TGF-β is the main signaling pathway opposing stimulatory effects of growth factors. It also promotes invasive cell behavior and metastasis associated with EMT. TGF-β inhibits mammary gland, normal epithelial cells, and breast cancer cells growth in culture. TGF-β shows markedly different biological effects on luminal MCF-7 and mesenchymal like MDA-MB-231 cells. HER2 positive MCF-7 cells are resistant to the growth inhibitory effect of TGF-β. HER2 positive MDA-MB-231 cells show aggressiveness through cooperation between HER2 and TGF-β.

In MDA-MB-231 cells which express a constitutively active ras, MA inhibits ras farnesylation allowing for cell cycle arrest. Flow cytometry data shows that MA induces G2/M phase arrest in these cells, so we speculate that the cells arrest at G2/M phase after ras inhibition following MA treatment and are no longer actively dividing, so they are not sensitive to Mbz thus the synergistic effect observed with MA 1st treatment with HER 2 positive cells is absent in wild type cells.

In MDA-MB-231/ErbB2 cells cell cycle arrest is halted by ras and HER2 activity. Giving MA first inhibits the constitutively active ras. HER2 effect on cell cycle persist preventing cell cycle arrest. MA exerts its cytotoxicity via a different pathway than cell cycle arrest. When Mbz is given second it affects the cells undergoing EMT by destabilizing the microtubule based membrane protrusions, the microtentacles, which are formed at an early stage of EMT [Whipple et al. 2010]. Since HER2 enhances EMT, more cells will be affected by Mbz, thus the additional benefit obtained with MA 1st treatment in HER2 positive cells.

In the wild type MCF-7 cancer cells the difference in cytotoxicity between the different treatment groups is influenced by MA concentration. At the lower MA concentrations MA 1st is significantly different from concurrent treatment, while at higher MA concentrations MA 1st becomes significantly different from Mbz 1st treatment, and shows no significant difference in cytotoxicity compared to MA alone and concurrent treatments. Mbz 1st treatment group is significantly different from the other two

combinations showing higher cell viability. It offers no additional benefit compared to treatment with single agents, thus it is considered antagonistic. It is also observed that when used alone, Mbz was less cytotoxic compared to concurrent and MA 1st treatment [Figure 5-12]. We conclude that MA interferes with Mbz mechanism of action blocking its cytotoxicity.

Mbz 1st treatment group in the HER2 transfected MCF-7/Her18 cancer cells gives the lowest percent cell viability compared to all other treatment groups. At MA dose of 60µM ,the difference between Mbz 1st and the three treatments(MA alone, MA 1st and concurrent treatments) is significant. One can conclude that Mbz1st shows additional benefit compared to single agent and other combination treatment groups. CI values presented in the synergy map do indicate that Mbz1st was synergistic in this cell line at different ratios and concentrations of MA and Mbz. [Figure 5-13]. Referring to figure 6-1 we see that in wild type cells cell cycle arrest is not inhibited, so when giving Mbz 1st it will arrest the cells in the M phase and fewer cells will move on to the G1 and S phases where MA exerts its arrest. In HER2 positive cells, HER2 blocks cell cycle arrest. If cell cycle arrest is blocked other mechanism of Mbz cytotoxicity become obvious. It is proposed that Mbz is a microtubule inhibitor with pleiotropic effects due to its structure that resembles different nucleotides [Martarelli et al 2008]. Benzimidazoles are known to inhibit glucose uptake and fumarate reductase activity. An increased role for fumarate reductase in cancer cells was recently reported [Esumi et al, 2009]. We conclude that

when cell cycle arrest is blocked we observe an additional benefit from combination treatment, while when cells undergo cell arrest one drug blocks the effect of the other.

Comparing the two different cell lines MDA-MB-231 and MCF-7, we can see a clear difference in the overall outcome from different treatment groups; summary in [Table 5-2]. We conclude that due to the variation in the genetic composition between MDA-MB-231 and MCF-7 cells cytotoxicity of the different MA and Mbz combination treatments varies in these two cell lines. The two HER2 transfected cell lines, MDA-MB-231/ErbB2 and MCF-7/Her18 cells differ in a number of genetic variables. MDA-MB-231/ErbB2 cells lack ER and PR and have constitutively active ras and mutant p53, while MCF-7/Her18 cells express ER and PR, and have wild type ras and p53. The presence of wild type p53 in cancer cells favors the G1/S cycle arrest with MA treatment which was observed in our PI flow cytometry experiments, in contrary to G2/M cycle arrest obtund in MDA-MB-231 cells that express a mutant p53. This could be one of the factors contributing to the difference in optimal sequence of drug administration.

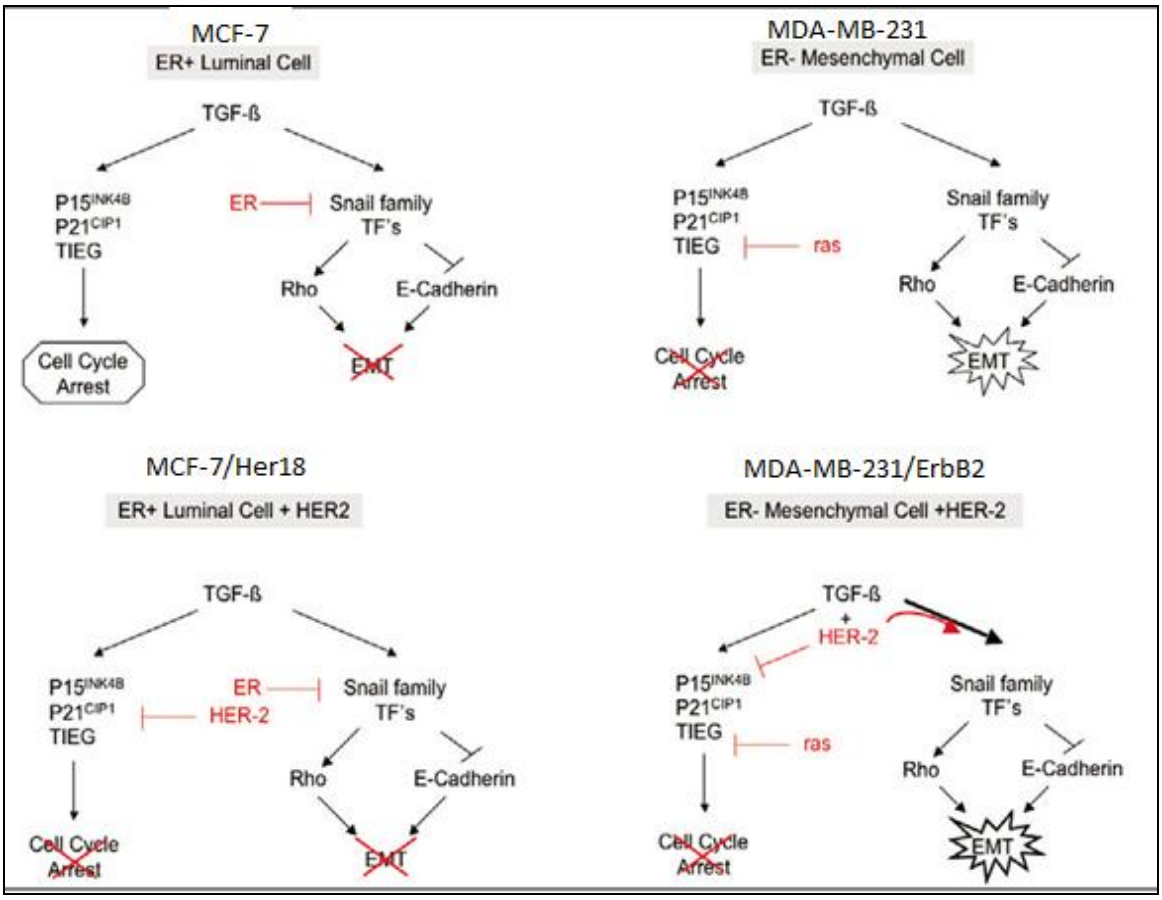

Figure 6-1- Model for context specific effect of HER2 overexpression on TGF-β signaling as proposed by Wilson et al 2005, Breast Cancer Research 7 (6): R1072.

6-B- Assessing the role of cell cycle arrest and apoptosis in the cytotoxicity of combined MA and Mbz treatments in the four breast cancer cell lines:

The improvement in cytotoxicity with sequential therapy was statistically significant in HER2 transfected MDA-MB-231 and MCF-7 cancer cells. The optimal sequence of drug administration was different in the two cell lines. We hypothesized that the final effect of the MA-Mbz combination treatment is the result of both apoptosis and cell cycle arrest. Flow cytometry analysis, which is capable of detecting apoptosis and cell cycle arrest, and western blotting of cyclins E and B and PARP were used to evaluate our hypothesis.

Flow cytometry studies using PI showed that Mbz arrests the cells at the G2/M phase in both cell lines [Figures 5:14-17], this is manifested by an increase in the proportion of cells in the G2/M phase following treatment with Mbz alone both in wild type and HER2 transfected cells. In 2002 the effect of Mbz on a number of cancer cells was evaluated. Propidium iodide staining of H460 cells at different time points following treatment with Mbz revealed an increase in G2-M phase cell cycle arrest at 12 hours post treatment [Sasaki et al, 2002]. Mbz inhibited the growth of cancer cells in vitro and in vivo by mitotic arrest. It depolymerized tubulin disrupting the function of microtubules [Martarelli et al 2008]. In our study these results stand true for the effect of Mbz on wild type and HER2 transfected MDA-MB-231 and MCF-7 breast cell lines.On the other hand, MA induced cell cycle arrest at different phases in MDA-MB-231 compared to MCF-7 cell lines. FTIs modulate the cell cycle in human tumor cell lines where cells

accumulate either in G0/G1 or G2/M phase. The G0/G1 blockade was correlated with wild type p53 [Mazierel et al 2004].

In wild type and HER2 transfected MDA-MB-231 cells MA arrested the cells at the G_2/M-phase [Figures 5: 14-15]. This effect is attributed to the mutant p53 expressed in MDA-MB-231 cells [Hui et al 2006]. There was no significant difference between concurrent and MA alone treatments in wild type and HER2 transfected cells in regard to cell cycle distribution. This explains our previous observations with single and combination treatment comparison in section (6-A). No significant difference in cell percent viability in MA single agent and concurrent treatments was observed; here too we see that the effect of concurrent treatment on cell cycle is not different from single agent MA. Our observation leads us to speculate that when given concurrently MA blocks any additional effect of Mbz on treated cells.

Cell cycle analysis of MDA-MB-231/ErbB2 cells shows that MA arrests the cells at G2/M and has an effect on S phase. A slight but statistically significant increase in S-phase compared to control was observed. Comparing MA 1^{st} treatment group in MDA-MB-231/ErbB2 cells with concurrent and Mbz1^{st} treatments reveals that MA 1^{st} triggered an increase in S and G2/M phases similar to MA single agent treatment, while the other two treatments did not affect the percentage of cells in S phase. This can explain the additional cytotoxic effect MA 1^{st} treatment has compared to the other groups, and drives

us to conclude that when Mbz is given before or with MA it interferes with MA action and prevent its effect on S-phase [Figure 5-15].

In MCF-7 breast cancer cell lines, single agent MA arrested the cells at G_1/S phase which was observed as an increase in the proportion of cells in the S phase. MCF-7 have wild-type p53 [Hui et al 2006]. Mbz 1^{st} treatment showed a significant decline in the percentage of cells in the G1 and S phases and a significant increase in the G2/M phase compared to the other two combination treatments [Figure 5-16]. This justifies our explanation that giving Mbz 1^{st} will arrest the cells in the M phase and fewer cells will complete the cycle going into the G1 and S phases where MA exerts its arrest. There was no statistical difference in the cell percentages in any of the cell cycle phases in concurrent and MA alone groups, thus again giving the drugs concurrently blocks the effect of Mbz on cell cycle.

In MCF-7/Her18 cells, MA arrested the cells at G_1/S phase and increased the proportion of cells in S phase. This observation indicates that HER2 expression does not influence the effect of MA on cell cycle. Mbz 1^{st} treatment in MCF-7/Her18 cells gave an additional benefit compared to wild type cells. We tried to explain our observations using cell cycle data, and found that the only difference that can contribute to this effect is that 80% of the cells were at the G2/M phase in the HER2 positive cells compared to 55% only in the wild type cells. This may account for the additional benefit observed with Mbz 1^{st} treatment in MCF-7/Her18 compared to MCF-7 cells.

Our final conclusion obtained from flow cytometry using PI staining is that MA arrests the two breast cancer cell lines MDA-MB-231 and MCF-7 at different stages. The expression of HER2 did not have an effect on MA or Mbz cell cycle arrest. Due to the low percentage of cells in the subdiploid portion, one can predict that apoptosis does not have a crucial role in cytotoxicity of the MA and Mbz treatment in wild type and HER2 transfected MDA-MB-231 and MCF-7 breast cancer cell lines.

Concomitant treatment with MA and the antimicrotubule agent paclitaxel increased apoptosis in anaplastic thyroid carcinoma [Yeung et al 2000]. Paclitaxel did not induce apoptosis when used as a single agent, while MA alone induced apoptosis to a lesser extent than the combination. As a single agent Mbz induced PARP cleavage in H460 and A549 cell-lines within 48hrs of treatment. The antimicrotubule Mbz inhibited cancer cells growth in vitro and in vivo by mitotic arrest, decreased angiogenesis, and induced apoptosis [Martarelli et al 2008]. Mbz induced apoptosis by phosphorylating Bcl-2 and preventing its binding to Bax [Orlow et al 2008]. Since the use of Mbz alone led to apoptosis, we hypothesized that when combined to MA a greater effect on apoptosis and synergy will be observed compared to the MA and Paclitaxel combination. Both MDA-MB-231/ErbB2 and MCF-7/Her18 cells showed an additional benefit of using MA and Mbz sequentially. We wanted to test whether this benefit was due to an increase in apoptotic cell death in these synergistic combinations compared to other treatment groups.

When MDA-MB-231/ErbB2 breast cancer cells were treated with MA (5µM), Mbz (1.25µM) or one of the combinations, harvested 12 or 24 hours after treatment, and stained with Annexin V-FITC and PI according to the protocol in (4-B-2a-2), our visual gain data presentation [Figure 5-18] did not show any significant gain in apoptotic cells in any of the treatment groups compared to control. No difference in staining among the different combination groups was observed, indicating that apoptosis did not occur neither at 12 nor 24 hours of treatment, and that it did not play a role in the additional cytotoxicity of MA 1st treatment group in this cell line.

Annexin staining flow cytometry experiments were done on the MCF-7 cell pair. Both MCF-7 and MCF-7/Her18 cancer cells were treated with MA (10µM), Mbz (5µM) or one of the combinations. Cells were harvested 12 or 24 hours after treatment, then were stained Annexin V-FITC and PI for flow cytometry analysis (according to 4-B-2a-2). Data did not show any significant difference in the staining with Annexin among the different treatment groups, indicating that apoptosis did not occur neither at 12 nor 24 hours of treatment [Figures 5: 19 and 20]. We conclude that apoptotic cell death does not contribute to the additional benefit observed with Mbz 1st treatment in MCF-7/Her18 cells. The absence of HER2 did not affect apoptosis, as observed when comparing wild type to HER2 transfected MCF-7 cells.

Mbz altered tubulin structure both in melanocytes and melanoma cells, yet it only induced apoptosis in the malignant cells. Six hours following the treatment of M14 and SKMel19 cells with 0.5µM Mbz, the cleavage of caspases 9, 7 and 3 and PARP were

detected. This indicates the activation of the intrinsic apoptosis pathway. Active Caspase 8 was detected 18 hours after treatment, which supports that the extrinsic pathway was activated at a later point [Orlow et al 2008]. Thus we believe that if apoptosis would take place with single agent or combination treatment it would have been observed in our 24hr sample. We conclude that apoptosis is not the main mechanism of cell death induced by Mbz in MDA-MB-231 and MCF-7 cells.

Wang and Macaulay reported concentration dependent cell changes with MA treatment. At concentrations above 10 µM cells became rounded and detached from the flask and an apoptotic peak was observed at about 12hr in all cell lines. They also reported that inhibition of ras farnesylation is maximum at 10 µM, and that apoptosis increase with increasing concentration. No effect on cell cycle was observed in medulloblastoma with MA treatment [Wang and Macaulay 1999]. Thus we conclude that the absence of apoptotic cell death could be related to the MA concentration used in the combination, as we used concentrations less than or equal to 10µM. Yeung et al used manumycin (54 µM) and paclitaxel (22 µM) either alone or in combination to treat anaplastic thyroid carcinoma ARO cells in vitro. They did observe an increase in apoptotic cell death and attributed the synergistic effect of the combination in part to this increase [Yeung et al 2000]. At these MA and Mbz concentrations, no additional apoptotic cell death was observed with combination treatments in our breast cancer cell lines.

All four cell lines were probed for cleaved PARP and cyclins E and B to determine the role of cell cycle arrest and apoptosis in MA and Mbz cytotoxicity. MA and Mbz induced G2/M phase cell cycle arrest in MDA-MB-231 cells. The increase in cyclin B was only observed in Mbz single agent and Mbz 1st treatment groups. The increase in cyclin B was observed at 12 and 24 hours with Mbz 1st treatment but only at 24 hours in single Mbz treatment [Figure 5-22]. We conclude that the effect of MA on cell cycle regulatory proteins either is not observed within the first 24 hours, or that MA effect on cell cycle is independent of cyclin B. In MDA-MB-231/ErbB2 cells, cyclin B levels were increased in Mbz 1st at 12 hours and in concurrent and Mbz 1st at 24 hours. We speculate that the effect of Mbz on cell cycle in these cells is delayed compared to wild type, as the increase in cyclin B was delayed to 24 hours compared to 12 hours in Mbz 1st treatment. A further time point is required to investigate this claim and observe increase in cyclin B with Mbz single agent. MA 1st treatment was synergistic in this cell line, yet we see no statistical difference in cyclin B levels compared to single MA treatment. In both concurrent and Mbz 1st treatments an increase in cyclin B due to Mbz effect was observed, when this effect was blocked in MA 1st treatment we were able to see synergism. This led us to conclude that the effect of MA on cell cycle is blocked in the presence of Mbz in concurrent treatment and Mbz 1st. When MA and Mbz effect is independent of cell cycle arrest we see synergism. This is also observed with cyclin E, as MA single agent showed a 4.5 folds increase in cyclin E in MDA-MB-231/ErbB2 cells, the increase was absent in combination treatment showing that Mbz blocks the effect of MA on cell cycle.

Since the increase in cyclin E observed with MA single agent treatment is absent in MA 1st treatment and no difference in cyclin B levels was observed in MA 1st compared to MA single agent; we conclude that the enhanced cytotoxicity observed with MA 1st compared to all other treatment groups is not mediated by synergy in cell cycle arrest.

MA induced G1/S phase arrest in wild type and HER2 transfected MCF-7 cells while Mbz induced a G2/M phase cell cycle arrest.

In MCF-7 Mbz 1st treatment showed 2.5 folds increase in cyclin B compared to MA 1st treatment. This reveals the antagonizing effect of MA on Mbz at the cell cycle level, since giving MA first blocked the effect of Mbz on cyclin B observed with Mbz single agent, concurrent and Mbz 1st treatments. Mbz1st treatment was synergistic in MCF-7/Her18 cells. At 24 hours Mbz 1st treatment showed increase in cyclins E and B compared to single agents and MA 1st treatment groups.

In agreement with the conclusion from flow cytometry studies, apoptosis did not play a major role in MA and Mbz cytotoxicity in the studied cell lines at the concentrations used for treatment. No bands were observed at 89 kDa in any of the four cell lines. In MDA-MB-231 cells we saw a band at 47kDa which is characteristic of necrotic cell death [Figure 5-21]. MCF-7/Her18 cells showed band at 40kDa which are characteristic of primary necrosis [Duriez and Shah 1997]. Both MDA-MB-231/ErbB2 and MCF-7 cells did not show any bands when probed for PARP. Observing variable patterns of PARP cleavage with MA treatment is not uncommon. Manumycin plus paclitaxel led to PARP

cleavage into an 89kDa and 24kDa fragments characteristic of apoptosis. Manumycin alone or in combination with docetaxel showed a different pattern of PARP cleavage not characteristic of apoptosis [Yeung et al 2000].

We do conclude that neither cell cycle arrest nor apoptosis plays a role in the synergistic activity observed in sequential treatment in HER2 expressing cells.

6-C- In vivo study of MA and Mbz combination treatment in nu/nu Swiss background athymic mice:

We used wild type and HER2 transfected MDA-MB-231 breast cancer cells to test our MA and Mbz combination in vivo. Mice were xenografted subcutaneously, and tumor volumes were assessed to evaluate the effect of treatment. Some of our observations from cell culture were also valid in vivo.

Sequence of drug administration influenced treatment outcome in cell culture. This was observed in mice with MDA-MB-231/ErbB2 cells. Concurrent treatment in these mice was statistically better than Mbz 1st. Concurrent treatment reduced tumor growth while Mbz 1st group had the largest tumors and did not show any effect.

Evaluating these groups in MDA-MB-231 cells ,one see that all treatment groups single and combination were not statistically different from control, this was also observed in vitro, where combination treatment did not exert any additional benefit over MA or Mbz

single agents in wild-type cells and MA1st treatment was superior to single agent in HER2 transfected cells.

When cells were introduced into female and male mice, gender became a new factor influencing the final outcome. MDA-MB-231 tumors harvested from male mice were noticeably smaller than those harvested from female mice in Mbz 1st treatment group. This triggered further investigation of the effect of gender on the final outcome of the MA and Mbz combination. We rearranged our data according to gender, and found out in MA single agent, concurrent and MA first groups female and male tumor volume profiles were superimposed. In Mbz single agent, the two profiles were different, with female tumors being smaller compared to male tumors. This difference was not statistically significant. We believe that this is due to the small sample size of 5 mice in each group.

We compared Mbz 1st treatment in MDA-MB-231 xenografted mice to MA single agent in male and female mice. Female mice treated with Mbz 1st showed larger tumor volumes compared to MA and Mbz single agents. We believe that MA blocked the effect of Mbz in female but not in male mice. The enhanced effect observed in Mbz 1st treatment in male mice was a result of MA and Mbz activity. In female mice the effect of Mbz 1st treatment was a result of MA alone and was inferior to Mbz single agent. A number of gender-related variations in drug effect and toxicity are identified and reported in literature. Hormonal influence and difference in metabolic capacity were identified among the most important differences between genders. Gender related variation in

metabolic capacity was identified in human and rodents where females showed 20-30% higher clearance of drugs metabolized by (CYP 450-3A) [Nicolson et al 2010, Goodson and Gillman's 2001]. It is believed that Mbz is metabolized by (CYP 450-3A4) since cimetidine increased Mbz concentration in plasma when given concurrently [Iosifidone et al 1997]. We do suspect that MA affected the levels of Mbz by altering its metabolism. This requires more in vivo experiments to compare Mbz pharmacokinetics given alone or combined with MA.

Swelling was observed in one animal receiving 5mg/kg MA and in three animals receiving combination treatment. This led us to believe that MA is the leading cause of toxicity, and since the kidneys were pale upon dissection we believed that renal failure was the cause of toxicity. Histopathology of the kidney and liver taken from animal # SC10-105300 which was xenografted with MDA-MB-231/ErbB2, received concurrent treatment and was sacrificed due to swelling revealed normal kidneys and showed necrotic, apoptotic and microangiopathic changes in the liver. Rare cases of hepatic dysfunction have been reported after Mbz administration [Will et al 1983]. A slight increase in liver enzymes was observed with the combination of MA and Paclitaxel [Yeung et al 2000]. Human hepatic cells were more sensitive to Mbz induced hepatotoxicity than mice and rats hepatocytes [Higa et al 1992]. Thus since the incidence of toxicity increased with combination treatment in mice, we do expect it to be high in humans too. Three out of the four mice showing this toxicity were females, this led us to

conclude that this toxicity has to do with Mbz metabolism that was altered when MA was added.

Little attention is paid to combinations with antagonistic outcome. These combinations should be utilized to increase the understanding of drugs and disease. In our combination of MA and Mbz, MA blocked the effect of Mbz in vitro and in vivo with some exceptions (concurrent treatment with MDA-MB-231/ErbB2 in vivo and MA 1^{st} in vitro, Mbz1^{st} in MCF-7/Her18 in vitro). Yet, by studying this combination we identified a number of factors that influenced the final outcome of treatment. Sequence of drug administration and targeted cancer cells were among the factors that influenced the final outcome of treatment both in vitro and in vivo. Ratio of MA to Mbz had an influence in vitro, and was also observed in vivo when gender was taken into consideration. The difference in drug handling between male and female mice gave different MA to Mbz ratio and lead to synergy in males and antagonism in females with Mbz 1^{st} treatment. In vivo studies revealed a higher incidence of toxicity when MA and Mbz are combined, and showed that gender had an influence on the final outcome of the MA and Mbz combination.

We do recommend that MA and Mbz not be given concomitantly due to the increased toxicity. We also recommend that this combination not be used for female patients until further evaluation of pharmacokinetics and pharmacodynamics of Mbz and MA alone and in combination.

CHAPTER-7- SUMMARY

We studied the combination of the farnesyl transferase inhibitor, manumycin A, and the antimicrotubule agent, mebendazole, in two different breast cancer cell lines. The combination was evaluated both in wild type and HER-2 transfected MDA-MB-231 and MCF-7 breast cancer cell lines. The sequence of drug administration was taken into consideration, where both concurrent and sequential treatments were evaluated.

7-A-The effect of single agent and combined treatment with MA and Mbz in all four breast cancer cell lines:

7-A-1- Single agents, MA and Mbz, treatment in wild type and HER2 transfected MDA-MB-231 and MCF-7 breast cancer cell lines:

- MA is effective in wild-type and HER2 transfected MDA-MB-231 (0.25-250µM) and MCF-7 (1-500µM), and shows the same potency in all four cell lines.
- Mbz is effective in wild-type and HER2 transfected MDA-MB-231 (1.25-50µM) and MCF-7 (5-80µM). It is more potent in MDA-MB-231 cells compared with MCF-7 cells.
- Both MA and Mbz have the same potency in wild type and HER-2 transfected cells of each cell line pair.

7-A-2- Combination treatment with MA and Mbz in wild type and HER2 transfected MDA-MB-231 and MCF-7 breast cancer cell lines:

7-A-2a- Synergy Heat Maps:

- At 1:1 ratio of MA to Mbz the synergy heat map revealed a region of synergism at concentrations (3.9-125) µM.
- At MA to Mbz ratios different from 1:1 the combination effect was dependent on MA to Mbz ratio and concentration.
- Drug concentration, sequence of administration, MA to Mbz ratio, and the targeted cells all played a role in the final outcome of combination treatment.

7-A-2b- Comparing single and combination treatment with MA and Mbz:

- Combination treatment with MA and Mbz had no additional benefit over treatment with single agents in wild type MDA-MB-231 and MCF-7 cancer cells.
- Combination treatment with MA and Mbz showed additional benefit over treatment with single agents in HER2 transfected MDA-MB-231 and MCF-7 cancer cells. Enhanced effect of combination was observed with sequential treatment.
- In MDA-MB-231/ErbB2 cells MA 1^{st} treatment showed additional benefit to single agent, while in MCF-7/Her18 Mbz 1^{st} treatment showed the additional benefit.

7-B-Assessing the role of cell cycle arrest and apoptosis in the cytotoxicity of combined MA and Mbz treatments in the four breast cancer cell lines:

7-B-1- Flow cytometry to cell cycle arrest and apoptosis:

Using PI staining our flow cytometry experiments revealed that:

- MA arrests the two breast cancer cell lines MDA-MB-231 and MCF-7 at different stages. MDA-MB-231 cells were arrested at G2/M phase and MCF-7 at G1/S phase.
- Mbz arrests both MDA-MB-231 and MCF-7 cells at G2/M phase.
- The expression of HER2 did not have affect cell cycle arrest induced by MA or Mbz.
- The low percentage of cells in the subdiploid portion indicates apoptosis does not have a crucial role in cell death induced by MA and Mbz treatment in wild type and HER2 transfected MDA-MB-231 and MCF-7 breast cancer cell lines.

Using Annexin-V-FITC staining our flow cytometry experiments revealed that:

- In MDA-MB-231 /ErbB2, MCF-7 and MCF-7/ Her18 there was no difference in AnnexinV-FITC staining among the different treatment groups, indicating that the role of apoptosis in cytotoxicity is minimal in these cell lines.

7-B-2- Western blotting to detect Cyclins E and B and cleaved PARP:

- Apoptosis did not play a role in cytotoxicity of single agent or combination MA and Mbz treatment at the dose used. No PARP bands were detected at 89kDa.
- When combined either MA or Mbz block the effect of the second agent on cell cycle arrest. Thus we conclude that cell cycle synergism does not play a role in the synergism of sequential treatment in HER2 transfected cells.

7- C- In vivo effect of MA and Mbz combination on MDA-MB-231 and MDA-MB-231/ErbB2 xenografts in nu/nu Swiss Background athymic mice:

Dose efficacy for MA and Mbz single agents:

- In MDA-MB-231 breast cancer cells MA dose of 2.5 mg/kg is statistically effective in reducing tumor size compared to control.
- In MDA-MB-231/ErbB2 breast cancer cells MA treatment in the range of (1-5 mg/kg) showed no statistical significance in decreasing tumor volume.
- In wild type and HER2 transfected MDA-MB-231 cells Mbz treatment in the range of (1-33 mg/kg) showed no statistical significance in decreasing tumor volume.

Combination Treatment of MA and Mbz:

In MDA-MB-231 breast cancer cells no statistical significance in the difference in tumor volume ratios (V/V0) was observed between the different groups. The repeated measures ANOVA p-value was (0.1633). The Tukey's multiple comparison test yielded p-value > 0.05 in all group comparisons.

In MDA-MB-231/ErbB2 breast cancer cells concurrent treatment was statistically different from control MA and Mbz 1st treatments with a p-value <0.001. MA single agent was significantly different from control MA ($p<0.01$) and Mbz 1st ($p<0.05$). Concurrent treatment had the lowest and Mbz 1st treatment gave the highest tumor volume ratios.

In MDA-MB-231 breast cancer cells comparing tumor weight in male to female mice in Mbz 1st treatment group revealed that the difference is statistically significant with p-value of 0.013 using repeated measures one way ANOVA followed by Tukey's post hoc ($p<0.05$). This emphasizes the role of gender in determining the effect of drug combination in the treatment of cancer.

Hepatotoxicity was increased with combination treatment. We speculate that it is related to the effect of MA on Mbz metabolism. Further investigation is required before deriving final conclusions.

REFERENCES

American Cancer Society, Inc. Breast Cancer Facts and Figures 2009-2010.

Annunziata C and O' Shaughnessy J. Poly (ADP-ribose) polymerase as a novel therapeutic target in cancer. Clinical Cancer Research 2010; 16 (18): 4517-4526.

Bagheri-Yarmand R, Nanos-Webb A, Biernacka A, Bui T, and Keyomars K. Cyclin E Deregulation Impairs Mitotic Progression through Premature Activation of Cdc25C. Cancer Research 2010; 70 (12): 5085-5095.

Bhattacharya B, Panda D, Gupta S, Banerjee M. Anti-mitotic activity of colchicines and the structural basis for its interaction with tubulin. Medicinal Research Renew 2008; 28(1): 155-183.

Banishree Saha and Dipankar Nandi. Farnesyltransferase inhibitors reduce Ras activation and ameliorate acetaminophen induced liver injury in mice. Hepatology 2009: 50: 1547-1557.

Barrington RE, Subler MA, Rands E, Omer CA, Miller PJ, Hundley JE, Koester SK, Troyer DA, Bearss DJ, Conner MW, Gibbs JB, Hamilton K, Koblan KS, Mosser SD, O'Neill TJ, Schaber MD, Senderak ET, Windle JJ, Oliff A, Kohl NE. A Farnesyltransferase Inhibitor Induces Tumor Regression in Transgenic Mice Harboring Multiple Oncogenic Mutations by Mediating Alterations in Both Cell Cycle Control and Apoptosis. Molecular and Cellular Biology 1998; 18 (1): 85-92.

Bhabatarak Bhattacharya, Dulal Panda, Suvroma Gupta, Mithu Banerjee. Anti-mitotic activity of colchicines and the structural basis for its interaction with tubulin. Medicinal Research Renew 2008; 28(1): 155-183.

Bouchalova K, Cizkova M, Cwiertka K, Trojanec R, Hajduch M. Triple negative breast cancer-current status and prospective targeted treatment based on HER1 (EGFR), TOP2A and C-MYC gene assessment. Biomedical Papers of Medical Faculty of the University of Palacky Olomouc Czech Republic 2009; 153(1):13–18.

Brunner TB, Hahn SM, Gupta AK, Muschel RJ, McKenna WG, Bernhard EJ. Farnesyltransferase Inhibitors: An Overview of the Results of Preclinical and Clinical Investigations. Cancer Research 2003; (63): 5656-5668.

Burdall S, Hanby A, Lansdown M and Speirs V. Breast Cancer cell lines: Friend or Foe? Breast cancer research-2003, vol 5 No 2:89-93.

Charafe_Jauffret E, Ginestier C, Monville F, Finetti P, Adlaide J, Ncervera I, Karri SE, Xerri L, Jacquemei J, Birnbaum D and Bertucci F. Gene expression profiling of breast cell lines identifies potential new basal markers. Oncogene 2006, vol 25: 2273-2284.

Christina Annunziata and Joyce O' Shaughnessy. Poly (ADP-ribose) polymerase as a novel therapeutic target in cancer. Clinical Cancer Research 2010; 16 (18): 4517-4526.

Christophe Tournigand, Thierry André, Emmanuel Achille, Gérard Lledo, Michel Flesh, Dominique Mery-Mignard, Emmanuel Quinaux, Corinne Couteau, Marc Buyse, Gérard

Ganem, Bruno Landi, Philippe Colin, Christophe Louvet, and Aimery de Gramont. FOLFIRI followed by FOLFOX6 or the reverse sequence in advanced colorectal cancer: a randomized GERCOR study. Journal of Clinical Oncology 2004; 22 (2): 229-237.

Chu Edward. Sequential versus combination therapy: where are we? Clinical Colorectal Cancer 2008; 7 (5):295.

Dayan AD. Albendazole, Mebendazole, and praziquantel: review of non-clinical toxicity and pharmacokinetics. Acta Tropica 2003, 86(2-3): 141-159.

Dixit D, Sharma V,Ghosh S, Koul N, Kumar P, and Seen E. Manumycin inhibits STAT3, telomerase activity, and growth of glioma cells by elevating intracellular reactive oxygen species generation. Free Radical Biology and Medicine 2009; 47.364-374.

Duriez P. and Shah G. Cleavage of poly (ADP-ribose) polymerase: a sensitive parameter to study cell death. Biochemistry and Cell Biology 1997; 75: 337-349.

Edelman M.J., Gandara D. R., Lau D. H., Lara P., Lauder I. J., and Tracy D. "Sequential Combination Chemotherapy in Patients with Advanced Nonsmall Cell Lung Carcinoma. Cancer 2001; 92 (1): 146-152.

Edward Chu. Sequential versus combination therapy: where are we? Clinical Colorectal Cancer 2008; 7 (5):295.

Esumi H, Kiyoshi K, and Tomitsuka E. Regulation of succinate-ubiquinone reductase and fumarate reductase activities in human complex II by phosphorylation of its flavoprotein subunit. Proc. Jpn. Acad. 2009, B 85: 258- 265.

European medicines evaluation agency (EMEA) 1999 Mebandazole summary report by CVMP (EMEA/MRL/625/99-final) EMEA, London.

European medicines evaluation agency (EMEA) 2001 Mebandazole summary report 2 by CVMP (EMEA/MRL/781/01-final) EMEA, London.

Frei E, Funk D, and Schrenk H. Serum albumin leads to false-positive results in the XTT and the MTT assay. BioTechniques 2007; 43:178-186 .

Freudenberg J, Wang Q, Katsumata M, Robin J, Nagatomo I, and Greene. The role of HER2 in early breast cancer metastasis and the origins of resistance to HER2-targeted therapies. Exp mol pathology 2009; 87(1):1-11.

G.J.Peters, C.L. van der Wilt, C.J.A. van Moorsel, S.R. Kroep, A.M. Bergman, S.P. Ackland. Basis for effective combination cancer chemotherapy with antimetabolites. Pharmacology and Therapeutics 2000; 87: 227-253.

Girish M Shah, Rashmi G. Shah, and Guy G. Poirier. Different cleavage pattern for poly (ADP-ribose) polymerase during necrosis and apoptosis in HL-60 cells. Biochemical and Biophysical Research Communications 1996; 229: 838-844.

Goodman and Gilman's; The Pharmacological Basis of therapeutics. Chapter 42, Drugs used in the chemotherapy of helminthiasis, page 1125. 10th edition 2001.

Goodman and Gilman's : The Pharmacological Basis of therapeutics, 10th edition 2001, page 18.

Gruver A, Peewah H, and Tubbs R. Out of the darkness and into the light: bright field in situ hybridization for delineation of ErbB2 (HER2) status in breast carcinoma. Journal of Clinical Pathology 2010; 63: 210-219.

Guisado E, Alvarez-Barrientos A, Mulero- Navarro S, Santiago-Josefat B, and Salguero P. The anti proliferative activity of resveratrol results in apoptosis in MCF-7 but not in MDA-MB-231 human breast cancer cells: cell-specific alteration of the cell cycle. Biochemical pharmacology 2002; 24:1375-1386.

Harasym T, Liboiron B, and Lawrence D. Mayer. Drug Ratio-Dependent Antagonism: a new category of multidrug resistance and strategies for its circumvention. Methods in Molecular Biology 596 "Multi-Drug Resistance in Cancer" 2009, chapter 13; 291-323.

Hastak K, Alli E, and Ford J. Synergistic chemosensitivity of triple-negative breast cancer cell lines to poly (ADP-ribose) polymerase inhibition, gemcitabine, and cisplatin. Cancer Research 2010, 70 (20): 7970-7980.

Higa F, Kitsukawa K, Gaja M, Shikiya K, Shigeno Y, Kinjo F and Saito A. Cytotoxicity of Mebandazole against established cell lines from human, rat, and mouse liver. Arch Toxicology 1992, 66 (3): 224-227.

Hortobagy et al. “New Cytotoxic Agents for the Treatment of Breast Cancer.” Oncology 1996; 10 (6): 21-29.

Hotchkiss R, Stressor A, McDunn J and Swanson P. Mechanisms of disease, cell death. NEJM 2009; 361: 1570-1583.

Hu J and Cheung NK. Methionine depletion with recombinant methioninase: In vitro and in vivo efficacy against neuroblastoma and its synergism with chemotherapeutic drugs. Internal Journal of Cancer 2009; 124: 1700–1706.

Hui L, Zheng Y, Yan Y, J Bargonetti and Foster DA. Mutant p53 in MDA-MB-231 breast cancer cells is stabilizedby elevated phospholipase D activity and contributes to survival signals generated by phospholipase D. Oncogene 2006, 25: 7305–7310.

Hudis C, Seidman A, Baselga J, Raptis G, Lebwohl D, Gilewski T, Moynahan M, Sklarin N, Fennelly D, Crown JP, Surbone A. Sequential dose-dense doxorubicin, paclitaxel, and cyclophosphamide for respectable high-risk breast cancer: feasibility and efficacy. Journal of clinical oncology 1999; 17:1.

Huff L, Sackett D, Poruchynsky M, and Fojo T. Microtubule-Disrupting Chemotherapeutics Result in Enhanced Proteasome-Mediated Degradation and Disappearance of Tubulin in Neural Cells. Cancer Research 2010; 70 (14): 5870-5879.

Hussein D and Taylor S. Farnesylation of Cenp-F is required for G2/M progression and degradation after mitosis. Journal of Cell Science 2002; 115 (17): 3403-3414.

Iosifidon E., Haagsma N., Olling M., Boon J. and Tanck M. Residue study of mebendazole and its metabolites Hydroxy-mebendazole and Amino-mebendazoles in Eel (Anguilla Anguilla) after both treatment.Drug metabolism and disposition 1997; 25 (3) : 317-320

Jingxuan Pan, Bo Chen, Chun-Hui Su, Ruining Zhao, Zhi_XiangXu, Lily Sun, Mong Hong Lee, and Sai-Ching Jim Yeung. Autophagy induced by Farnesyl transferase inhibitors in cancer cells" Cancer Biology and Therapy 2008:7(10):l679-1684.

Johnson D and Walker C. Cyclins and cell cycle checkpoints. Annual Reviews of Pharmacology and Toxicology 1999; 399 295-312.

Julien Mazieres, Anne Pradines, and Gilles Favre. Perspectives on farnesyl transferase inhibitors in cancer therapy. Cancer Letters 2004; 206: 159-167.

Jun Zhou, and Paraskevi Giannakakou. Targeting Microtubules for Cancer Chemotherapy. Current Medicinal Chemistry-Anti-Cancer Agents, 2005; 5:65-71.

Kim R, Emi M, Tanabe K, Uchida Y, and Arihiro K. The role of apoptotic or non apoptotic cell death in determining cellular response to anticancer treatment. EJSO 2006; 32:269- 277.

Kristen M. Leu, Leo J. Ostruszka, Donna Shewach, Mark Zalupski, Vernon Sondak, J. Sybil Biermann, Julia shin- Jung Lee, Carol Couwlier,KrisindaPalazzolo, and Laurence Baker. Laboratory and clinical evidence of synergistic cytotoxicity of sequential

treatment with gemcitabine followed by docetaxel in the treatment of sarcoma. Journal of Clinical Oncology 2004; 22(9):1706-1712.

Kuhn D, Balkis M, Chandra J, Mukherjee K, and Ghannoum P. Uses and Limitations of the XTT Assay in Studies of Candida Growth and Metabolism. Journal of Clinical Microbiology 2003, 41 (1): 506-508.

Lacroix M. and Leclercq G. Relevance of Breast Cancer Cell-lines as Models for Breast tumors: an Update. Breast Cancer Research and Treatment 83: 249-289, 2004.

Leo A. D., Crown J., Nogaret J.-M., Duffy K., Bartholomeus S., Dolci S., Rowan S., O'Higgins N., Paesmans M., Larsimont D., Riva A., and Piccart M. " A Feasibility study evaluating docetaxel-based sequential and combination regimens in the adjuvant therapy of node-possitive breast cancer" Annals of Oncology 2000, 11: 169-175.

Leu K, Ostruszka L, Shewach D, Zalupski M, Sondak V, Biermann J, Lee J, Couwlier C, Palazzolo K, and Baker L. Laboratory and clinical evidence of synergistic cytotoxicity of sequential treatment with gemcitabine followed by docetaxel in the treatment of sarcoma. Journal of Clinical Oncology 2004; 22(9):1706-1712.

Lostumbo A, Mehta D, Setty S, and Nunez R. Flow cytometry: a new approach for the molecular profiling of breast cancer. Experimental and Molecular Pathology 2006; 80 (1): 46-53.

Manabu E, Ryungsa K, Kazuaki T, Yoko U, and Tetsuya T. Targeted therapy against Bcl-2 related proteins in Breast cancer cells. Breast cancer research 2005; 7 (6) : R940-951.

Martarelli et al. Mebendazole inhibits growth of human adrenocortical carcinoma cell lines implanted in nude mice. Cancer Chemotherapy and Pharmacology 2008; 61:809-817.

Martinez-Lacaci E, Bianco C, De Santis M, and Salamon D. Epidermal growth factor-related peptides and their cognate receptors in breast cancer. Chapter2. Breast Cancer: Molecular genetics, pathogenesis, and therapeutics. Humana Press 1999; 31- 47.

Mathews and Farewell. Using and understanding medical statistics, 3rd edition. Chapters 6 and 7, page74, 75, and 78. 1996.

Mayer L, Harasym T, Tardi P, Harasym N, Shew C, Johnstone S, Ramsay E, Bally M, and Janoff A. Ratiometric dosing of anticancer drug combinations: Controlling drug ratios after systemic administration regulates therapeutic activity in tumor-bearing mice. Molecular Cancer Therapy 2006; 5 (7): 1854-1863.

Mayer L and Janoff A. Optimizing combination chemotherapy by controlling drug ratios. Molecular interventions 2007; 7 (4): 216-223.

Mazierel J, Pradines A, Favre G. Perspectives on farnesyl transferase inhibitors in cancer therapy. Cancer Letters 2004; 206: 159-167.

Mittendorf E, Liu Y, Tucker SL, McKenzie T, Qiao N, Akli S, Biernacka A, Liu Y, Meijer L, Keyomarsi and Hunt K. A novel interaction between HER2/neu and cyclin E in breast cancer. Oncogene 2010; 1-12.

Mukhopadhyay T, Sasaki J, Ramesh R, and Roth J. Mebendazole elicits a potent antitumor effect in human cancer cell lines both in vitro and in vivo. Clinical Cancer Research 2002; 8:2963-2969.

Naoto Takahashi, Wei Wei Li, Debabrata Banerjee, Kathleen Scotto and Joseph Bertino. Sequence-dependent enhancement of cytotoxicity produced by ecteinascidin 743 (ET-743) with doxorubicin or paclitaxel in soft tissue Sarcoma cells. Clinical Cancer Research 2001; 7:3251-3257.

Nicolson T. Mellor H & Roberts R. Gender differences in drug toxicity. Trends of pharmacological sciences 2010, 31(3):108-114.

Nielsen et al. The farnesyl protein transferase inhibitor SCH66336 synergizes with taxanes in vitro enhances their antitumor activity in vivo. Cancer Chemotherapy and Pharmacology 2000, (46): 387-393.

Norton L. A Gompertzian model of human breast cancer growth. Cancer Research 1998; 48: 7067-71.

Pan J, Chen B, Su CH, Zhao R, Sun L, Lee MH, Yeung J SC Autophagy induced by farnesyltransferase inhibitors in cancer cells. Cancer Biology and Therapy 2008; 7(10):1679-1684.

Patricia Servais I Beatrice Gulbis, Dominique Fokan and Paul Galand. Effects of the Farnesyltransferase inhibitor UCF-1C/Manumycin on growth and p21- Ras posttranslational processing in NIH3T3 cells. Int.J.Cancer 1998: 76: 601-608.

Patrick J. Duriez and Girish M. Shah. Cleavage of poly (ADP-ribose) polymerase: a sensitive parameter to study cell death. Biochemistry and Cell Biology 1997; 75: 337-349.

Peters G, C.L. van der Wilt, C.J.A. van Moorsel, S.R. Kroep, A.M. Bergman, S.P. Ackland. Basis for effective combination cancer chemotherapy with antimetabolites. Pharmacology and Therapeutics 2000; 87: 227-253.

Pfuma E. Pharmacokinetics and pharmacodynamics of combination CZ48 and Manumycin A in an athymic mouse model. 2009

Pusztai L. Markers predicting clinical benefit in breast cancer from microtubule-targeting agents. Annals of Oncology 2007; 18 supp (12): xii 15 –xii20.

O'Regan R M and Khuri F R. Farnesyl Transferase inhibitors: the next targeted therapies for breast cancer? Endocrine Related Cancer 2004; 11: 191-205.

Orlow S, Doudican N, Rodriguez A, Osman I. Mebendazole induced apoptosis via Bcl-2 inactivation in chemoresistant melanoma cells. Molecular Cancer Research 2008; 6 (8):1308-1315.

Rodriguez- Caabeiro F, Criado-Fornelio A, A. Jimenez-Gonzalez, L. Guzmen, A. Igual, A. Perez, M. Pujol. Experimental Chemotherapy and toxicity in mice of three Mebendazole polymorphic forms. Chemotherapy 1987; 33: 266-271.

Salomon A and Theiry J. Host microenvironment in breast cancer development: Epithelial–mesenchymal transition in breast cancer development. Breast Cancer research 2003, 5 (2): 101-106.

Sasaki J, Ramesh R, Chada S, Gomyo Y, Roth J, and Mukhopadhyay T. The anthelmintic drug Mebendazole induces mitotic arrest and apoptosis by depolymerizing tubulin in non-small cell lung cancer cells. Molecular Cancer Therapeutics 2002; 1: 1201-1209.

Sebti S M. Blocked pathways: FTIs shut down oncogene signals. The Oncologist 2003; 8(3):30-38.

Servais P, Gulbis B, Fokan D and Galand P. Effects of the Farnesyltransferase inhibitor UCF-1C/Manumycin on growth and p21- Ras posttranslational processing in NIH3T3 cells. International Journal of Cancer 1998: 76: 601-608.

Shah G, Shah R, and Poirier G. Different cleavage pattern for poly (ADP-ribose) polymerase during necrosis and apoptosis in HL-60 cells. Biochemical and Biophysical Research Communications 1996; 229: 838-844.

Shah U and Goldberg R. Sequential versus combination therapy into treatment of patients with advanced colorectal cancer. Clinical Colorectal Cancer 2008; 7(5):315-320.

She M, Yang H, Sun L, and Yeung J SC. Redox control of Manumycin A induced apoptosis in anaplastic thyroid cancer cells; involvement of the xenobiotic apoptotic pathway. Cancer Biology and Therapy 2006; 5 (3):275-280.

Shi B, Yaremko B, Hajian G, Terracina G, Bishop W, Liu M, and Nielsen L. The farnesyl protein transferase inhibitor SCH 66336 synergizes with taxanes in vitro and enhances their antitumor activity in vivo. Cancer Chemotherapy and Pharmacology 2000; 46387-393.

Sudakin V and Timothy J. Yen. Targeting Mitosis for Anti-Cancer Therapy. Biodrugs, 2007; 21 (4): 225-233.

Suzuki N, Urano J and Tamanoi F. Farnesyltransferase Inhibitors Induce Cytochrome c Release and Caspase-3 Activation Preferentially in Transformed Cells. Cell Biology1998, 95:15356-61.

Takahashi N, Li W, Banerjee D, Scotto K and Bertino J. Sequence-dependent enhancement of cytotoxicity produced by ecteinascidin 743 (ET-743) with doxorubicin or paclitaxel in soft tissue Sarcoma cells. Clinical Cancer Research 2001; 7:3251-3257.

Tardi P, Dos Santos N, Harasym T, Johnston S, Zisman N, Tsang A, Bermudes D, and Mayer L. Drug-ratio dependent antitumor activity of irinotecan and cisplatin combinations in vitro and in vivo.

Tian Hi, Fei Goo, Ning Li,ShengtingLi, Guang hang Yin Geng Tian,Shangang Tia, kai Wang, Xiuqing zhang,Huanming Yang, Anders Lade Nielsen and Lars BoLund. An improved method for genome wide DNA methylation profiling correlated to transcription and genomic instability in two breast cancer cell lines. Genomics 2009; 10: 1-15.

Usman Shah and Richard Goldberg. Sequential versus combination therapy into treatment of patients with advanced colorectal cancer. Clinical Colorectal Cancer 2008; 7(5):315-320.

Vichai V and Kirtikara K. Sulforhodamine blue colorimetric assay for cytotoxicity screening. Nature protocols 2006; 1 (3): 1112-1116.

Wang W and Macaulay R. Apoptosis of medulloblastoma cells in vitro follows inhibition of farnesylation using manumycin A. International Journal of Cancer 1999; 82,430-434.

Whipple R, Matrone M, Cho E, Balzer E, Vitolo M, Yoon J, Loffe O, Tuttle K, Yang J, and Martin S. Epithelial-to-mesenchymal transition promotes tubulin detyrosination and microtentacles that enhance endothelial engagement. Cancer Research 2010, 70 (20): 8127-8137.

Whyte J, Bergin O, Bianchi A, McNally S and Martin F. Mitogen-activated protein kinase signalling in experimental models of breast cancer progression and in mammary gland development. Breast cancer research 2009; 11: 209.

Wiechec E and Hansen L. The effect of genetic variability on drug response in conventional breast cancer treatment. European Journal of Pharmacology 2009; 625:122-130.

Will JA, Van Cauteren H, Marsboom R, and Vandenberghe J. Safety studies evaluating the effect of Mebendazole on liver function in dogs. Journal of American Veterinary Medicine Association 1983, 183 (1): 93-98.

Wilson C, Cajulis E, Green J, Olsen T, Chung Y, Damon M, Dering J, Calzone F, and Slamon D. HER-2 overexpression differentiates growth factor beta responses in luminal versus Mesenchymal human breast cancer cells. Breast cancer Research 2005; 7 (6): R1058- 1079.

Xu G, Pan J, Martin C, and Yeung J S-C. Angiogenesis inhibition in the in vivo antineoplastic effect of manumycin and paclitaxel against anaplastic thyroid carcinoma. The Journal of Clinical Endocrinology and Metabolism 2001; 86 (4): 1769-1777.

Yarmand R, Biernacka A, Hunt K, and Keyomarsi K .Low Molecular Weight Cyclin E Overexpression Shortens Mitosis, Leading to Chromosome Missegregation and Centrosome Amplification .Cancer Research 2010; 70 (12): 5074–5084.

Yeung et al. Manumycin Enhances the Cytotoxic Effect of Paclitaxel on Anaplastic Thyroid Carcinoma Cells. Cancer Research 2000, 60: 650-656.

Yeung et al. Farnesyltransferase Inhibitors induce DNA Damage via reactive Oxygen Species in Human Cancer Cells. Cancer Research 2005; 65: 3671-3681.

Zhou J and Giannakakou P. Targeting Microtubules for Cancer Chemotherapy. Current Medicinal Chemistry-Anti-Cancer Agents, 2005; 5:65-71.

Zhou J, Chanel Vos C, Gjy rezi A, Yoshida M, Khuri F, Tamami F, and Giannakakou P. The protein farnesyl transferase regulates HDAC6 activity in microtubule-dependent manner. The Journal of Biological Chemistry 2009; 284 (15): 9648-9655.

Zoli W, Ricotti L, Dal Susino M, Brazanti F, Frassineti GL, Folli S, Tesei A, Bacci F, and Amadori D. Docetaxel and Gemcitabine activity in NSCLC cell lines and in primary cultures from human lung cancer. British Journal of Cancer 1999; 81 (4): 609-15.